# PVAm-PVA Composite Membranes Incorporated with Carbon Nanotubes and Molecular Amines for Gas Separation and Pervaporation

by

Yijie Hu

A thesis
presented to the University of Waterloo
in fulfillment of the
thesis requirement for the degree of
Doctor of Philosophy
in
Chemical Engineering

Waterloo, Ontario, Canada, 2013

# AUTHOR's DECLARATION

I hereby declare that I am the sole author of this thesis. This is the true copy of the thesis, including any required final revisions, as accepted by my examiners.

I understand that my thesis may be made electronically available to the public.

# Abstract

This study deals with polyvinylamine (PVAm)-poly(vinyl alcohol) (PVA) based composite membranes incorporated with carbon nanotubes (CNTs) and molecular amines (e.g., piperazine (PZ), triethanolamine (TEA), *N*-methyldiethanolamine (MDEA), PZ/TEA and PZ/MDEA blends, diethylenetriamine (DETA) and triethylenetetramine (TETA)) for $CO_2$ separation, solvent dehydration by pervaporation, and hydrogen purification. The effects of the parameters involved in the procedure of membrane formation and operating conditions on the membrane performance were investigated.

Composite membranes comprising of a skin layer of PVAm-PVA incorporated with CNTs and a microporous polysulfone substrate were developed for $CO_2$ separation from flue gas and dehydration of ethylene glycol by pervaporation. The membranes were characterized with Fourier transform infrared (FTIR), Raman spectroscopy, X-ray diffraction (XRD), contact angle measurement and water sorption uptake, using dense films of PVAm-PVA/CNTs, to determine the effects of CNTs on the intermolecular interactions, degree of crystallinity, surface hydrophilicity, and degrees of swelling of the membranes. For $CO_2/N_2$ separation, adding CNTs in the membrane was shown to enhance $CO_2$ permeance while retaining a similar $CO_2/N_2$ selectivity; a $CO_2$ permeance of 18.5 GPU and a $CO_2/N_2$ ideal selectivity of 64 were obtained at 0.6 MPa feed pressure. For pervaporative dehydration of ethylene glycol, the incorporation of CNTs into the membrane was shown to increase both the permeation flux and separation factor, and at 70℃ a permeation flux of 146 g/($m^2$.h) and a separation factor of 1160 were achieved at 1 wt% water in feed using a PVAm-PVA/CNT composite membrane containing 2 wt% MWNTs.

Novel facilitated transport membranes containing both PVAm as fixed carriers and various molecular amines as mobile carriers were fabricated and used for $CO_2$ separation from $N_2$ and

$H_2$, as well as $CO_2$ separation from ethanol fermentation off gas. For membranes containing a single amine (i.e., PZ, DETA or TETA), the $CO_2$ permeance increased with an increase in the amine content in the membrane until the amine content is sufficiently high, beyond which a further increase in the amine content would decrease the membrane performance. The facilitation in $CO_2$ transport was more significant with membranes containing mixed amines (e.g., PZ/TEA and PZ/MDEA). Among all the molecular amines tested, TETA was shown to be most effective in facilitating $CO_2$ transport in terms of $CO_2/N_2$ permselectivity. Using a PVAm-PVA/TETA composite membrane with a TETA to polymer (i.e., PVAm plus PVA) mass ratio of 150/100, a $CO_2$ permeance of 22.6 GPU and a $CO_2/N_2$ selectivity of 86.5 were obtained at 0.6 MPa feed pressure for the removal of $CO_2$ from flue gas, a $CO_2$ permeance of 23.3 GPU and a $CO_2/H_2$ selectivity of 28.5 were obtained at 0.6 MPa feed pressure for $CO_2$ separation from $H_2$, a water vapor permeance of 16700 GPU was obtained at 25℃ and 2.5 mol% water vapor concentration in the feed for dehydration of ethanol fermentation off gas.

Keywords: Polyvinylamine; poly(vinyl alcohol); carbon nanotubes; molecular amine; composite membranes; facilitated transport; gas separation; carbon dioxide; pervaporation; ethylene glycol dehydration; gas dehydration

# Acknowledgements

I would like to carry out my sincere appreciation and gratitude to Dr. Xianshe Feng for giving me such a great opportunity to study in University of Waterloo. His vision and knowledge provide me guidance for my future life and career, and his advice, encouragement and support throughout the course of this study and in the preparation of this thesis are invaluable.

I wish to thank all my colleagues from our membrane group for all their assistance, support and advice in the past four years during my study, including Dr. Gil J. Francisco, Dr. Runhong Du, Dr. Chenggui Sun, Dr. Prodip Kundu, Yiyi Shangguan, Charlie J. Ulloa, Shahab Eslami, Muhammad Farooq Usman, Ying Zhang, Jingjing Sun, Dihua Wu, Xincheng Xu, Yifeng Huang, Kevin Bailey, Melanie Snow, Min Guan, Boya Zhang and Shuixiu Lai. I would like to thank Dr. Yin Liu for FTIR and XRD tests, Dr. Sandro Eugenio for SEM tests, and Dr. Jinyong Luo and Dr. Baoliang Peng for their invaluable advices for my research.

I would like to express my gratitude to my PhD examination committee members, Dr. Mladen Eic, Dr. Shirley Tang, Dr. Joao Soares and Dr. Eric Croiset, for their comments on my research and thesis.

I would like to give my special thanks to my parents and grandparents for their love and support to encourage me complete this thesis.

I would like to thank all my best friends for their support and encouragement.

Research support from the Natural Sciences and Engineering Research Council (NSERC) of Canada is gratefully acknowledged.

# Table of Contents

# List of Figures

# List of Tables

# List of Symbols

$A$ Membrane area for permeation, $cm^2$

$D$ Diffusivity coefficient, $cm^2/s$

$E$ Activation energy, kJ/mol

$J$ Gas permeance, $cm^3(STP)/cm^2.s.cmHg$

$l$ Membrane thickness, cm

$M_w$ Weight average molecular weight

$N$ Gas permeation flux, $cm^3(STP)/cm^2.s$

$P$ Permeability coefficient, $cm^3(STP).cm/cm^2.s.cmHg$

$p$ Gas pressure, cmHg

$p^s$ Saturated vapor pressure, cmHg

$\Delta p$ Pressure difference across membrane, cmHg

$Q$ Gas permeation rate, $cm^3(STP)/s$

$R$ Gas constant, J/mol.K

$S$ Solubility coefficient, $cm^3(STP)/cm^3$ polym..cmHg

$T$ Temperature, K

$T_c$ Critical temperature, K

$V$ Volume, $cm^3$

$x$ Dimensionless gas mole fraction in feed side

$y$ Dimensionless gas mole fraction in permeate side

*Greek letters*

$\alpha$ Dimensionless permeability/permeance ratio or selectivity

$\gamma$ Activity coefficient

$\theta$ Diffraction angle

# Chapter 1

## Introduction

---

### 1.1 Background

Due to their technological and economic advantages over competing separation technologies, membrane processes for gas and liquid separations have been increasingly developed in the past few decades. The “heart” of a membrane process is the membrane itself. To fully exploit the growing opportunities for membrane separation, membranes with improved performance are needed. Some basic requirements for membranes include permeability, selectivity and stability. High selectivity and permeability are always desirable since a lower driving force and a smaller membrane area are needed to achieve a given separation.

Though nonporous polymeric membranes can provide a high selectivity, the mass transport rate through the membrane is usually slow. Thus, asymmetric polymeric membranes are more commercially attractive since they consist of two structurally distinct layers: one is a thin dense selective skin (e.g., a barrier layer), and the other a thick porous substrate whose main function is to provide physical support to the thin skin. The permeation flux can be substantially enhanced by using the asymmetric structure. Asymmetric membranes can be subdivided into two categories: integrally skinned membranes and composite membranes. The difference between the two types of asymmetric membranes mainly lies in whether the skin and the support are made

from the same polymer material. A composite membrane is generally considered to consist of a skin layer and a support that are made separately and from two different materials. Because different polymers may be used, composite membranes have the advantage of combining the properties that may not be available in a single material. Several methods have been developed to prepare composite membranes, including direct coating, interfacial polymerization and in situ polymerization [Feng and Huang, 1997]. Among these methods, direct coating of a polymer solution onto a microporous support is widely used.

Polyvinylamine (PVAm) is a water soluble polymer with abundant primary amine groups in its backbone. However, membranes made from linear PVAm often have a high crystallinity due to strong intermolecular interactions [Yi *et al.*, 2006]. A high crystallinity will not only cause membrane brittleness but also reduce the permeability of the membrane. On the other hand, poly(vinyl alcohol) (PVA) is also a hydrophilic polymer with good membrane forming properties and mechanical strength, easy to process and readily available. Therefore, blending PVAm with a more robust polymer (e.g., PVA) is expected to help decrease the membrane crystallinity due to potential interactions between the functional groups of PVAm and PVA chains, and improve the mechanical property and/or permselectivity of the membrane [Deng *et al.*, 2009]. In addition, the hydrophilic nature of PVA along with PVAm will make the membrane easily swollen by water. Moderate membrane swelling will favor the permeation of both gas molecules (e.g., $CO_2$) and water molecules through the membrane. Therefore, composite membranes based on PVAm-PVA blend polymers can be employed for certain applications of gas separation, pervaporation and vapor permeation.

Conventional polymeric membranes based on the solution-diffusion mechanism usually exhibit a “trade-off” relationship between the permeability and selectivity, that is, a high

permeability and a high selectivity can hardly be achieved simultaneously. Thus, to develop advanced membranes for future applications, two potential approaches can be considered to address this issue. The first approach to membrane development is to use polymer-inorganic nanocomposite, where nanofillers are dispersed in a polymer matrix, and such membranes are sometimes referred to as mixed matrix membranes (MMMs) [Chung *et al.*, 2007; Cong *et al.*, 2007a]. Zeolites, silica and carbon molecular sieves have been studied intensively as fillers for fabrication of MMMs [Kim and Lee, 2001; Vu *et al.*, 2003; Huang *et al.*, 2006]. More recently, carbon nanotubes (CNTs) have attracted significant attention as a new type of nanofillers due to their superior separation and mechanical properties. CNTs are rolled-up cylinders of graphite sheets with a nanometer diameter and a tubular structure. The as-produced CNTs tend to assemble into bundles due to strong van der Waals attraction among the tubes [Georgakilas *et al.*, 2008]. Thus, the effectiveness of using CNTs in MMMs to improve the separation performance depends to a large extent on the ability to disperse the CNTs uniformly in the polymer matrix. Attaching functional groups to the CNTs is considered to be an effective way to prevent nanotube aggregation, which helps better disperse the CNTs in a polymer matrix [Sahoo *et al.*, 2010], and surface treatment of CNTs with strong acids (e.g., sulfuric acid, nitric acid) is commonly used for this purpose [Choi *et al.*, 2007]. CNT-incorporated membranes have been reported to have extraordinarily high transport rate to both gases and liquid water [Majumder *et al.*, 2005; Holt *et al.*, 2006] due to the inherent smoothness of CNT walls [Kim *et al.*, 2007a], and some efforts have been made to study CNT-incorporated membranes for gas separation and pervaporation applications [Cong *et al.,* 2007b; Choi *et al.*, 2009; Murali *et al.,* 2010; Shirazi *et al.*, 2011]. Thus, considering the good affinity of amine groups in PVAm to both $CO_2$ molecules and water molecules as well as the fast transport properties of CNTs, PVAm-PVA composite

membranes modified by CNTs were developed and investigated for separating $CO_2$ from flue gas and solvent dehydration by pervaporation in the present work. To the best of our knowledge, no prior work has been found in the literature about PVAm/PVA blend membranes modified by CNTs for $CO_2$ separation or PVAm/PVA based membranes for pervaporation applications.

On the other hand, facilitated transport membranes, which are based on the reversible reaction between the specific gas molecules and the reactive carriers contained in the membrane, may offer an effective method to obtain high selectivity without compromising permeability. There are two major types of facilitated transport membranes based on the mobility of the carriers in the membrane. The carrier molecules can be mobile in the membrane where the carriers can diffuse freely across the membrane (similar to liquid membranes), or immobilized in the membrane matrix where the carriers are fixed to certain sites of the matrix (i.e., fixed-site-carrier membranes). Liquid membranes normally possess a high permeability and a high selectivity, but they have not yet been commercialized due to their instability and carrier loss problems. Through fixation of carriers onto polymer backbones via chemical bonds, fixed-site-carrier membranes generally exhibit a high stability. In view of the primary amine groups present in the PVAm/PVA blend, the blend polymer may exhibit facilitated transport to $CO_2$. Moreover, research efforts were devoted to facilitated transport membranes containing both mobile and fixed carriers used for $CO_2$ separation, which may combine the advantages of both liquid and fixed-site-carrier membranes. These novel facilitated transport membranes have shown promising results in $CO_2$ separation [Zou and Ho, 2006; Yuan *et al.*, 2011]. Since the amine groups from PVAm could be considered as fixed carriers to facilitate the transport of $CO_2$, additional molecular amines can be incorporated into the membrane to be used as mobile carriers. Therefore, several molecular amines were incorporated into PVAm-PVA composite

membranes in this study, and the as-prepared membranes were then investigated for the removal of $CO_2$ from flue gas. Based on these results, the most effective molecular amine in facilitating $CO_2$ transport was chosen and the membranes containing this amine were then investigated for $CO_2$ separation from $H_2$, and $CO_2$ dehydration from ethanol fermentation off gas.

## 1.2 Research objectives

The objectives of this research were to study PVAm-PVA composite membranes incorporated with CNTs and different molecular amines for $CO_2$ separation and water permeation. The research consisted of the followings:

1) To develop a polymer-inorganic nanocomposite membrane incorporated with CNTs used for $CO_2$ separation and solvent dehydration by pervaporation.
2) To develop a novel facilitated transport membrane containing both fixed and mobile carriers used for $CO_2$ separation and gas dehydration.
3) To study the effects of main parameters involved in membrane formation and operating conditions on the separation performance of the membranes.

## 1.3 Outline of the Thesis

The thesis consists of nine chapters. The scope of each chapter is listed as follows:

Chapter 1 presents an overview of the objectives and the rationale of selecting PVAm-PVA blend polymers as the membrane material and potential modifications of the membranes. A literature review on the solution-diffusion mechanism for permeation and its various applications ($CO_2$ separation, pervaporation and vapor permeation), and typical membranes used for these applications are presented in Chapter 2.

PVAm-PVA membranes incorporated with CNTs were developed and then investigated for $CO_2/N_2$ and other gas separations and the dehydration of ethylene glycol by pervaporation, as presented in Chapters 3 and 4, respectively.

On the other hand, Chapters 5 and 6 are concerned with the development of PVAm-PVA composite membranes incorporated with molecular amines for use in $CO_2$ separation from flue gas (i.e., $CO_2/N_2$ separation). Namely, piperazine (PZ) was incorporated into the membrane and investigated in Chapter 5, and diethylenetriamine (DETA) and triethylenetetramine (TETA) were examined in Chapter 6.

Based on the investigations in Chapters 5 and 6, TETA was shown to be the most effective molecular amine in facilitating $CO_2$ transport in terms of $CO_2/N_2$ permselectivity. Therefore, the applications of the PVAm-PVA composite membranes incorporated with TETA (including $H_2$ purification and $CO_2$ dehydration from ethanol fermentation off gas) are subsequently presented in Chapters 7 and 8, respectively.

Chapter 9 summarizes the general conclusions drawn from the study, original contributions of the thesis work, and recommendations for future work. In order to have a clear understanding of this thesis, Fig. 1-1 is hereby presented to describe the relationship of each chapter.

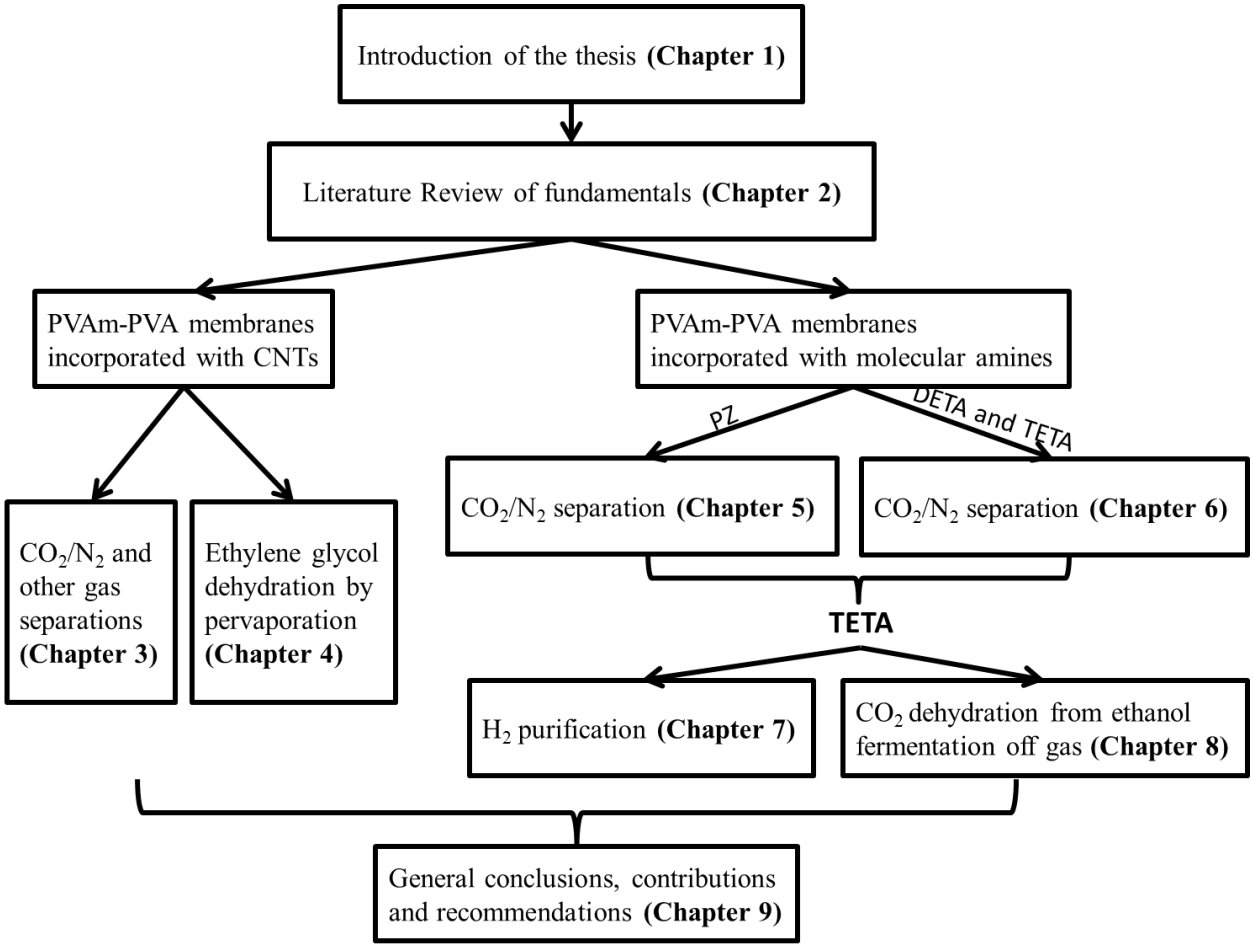


Fig. 1-1 Relationship of each chapter in this thesis

# Chapter 2

## Literature Review

---

Membrane separation processes are developing rapidly, and they have received remarkable attentions as one of the major separation processes. Membrane technology is considered to be a promising alternative to such conventional separation techniques as distillation, absorption and adsorption due to its inherent merits of dramatically lowered energy consumption, smaller footprints, lower operating and capital costs, light weight, ease of operation and environmental friendliness [Mulder, 1991; Baker, 2004]. Nowadays, membrane-based separation has been widely used in industrial gas separations and liquid separations.

This chapter serves to provide an overview of the fundamentals of gas separation, pervaporation and vapor permeation, as well as the membranes used in these areas. Various methods of modification of polymeric membranes targeted at the above applications in order to achieve a higher separation performance are also reviewed, which is relevant to the present thesis work.

### 2.1 Membrane separation processes

Membrane separation is based on the selective transport of one component over the other in a mixture through a membrane under a driving force [Koros, 2004]. Fig. 2-1 illustrates the basic concept of a membrane separation process, in which the driving force is often a pressure or

concentration gradient across the membrane [Ismail *et al.*, 2009].

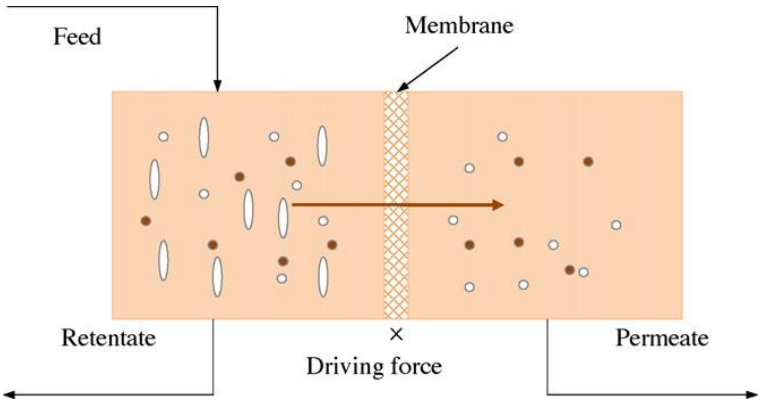


Fig. 2-1 The basic concept of membrane separation process [Ismail *et al.*, 2009]

Membrane-based gas separation is a pressure-driven process and has found applications in air separation, hydrogen recovery and acid gas separation. Since $CO_2$ is one of the most important greenhouse gases contributing to the climate change, its recovery from various emission sources is a crucial scientific and technological challenge which is gaining tremendous attention. $CO_2$ separation from $N_2$, $H_2$, $CH_4$ (e.g., $CO_2/N_2$, $CO_2/H_2$ and $CO_2/CH_4$) is directly related to flue gas separation, hydrogen purification and natural gas sweetening. Among them, to capture $CO_2$ from flue gas produced by the combustion of fossil fuels and biomass from the power plants efficiently and economically is essential since more than one-third of all $CO_2$ emissions are from the existing power plants over the world [Zhao *et al.*, 2008a; Brunetti *et al.*, 2010].

Pervaporation is a membrane process for liquid separation. Normally, pervaporation works best for removing a minor component from a liquid mixture. Pervaporation also has demonstrated incomparable advantages in separating close-boiling and azeotropic mixtures [Nureshi and Blaschek, 1999]. It has a broad range of applications mainly in the following three areas [Smitha *et al.*, 2004]: (i) dehydration of organic solvents (e.g., alcohols, ethers, esters, acids and glycols), (ii) removal of dilute organic compounds from aqueous streams (e.g., removal of

volatile organic compounds, recovery of aroma), (iii) separation of organic-organic mixtures (e.g., methyl *tert*-butyl ether/methanol). Among them, dehydration of organic solvents is the best developed.

Vapor permeation is generally considered the permeation of condensable gases such as water vapor and volatile organic compounds (VOCs), and can be used to separate various vapors from gas or vapor streams. The recovery of VOCs from various emission sources (e.g., gasoline) and monomers (e.g., vinyl chloride, ethylene, or propylene) from polymerization off gases are important to mitigate the environmental pollution and health problems [Baker, 2004]. Besides, water vapor permeation is also of industrial importance for dehydration of gases. Representative applications can be found in the drying of natural gas [Liu *et al.*, 2001], compressed air [Wu *et al.*, 2002], or flue gas [Sijbesma *et al.*, 2008], packaging materials, and humidity control in closed spaces (e.g., air conditioning in buildings, aviation and space flight) [Metz *et al.*, 2005a].

Depending on the feed mixtures to be separated and the mass transport mechanism used, the membranes may be classified as porous or dense. Generally speaking, porous membranes with pores ranging from 100 nm (for ultrafiltration) or up to 10 $\mu m$ (for microfiltration) are normally used to separate mixtures with large sizes based on size-sieving mechanism. On the other hand, gas separation, pervaporation and vapor permeation that deal with small molecules require the membranes to be nonporous. The mass transport through these membranes is best described by the solution-diffusion mechanism. Therefore, to develop membranes for effective gas separation, pervaporation and vapor permeation, a good understanding of the transport mechanism is important, and the basic principles will be reviewed briefly in the following.

## 2.2 Solution-diffusion mechanism

The solution-diffusion is generally accepted to describe mass transport through dense membranes. The permeant molecules are believed to dissolve in the membrane material and then diffuse through the membrane down a concentration gradient to reach the other side of the membrane [Pandey and Chauhan, 2001]. Separation of different permeants is achieved due to the difference in the amount of material that dissolves in the membrane and the rate at which the material diffuses through the membrane [Ismail *et al.*, 2009].

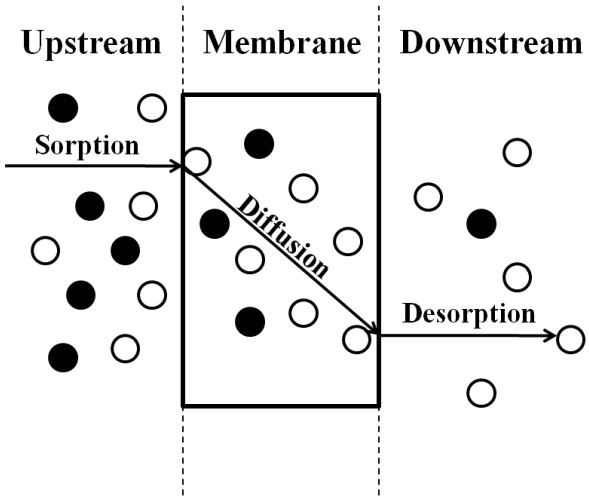


Fig. 2-2 Schematic description of solution-diffusion mechanism

The solution-diffusion mechanism considers three consecutive steps: 1) sorption of permeants into the upstream side of the membrane; 2) diffusion through the membrane under a concentration gradient; and 3) desorption from the downstream side of the membrane (see Fig. 2-2) [Wijmans and Baker, 1995; Pandey and Chauhan, 2001]. The sorption and desorption of permeants are usually very fast, and a sorption equilibrium is thus assumed to be established rapidly between both the permeant-membrane interfaces. On the other hand, the slowest molecular diffusion is considered to be the rate-determining step in permeation [Feng and Huang, 1997]. Therefore, the diffusion of a permeant from a high concentration feed (upstream)

to a low concentration (downstream) side forms the basis of the mass transport model.

The permeability coefficient ($P$) is generally used to characterize how permeable the membrane is, which can be viewed as the product of a solubility coefficient ($S$) and a diffusion coefficient ($D$):

$$P = DS \tag{2-1}$$

The solubility coefficient is a thermodynamic parameter and provides a measure of quantity of permeant molecules that dissolve in the membrane. It is affected by the condensability of the permeant and the interaction between the permeant and the membrane. The diffusion coefficient is a kinetic parameter that describes the mobility of permeant molecules, which is normally governed by the size of the permeant molecules as they move through the transient voids offered by the free volume in the membrane [Zou *et al.*, 2008].

The ability of a membrane to separate a mixture is measured by its selectivity. In a binary mixture system consisting of components $i$ and $j$ with component $i$ as the fast permeating species, the selectivity can be measured by the ratio of their permeability coefficients [Koros, 2002], which is sometimes called ideal separation factor:

$$\alpha_{i/j} = \frac{P_i}{P_j} = \left(\frac{D_i}{D_j}\right) \times \left(\frac{S_i}{S_j}\right) \tag{2-2}$$

Obviously, the ideal separation factor is dependent on not only the diffusivity selectivity ($D_i/D_j$) but also the solubility selectivity ($S_i/S_j$). The diffusivity selectivity depends mainly on the size-sieving capability of the membrane (e.g., the ability for a polymer to separate diffusing molecules of different sizes), which is determined by the free volume of the membrane and the size of the permeants. The size-sieving ability of a polymer is related to a number of parameters such as chain mobility and structure of the polymer [Matteucci *et al.*, 2008]. The solubility selectivity is primarily associated with the condensability of the permeant molecules and the

affinity between the permeants and the polymer matrix.

The solution-diffusion mechanism applies to gas separation, pervaporation and vapor permeation processes. In terms of the physical phases of the feed and permeate, gas separation and pervaporation can be differentiated: the feed in gas separation and pervaporation is a gas and a liquid, respectively, while the permeate is a gas (or vapor) in both processes. Vapor permeation is similar to gas separation, where both of the feed and permeate phases are gaseous. All these processes involve diffusion of molecules in a dense polymer. Once dissolved in the membrane, the permeant moves by molecular diffusion. Sometimes, similar membranes can be used in different processes. For instance, poly(vinyl alcohol) membranes may be used for the removal of carbon dioxide from flue gases, dehydration of alcohols and gas dehydration as long as the membranes are defect-free.

In gas separation, a gas mixture at an elevated pressure passes along the surface of a membrane that is selectively permeable to one component of the feed mixture, and this component is thus enriched in the permeate side of the membrane. In vapor permeation, the transport of permeating components is carried out from a vapor feed mixture to a permeate vapor phase. The permeate vapor is taken out by vacuum or sweeping gas applied on the permeate side. Vapor permeation is different from permanent gas permeation due to their different degrees of condensabilities. Unlike gas separation and vapor permeation, phase change of permeating species from liquid to vapor state takes place in pervaporation. In pervaporation, a liquid mixture contacts one side of a membrane, and the permeate is removed as a low pressure vapor from the other side of the membrane. The pressure difference across the membrane is usually small, and the driving force for pervaporation is provided by lowering the vapor partial pressure (or activity) on the permeate side of the membrane via vacuum or inert purge [Feng and Huang,

1997]. The partial vapor pressure of a component on the permeate side of the membrane affects its permeation rate significantly. Hence, the downstream vapor pressure must be maintained as low as economically feasible to maximize the driving force for the permeation.

## 2.3 $CO_2$ separation membranes

Based on membrane structures, transport mechanisms or applications, $CO_2$ separation membranes can be classified into different categories. The inorganic membranes, polymeric membranes, nanocomposite membranes incorporated with nanofillers (especially carbon nanotubes (CNTs)), and facilitated transport membranes based on $CO_2$-carrier interactions will be discussed.

### 2.3.1 Inorganic membranes

Inorganic membranes are usually formed from metals, metal oxides, zeolites, ceramics, carbons and glasses, which can be dense or porous. Porous inorganic membranes from zeolites and carbon molecular sieves are favorable for gas separation due to their excellent size-sieving ability. The transport mechanism in porous media mainly includes [Noble and Stern, 1995] Knudson diffusion, surface diffusion, capillary condensation and molecular sieving. Among these, Knudson diffusion and molecular sieving are more important for most membranes. The mechanism of mass transport depends largely on the pore size and the size of diffusing gas molecules [Ockwig and Nenoff, 2007].

Inorganic membranes have been studied to separate gas mixtures because of their thermal, chemical and mechanical stabilities as compared to polymeric membranes. The well defined pore sizes and shapes of the membrane resulting from narrow pore distributions ensure good permselectivity [Chung *et al.*, 2007]. However, the intrinsic brittleness, high handling cost and

poor processability has affected the large scale industrial application of inorganic membranes for gas separation. Currently, inorganic membranes aiming at gas separation is still on the laboratory scale, and there is no commercial application yet for gas separation, to our best knowledge.

### 2.3.2 Polymeric membranes

In membrane-based gas separations, conventional polymeric membranes (e.g., cellulose acetate, polyimide and polysulfone membranes) based on the solution-diffusion mechanism have been employed in commercial applications. Polymeric membranes have received considerable attention since they compete favorably with other conventional gas separation techniques (e.g., pressure swing adsorption, amine absorption and cryogenic distillation).

#### 2.3.2.1 Free volume and its effect on polymeric membranes

The macroscopic space which a polymer occupies is not completely filled by its chains. Gaps between the chains cannot be filled due to conformational constraints (bond angles, steric hindrance), especially in the case of amorphous polymers. A fraction of these gaps is large enough to accommodate gas molecules and such gaps are considered to be the "free volume" [Maier, 1998]. As stated previously, the molecular diffusion process is the rate-determining step for mass transport in nonporous polymeric membranes based on the solution-diffusion mechanism. Hence, the free volume will significantly affect the gas diffusion. Consequently, the free volume is of vital importance for the separation performance of polymeric membranes. The free volume elements usually include pores, channels and cavities, and the sizes and distribution of free volume elements play a key role in determining the permeability and separation characteristics [Park *et al.*, 2007].

The free volume, whether static voids created by inefficient chain packing or transient gaps generated by thermally induced chain segment rearrangement, provides penetrants with a low-

resistance avenue for transport [Merkel *et al.*, 2002]. The larger and more these pathways are, the faster the molecules migrate through a polymer. Thus, amorphous polymers generally possess a higher free volume and gas permeability than semi-crystalline polymers.

Park *et al.* [2007] demonstrated that polymers with an intermediate cavity size and a narrow cavity size distribution could yield both a high permeability and a high selectivity. In principle, these polymers could be obtained by controlling the free-volume element formation through a spatial rearrangement of the rigid polymer chain segments in the glassy phase. The microstructure of polymer materials can be tailored by thermally driven segment rearrangement. Based on this, the so-called thermally rearranged (TR) polymers with well connected and narrowly distributed free-volume element sizes appropriate for molecular separations are obtainable. The unusual large cavities of TR polymers may contribute to their high gas permeability, whereas the constriction formed by cavity coalescence is presumably responsible for their precise discrimination among gas molecules [Park *et al.*, 2007].

Effectively controlling the free volume element size and distribution of polymeric membranes could yield a good permeability and selectivity. For amorphous glassy polymers, attempts can be made to increase the chain stiffness by incorporating rigid and bulky groups into the polymer chain, which in turn, by affecting the packing density, increases the free volume [Maier, 1998]. However, the distribution of the "gap" diameters is different for different polymers. Therefore, it's far more difficult to control the free volume element size distribution than the size itself for polymers.

**2.3.2.2 Robeson upper bound**

Robeson [1991] did a comprehensive analysis of the permeability data for binary gas mixtures from a list of He, $H_2$, $O_2$, $N_2$, $CH_4$, and $CO_2$ in conventional polymeric membranes

reported in the literature and concluded that there was a permeability/selectivity trade-off relationship, that is, a membrane with a high gas permeability was often associated with a low gas pair selectivity, and vice versa. An "upper bound" in the permeability and selectivity plot was observed, above which virtually no data existed for polymeric membranes (see Fig. 2-3).

The theoretical work of Freeman [1999] shows that the polymer structure has no influence on the slope of the upper bound, which is merely dependent on the penetrant size ratio for a gas pair. In addition, the fundamental characteristics of polymers with outstanding gas separation properties for one pair of gases are often shared by polymers having good separation properties for other gas pairs.

Therefore, the Robeson upper bound is based on polymers with chain stiffness and strong size-sieving capability, which are characteristics typical of glassy polymers. To achieve higher selectivity/permeability combinations and surpass the upper bound, materials that do not obey these simple rules will be required. Two options can be considered: one is forcing diffusing molecules to follow different mechanisms other than the solution-diffusion mechanism when transporting across the membranes by properly controlling membrane structures; the other is to find out the solubility selectivity that will dominate the polymeric membranes according to Freeman's theory.

Fixed-site-carrier membrane in the category of facilitated transport membrane is one example that does not follow the simple solution-diffusion mechanism [Kim *et al.*, 2004; Yi *et al.*, 2006; Cai *et al.*, 2008]. The facilitated transport dominant in mass transfer across the membrane is based on reversible reactions or interactions between $CO_2$ molecules and carriers present in the polymer matrix. The separation performance in terms of $CO_2$ permeability and $CO_2/CH_4$ selectivity for fixed-site-carrier membrane was observed to exceed the Robeson upper

bound displayed by simple polymeric membranes [Cai *et al*., 2008]. On the other hand, the solubility selectivity-dominant polymeric membranes mainly include those containing ether moieties as backbones or linkages. For instance, poly (ethylene glycol) segments possess regularly spaced polar ether linkages along the backbone, and the introduction of ether moieties into the polymer membrane could be used to promote specific chemical interactions with $CO_2$ molecules, thereby facilitating molecular transport of $CO_2$. An unusually high $CO_2$ selectivity was constantly observed in such membranes [Patel *et al.*, 2003, 2004; Lin *et al.*, 2006a, 2006b]. Compared to the diffusivity selectivity-dominant membranes, the solubility selectivity-dominant membranes tend to show many distinct properties; for instance, the membrane may be reversely selective (e.g., more permeable to larger molecules such as $CO_2$ than to smaller molecules such as $H_2$) [Patel *et al.*, 2003, 2004; Lin *et al.*, 2006a]. The plasticization of the polymer induced by $CO_2$ could further improve the membrane selectivity, and thus a decrease in temperature does not necessarily reduce the permeability and may enhance the selectivity dramatically [Lin *et al.*, 2006a, 2006b].

Recently, Robeson [2008] revisited his "upper bound" (see Fig. 2-3). The prior upper bound relationship is mainly based on homogeneous polymer membranes, and several approaches involving heterogeneous membranes are demonstrated to be able to shift the upper bound. For instance, surface modification [Chung *et al.*, 2006], mixed matrix approach [Chung *et al.*, 2007; Husain and Koros, 2007], carbon molecular sieving membranes produced by carbonization of aromatic polymer membranes [Kim *et al.*, 2005] can yield permselective properties that are well above the prior upper bound.

As Fig. 2-3 shows, compared to the prior upper bound, the present upper bound shifts towards higher permeability and selectivity with the development of advanced polymers and

membranes in recent years. In particular, certain TR polymers exhibit exceptional separation capabilities, even surpassing the present upper bound [Park *et al.*, 2007].

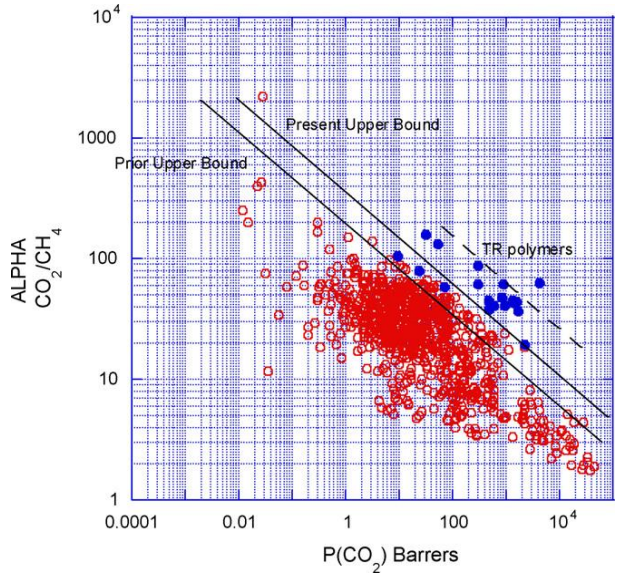


Fig. 2-3 Robeson upper bound and revisited upper bound for $CO_2/CH_4$ system [Robeson, 2008]

### 2.3.3 Nanocomposite membranes

Polymer nanocomposites have attracted significant attention for application in areas such as microelectronics, optics and catalysis due to their unique properties [Merkel *et al.*, 2002]. Nanocomposites may also be useful for developing membranes for molecular separation such as seawater desalination. The incorporation of fillers with at least one dimension in the nanometer range into a continuous polymer phase can generate nanocomposite membranes [Lebrun *et al.*, 2006]. Fifty years ago, the nanocomposite membrane had been studied for gas separation. Nowadays, various nanofillers such as silica, zeolites, carbon molecular sieves and activated carbons are widely utilized in studies of nanocomposite gas separation membranes, and recently carbon nanotubes (CNTs) have also received significant interest as a new type of nanofillers because of their unique structures and properties.

#### 2.3.3.1 Overview of nanocomposite membranes

Nanocomposite membranes are usually classified according to the states of the nanofillers and the continuous phase, as shown in Table 2-1.

Table 2-1 Types for nanocomposite membranes

| No. | Nanofillers | Continuous phase | Examples | References |
|---|---|---|---|---|
| 1 | Inorganic | Organic | $SiO_2$, $TiO_2$/PMP[a] | [Shao *et al.*, 2009a] |
| 2 | Inorganic | Inorganic | ZSM-5 zeolite/carbon | [Liu *et al.*, 2006] |
| 3 | Organic | Organic | PS/PI, PSVP/PI[b] | [Xu *et al.*, 2002] |
| 4 | Organic | Inorganic | Vinyl groups/silica | [Kruk *et al.*, 2002] |

[a] PMP: poly(4-methyl-2-pentyne).

[b] PS: polystyrene, PSVP: poly(styrene-co-4-vinylpyridine), PI: polyimide.

Nanocomposite membranes based on inorganic nanofillers have attracted a lot of attention. Polymer-inorganic nanocomposite membranes, comprising of inorganic nanofillers dispersed at a nanometer level in a polymer matrix, which is sometimes referred to as mixed matrix membranes (MMMs), have been a focus of research for gas separation in recent years [Chung *et al.*, 2007; Cong *et al.*, 2007a].

In gas separation, the Robeson upper bound indicates that a rather general trade-off relationship exists between permeability and selectivity for polymeric materials. Based on the structure-property relation, modified polymers may have improved permeability and/or selectivity below the "upper bound" line but can hardly across it. On the other hand, certain inorganic materials have permselectivity beyond the upper bound limit based on molecular sieving mechanism. Nevertheless, the immediate application of inorganic membranes is still seriously hindered by the lack of technology to form defect-free membranes, the extremely high cost for the membrane production, and handling issues (e.g., inherent brittleness). In view of this, the mixed matrix membrane approach that combines advantages of both polymeric and inorganic materials may provide an alternate cost-effective membrane with separation properties above the upper bound limit. MMMs may benefit from the addition of the inorganic particles with their

inherent superior separation characteristics. In the meantime, the fragility associated with the inorganic membranes may be avoided by using a flexible polymer as the continuous phase [Chung *et al.*, 2007].

Due to the different physical properties, especially the difference in density between inorganic fillers and polymers, precipitation of inorganic fillers may occur during the MMM preparation, leading to non-uniform distribution of the inorganic fillers in the polymer phases in the resulting composite membrane [Chung *et al.*, 2007]. The agglomeration of inorganic fillers will cause pinholes, acting as non-selective defects in the MMM. This situation is especially serious at a high loading content of the inorganic fillers in the MMM. One possible solution to this issue is the use of polymer solutions at a relatively high concentration to increase the solution viscosity in order to slow down the filler sedimentation. Alternatively, if the membrane can form rapidly, the fillers will not have enough time to precipitate. In addition, if one can attach the organic functional groups to the surface of inorganic fillers, it will not only provide a better dispersion of inorganic fillers in the polymer matrix, but also enhance the penetrants adsorption capacity, resulting in improved separation performance [Cong *et al.*, 2007a].

The gas transport behavior in polymer-inorganic nanocomposite membranes is considerably influenced by a variety of factors including: (1) properties of the polymer and inorganic materials (2) their compatibility, (3) membrane formation process, and (4) morphology of the membrane formed [Ahn *et al.*, 2008].

Due to the large difference between the polymer and the inorganic materials in their properties and strong aggregation of the nanofillers, nanocomposite membranes cannot be prepared by such common methods as melt blending. The most commonly used methods for the fabrication of nanocomposite membranes can be divided into the following three types: solution

blending, in situ polymerization and sol-gel [Cong *et al.*, 2007a]. Among them, solution blending is a simple way to fabricate polymer-inorganic nanocomposite membranes. A polymer is first dissolved in a solvent to form a solution, and then inorganic nanofillers are added into the solution and dispersed under vigorous agitation. The nanocomposite membrane is then cast by removing the solvent. The solution blending method is easy to handle and suitable for all kinds of inorganic materials, and the concentrations of the polymer and inorganic components can be easily controlled. However, the inorganic ingredients are inclined to aggregate in the membranes when the contents of the inorganic materials are considerably high.

**2.3.3.2 Effect of nanofillers on the separation performance**

The content, shape and size of nanofillers are important to the separation performance of nanocomposite membranes. To explain how the nanofillers can affect the separation performance of nanocomposite membranes, the following four aspects can be considered:

*Maxwell model*

According to the Maxwell model [1873], adding impermeable inorganic nanofillers to a polymer is typically expected to reduce the gas permeability. On one hand, the membrane solubility decreases due to reduction of polymer volume available for sorption upon the addition of nanofillers. On the other hand, a decrease in the diffusivity is obvious due to increased tortuosity and thus the penetrant diffusion pathway length. Both factors serve to decrease permeability with an increase in the filler content. For example, the permeabilities of $CO_2$, $H_2$ and air all suffered a reduction in polycarbonate/$Co_{0.6}Zn_{0.4}Fe_2O_4$ nanocomposite membranes [Vijay *et al.*, 2006]. However, this is not always the case and different trends have also been observed, which indicates non-Maxwellian effects [Merkel *et al.*, 2002, 2003a; Gomes *et al.*, 2005]. That is, the addition of nanofillers is not necessarily associated with a decrease in gas

permeability. The problem with the Maxwell model lies in its neglect of the interactions between the nanofillers and the polymer chains, and between the nanofillers and the penetrants. In most cases, these interactions are strong enough to change the diffusivity and solubility of penetrants significantly.

*Free-volume increase*

It is believed that the nanofillers will increase the free volume of the membrane. This provides a qualitative understanding of the interaction between the polymer chain and nanofillers. The nanofillers may disrupt the polymer chain packing and increase the free volume between the polymer chains, enhancing gas diffusion and finally leading to an increase in gas permeability. This hypothesis is consistent with many experimental observations [Merkel *et al.*, 2002, 2003a, 2003b; Gomes *et al.*, 2005]. Gomes *et al.* [2005] introduced fumed silica nanoparticles into poly(1-trimethylsilyl-1-propyne) (PTMSP) and evaluated the performance of the nanocomposite membranes for butane/methane separation. The incorporation of fumed silica into the polymer matrix can increase the free volume without creating non-selective defects, resulting in an increased gas permeability; however, if too much fumed silica is incorporated that leads to free volume elements large enough to permit non-selective Knudsen transport, a decrease in butane/methane selectivity will be obtained.

*Solubility increase*

It is assumed that the gas permeability in the membrane will be increased by the interaction between the penetrants and the nanofillers. Functional groups such as hydroxyl on the surface of the inorganic nanofillers may interact with polar gases (e.g., $CO_2$ and $SO_2$), resulting in an increase in the gas solubility in the nanocomposite membranes, which in turn, increases the gas permeability. Kim and Lee [2001] reported a PEBAX/silica nanocomposite membrane with a

high $CO_2$ permeability as well as a high $CO_2/N_2$ selectivity, which are presumably due to strong interactions between $CO_2$ molecules and the residual hydroxyl groups on the silica domain.

*Nanogap hypothesis*

According to this hypothesis, due to poor compatibility of the nanofillers (such as silica and carbon nanotubes) surface and the polymer, the polymer chains do not tightly contact the nanofillers, thus forming a narrow gap surrounding the fillers. Therefore, the gas diffusion path was shortened and the apparent gas diffusivity and permeability were increased. In the meantime, this may also explain why the addition of the nanofillers enhances gas permeability but does not affect the gas selectivity [Cong *et al.*, 2007b, 2007c].

**2.3.3.3 Overview of carbon nanotubes**

Since the discovery of carbon nanotubes (CNTs) by Iijima [1991], they have received much attention for their many potential applications in superconductors, electrochemical capacitors, nanowires and nanocomposite materials. CNTs consist of graphitic sheets, rolled up into a cylindrical shape [Tasis *et al.*, 2006]. CNTs possess high flexibility, low density, large aspect ratio (>1,000) and thus extremely large surface area [Sears *et al.*, 2010; Spitalsky *et al.*, 2010]. Besides, the remarkable mechanical, thermal and electrical properties of CNTs also make them promising reinforcement materials. The unique mechanical properties arise from the presence of carbon-carbon bond in the graphite layers, even a small amount of CNTs can substantially improve the mechanical strength of polymer nanocomposites [Murali *et al.*, 2010]. CNTs can be synthesized to have diameters of several Å̊s or tens of nms, and their lengths can be up to several mms. Additionally, these tubes can be synthesized as singular tubes (e.g., single walled nanotubes (SWNTs)) or as a series of shells of different diameters spaced around a common axis (e.g., multiwalled nanotubes (MWNTs)), as shown in Fig. 2-4. SWNTs have outer diameters in

the range of 1-3 nm and inner diameters of 0.4-2.4 nm, whereas MWNTs can have outer diameters ranging from ~2 nm (double walled nanotubes) up to ~100 nm with tens of walls [Kim *et al.* 2006; Sanip *et al.*, 2011]. Particularly, the inner core diameter of SWNTs can be as low as 4 Å, which is identified as possible selective nanopores in membrane materials [Qin *et al.*, 2000; Wang *et al.*, 2000]. CNTs are synthesized in a variety of ways, such as arc discharge, high pressure carbon monoxide, and chemical vapor deposition [Sahoo *et al.*, 2010].

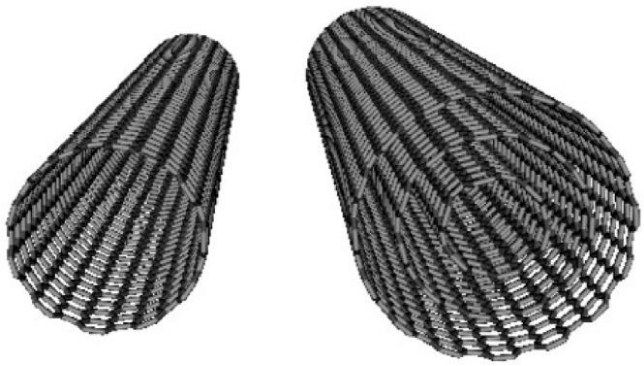

Fig. 2-4 Sketch of the structure of (a) SWNTs and (b) MWNTs [Ismail *et al.*, 2009]

However, due to strong van der Waals attraction among the tubes, CNTs tend to form stabilized bundles, which in turn result in the formation of tight bundles and hollow ropes [Georgakilas *et al.*, 2008]. Furthermore, the relatively smooth CNT surfaces, which lack interfacial bonding, have limited load transferring from the matrix to the CNTs [Abdalla *et al.*, 2007]. The difficulties associated with dispersion of the entangled CNTs during processing and poor interfacial interactions between CNTs and polymer matrix may impose significant limitations to effective use of CNTs. However, several processing methods appear to work, including sonication of nanotubes in the presence of polymers, in situ polymerization of monomers in the presence of CNTs, and chemical modification or functionalization [Lin *et al.*, 2003].

Among the above approaches, chemical functionalization of CNTs is shown to be effective.

By introducing functional groups to the CNTs, it is possible to obtain homogeneous and fine dispersion of CNTs in the polymer matrix which at the same time will activate the CNT surfaces by creating such active functional groups as carboxyl acid or hydroxyl groups [Ismail *et al.*, 2009]. The functionalization of CNTs can be done by either non-covalent or covalent functionalization. Non-covalent functionalization of nanotubes is of particular interest because it does not compromise the physical properties of CNTs, while the solubility and processability may be improved. It mainly involves surfactants, biomacromolecules or "wrapping" with polymers [Sahoo *et al.*, 2010]. The polymer wrapping technique is extensively studied by many researchers. For example, many polymers such as chitosan [Aroon *et al.*, 2010], cyclodextrin [Chen *et al.*, 2001] and glucosamine [Pompeo and Resasco, 2002] have been used as the wrapping agents to functionalize CNTs. On the other hand, covalent functionalization can be accomplished by modification of surface-bound carboxylic acid groups on the nanotubes. Generally, functional groups such as -COOH or -OH can be produced on the CNTs during oxidation by oxygen, air, concentrated sulfuric acid, nitric acid or aqueous hydrogen peroxide [Liu *et al.*, 1998]. The most commonly used modification is surface treatment with strong acids [Choi *et al.*, 2007]. The number of -COOH groups on the surface of CNT depends on the temperature and time of acid treatment [Georgakilas *et al.*, 2002]. The acid modified CNTs have -COOH and -OH groups, which are helpful to disperse in water and various organic solvents. Moreover, the presence of these functional groups may interact with the polymer and eventually affect the mobility and crystallinity of the polymer chains [Ismail *et al.*, 2009].

#### 2.3.3.4 Carbon nanotube based membranes used in gas separation

The increasing interest in using CNTs for membrane applications can be attributed to their unique properties that are favorable to separation: high aspect ratio and surface area, simple

functionalization and dispersion in polymer, enhancement of mechanical strength with a small amount of filler, and also the potentially good control of pore dimension at the nanometer scale [Ismail *et al.*, 2008]. Nanocomposite membranes containing CNTs are believed to combine the advantages of both the polymer and carbon phases.

A theoretical study [Skoulidas *et al.*, 2002] predicts a rapid mass transport in CNTs due to smooth nanotube walls, which may be several orders of magnitude higher than in many other porous fillers, making CNTs an ideal candidate filler material for membranes. The remarkably high transport rate may benefit from the inherent smoothness of CNT walls [Kim *et al.*, 2007a]. CNT-incorporated membranes have been reported to have extraordinarily high transport rate to both gases and liquid water [Hinds *et al.*, 2004; Majumder *et al.*, 2005; Holt *et al.*, 2006], and some efforts have been made to study CNT-incorporated membranes for gas separation.

For instance, Cong *et al.* [2007b] reported that impregnation of brominated poly(2,6-diphenyl-1,4-phenylene oxide) membrane with CNTs had increased $CO_2$ permeability while maintained a similar $CO_2/N_2$ selectivity as compared to the pure polymer membrane. The increased permeability and unchanged selectivity of the membranes with the addition of CNTs can be explained based on the nanogap hypothesis discussed earlier. In addition, MWNTs were shown to be more effective to increase the gas permeability than SWNTs. Kim *et al.* [2006] found that the permeabilities of He, $H_2$ and $CO_2$ increased by adding 2 wt% CNTs in the membrane. However, there was no difference in the gas permeability when the CNT content was increased further to 10 wt% in the polymer matrix. The presence of high diffusivity CNT tunnels within the poly(imide siloxane) matrix can increase the diffusion coefficients of $O_2$, $N_2$ and $CH_4$, leading to an increase in gas permeability.

In general, a higher gas permeability was generally observed in CNTs-polymer

nanocomposite membranes [Choi *et al.*, 2006; Kim *et al.*, 2007b; Weng *et al.*, 2009; Aroon *et al.*, 2010; Murali *et al.*, 2010; Sanip *et al.*, 2011], whereas the selectivity could be reduced or remained the same [Cong *et al.*, 2007b; Ge *et al.*, 2011], or enhanced [Murali *et al.*, 2010; Sanip *et al.*, 2011]. Furthermore, CNTs well aligned in the membrane will lead to a higher gas permeability than the permeability of the membrane with randomly dispersed CNTs [Sharma *et al.*, 2009].

### 2.3.4 Facilitated transport membranes

As mentioned before, by incorporating active carriers into membranes, permeation of certain gases can be enhanced by using facilitated transport membranes. To some extent, this type of membranes is similar to biological cell membranes. The carrier in a facilitated transport membrane interacts or reacts specifically and reversibly with a target permeant to form a permeant-carrier complex, which diffuses to the downstream side of the membrane, where the complex decomposes and releases the permeant and carrier.

There are two major types of facilitated transport membranes based on the mobility of the carriers in membranes. The carrier molecules can be mobile in the membrane (e.g., liquid membranes) where the carriers can diffuse in the membrane, or immobilized in the membrane matrix where the carriers are fixed to certain sites of the matrix. Both types of facilitated transport are discussed below.

#### 2.3.4.1 Liquid membranes

Since diffusivities in liquids are orders of magnitude higher than diffusivities in solids, much higher permeabilities in liquid membranes can be expected than permeabilities of typical solid membranes. Thus, liquid membranes have been studied in past years, but their practical applicability is still limited due to membrane instability.

Generally, liquid membranes are comprised of supports, liquids and carriers. The selection of supports is very important to the separation performance of liquid membranes. Firstly, the support could affect the overall permeability if its porosity is not large enough. In addition, a suitable support should provide a sufficient stability of the liquid membrane. The liquid membranes can be further subdivided into immobilized liquid membranes (ILM) and supported liquid membranes (SLM). A liquid is held inside the pores of a porous support by means of capillary forces in an ILM, where the support has to be wettable by the liquid under such condition. In a SLM, the liquid is located on top of the porous support [Krull *et al.*, 2008].

Because of similar magnitude of gas diffusivities in a liquid, the selectivity of a liquid membrane is based mainly on the sorption selectivity of a gas pair in the liquid. In case the sorption selectivity is very low or lacking, carrier species interacting selectively with a gas species may be employed. The carriers should be soluble in the liquids, and a permeant molecule (e.g., $CO_2$) should be reversibly bound to a carrier and transported across the membrane via facilitated transport mechanism, resulting in an enhanced permeability. Materials with amine functional groups are generally considered as possible carriers in liquid membranes for $CO_2$ permeation. Thus, the amines used for $CO_2$ absorption may be the potential carriers for $CO_2$ separation by facilitated transport based on the fast reaction kinetics of amine and $CO_2$. Monoethanolamine, diethanolamine and ethylenediamine have been utilized as the facilitating carriers for $CO_2$ separation in either SLM or ILM configuration [Teramoto *et al.*, 1996, 1997; Gorji and Kaghazchi, 2008]. Besides, dendrimers containing abundant terminal groups in a highly branched molecular structure are another potential carrier materials for $CO_2$ transport [Inoue, 2000]. Poly(amidoamine) (PAMAM) dendrimers of generation 0 with an ethylenediamine core have a large amount of primary and tertiary amine groups, and they are

shown to be effective carriers for $CO_2$ separation [Kovvali *et al.*, 2000; Kovvali and Sirkar, 2001, Duan *et al.*, 2006; Kouketsu *et al.*, 2007].

The long term stability of a liquid membrane is largely dependent on the volatility of the membrane liquid. Hence, low to non-volatile liquids (e.g., glycerol, ionic liquids, and liquid molten salts) are desired to avoid a breakdown of the membrane function due to evaporation. However, the use of aforementioned liquids is still limited even though they can improve the membrane stability to some extent because the carrier washout under a higher transmembrane pressure cannot be prevented [Krull *et al.*, 2008]. Although the permeability and selectivity of liquid membranes seem to have improved significantly over the past decade, their long-term stability remains a major technical challenge for practical applications.

**2.3.4.2 Fixed-site-carrier membranes**

One way to improve membrane stability is to immobilize the carriers within the membranes. In a fixed-site-carrier membrane, the carriers are covalently bond directly to the polymer backbone. Carrier molecules can only vibrate within some distance near the equilibrium position but cannot move freely. The target permeant reacts at one carrier site and then hops to the next carrier site, moving from upstream to downstream side via the "hopping" mechanism [Cussler *et al.*, 1989]. Obviously, the interaction between permeating species and carriers is depressed in fixed-site-carrier membrane as compared to liquid membranes with mobile carriers. This results in a relatively lower permselectivity in fixed-site-carrier membranes. Nevertheless, from a membrane stability point of view, fixed-site-carrier membranes are preferred.

Currently, the research of fixed-site-carrier membrane for $CO_2$ separation has mainly focused on amine based polymers. Various amine based polymers are used: polyvinylamine with primary amine groups [Kim *et al.*, 2004, 2013; Deng *et al.*, 2009; Deng and Hagg, 2010; Yuan *et*

*al.*, 2011; Qiao *et al.*, 2013], polyallylamine with primary amine groups [Zou and Ho, 2006; Huang *et al.*, 2008; Cai *et al.*, 2008], pentaerythrityl tetraethylenediamine dendrimer with both primary and secondary amine groups [Wang *et al.*, 2007], and poly(N-Vinyl-γ-sodium aminobutyrate) containing secondary amine and carboxylate groups [Zhang *et al.*, 2002a]. Fixed-site-carrier membranes based on these polymers all exhibited excellent separation performance in terms of $CO_2$ permeation rate and selectivity. For example, polyallylamine/poly(vinyl alcohol) blend membranes showed a selectivity for $CO_2$ over $N_2$ and $CO_2$ over $CH_4$ of 80 and 58, respectively [Cai *et al.*, 2008].

In fixed-site-carrier membranes containing sufficient amine groups, $CO_2$ is mediated based on the weak acid-base reaction between $CO_2$ and amine moiety in dry state. While in water-wet membrane, water also plays a role in the $CO_2$ transport because of membrane swelling [Liu *et al.*, 2008]. The reaction of $CO_2$ with primary and secondary amines is usually described by the zwitterion mechanism including the following steps [Little *et al.*, 1992; Zou and Ho, 2006; Yuan *et al.*, 2011]:

$$CO_2 + R_1R_2NH \underset{k_2}{\overset{k_1}{\rightleftharpoons}} R_1R_2\overset{+}{N}H\overset{}{C}OO^- \tag{2-3}$$

$$R_1R_2\overset{+}{N}H\overset{}{C}OO^- + R_1R_2NH \underset{k_4}{\overset{k_3}{\rightleftharpoons}} R_1R_2NCOO^- + R_1R_2NH_2^+ \tag{2-4}$$

$$R_1R_2NH^+COO^- + H_2O \rightleftharpoons R_1R_2NCOO^- + H_3O^+ \tag{2-5}$$

$$R_1R_2NCOO^- + H_2O \rightleftharpoons R_1R_2NH + HCO_3^- \tag{2-6}$$

where $R_1$ and $R_2$ are functional groups or hydrogen. In the first step, $CO_2$ reacts with primary or secondary amines to form zwitterion as an intermediate. The next step is the subsequent removal of the proton from the zwitterions by a base or $H_2O$, forming carbamate ions. The carbamate ion is not stable and reacts with $H_2O$ to form bicarbonate. Hence, the facilitated transport of $CO_2$ is

conveyed in the $CO_2$-amine complex forms in terms of carbamates and bicarbonates. On the other hand, tertiary amines cannot react with $CO_2$ directly. It is suggested that such amines have a base-catalytic effect on the hydration of $CO_2$ [Donaldson and Nguyen, 1980; Vaidya and Kenig, 2007; Yu *et al.*, 2010], represented as follows:

$$R_1R_2R_3N + H_2O + CO_2 \underset{k_2}{\overset{k_1}{\rightleftharpoons}} R_1R_2R_3NH^+ + HCO_3^- \tag{2-7}$$

$CO_2$ reacts with tertiary amines and water to produce bicarbonate within the membrane, diffusing in the form of bicarbonate ions.

As mentioned earlier, owing to the enhanced transport of $CO_2$ bound to the carriers, SLMs or ILMs display both high $CO_2$ permeance and $CO_2$/light gas selectivity. However, the possible instability issue of the membranes caused by the solvent evaporation and carrier washout poses a great challenge if large scale industrial application is considered. In order to overcome this limitation, research efforts were devoted to develop facilitated transport membranes with fixed-site-carriers. By covalently bonding the carriers to the polymer backbone, fixed-site-carrier membranes normally show improved stability than the liquid membranes. In view of the above considerations, facilitated transport membranes containing both mobile and fixed carriers may combine the excellent $CO_2$ permselectivity and good stability since the additional mobile carriers could be well retained in the polymer structure and both the mobile and fixed carriers can be used to facilitate the transport of $CO_2$ molecules. Pioneering work of the novel facilitated transport membranes containing poly(allylamine) or polyethylenimine as the fixed carriers and amino acid salts as mobile carriers designed for $CO_2$/light gas separation have been done recently [Tee *et al.*, 2006; Zou and Ho, 2006; Bai and Ho, 2009].

## 2.4 Pervaporation dehydration membranes

Pervaporation, also considered to be a solution-diffusion-evaporation three-step process, is based on the selective solution and diffusion in the membrane, not the relative volatility of the components in the feed [Feng and Huang, 1997], which makes it an energy efficient separation technology compared to distillation.

Pervaporation membranes should exhibit good sorption characteristics for the preferentially permeating component. In general, polymeric materials are utilized to make pervaporation membranes. Recently, nanocomposite membranes modified by various inorganic nanofillers such as CNTs have also attracted considerable attention. Therefore, these membranes will be discussed in the following.

### 2.4.1 Polymeric membranes

Both rubbery and glassy polymers have been used to form pervaporation membranes. In addition to high permeation flux and high selectivity, which are always required, the membrane needs to be stable in terms of mechanical, chemical and thermal resistance. Among these requirements, the membrane selectivity that forms the basis for separating a mixture should be emphasized. Therefore, there are some criteria for selection of polymer materials in order to develop a successful pervaporation membrane.

#### 2.4.1.1 Selection of membrane materials

The high polarity of water molecules makes hydrophilic membranes more selective to water permeation. In addition, water molecules are usually smaller than organic compounds in aqueous-organic mixtures. Obviously, a hydrophilic membrane favors both the solubility and diffusivity aspects for selective permeation of water. Thus it is necessary to use hydrophilic

polymer membranes for dehydration of organic solvents. Nevertheless, the polymer materials for dehydration membranes should maintain a proper balance of hydrophilicity and hydrophobicity to maintain the membrane stability to prevent excessive swelling or dissolution of the membrane by water.

Rubbery organophilic polymer membranes are favorable to the selective removal of organic compounds from water since the rubbery polymers preferentially absorb and permeate the organic components. For the separation of organic/organic mixtures, it is not yet very clear which kind of membranes are more appropriate, and both hydrophilic and organophilic polymers exhibit some pervaporation selectivities.

Since the dehydration of organic solvents currently represents the main applications of pervaporation, hydrophilic membranes used for this purpose will be reviewed in the following.

#### 2.4.1.2 Hydrophilic polymeric membranes

Hydrophilic polymers have a great affinity to water, which is caused by functional groups in the polymer chains that are able to interact with water molecules via hydrogen bonding or dipole-dipole interaction. Poly(vinyl alcohol) (PVA), poly(acrylic acid) (PAA), chitosan and polyelectrolytes are the most widely used hydrophilic polymers. The hydroxyl groups in PVA can form strong hydrogen bonding, leading to a high selectivity for water permeation in solvent dehydration. However, PVA can be swollen easily in water, and to some extent dissolution can occur at elevated temperatures. Thus, to improve the membrane stability, PVA membranes need to be modified to constrain their swelling in aqueous solutions. In general, crosslinking, blending and incorporating with inorganic fillers are commonly used to reduce membrane swelling [Xiao *et al.*, 2006; Amnuaypanich *et al.*, 2009], though a trade-off relationship between the membrane permeability and selectivity is often observed. PVA membranes are thus often crosslinked

chemically or thermally to improve the mechanical strength and long-term stability. Dialdehydes, such as glutaraldehyde, are commonly used crosslinking agents for PVA to form a crosslinked polyacetal structure in the presence of a strong acid as a catalyst [Ahn *et al.*, 2005]. The commercial pervaporation membrane developed by GFT Co. for solvent dehydration is made from chemically crosslinked PVA [Feng and Huang, 1997].

PAA is another typical polymer suitable for pervaporation dehydration. It has a high charge density and thus a high hydrophilicity. High molecular weight PAA is effective for forming thin films with good mechanical strength. The carboxyl groups on the side chains are readily available for crosslinking if improved resistance of PAA is needed [Zhao and Huang, 1990]. Another way to stabilize the PAA-based membranes is to use certain polycations, instead of alkali metals, to form a stable polyion complex [Karakane *et al.*, 1991]. Karakane *et al.* [1991] fabricated a PAA-based polyion complex membrane with a permeation flux of 1.6 kg/($m^2$.h) and a separation factor of 3,500 for separating a water/ethanol mixture (5/95 wt%) at 60℃.

Chitosan is the *N*-deacetylated product of chitin and the second most abundant natural polymer next to cellulose. The reactive amine groups and the primary and secondary hydroxyl groups are available for chemical modifications. Therefore, chitosan membranes can be easily crosslinked using sulfuric acid and aldehydes to improve the separation performance of the membranes [Sridhar *et al.*, 2001]. Dehydration of ethylene glycol and isopropanol using chitosan membranes has been attempted [Feng and Huang, 1996; Nawawi and Huang, 1997], in order to upgrade ethylene glycol used in aircraft deicing and purification of isopropanol in the electronic manufacturing industry.

### 2.4.2 Nanocomposite membranes

#### 2.4.2.1 Overview of nanocomposite membranes

Similar to the polymer-inorganic nanocomposite membranes used in gas separation, various nanofillers such as $TiO_2$ and $SiO_2$ nanoparticles, zeolites and CNTs are incorporated into polymeric membranes to form nanohybrid pervaporation membranes mainly for solvent dehydration. The polymers commonly used for constructing the nanocomposite membranes include the hydrophilic PVA and chitosan. The basic principles related to nanocomposite membranes and their formations have been introduced previously, and some successful examples of nanocomposite pervaporation membranes will be discussed here.

Amnuaypanich *et al.* [2009] fabricated MMMs from a semi-interpenetrating polymer network of natural rubber and crosslinked PVA incorporated with zeolite 4A. The natural rubber was expected to limit the swelling of the membranes in water, while PVA, on the other hand, was considered to improve the water sorption due to its hydrophilicity. Zeolite 4A with a uniform porous structure could provide an alternative route for the transport of water molecules through the membranes, which helps enhance the water selectivity of the membranes due to molecular sieving effect of the zeolites. Ethanol dehydration was performed, and the results showed that at a low water concentration in the feed, increasing the zeolite loading could improve both the total permeation flux and the separation factor. However, as the feed water concentration increased, although the total permeation flux increased, the separation factor was reduced because the membranes were substantially swollen, causing a loose structure of the surrounding polymer networks.

Liu *et al.* [2005] functionalized silica nanoparticles with sulfonic acid groups on their surfaces, which were then used for crosslinking chitosan in situ to prepare chitosan-silica nanocomposite membranes. Crosslinking of chitosan reduced its degree of swelling in water and alcohol/water mixtures, resulting in an increase in its permselectivity for pervaporation

dehydration of ethanol-water mixtures. However, unlike the normally observed reduction in permeation flux due to chemical crosslinking, the nanocomposite membrane exhibited fairly high permeation rates since the silica particles would provide extra free volumes to the polymer chain, consequently offering spaces for water molecules to permeate through the membranes.

Enhanced permeation flux for dehydration of organic solvents is frequently observed when nanocomposite pervaporation membranes are used [Liu *et al.*, 2005; Huang *et al.*, 2006; Zhang *et al.*, 2007; Amnuaypanich *et al.*, 2009; Dong *et al.*, 2009; Zhao *et al.*, 2009]. The nanofillers in the membranes either serve as "spacers" for polymer chains to provide extra space for water permeation (e.g., silica, $TiO_2$), or promote water transport due to the molecular sieving effect (e.g., zeolite). In addition, some nanocomposite pervaporation membranes also exhibit high selectivities that are important for industrial applications.

#### 2.4.2.2 Carbon nanotube based membranes used in pervaporation

CNT-incorporated membranes are also extensively studied in pervaporation for alcohol dehydration and organic-organic separation [Peng *et al.*, 2007a, 2007b; Choi *et al.*, 2007, 2009; Penkova *et al.*, 2010; Shirazi *et al.*, 2011; Ong *et al.*, 2011; Sieffert and Staudt, 2011].

For instance, PVA membranes loaded with MWNTs were prepared for ethanol dehydration by pervaporation, and it was found that the flux of the membrane was increased with the addition of MWNTs, whereas the separation factor remained unchanged up to 1.0 wt% MWNTs and then began to decrease with a further increase in the amount of MWNTs in the membrane [Choi *et al.*, 2009]. Peng *et al.* [2007a] studied the pervaporation separation of benzene/cyclohexane mixtures using PVA membranes modified with chitosan-wrapped MWNTs, and they observed an increase in both the permeation flux and separation factor. This seems to suggest that incorporating CNTs in the membrane could tune the packing of hydrophilic chains at the interface, thereby increasing

the free volume, and provide internal nanochannels for water permeation through the nanoscale openings of CNTs. Similarly, polyamide membranes filled with 2 wt% CNTs were shown to have both a higher selectivity and permeability than the pure polyamide membrane for pervaporation of methanol/methyl *tert*-butyl ether mixtures [Penkova *et al.*, 2010]. However, it should be pointed out that the nanofillers are the dispersed phase in the membranes, and the enhanced permeation cannot be attributed merely to the fast mass transport in the nanotubes, as the nanofillers will affect the surface and bulk properties of the composite membrane, thereby influencing the solubility and diffusivity of a permeant in the membrane.

## 2.5 Water vapor permeation

In general, the diffusivity of gas and vapor increases with decreasing molecular sizes (i.e., smaller kinetic diameter), whereas their solubility tends to increase with an increase in their condensability (i.e., higher critical temperature). Water molecules with a kinetic diameter of 0.25 nm are smaller than such permanent gases as $CO_2$, $N_2$ and $CH_4$ (with kinetic diameters of 0.33, 0.364 and 0.38 nm [Breck, 1974], respectively). Hence, water has much higher diffusivity than these gases. On the other hand, water is more condensable than $CO_2$, $N_2$ and $CH_4$, as indicated by their critical temperatures of 647, 304, 126 and 190 K [Reid *et al.*, 1987], respectively. Thus, water is likely to have a higher solubility in polymers. Apparently, both the diffusivity selectivity and solubility selectivity favor water permeation over permanent gases. Therefore, polymers are normally much more permeable to water vapor than carbon dioxide, nitrogen and methane. Among the available polymers, hydrophilic rubbery ones display a good combination of high water vapor permeability and high water vapor/permanent gas selectivity [Potreck *et al.*, 2009; Reijerkerk *et al.*, 2011a; Lin *et al.*, 2012]. Rubbery polymers tend to show a higher water vapor

diffusivity due to their flexible polymer chains (compared with glassy ones). On the other hand, hydrophobic polymers normally have a lower solubility selectivity than hydrophilic polymers, and glassy polymers usually have a relatively higher diffusivity selectivity than rubbery polymers due to rigid structure and stronger size-sieving ability of glassy polymers. For example, a water vapor permeance up to 2000 GPU and a $H_2O/CH_4$ selectivity up to 1500 were observed using a Pebax thin film composite membrane for natural gas dehydration [Lin *et al.*, 2012].

Recall the "Robeson upper bound" commonly observed for gas separation using polymer membranes, that is, a high permeability is accompanied with a low selectivity. However, this relationship does not hold for the permeation of water vapor in gas dehydration using polymer membranes [Metz *et al.*, 2005b]. Conversely, most of the highly selective polymers also possess a very high permeability. Besides, for different polymers, the water vapor permeability and water vapor/gas selectivity can vary by 5 and 7 orders of magnitude, respectively [Metz *et al.*, 2005b].

Due to hydrogen bonding and other polar interactions with the polymer, water molecules may interact with polymer to cause plasticization in the membrane; or interact with other water molecules to form water clusters, especially for polymers that are hydrophobic or weakly hydrophilic [Huang *et al.*, 2003]. Clustering of water molecules will result in an increase in the permeant size. The water clusters formed in the polymer are less mobile, and they will significantly obstruct the transport of other gas molecules along the diffusion pathway. Besides, the water clusters are more effective to swell the membrane than the unassociated water molecules, thereby enhancing plasticization effects [Chen *et al.*, 2011]. At low vapor activities, water molecules are inclined to interact with polymer more favorably and strongly than with themselves. In this case, water behaves like a common plasticizing agent. As the vapor activity increases, more and more water molecules will be absorbed in the membrane, leading to a higher

tendency to form water clusters [Modesti *et al.*, 2004].

Concentration polarization occurs when there is a concentration gradient formed at the surface of the membrane, which usually exists in membrane separation processes dealing with liquids such as pervaporation, ultrafiltration and reverse osmosis. However, in gas separation, the effects of concentration polarization are normally negligible because of the small stage cut used in the lab scale test, where only a very small portion of the feed components permeating through the membrane will not result in significant change in feed gas composition on the surface of the membrane. Nevertheless, in case of water vapor permeation for gas drying, the concentration polarization effects may need to be taken into account because the high transport rate of water vapor through the membrane compared to the slower diffusion in boundary layers could induce concentration polarization at both the feed and permeate side of the membrane [Metz *et al.*, 2005b; Chen *et al.*, 2011].

The permselectivity for water vapor through many hydrophilic polymeric membranes has been reported. Landro *et al.* [1991] reported a high $H_2O/CH_4$ selectivity of $10^3$~$10^4$ through amorphous polyurethane membranes. Huang *et al.* [2003] studied water vapor separation from 1-propanol and acetic acid using polyimide dense membranes. Du *et al.* [2010a] investigated the water vapor transport through poly(*N,N*-dimethylaminoethyl methacrylate) composite membrane for natural gas dehydration and found that the water vapor permeance increased almost exponentially with an increase in water vapor concentration in the feed. Reijerkerk *et al.* [2011a] developed a highly hydrophilic, poly(ethylene oxide) based block copolymer membrane for simultaneous removal of water vapor and carbon dioxide from flue gas and achieved a very high water vapor permeability.

# Chapter 3

## PVAm/PVA blend membranes and nanocomposites incorporated with carbon nanotubes for $CO_2$ separation

---

### 3.1 Introduction

$CO_2$ capture and separation from a variety of emission sources is essential from an environmental perspective. One strategy for $CO_2$ emission control is post-combustion capture. In this case, $CO_2$ is separated from flue gas after combustion of fossil fuels [Brunetti *et al.*, 2010]. Among the current viable separation technologies for $CO_2$ capture, membrane-based gas separation is promising from energy and environmental points of view, and it is gaining growing interest for greenhouse gas emission control in recent years.

As mentioned previously, introducing amino groups to the polymer chains is expected to facilitate $CO_2$ transport by taking advantage of the selective weak acid-base interactions between the amino groups and $CO_2$ molecules. Therefore, in this chapter, PVAm/PVA blend membranes were prepared and studied for $CO_2$ separation. The effects of feed pressure, temperature, membrane composition and heat-treatment of the membrane on the separation performance were studied. Furthermore, considering the unique properties of carbon nanotubes (CNTs), a novel nanocomposite membrane was developed by uniformly dispersing CNTs into PVAm/PVA blend polymer matrix using solution blending method. The effects of CNT loadings on the membrane

permselectivity were investigated, and the membranes were characterized to understand the function of CNTs in the nanocomposite membranes. Asymmetric PVAm-PVA/CNT membranes formed on a microporous support were then developed to improve the gas permeance of the membranes.

## 3.2 Experimental

### 3.2.1 Materials

Polyvinylamine (PVAm) (Lupamin 9095, $M_w = 340{,}000$) was supplied from BASF and poly(vinyl alcohol) (PVA) (99% hydrolyzed, $M_w = 133{,}000$) was obtained from Polysciences Inc.. Both polymers were used as received without further purification. Multi-walled carbon nanotubes (MWNTs) (purity$>$95%) were supplied by Shenzhen Nanotech Ltd., China. The average sizes of MWNTs were about 20-40 nm in diameter and 1-2 $\mu m$ long. Nitric and sulfuric acids were purchased from Fisher Scientific. Polysulfone (PSf) microfiltration membrane with a nominal pore size of 0.2 $\mu m$, provided by Pall Corporation, was used as a substrate in preparing asymmetric membranes. The PSf membrane was thoroughly rinsed with dilute NaOH solution and then with water to clean the membrane surface before use. All gases used, nitrogen ($N_2$), oxygen ($O_2$), methane ($CH_4$), helium (He), hydrogen ($H_2$), and carbon dioxide ($CO_2$), were provided by Praxair Canada Inc..

### 3.2.2 Membrane preparation

*Purification of MWNTs*

To disperse the MWNTs in various solvents and polymer matrix, the MWNTs were treated with concentrated nitric acid (70 wt%) and sulfuric acid (98 wt%) mixed at a ratio of 1:3 v/v.

One g of the pristine MWNTs was added to 200 mL of the acid mixture in a round-bottom flask, and the mixture was sonicated for 0.5 h and subsequently refluxed at 90℃ for 2 h. After cooling, the mixture was washed with deionized water to remove the acids until the liquid became neutral. After filtration with a membrane filter (nominal pore size 0.2 $\mu m$) under vacuum, the filtrate (i.e., wet MWNT powder) was dried in a vacuum oven at 80℃.

*Preparation of PVAm/PVA blend membranes*

PVAm/PVA blend membranes were prepared on a Teflon plate. The polymer solution of PVAm/PVA blend was prepared by adding an aqueous solution of PVA to an aqueous solution of PVAm at same concentrations (8 wt%). The aqueous solution of PVA was obtained by dissolving PVA powder in water at 90℃ for 3 h. The aqueous solution of PVAm was obtained by mixing PVAm with water at room temperature for 3 h. The final composition of the blend solution was determined by adjusting the weight ratio of the two solutions. After stirring overnight, the polymer blend solution was cast onto a Teflon plate to form a film of the polymer solution of desired thickness. After casting, the membrane was dried in an oven at 55℃ overnight. Some of the membranes were also heat-treated at 120℃ in a convection oven in order to evaluate whether heat-treatment will influence the membrane performance. The thickness of the dry membranes was about 20-35 $\mu m$.

*Preparation of PVAm-PVA/CNT nanocomposite membranes*

PVAm-PVA/CNT nanocomposite membranes were prepared by casting a blend of PVAm/PVA solution containing a pre-determined amount of MWNTs (0.5-3 wt%). Firstly, a polymer solution of PVAm-PVA blend was prepared by adding an aqueous solution of PVA to an aqueous solution of PVAm at same concentrations, followed by vigorous stirring for more than 6 h. A 3 wt% MWNT in water suspension was prepared by dispersing the acid-treated

MWNTs in deionized water, and the solution was sonicated for 1 h using an ultrasonic cleaner to facilitate the dispersion. The MWNTs suspension was then added dropwise to the PVAm-PVA blend solution under vigorous stirring to form a uniform suspension, which was then used for membrane fabrication. After stirring overnight, the solutions were further sonicated for 1 h to homogenize and then kept at room temperature for at least 24 h to remove air bubbles. To prepare the membrane casting solutions containing different amounts of MWNTs, the mass ratio of PVAm to PVA was maintained at 60/40, whereas the mass ratio of MWNT to polymer (i.e., PVAm plus PVA) was varied: 0.5/99.5, 1.0/99.0, 1.5/98.5, 2.0/98.0, 2.5/97.5, and 3.0/97.0. PVAm-PVA/CNT dense membranes were formed by casting the solution onto a Teflon plate, followed by drying at 55℃ for more than 12 h. The membrane thickness was determined to be about 20-30 $\mu m$.

*Preparation of PVAm-PVA/CNT asymmetric membranes*

PVAm-PVA/CNT asymmetric membranes were prepared by the solution coating technique. A PVAm-PVA/CNT blend solution was placed into a wide-mouth glass bottle, and the PSf substrate was placed inside the bottle cap. They were then carefully assembled to form a pressure tight seal. The bottle assembly was placed vertically upside-down for 0.5 h to ensure a sufficient contact between the PSf substrate and the blend solution. Then it was placed upright in an oven at 55℃ for 1 h. The above steps were repeated for multiple coatings. Eventually, the membranes were dried at 55℃ overnight, resulting in an asymmetric membrane comprising of a thin dense layer of PVAm-PVA/CNT and a microporous PSf substrate.

For all the PVAm-PVA/MWNT blends, the mass ratio of PVAm to PVA was kept at 60/40, the mass ratio of MWNTs to polymer was maintained at 0.5/99.5, and the polymer concentration in the blend was varied, as shown in Table 3-1. Five different polymer concentrations, which are

denoted as Con A, B, C, D and E, respectively, in decreasing order, were used in membrane coating. A high concentration (e.g., A and B) was used to coat the first layer. Then lower concentrations (e.g., C, D and E) were used to coat the subsequent layers. PVAm-PVA/CNT asymmetric membranes with different combinations of five concentrations were then fabricated.

Table 3-1 Polymer concentration in PVAm-PVA/MWNT blend solutions

| Abbreviation | PVAm-PVA polymer concentration (wt%) | PVAm concentration (wt%) | PVA concentration (wt%) | Mass ratio of MWNTs to polymer |
|---|---|---|---|---|
| Con A | 8.70 | 5.22 | 3.48 | 0.5/99.5 |
| Con B | 6.53 | 3.92 | 2.61 | 0.5/99.5 |
| Con C | 4.65 | 2.83 | 1.89 | 0.5/99.5 |
| Con D | 3.25 | 1.95 | 1.30 | 0.5/99.5 |
| Con E | 2.30 | 1.38 | 0.92 | 0.5/99.5 |

### 3.2.3 Membrane characterization

The Fourier transform infrared (FTIR) spectra of the CNTs before and after acid treatment, and the PVAm-PVA/CNT nanocomposite dense membranes with different CNT contents were determined between 4000 and 400 $cm^{-1}$ using a Bio-Rad FTS 300 FTIR spectrometer. Each spectrum was collected by cumulating 16 scans at a resolution of 2 wavenumbers.

The Raman spectra of the CNTs before and after acid treatment and the PVAm-PVA/CNT nanocomposite dense membranes with different CNT contents were recorded using Bruker SENTERRA Raman microscope ($\lambda = 785\ \mathrm{nm}, 10\mathrm{mW}$) at room temperature.

A Bruker D8 Focus X-ray diffractometer (XRD) was used to study the solid-state morphology of the PVAm-PVA/CNT nanocomposite dense membranes. X-rays of 1.5406 Å wavelength were generated by a CuK-$\alpha$ source, and the XRD patterns were recorded at a diffraction angle ($2\theta$) of from 5° to 60° to examine the crystal structure.

### 3.2.4 Gas permeation measurements

The schematic diagram of the experimental setup for gas permeation through the membrane is shown in Fig. 3-1. The apparatus consisted of a circular stainless steel membrane cell with an effective permeation area of 22.9 $cm^2$. The membrane was hydrated in water first. After the membrane surface was blotted dry, the membrane was then quickly mounted into the permeation cell. A pure gas (e.g., $CO_2$, $N_2$, $CH_4$, $H_2$, $O_2$ and He) was fed through a humidifier, and the gas saturated with water vapor was admitted to the permeation cell. The feed gas pressure was varied in the range of 0.15-0.6 MPa, while the permeate was maintained at atmospheric pressure. A thermostatted water bath was used to control the temperature, and the test temperature was 25℃ unless specified otherwise. The permeation rate was measured by a bubble flow meter, and the permeance ($J$) of the gas through the membrane was calculated by:

$$J = \frac{V}{At\Delta p}\frac{273.15}{T_0}\frac{p_0}{76} \tag{3-1}$$

where $J$ is the membrane permeance $[cm^3(STP)/(cm^2 \cdot s \cdot cmHg)]$, $V$ is the volume ($cm^3$) of the permeate collected at ambient conditions (temperature $T_0$ ($K$), pressure $p_0$ ($cmHg$)) over a period of time $t$ ($s$), $A$ the effective area of the membrane ($cm^2$), $\Delta p$ the transmembrane pressure difference ($cmHg$). Permeance is customarily expressed in the unit of $GPU$, and $1\ GPU = 10^{-6}\ cm^3(STP)/(cm^2 \cdot s \cdot cmHg)$. The membrane permeability ($P$) is equal to permeance multiplied by the effective thickness of the membrane:

$$P = J \times l \tag{3-2}$$

where $P$ is the membrane permeability $[cm^3(STP) \cdot cm/(cm^2 \cdot s \cdot cmHg)]$ and $l$ is the effective membrane thickness ($cm$). The membrane permeability is customarily expressed in the unit of $Barrer$, and $1\ Barrer = 10^{-10}\ cm^3(STP) \cdot cm/(cm^2 \cdot s \cdot cmHg)$. The thickness of the membrane was measured at 10 different locations (2 in the center and 2 in each quadrant) using a

Mitutoyo micrometer and the average value was used.

The membrane selectivity for permeation of a pair of gases was characterized by the ideal separation factor ($\alpha_{i/j}$), which is defined as the permeability ratio or permeance ratio:

$$\alpha_{i/j} = \frac{J_i}{J_j} = \frac{P_i}{P_j} \tag{3-3}$$

where subscripts $i$ and $j$ represent the more permeable and less permeable gases, respectively.

To evaluate the experimental error, replicates on permeance measurements were examined. The experimental error was shown to be less than 2% for a given membrane sample. Membrane samples from the same batch of membrane fabricated showed a relative difference of within 5% in permeance, which can be considered to represent the experimental error in the permeance measurements. The batch to batch variation in the permeance of the membranes was within 5-8%, indicating a good reproducibility of the membranes fabricated.

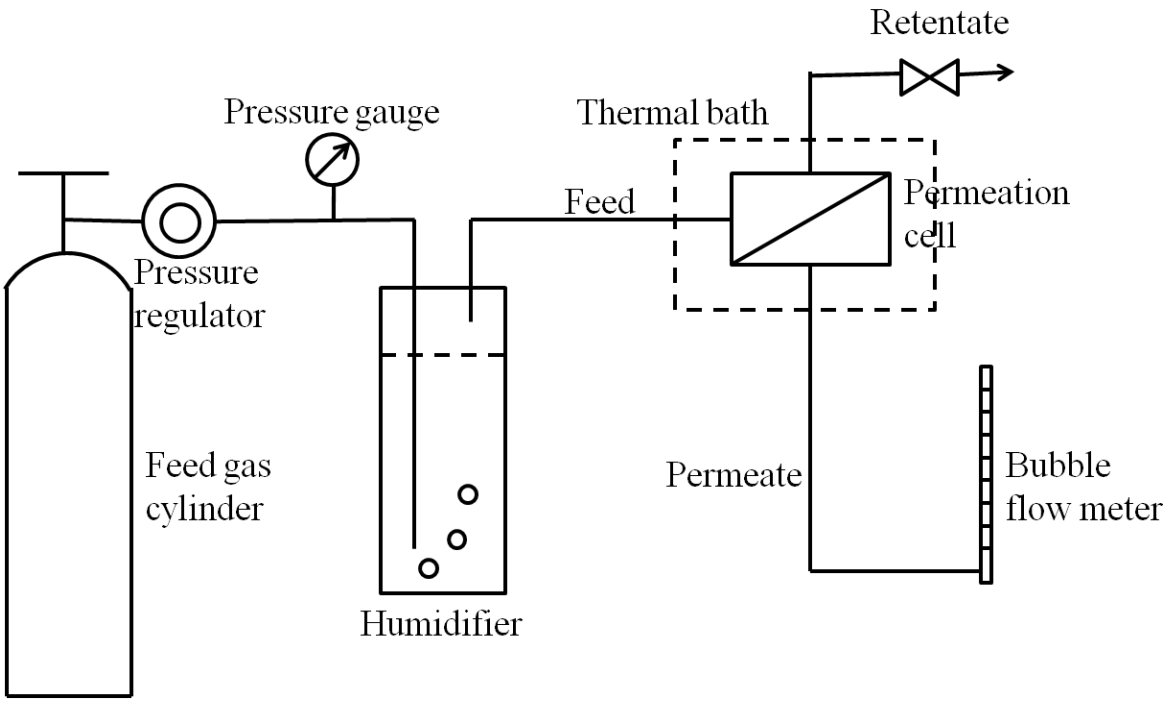


Fig. 3-1 Schematic diagram of gas permeation experiment

## 3.3 Results and discussion

### 3.3.1 Performance of PVAm/PVA blend membranes

Because of the low viscosity of PVAm, pure PVAm membranes were difficult to fabricate from solution casting. Thus, as mentioned before, it was proposed to blend PVAm with a more mechanically robust polymer like PVA. In the PVAm and PVA blend, the PVA ($M_w = 133{,}000$) was believed to be entangled with the PVAm ($M_w = 340{,}000$) chains, as illustrated in Fig. 3-2. The interaction between amino groups in PVAm and hydroxyl groups in PVA via hydrogen bonding is responsible for the entangled network structure. The interaction will help improve the membrane stability since both PVAm and PVA are highly hydrophilic. Because of the relative high crystallinity of PVAm derived from its highly linear, structured polymer chains, the polymer blending may also improve the membrane permselectivity.

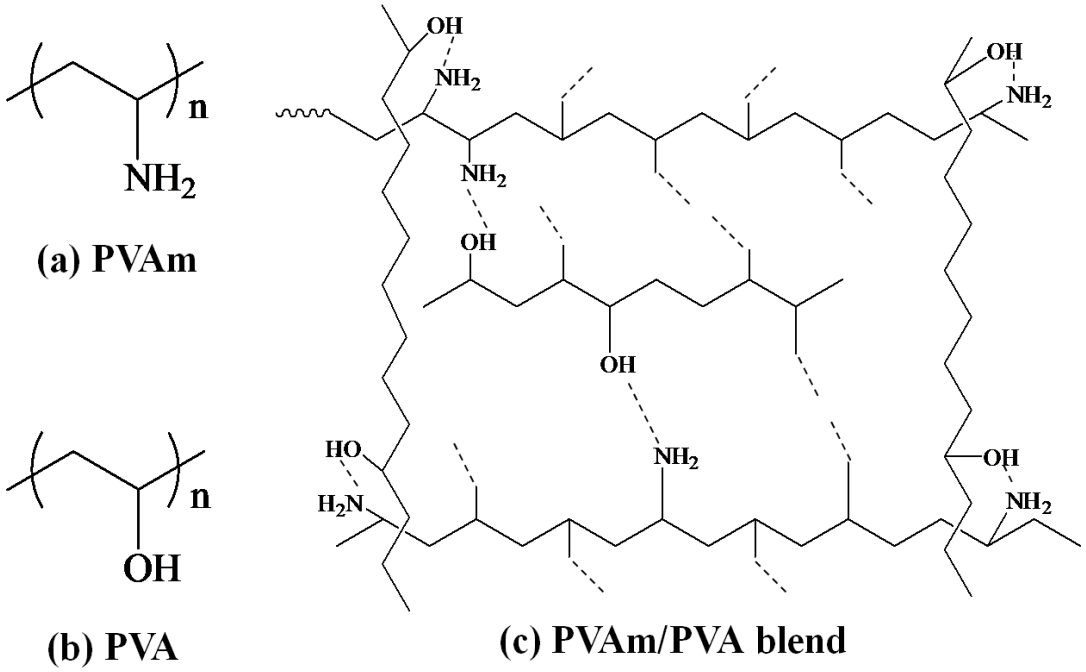


Fig. 3-2 Schematic diagram of PVAm/PVA blend polymer framework

In the following, the effects of gas pressure, operating temperature, the composition of the

polymer blend and heat-treatment of membranes on the separation performance of the PVAm/PVA blend membranes were investigated.

*Effect of pressure*

Pure gas permeation tests were conducted with $CO_2$, $N_2$, $CH_4$, $H_2$, $O_2$ and He at different pressures. Fig. 3-3 shows the gas permselectivity through the PVAm/PVA blend membranes. It's clear that the membranes show an obviously higher permeability of $CO_2$ than other gases tested here. The permeability of different gases through the membrane follows the order of $N_2 < CH_4 < He \approx O_2 < H_2 < CO_2$. The PVAm/PVA blend membrane exhibited the best selectivity for the gas pair $CO_2/N_2$, which is of interest to $CO_2$ capture from flue gas.

According to the solution-diffusion mechanism, the permeability through the membrane is given by the product of solubility and diffusivity of the penentrant in the membrane. Penetrant size and shape mainly affects its diffusivity. The smaller the penetrant is, the faster it will diffuse through the membrane. As shown in Table 3-2, the kinetic diameter of $CO_2$ is smaller than $O_2$, $N_2$ and $CH_4$, but larger than the diameters of He and $H_2$. Clearly, the high $CO_2$ permeability should be attributed to the solubility aspect. The solubility primarily depends on the penetrant condensability as well as the penetrant-membrane interactions. The critical temperature of the penetrants can reflect their condensabilities. $CO_2$ is more condensable than any other gas tested ($CO_2$ has the highest critical temperature, as shown in Table 3-2), which results in a high solubility of $CO_2$ in membrane matrix. Moreover, the solubility of $CO_2$ in the membrane can be further enhanced due to the weak acid-base interactions between $CO_2$ molecules and the amine moieties in PVAm. Thus it's obvious that the solubility aspect favors $CO_2$ permeation.

Fig. 3-3 also shows the ideal selectivities of $CO_2/N_2$, $CO_2/CH_4$, and $CO_2/H_2$, which are of industrial interests for flue gas separation, natural gas sweetening and hydrogen recovery,

respectively. Specifically, for the $CO_2/N_2$ gas pair, $CO_2$ is more condensable than $N_2$ and interacts with the membrane matrix favorably, therefore, $S_{CO2}/S_{N2} > 1$. On the other hand, $CO_2$ is smaller than $N_2$, so $D_{CO2}/D_{N2} > 1$. This explains the high $CO_2/N_2$ selectivity because of the favorable solubility selectivity and diffusivity selectivity. The high $CO_2/N_2$ permselectivity in the membrane suggests that the PVAm/PVA blend membrane can be used to separate $CO_2$ from flue gas.

Table 3-2 Properties of several gases

| Molecule | $k(\times 10^{10}$ m)[a] | $\sigma(\times 10^{10}$ m)[b] | $T_c$(°C)[c] |
|---|---|---|---|
| He | 2.6 | 2.551 | -277.0 |
| $H_2$ | 2.89 | 2.827 | -240.0 |
| $CO_2$ | 3.3 | 3.941 | 31.0 |
| $O_2$ | 3.46 | 3.467 | -118.6 |
| $N_2$ | 3.64 | 3.798 | -147.0 |
| $CH_4$ | 3.8 | 3.758 | -82.8 |

[a]: Kinetic diameter calculated from the minimum equilibrium cross-sectional diameter [Makino *et al.*, 1983];

[b]: Lennard-Jones collision diameter [Hines and Maddox, 1985];

[c]: Critical temperature [Knudsen, 1952].

Furthermore, the gas permeabilities in the membranes are independent of the pressure, except for $CO_2$ whose permeability increases as the transmembrane pressure increases when the feed gas pressure is relatively low. However, the $CO_2$ permeability levels off with a further increase in the transmembrane pressure when the $CO_2$ feed pressure is high enough. The different trends in $CO_2$ and other gas permeabilities with respect to pressure observed here could be attributed to the following: The amino groups present in the PVAm/PVA blend membrane can act as carriers for facilitated transport of $CO_2$. Increasing $CO_2$ pressure will enhance the rate of reaction between $CO_2$ and the carriers, which leads to an increase in the $CO_2$ permeability. However, when the carriers are saturated, the permeability will level off. On the other hand, $N_2$ does not have any reactions with the carriers and $N_2$ permeation follows the solution-diffusion

mechanism. Therefore, the $N_2$ permeability is independent of the transmembrane pressure.

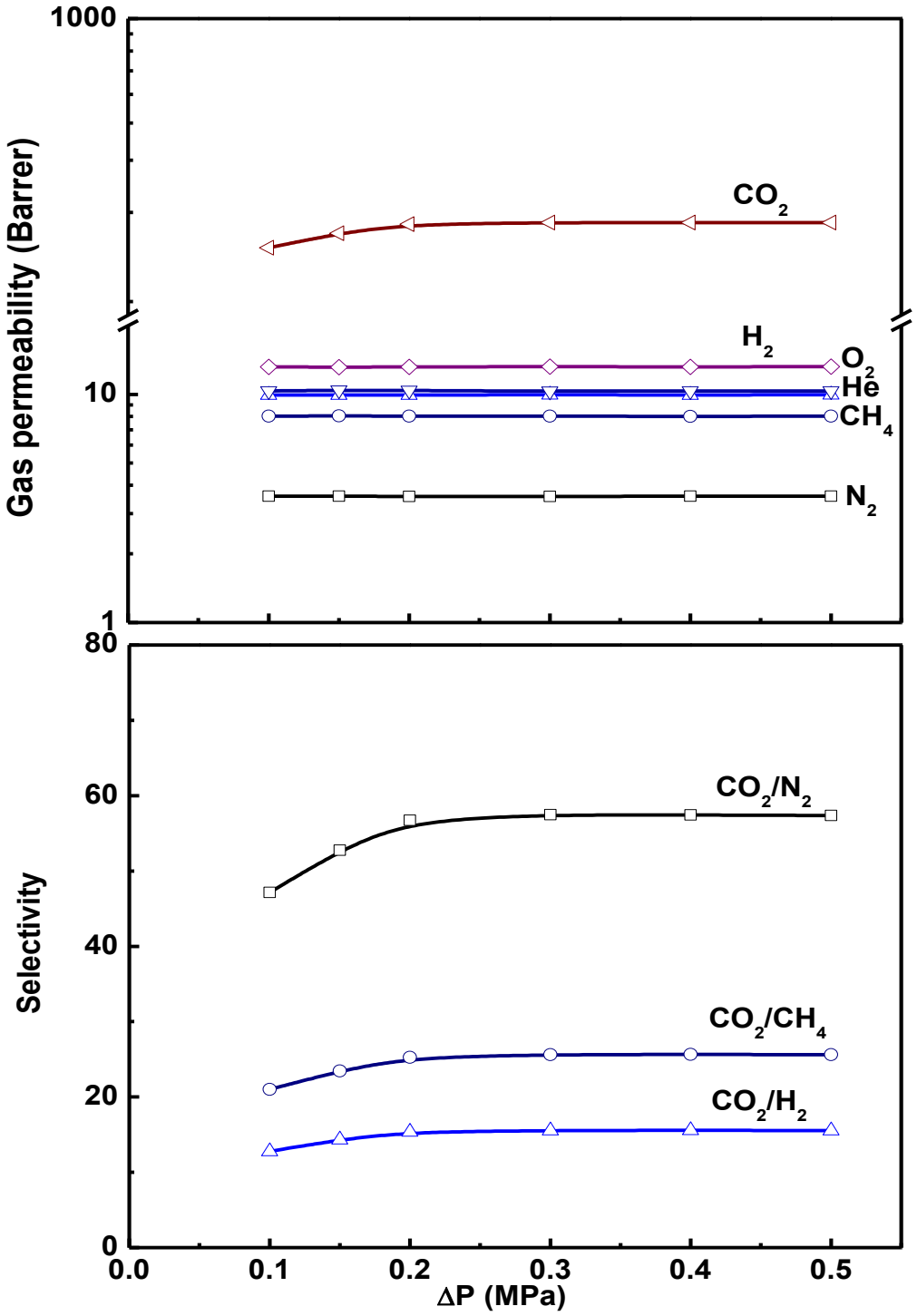


Fig. 3-3 Pressure dependence of permeability and selectivity of various gases through the PVAm/PVA blend membrane. PVAm/PVA blend ratio: 60/40 w/w.

*Effect of operating temperature*

The effects of operating temperature on the permselectivity of the PVAm/PVA blend membranes were examined. The permeability measurements were carried out in a range of 25-80℃ at a transmembrane pressure difference of 0.3 MPa. Since $CO_2$ separation from flue gas is a subject of main interest, we will only focus on $CO_2$ and $N_2$ in the following discussion. Fig. 3-4 shows that the permeabilities of both $CO_2$ and $N_2$ increase with an increase in temperature, and the temperature dependence of the permeability appears to follow an Arrhenius type of relation. However, $N_2$ permeability is affected by temperature more significantly than $CO_2$ permeability, resulting in a significant reduction in $CO_2/N_2$ selectivity when temperature increases.

In general, an increase in temperature will lead to an increase in the diffusivity and a decrease in the solubility. Thus the overall change in the permeability reflects the joint effects of enhanced diffusivity and reduced solubility. The gas diffusivity is generally a stronger function of temperature than solubility [Ghosal and Freeman, 1994], and thus a higher gas permeability is observed at higher temperatures. Moreover, compared to $N_2$, $CO_2$ is more condensable and its temperature-effect of dissolution is expected to be more significant. The increased segmental motion in the polymer chains derived from an increase in temperature will also decrease the ability of the membrane to discriminate based on penetrant size, thus leading to a reduction in diffusivity selectivity and eventually the overall permeation selectivity. Therefore, an increase in temperature will tend to elevate $N_2$ permeability more significantly than $CO_2$.

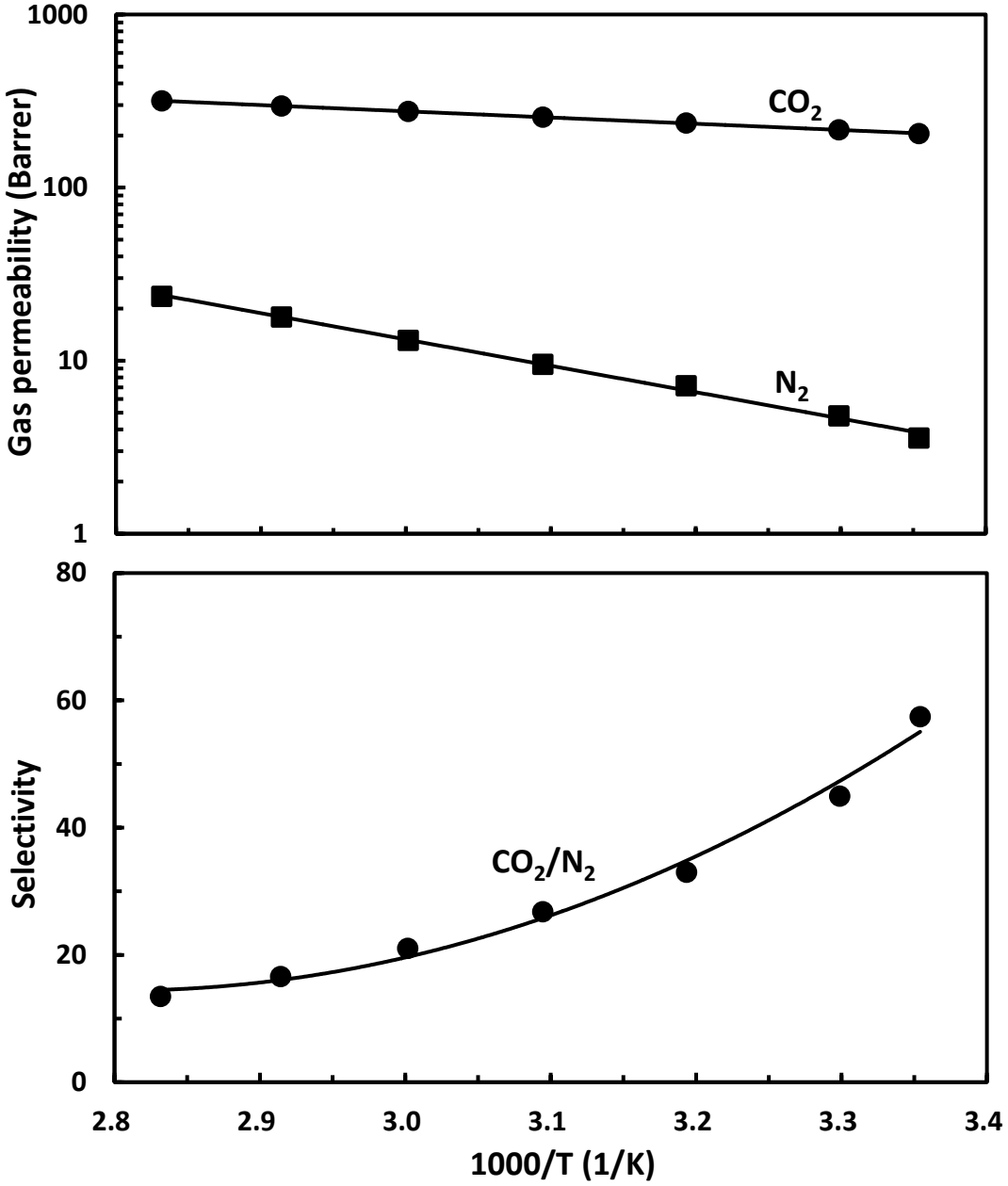


Fig. 3-4 Temperature dependence of permeability and selectivity of $CO_2$ and $N_2$ through the PVAm/PVA blend membrane at 0.3 MPa. PVAm/PVA blend ratio: 60/40 w/w.

The calculated activation energy of permeation is illustrated in Fig. 3-5. In membrane applications, it is a measure of the energy needed for pores to open and penetrants to diffuse through the membrane matrix. It appears that $CO_2$ tends to have a lower activation energy of permeation than $N_2$, which is in accordance with the trend observed in other studies [Du *et al.*, 2006]. A low activation energy indicates that $CO_2$ can permeate through the membrane more

easily.

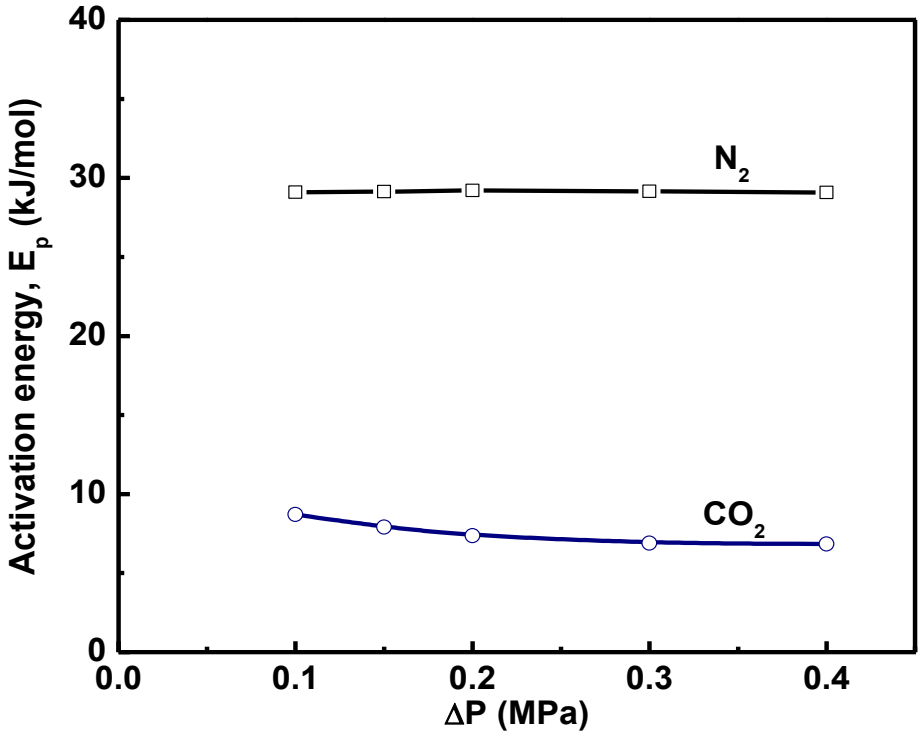


Fig. 3-5 Activation energies of $CO_2$ and $N_2$ in PVAm/PVA blend membrane

*Effect of blend ratio*

As stated previously, the interactions between PVAm and PVA may have important impacts on the separation performance of the PVAm/PVA blend membranes. Thus, three different PVAm to PVA blend ratios were considered: 50/50, 60/40 and 80/20 w/w. Besides, pure PVA membrane was also included for purpose of comparison.

Fig. 3-6 and 3-7 show the permeabilities of $CO_2$ and $N_2$ and their selectivity for different PVAm/PVA blend ratios in the membrane, respectively. Compared to a plain PVA membrane, the PVAm/PVA blend membranes tend to have a significantly higher $CO_2$ permeability. For example, the $CO_2$ permeability of the membrane with a PVAm/PVA blend ratio of 80/20 is more than 3 times that of pure PVA membrane at 0.5 MPa. Since $N_2$ permeability is almost a constant, the PVAm/PVA blend membranes also exhibit a higher $CO_2/N_2$ selectivity than plain PVA

membrane. On the other hand, when the content of PVAm in the membrane increases, $CO_2$ permeability and $CO_2/N_2$ selectivity of the PVAm/PVA blend membranes tend to increase. However, the permselectivity does not change monotonically with the blend ratio. Membranes with PVAm/PVA blend ratios of 60/40 and 80/20 do not have considerable difference in the separation performance.

PVAm possesses the amino carriers that can specifically interact with $CO_2$ to facilitate $CO_2$ transport through the membranes. Hence, it's obvious that PVAm/PVA blend membranes outperform pure PVA membrane for $CO_2/N_2$ separation. In the meantime, the trend of $CO_2$ permeability with respect to pressure observed here is typical of facilitated transport. An increase in the number of free carriers resulting from a higher PVAm content will enhance $CO_2$ permeability. However, when the membrane contains sufficient carriers readily available for facilitated transport of $CO_2$, a further increase in the number of the carriers will not result in a significant increase in $CO_2$ permeability. The membrane with a PVAm/PVA blend ratio of 80/20 has only a slightly higher $CO_2$ permselectivity than the membrane with a PVAm/PVA blend ratio of 60/40. In addition, the polymer solution with a PVAm/PVA blend ratio of 80/20 is much less viscous than a polymer solution with a blend ratio of 60/40. From a membrane formation point of view, a blend ratio of 60/40 is more appropriate to produce defect-free membranes.

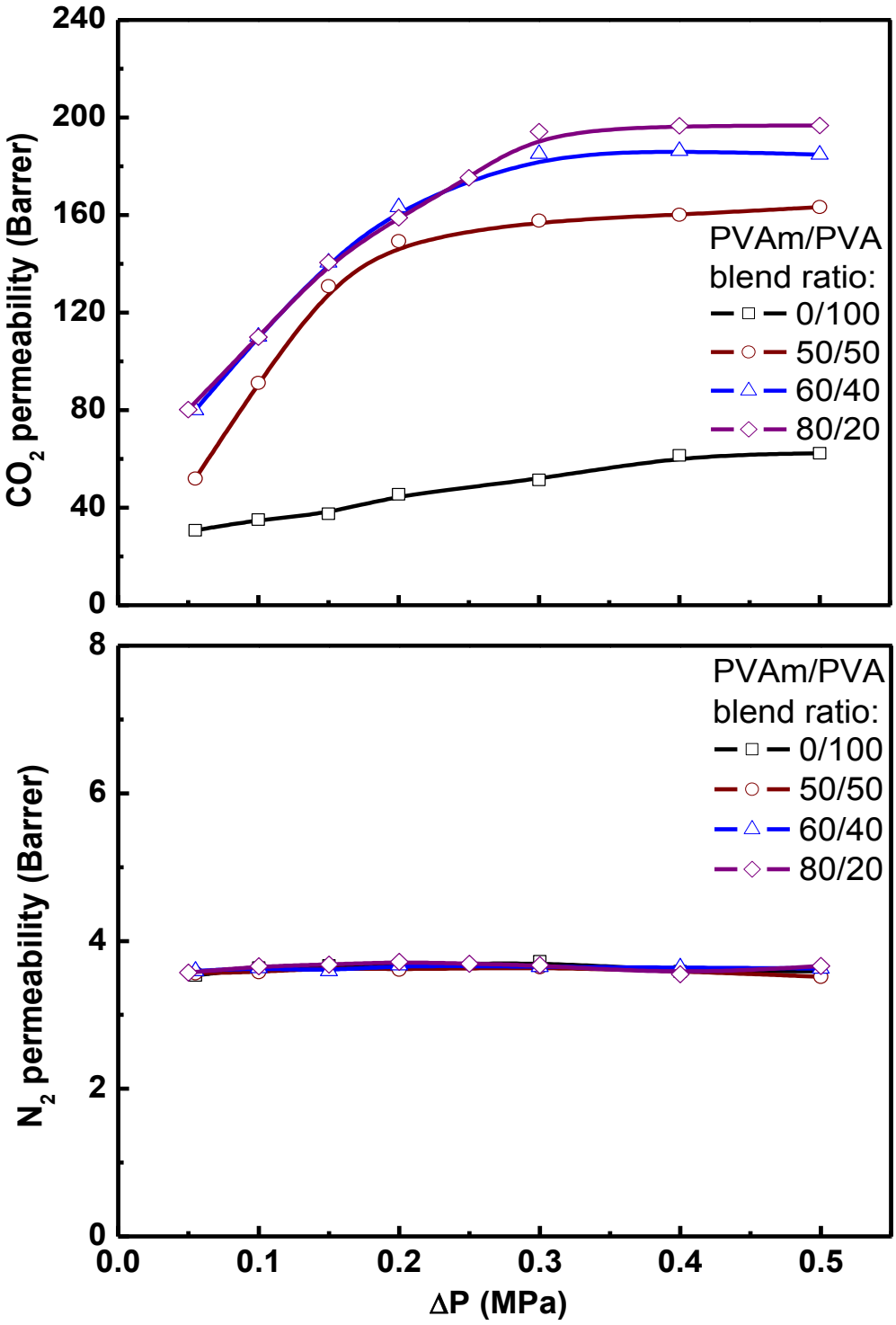


Fig. 3-6 Effect of PVAm/PVA blend ratio (w/w) on $CO_2$ and $N_2$ permeability of the membrane

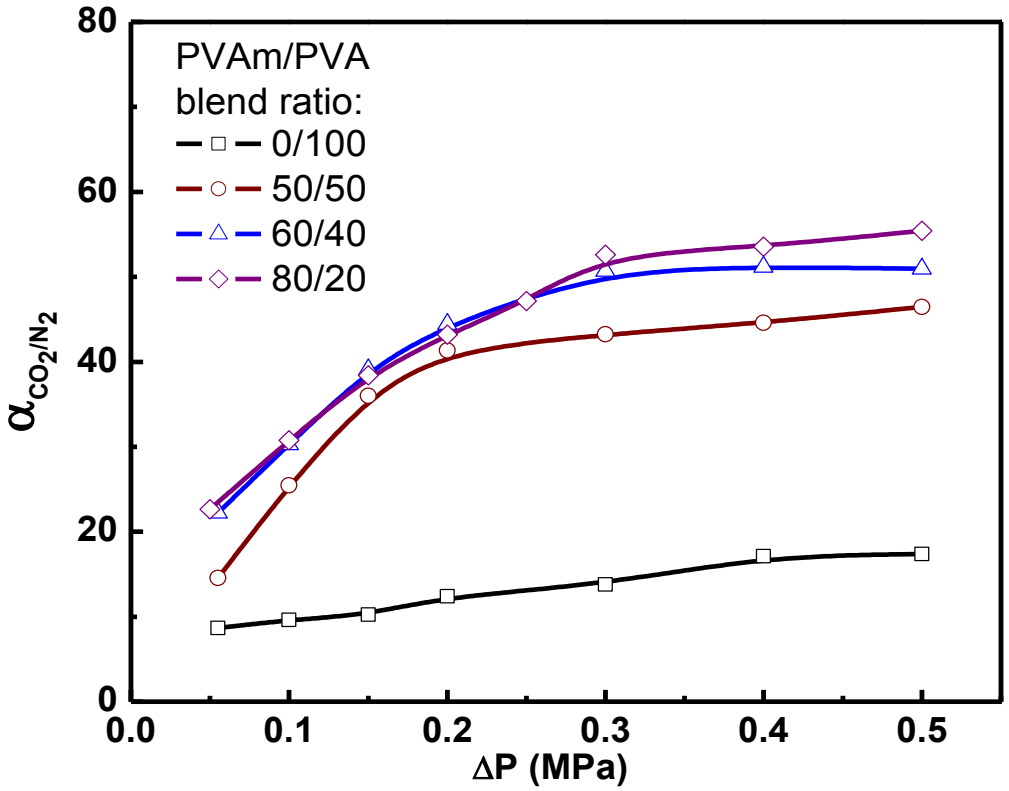


Fig. 3-7 Effect of PVAm/PVA blend ratio (w/w) on $CO_2/N_2$ selectivity of the membrane

*Effect of heat-treatment*

Heat-treatment has been shown to stabilize membranes and improve the membrane selectivity noticeably [Zhao *et al.*, 2006]. To study the effect of heat-treatment time on the separation performance of the PVAm/PVA blend membranes for $CO_2$ separation, the membrane samples were heat-treated at 120℃ for different periods of time (15 to 60 min). Fig. 3-8 and 3-9 show the permeability and selectivity of the membranes at a transmembrane pressure difference of 0.1, 0.2, 0.3 and 0.4 MPa, respectively.

As anticipated, the heat-treated membranes permeate both $CO_2$ and $N_2$ more slowly than the membrane without heat-treatment. The heat-treatment allows the polymer chains to pack more closely, and thus reduces free volume of the polymer (e.g., densifies the membrane) [Zhao *et al.*, 2006]. The membrane densification leads to the reduction of gas permeability and stabilization of membrane structure. In addition, it is shown that the prolonged heat-treatment does not have a

significant influence on the gas permeability, which may be attributed to the fact that the membrane will not be densified infinitely when the heat-treatment time is extended.

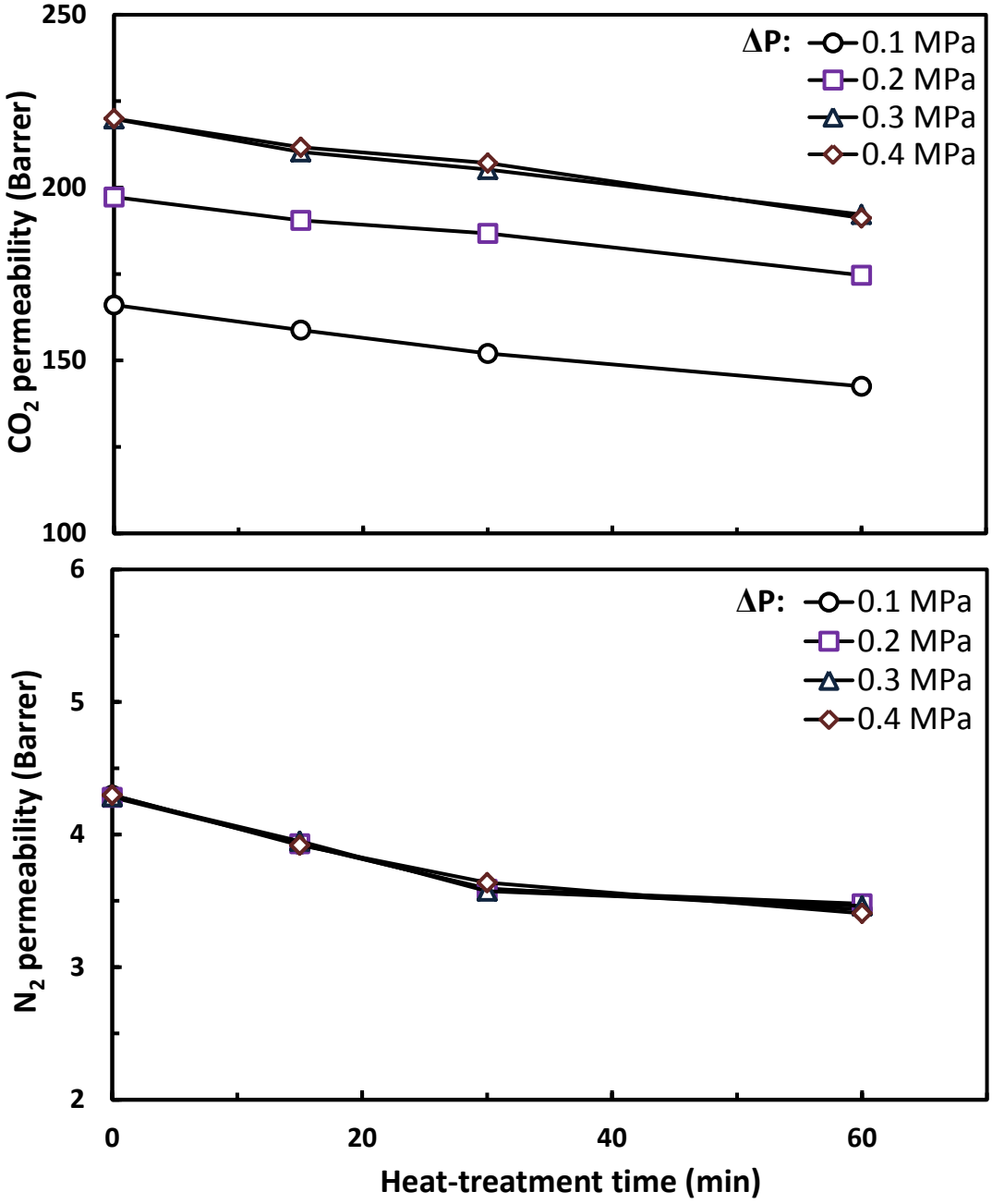


Fig. 3-8 Effect of heat-treatment on $CO_2$ and $N_2$ permeability in PVAm/PVA blend membrane. PVAm/PVA blend ratio: 60/40 w/w.

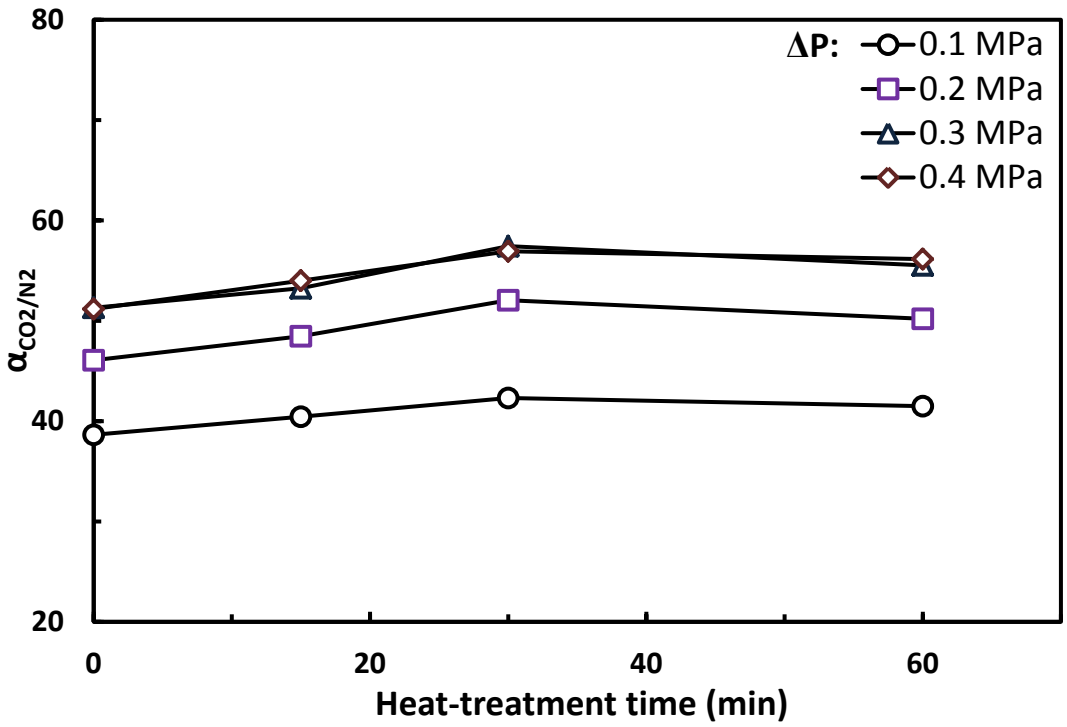


Fig. 3-9 Effect of heat-treatment on $CO_2/N_2$ selectivity in PVAm/PVA blend membrane. PVAm/PVA blend ratio: 60/40 w/w.

Fig. 3-9 depicts the effect of heat-treatment time on $CO_2/N_2$ selectivity of the PVAm/PVA blend membrane. Unlike the generally observed significant increase in the selectivity [Zhao *et al.*, 2006], only a slight variation in the selectivity was observed with extended heat-treatment time. In order to have a good understanding about this, let us look at the PVAm and PVA again. As shown in Fig. 3-2, the formation of the PVAm/PVA network structure is essentially a physical crosslinking process. Moreover, heat-treatment may also cause some physical crosslinking via rearrangement of crystallites in the polymer matrix [Deng *et al.*, 2009]. In other words, the PVAm/PVA blend membrane is physically crosslinked to a certain extent before heat-treatment. Hence, additional physical crosslinking due to heat-treatment will not be significant enough to further affect the membrane selectivity. However, a moderate heat-treatment of the membrane is still desired to ensure the long term membrane stability, and a heat-treatment time of 15-30 min may be suitable.

### 3.3.2 Membrane characterization

Pristine MWNTs were first acid-treated and then incorporated into the PVAm/PVA blend polymer matrix to prepare PVAm-PVA/CNT nanocomposite dense membranes. The chemical structures of MWNTs before and after acid treatment and the structures of the nanocomposite membranes with different CNT contents were studied by FTIR.

Fig. 3-10 shows the FTIR spectra of the pristine and acid-treated MWNTs, the PVAm/PVA blend membrane, and the PVAm-PVA/CNT nanocomposite membranes containing 1 and 3 wt% CNTs. It is clear that, like graphite, the FTIR spectrum of pristine MWNTs has no characteristic absorption peak (Fig. 3-10(a)). For acid-treated MWNTs, the peak at 1730 $cm^{-1}$ can be attributed to C=O stretching vibration of the carboxylic groups [Cong *et al.*, 2007b; Weng *et al.*, 2009; Wu *et al.*, 2010]. The FTIR spectra of PVAm/PVA blend membranes (Fig. 3-10(b)) show the characteristic bands at 1090 $cm^{-1}$ (-C-O stretching), 1140 $cm^{-1}$ (crystallization-sensitive band of PVA) and 1585 $cm^{-1}$ (-$NH_2$ bending) [Smitha *et al.*, 2005; Deng *et al.*, 2009]. However, the peak observed at 1730 $cm^{-1}$ (corresponding to the CNTs) does not appear to have a significant increase with an increase in the CNT content. This may be attributed to the fact that only a small amount of CNTs was loaded in the membrane and a small change in the CNT loading is not sufficient to cause a big change in the peak intensity.

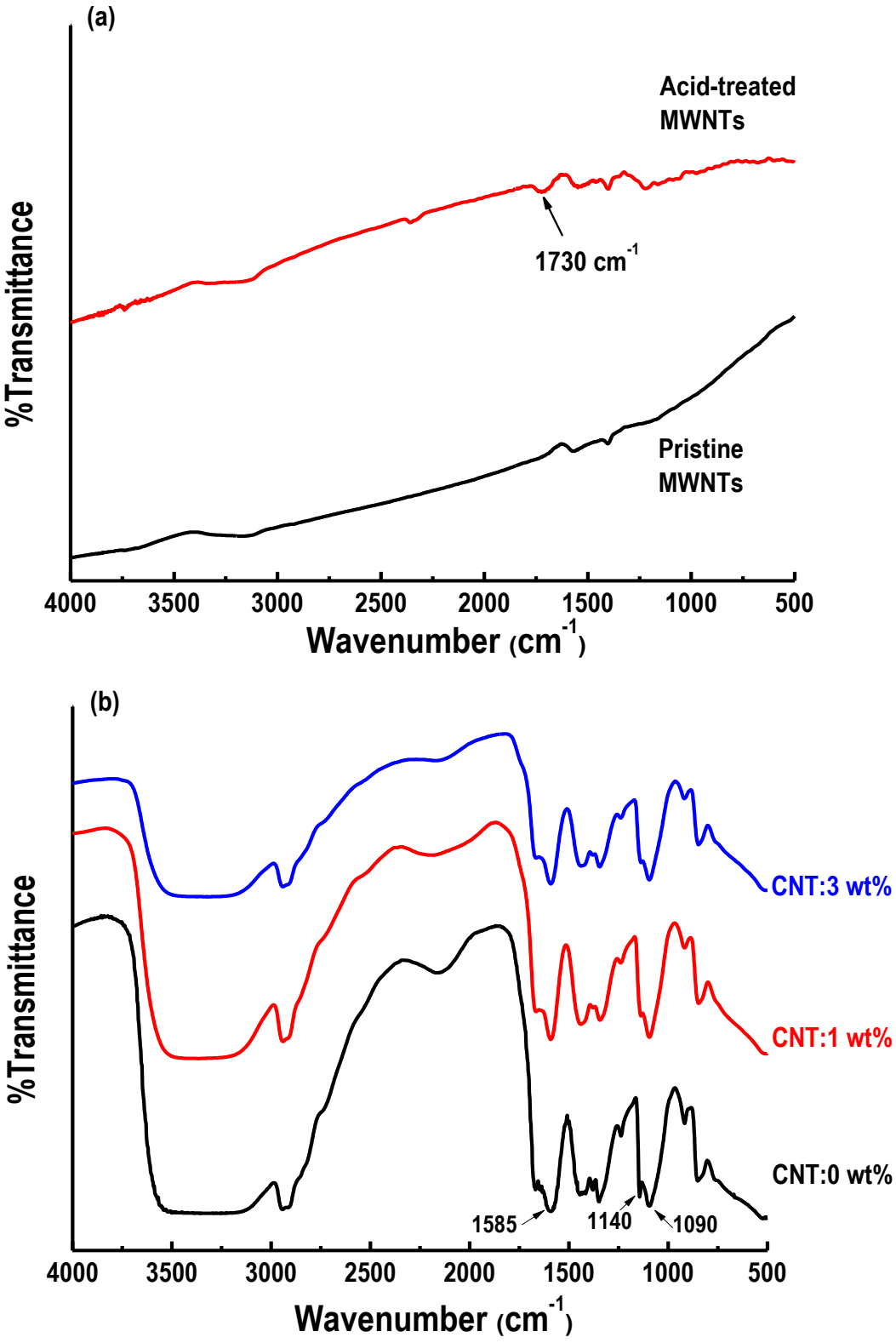


Fig. 3-10 FTIR spectra of (a) pristine MWNTs and acid-treated MWNTs, and (b) PVAm-PVA/CNT nanocomposite membranes with different contents of CNTs.

The FTIR spectra presented above for the composite membranes with and without MWNTs are similar, and there is no clear indication of the presence of acid-treated MWNTs in the nanocomposite membranes or possible interactions between MWNTs and the polymer matrix. Similar cases can be found for other CNT-polymer composite membranes using FTIR spectroscopy [Sharma *et al.*, 2010; Majeed *et al.*, 2012]. On the other hand, the Raman spectroscopy is considered to be a useful tool to study carbonaceous materials. Several publications demonstrate that Raman spectroscopy is more effective in analyzing CNT-polymer composite membranes [Penkova *et al.*, 2010; Kumar *et al.*, 2010; Akieh *et al.*, 2011; Majeed *et al.*, 2012]. Therefore, to further confirm the effectiveness of acid-treatment of MWNTs and the incorporation of acid-treated MWNTs into the PVAm/PVA polymer matrix, the Raman spectra of MWNTs before and after acid-treatment as well as the Raman spectra of the nanocomposite membranes with different MWNT contents were obtained.

In Fig. 3-11(a), two characteristic peaks appear in the spectra for both MWNT samples before and after acid-treatment: One is at 1325 $cm^{-1}$ as D-band (which corresponds to disordered graphite, amorphous carbon or defective structures on the side-walls of MWNTs), and the other is at 1566 $cm^{-1}$ as G-band (which is derived from $sp^2$-bond crystalline carbon and is an indication of ordered carbon nanotube structure). The D/G intensity ratio is often considered to be an indicator of the quality of a carbon nanotube sample. It is calculated that the D/G ratio was increased from 1.80 to 2.25 after the acid treatment, which can be attributed to the increased degree of disorder due to the presence of carboxylate groups from acid treatment [Akieh *et al.*, 2011; Surapathi *et al.*, 2011]. In Fig. 3-11(b), comparing to the spectrum of PVAm/PVA membranes without MWNTs, the characteristic D- and G-bands assigned to MWNTs are apparent in the spectra of MWNT-incorporated membranes. Hence, the Raman spectra confirm

the presence of acid-treated MWNTs in the PVAm-PVA/CNT nanocomposite membrane, which is not quite visible in the FTIR spectra.

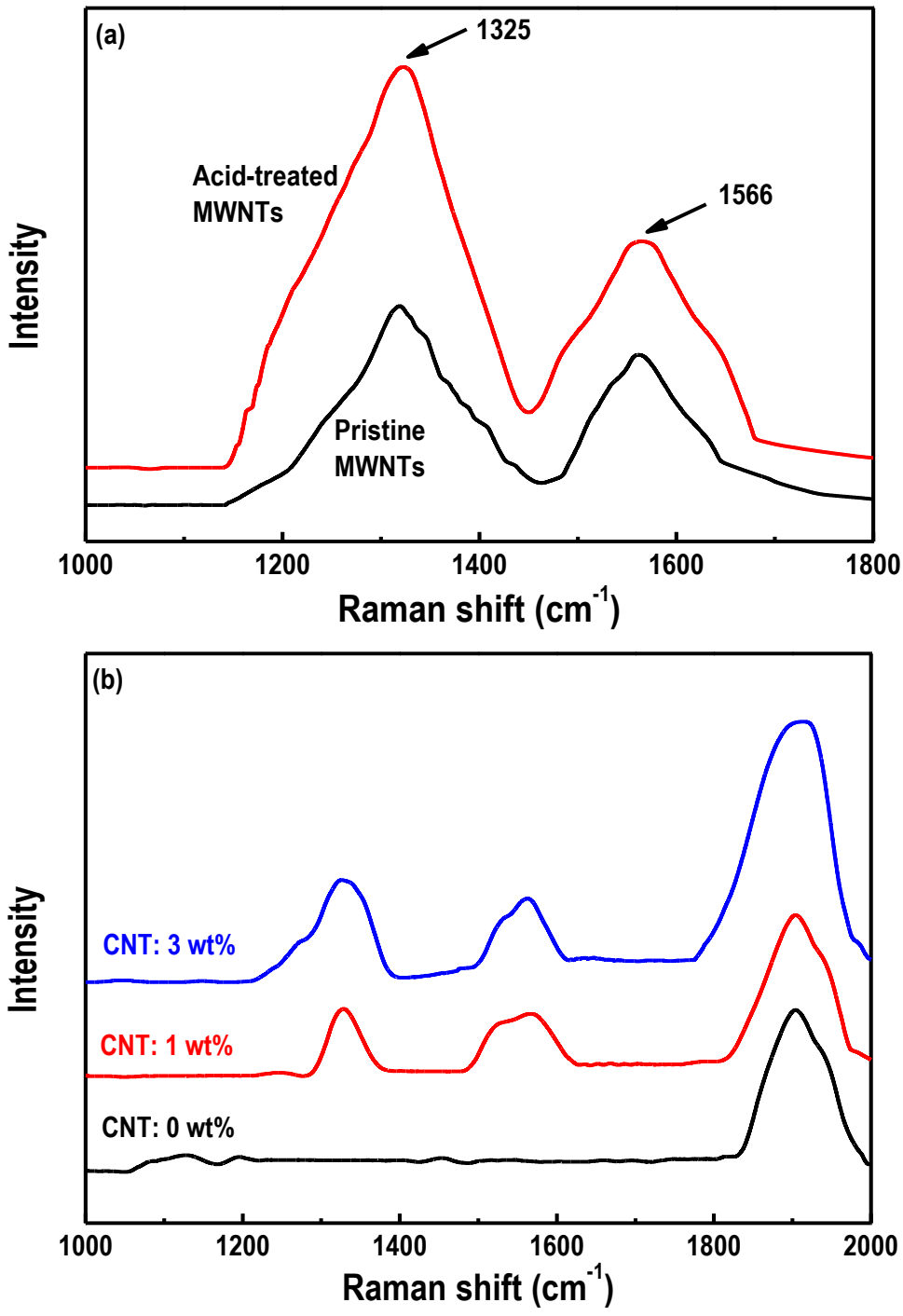


Fig. 3-11 Raman spectra of (a) pristine MWNTs and acid-treated MWNTs, and (b) PVAm-PVA/CNT nanocomposite membranes with different contents of CNTs.

The crystallinity of polymers is one of the important factors that affect the mass transport properties. It has been observed that the crystalline phase of a polymer is quite impermeable and the permeability in a semi-crystalline polymer membrane is substantially lower than in an amorphous membrane because of both the reduced spaces available for diffusion and the tortuous paths around the crystallites [Khulbe *et al.*, 2000]. Since PVAm has a high crystallinity due to the long, linear polymer chains and highly ordered structure, incorporating MWNTs into PVAm/ PVA polymer matrix is expected to lower the crystallinity of the polymer.

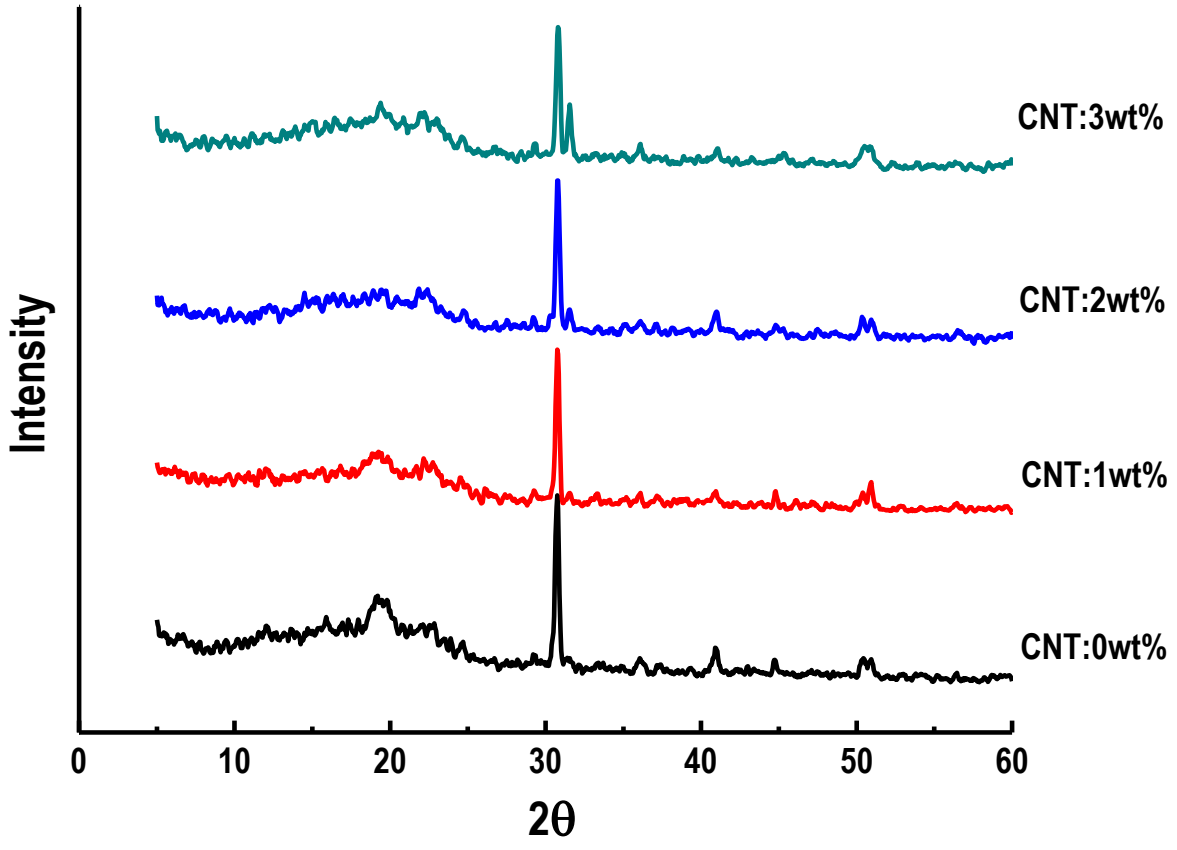


Fig. 3-12 XRD patterns of PVAm-PVA/CNT nanocomposite membranes with different contents of CNTs

Fig. 3-12 shows the XRD patterns of the PVAm-PVA/CNT nanocomposite membranes with different MWNT contents, and all these membranes displayed a semi-crystalline structure. A sharp diffraction peak was observed with the PVAm/PVA blend. Furthermore, the lowered peak intensities at $2\theta$ of 19 and 30.5 due to addition of MWNTs indicate a decrease in the relative

crystallinity of the nanocomposite material. As the content of MWNTs increased to 2 and 3 wt%, a peak at $2\theta$ of 31.5 was observed. Generally, introducing nanofillers into a polymer matrix produces more free volumes. However, when the MWNT loadings is sufficiently high (≥2 wt%), agglomeration of the MWNTs tends to occur. In addition, because of the interactions between MWNTs and the polymer matrix, the crystallinity of the membrane may decrease when the content of MWNTs increases. On the other hand, the presence of crystalline MWNTs will also contribute to the increase in the crystallinity. These two opposing effects determine whether the membrane crystallinity increases or decreases as the MWNT content increases.

### 3.3.3 Performance of PVAm-PVA/CNT nanocomposite membranes

Based on prior work regarding effective use of CNTs in gas separation reviewed in Chapter 2, the introduction of CNTs into a polymer matrix is expected to further improve the separation performance of PVAm/PVA blend membrane. Therefore, the PVAm-PVA/CNT nanocomposite membranes were developed and tested. As expected, the content of CNTs in the membrane is important to the membrane performance. Hence, the effects of CNT loadings in the membrane were investigated.

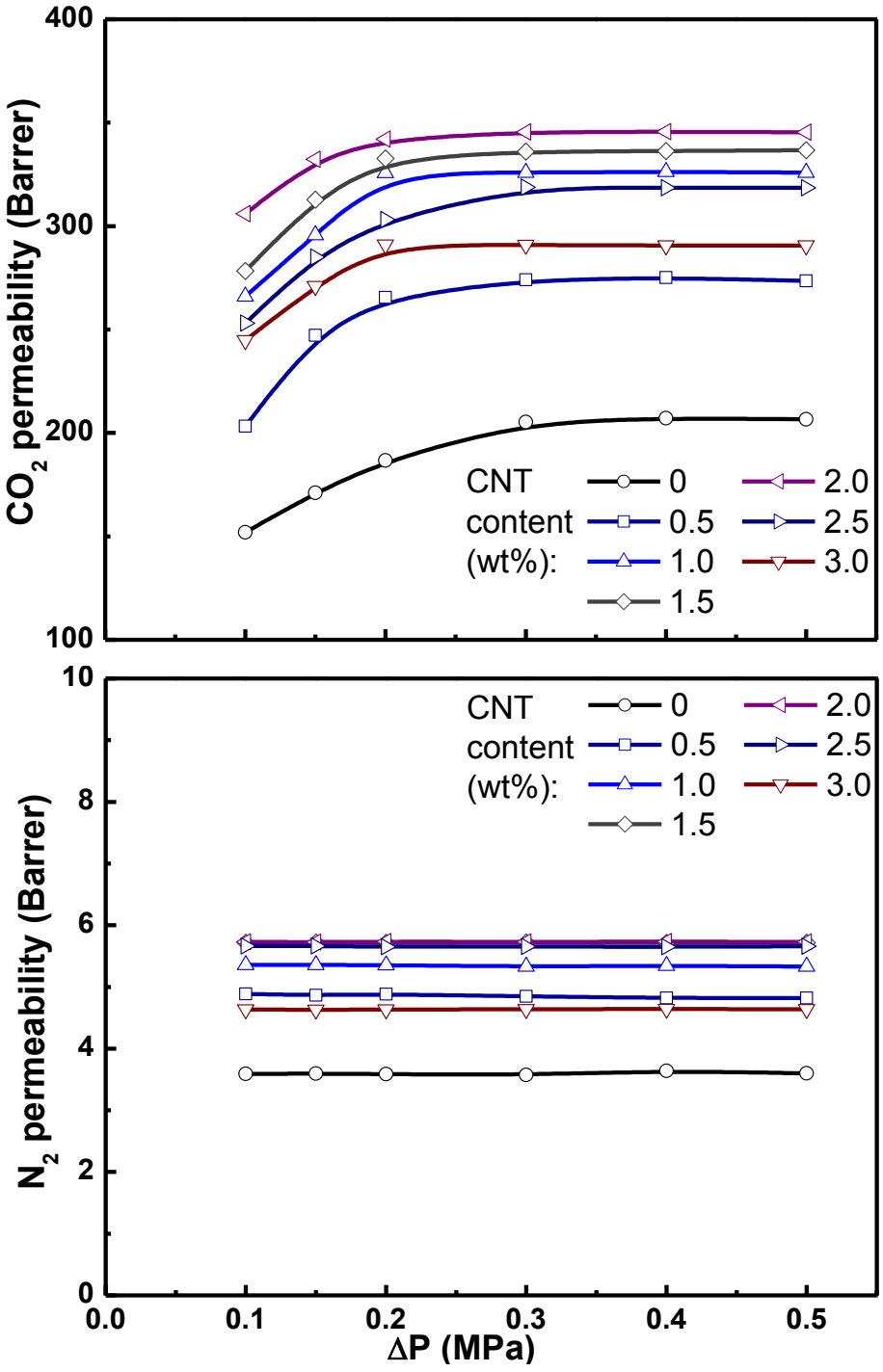


Fig. 3-13 Effect of CNT content (wt%) on $CO_2$ and $N_2$ permeability of PVAm-PVA/CNT nanocomposite membranes

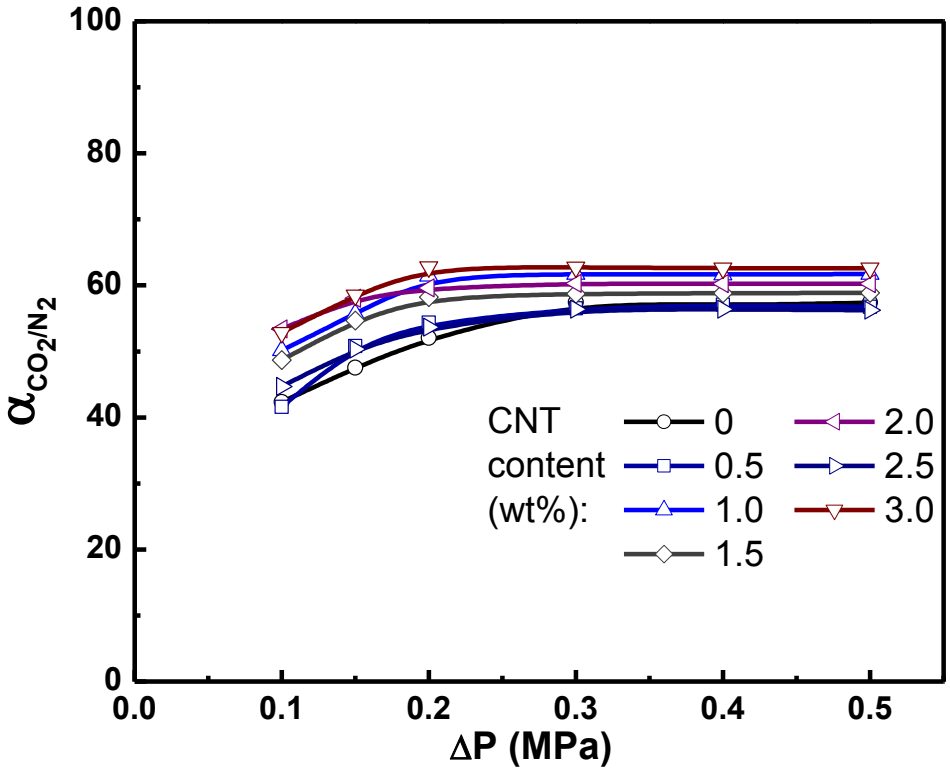


Fig. 3-14 Effect of CNT content (wt%) on $CO_2/N_2$ selectivity of PVAm-PVA/CNT nanocomposite membranes

Fig. 3-13 and 3-14 show the effects of CNT content in the membrane on the permeability and selectivity of the membranes for $CO_2/N_2$ separation, respectively. Compared to the PVAm/PVA blend membrane without CNT fillers, the PVAm-PVA/CNT nanocomposite membranes with the same PVAm/PVA blend ratio of 60/40 (w/w) exhibit an enhanced $CO_2$ permeability and, to a lesser extent, an enhanced $CO_2/N_2$ selectivity. The $CO_2$ permeability of nanocomposite membranes initially increases with an increase in CNT content from 0.5 to 2 wt%, and then begins to decrease if the CNT content is further increased, whereas the addition of CNTs does not change the membrane selectivity significantly. This is more clearly shown in Fig. 3-15. For example, at a transmembrane pressure of 0.3 MPa, the PVAm/PVA blend membrane has a $P_{CO_2}$ of 205 Barrer and $\alpha_{CO_2/N_2}$ of 57. When the membrane is filled with 2 wt% CNTs, the $P_{CO_2}$ of the membrane reaches 345 Barrer, which is 1.5 times that of the PVAm/PVA blend membrane, while the selectivity remains almost the same ($\alpha_{CO_2/N_2} = 60$).

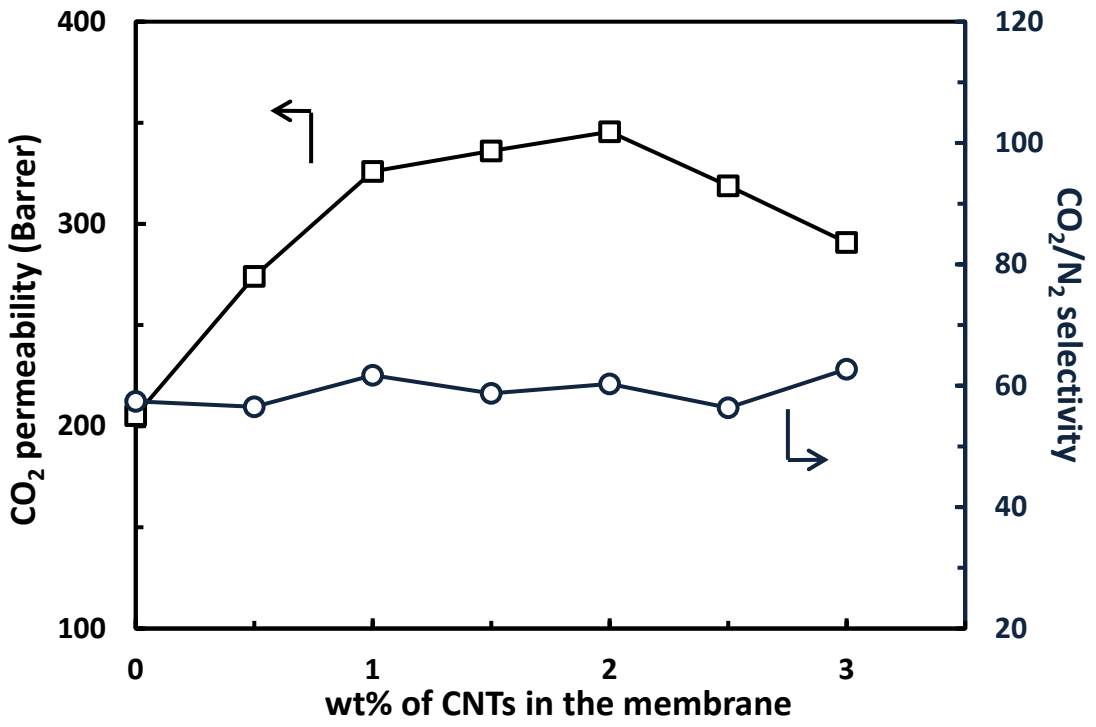


Fig. 3-15 The $CO_2$ permeability and $CO_2/N_2$ selectivity of PVAm-PVA/CNT nanocomposite membranes as a function of the CNT content in the membranes at a transmembrane pressure of 0.3 MPa

Because of CNTs in the membrane, there're three possible routes for gas molecules to permeate through the PVAm-PVA/CNT nanocomposite membrane, as illustrated in Fig. 3-16:

(1) The gas molecules permeate through the polymeric phase in the membrane. The contribution of this part of mass transport to the overall permeability and selectivity is similar to PVAm/PVA blend membranes without CNT fillers.

(2) When orientated vertically with respect to the membrane surface, MWNTs can act as channels that allow $CO_2$ and $N_2$ molecules to pass through easily. It should be pointed out that the inner diameters of MWNTs (20-40 nm) are far larger than the kinetic diameters of $CO_2$ (0.33 nm) and $N_2$ (0.364 nm). As a result, compared to PVAm/PVA polymeric membranes, a higher gas permeability may be achieved in PVAm-PVA/CNT nanocomposite membranes while the overall selectivity may be lower depending on how much gas will flow through the nanotubes.

(3) MWNTs are likely distributed randomly in the polymer matrix, and the gas molecules

have to experience a more tortuous path due to the presence of nanofillers with impermeable walls. Therefore, a decrease in permeability is expected. Nevertheless, the randomly distributed MWNTs may interact with the polymer chains via its functional groups and disrupt the polymer chain packing, which will help increase the overall free volume and hence enhance the gas permeability [Kim *et al.*, 2006; Cong *et al.*, 2007b; Weng *et al.*, 2009]. Besides, the interactions between the polymer and CNTs may help reduce the free volume elements (e.g., microvoids in the membrane), which will result in an increase in selectivity.

The experimental data show that the PVAm-PVA/CNT nanocomposite membrane has a higher gas permeability without compromising its selectivity.

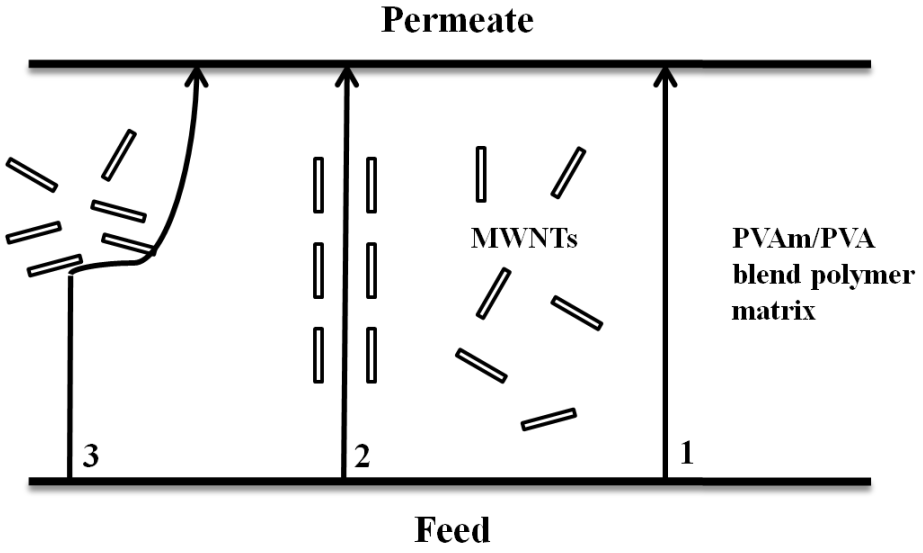


Fig. 3-16 Schematic diagram to show three possible routes for gas permeation in PVAm-PVA/CNT nanocomposite membranes

However, the permeability of nanocomposite membrane is shown to decrease when the CNT loadings exceed 2 wt%. This can be explained by the following. First, as shown in Fig. 3-12, the crystallinity of the membrane increases as CNT loading increases from 2 wt% to 3 wt%, which tends to reduce the gas permeability. In addition, CNTs tend to aggregate more severely as the CNT loading in the membrane increases. The tortuosity of the pathway for gas molecules to

diffuse through the continuous polymer phase in the membrane is thus increased due to presence of CNTs. If the decrease in permeability caused by the tortuous path outweighs the increase in permeability due to increased free volume, a reduced permeability will be observed. If both $CO_2$ and $N_2$ permeabilities decrease at a similar extent, the $CO_2/N_2$ selectivity will not change.

Table 3-3 lists the $CO_2/N_2$ separation performance of PVAm-PVA/CNT nanocomposite membrane developed in this study with other membranes reported in the literature, including four CNTs-based nanocomposite membranes and three facilitated transport membranes. As shown in this table, the PVAm-PVA/CNT nanocomposite membrane is found to compare favorably with other membranes for $CO_2/N_2$ separation.

Table 3-3 Membrane performance for $CO_2/N_2$ separation

| Membrane | System ($CO_2$ vol%) | Feed pressure (kPa) | Temp (K) | $\alpha$ | $P_{co_2}$ (Barrer) | CNT loadings (wt%) | Reference |
|---|---|---|---|---|---|---|---|
| $BPPO_{dp}$-MWNT | Pure $CO_2$ and $N_2$ | 170.3 | 298 | 32 | 148 | 5 | [Cong *et al.*, 2007b] |
| PDMS-SWNT | Pure $CO_2$ and $N_2$ | 405 | 308 | 13.3 | 191 | 2 | [Kim *et al.*, 2006] |
| Pebax-MWNT on PES support | Pure $CO_2$ and $N_2$ | 1000 | 303 | 78.5 | 330 | 2 | [Murali *et al.*, 2010] |
| PES-MWNT | Pure $CO_2$ and $N_2$ | 200 | 298 | 30 | 4.5 | 5 | [Ge *et al.*, 2011] |
| PVAm-PVA on PSf support | $CO_2/N_2$ (10%) | 200 | 298 | 174 | 64.5 | N/A | [Deng *et al.*, 2009] |
| PAAm-PVA on PSf support | $CO_2/N_2$ (20%) | 110 | 298 | 80 | 72 | N/A | [Cai *et al.*, 2008] |
| DNMDAm-TMC on PSf support | $CO_2/N_2$ (20%) | 110 | 298 | 70 | 86.5 | N/A | [Yu *et al.*, 2010] |
| PVAm-PVA/MWNT | Pure $CO_2$ and $N_2$ | 401.3 | 298 | 60.3 | 345.5 | 2 | This study |

### 3.3.4 Performance of PVAm-PVA/CNT asymmetric membranes

The PVAm-PVA/CNT nanocomposite membrane discussed above exhibits a good $CO_2$ permeability. To get a high permeance, which is important for practical applications, asymmetric membranes with a thin skin layer and a microporous substrate were fabricated and evaluated.

As mentioned in section 3.3.2, five different concentrations (e.g., Con A, B, C, D and E) of the polymers were used to prepare asymmetric membranes by the solution coating method. A

higher concentration (e.g., A and B) was used for the first coat, and then a lower concentration (e.g., C, D and E) was used in subsequent coats. Generally speaking, any defects on the membrane surface will make the membrane less selective or non-selective. The purpose of using multiple coatings is to ensure that there will be no open pores on the membrane surface. The resulting coating thickness is determined by the concentration of the coating solution. It is expected using a lower polymer concentration in subsequent coatings will help plug the defects that may be present in the initial coating without causing a significant increase in the mass transfer resistance of the membrane.

Table 3-4 Polymer concentrations of coating solutions in preparing PVAm-PVA/CNT asymmetric membranes

| No. of the membrane | 1st coating | 2nd coating | 3rd coating | Number of coating times |
|---|---|---|---|---|
| 1 | N/A | N/A | N/A | Dense membrane |
| 2 | Con A | N/A | N/A | 1 |
| 3 | Con A | Con C | N/A | 2 |
| 4 | Con A | Con D | N/A | 2 |
| 5 | Con A | Con E | N/A | 2 |
| 6 | Con B | Con B | N/A | 2 |
| 7 | Con B | Con C | Con C | 3 |
| 8 | Con B | Con D | Con D | 3 |
| 9 | Con B | Con E | Con E | 3 |

Table 3-5 Gas permeation performance through PVAm-PVA/CNT asymmetric membranes (at a transmembrane pressure of 0.1 MPa)

| Membrane | Permeance (GPU) | | $CO_2/N_2$ Selectivity |
|---|---|---|---|
| | $CO_2$ | $N_2$ | |
| 1 Dense | 8.1 | 0.19 | 41.6 |
| 2 (A) | 246.0 | 192.1 | 1.3 |
| 3 (A+C) | 11.1 | 0.24 | 45.8 |
| 4 (A+D) | 14.8 | 0.32 | 45.5 |
| 5 (A+E) | 19.4 | 1.2 | 16.2 |
| 6 (B+B) | 79.8 | 16.1 | 5.0 |
| 7 (B+2C) | 9.8 | 0.20 | 48.9 |
| 8 (B+2D) | 12.5 | 0.25 | 50.8 |
| 9 (B+2E) | 14.9 | 0.29 | 51.2 |

The concentrations of the polymers used in the coating solutions during fabrication of

PVAm-PVA/CNT asymmetric membranes are listed in Table 3-4. A dense membrane is denoted as Membrane 1 for comparison. The permselectivity of the membranes at a transmembrane pressure of 0.1 MPa are shown in Table 3-5. As shown in this table, though Membranes 2 and 6 have a rather high $CO_2$ permeance, their selectivities are poor. Membrane 5 also shows a poor selectivity. The permeance and selectivity of the remaining membranes (e.g., Membranes 1, 3, 4, 7, 8 and 9) at different pressures are shown in Fig. 3-17 and 3-18, respectively.

The data in Fig. 3-17 shows that all the PVAm-PVA/CNT asymmetric membranes have a higher gas permeance than the dense membrane without compromising their selectivities. In addition, both dense and asymmetric membranes have similar behavior with respect to gas pressure. Membrane 9 (B+2E) displays the best $CO_2/N_2$ separation performance. Compared to the dense membrane, this membrane shows an 80% increase in $CO_2$ permeance and a 20% increase in $CO_2/N_2$ selectivity at a transmembrane pressure of 0.1 MPa.

In Fig. 3-18, it was shown that all these asymmetric membranes tended to have a higher $CO_2/N_2$ selectivity than dense membrane. In the process of preparation of asymmetric and dense membranes, both the mass ratio of PVAm to PVA (i.e., 60/40) and the mass ratio of MWNTs to polymer (i.e., 0.5/99.5) were identical, however, the concentration of the polymer in the coating solution was different. As mentioned before, the polymer concentration in the blend for dense membrane was 8 wt%, and the polymer concentration used for asymmetric membranes can be seen in Table 3-1. A higher polymer concentration indicates more amine carriers available for facilitated transport of $CO_2$ through the membrane, thus a higher selectivity. Therefore, a slightly higher polymer concentration in the asymmetric membranes makes them show a higher $CO_2/N_2$ selectivity than dense membrane.

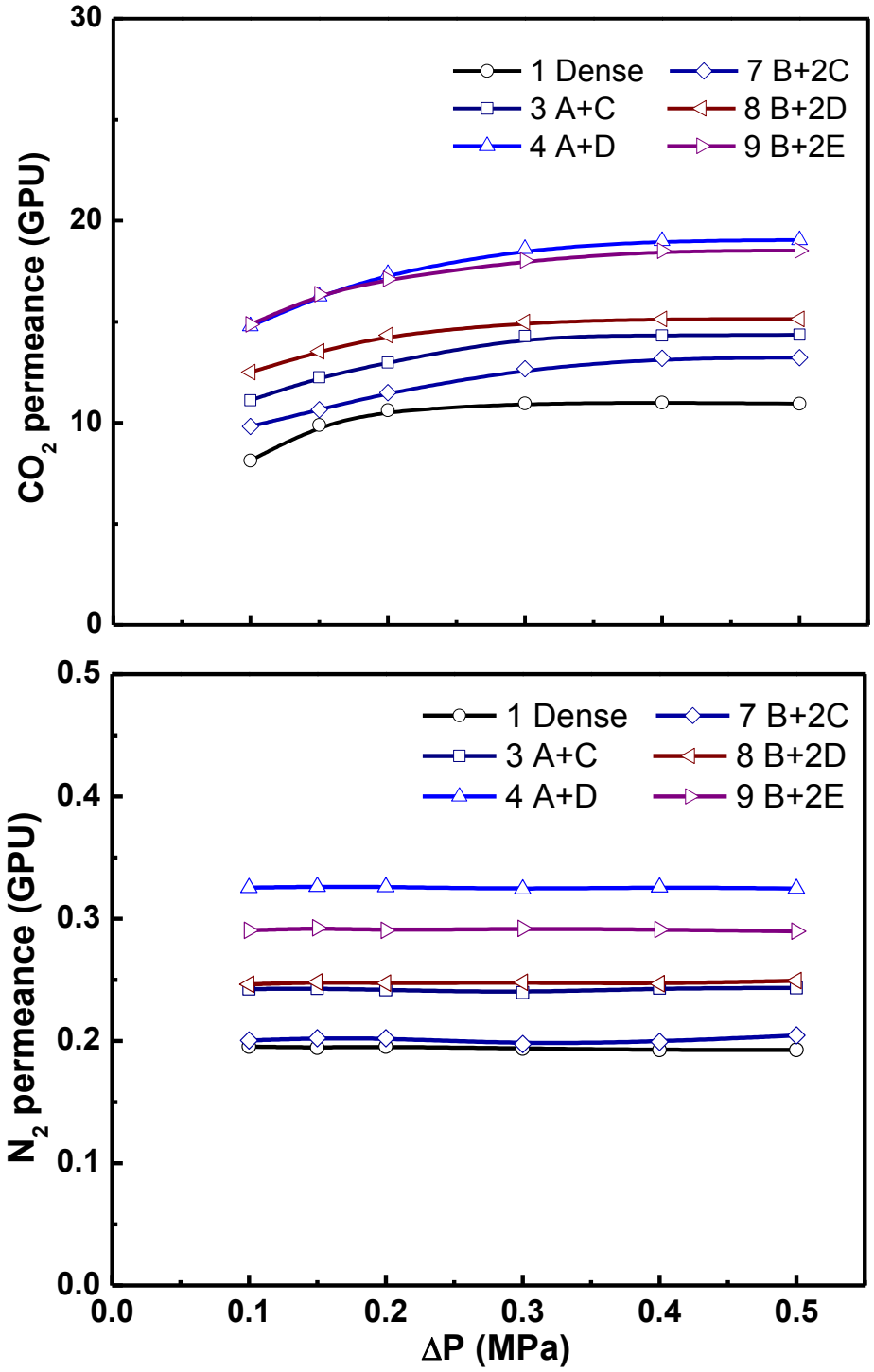


Fig. 3-17 Permeance of $CO_2$ and $N_2$ in dense and asymmetric PVAm-PVA/CNT membranes

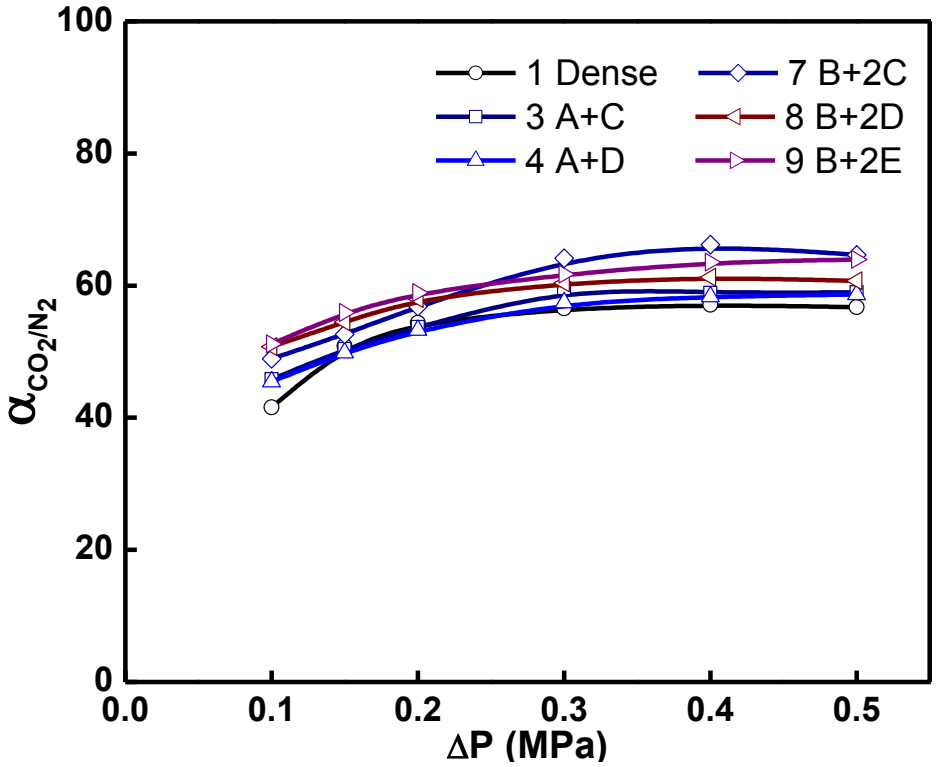


Fig. 3-18 $CO_2/N_2$ selectivity in dense and asymmetric PVAm-PVA/CNT membranes

The permeation behavior of gases through the asymmetric membranes observed here lies in the different effective membrane thickness due to the polymer concentration used. A lower polymer concentration will produce membranes with a thinner selective layer and thus a higher gas permeance. Similarly, a thicker layer provides a longer distance and greater resistance for the gas molecules to cross, thereby causing the gas permeance to decrease. On the other hand, if a membrane layer is very thin, there is more chance to have defects on the membrane surface. The results here show that it is possible to prepare asymmetric membranes with improved permeance without sacrificing the membrane selectivity via the multiple coating approach using varying concentrations of the coating solutions.

## 3.4 Conclusions

PVAm/PVA blend membranes were prepared by solution casting method and the membrane

permselectivities to $CO_2$, $N_2$, $CH_4$, $H_2$, $O_2$ and He were studied. The following conclusions can be drawn:

(1) The permeability of the blend membranes followed the order of $N_2 < CH_4 < He \approx O_2 < H_2 < CO_2$, and the membrane was found to exhibit promising separation performance for $CO_2$ removal from flue gas (e.g., $CO_2/N_2$ separation). The amino groups in PVAm could facilitate $CO_2$ transport.

(2) The gas permeability through the PVAm/PVA blend membranes increased with an increase in temperature, and the temperature dependence of the membrane permeability followed an Arrhenius type of relationship.

(3) A higher PVAm/PVA blend ratio correlates to a higher $CO_2$ permeability and $CO_2/N_2$ selectivity. An appropriate blend ratio for fabricating PVAm/PVA blend membranes was found to be 60/40 (w/w).

(4) Heat-treatment slightly reduced membrane permeability due to densification of the membrane but had little impact on the membrane selectivity. A preferred range of heat-treatment time was 15-30 min at 120℃.

To improve the membrane performance, CNTs were incorporated into the membrane to form a nanocomposite. The structures of the CNTs and the PVAm-PVA/CNT nanocomposite membranes with different CNT loadings were characterized. The separation performance of PVAm-PVA/CNT nanocomposite membranes was investigated, and the following conclusions can be drawn:

(1) The FTIR spectra confirmed the presence of carboxylic acid groups due to acid treatment of the CNTs, and the Raman spectra confirmed the presence of acid-treated CNTs in the PVAm-PVA/CNT nanocomposite membrane, which was not quite visible in the FTIR spectra. In

addition, the semi-crystalline structure of the blend polymer was verified with XRD, and the membrane crystallinity was shown to be decreased by the addition of CNTs.

(2) Adding CNTs in the membrane enhanced $CO_2$ permeability while retaining a similar $CO_2/N_2$ selectivity until a CNT loading of 2 wt%; a higher CNT loading tended to decrease the gas permeability gradually. In general, the PVAm-PVA/CNT nanocomposite membrane was found to compare favorably with other membranes reported in the literature in terms of $CO_2/N_2$ permselectivity.

(3) Asymmetric PVAm-PVA/CNT membranes were prepared by multiple coating using polymer solutions of varying concentrations. By introducing asymmetricity into the membrane structure, membranes with increased permeance were obtained.

# Chapter 4

## Pervaporation membranes based on PVAm-PVA composite membranes incorporated with carbon nanotubes for dehydration of ethylene glycol*

---

### 4.1 Introduction

Pervaporation is recognized as an energy-efficient alternative to conventional distillation, especially in separating close-boiling and azeotropic mixtures [Shao and Huang, 2007]. In recent years, advanced pervaporation membranes with improved separation performance have been sought for various applications, including dehydration of organic solvents, removal of dilute organic compounds from aqueous streams and the separation of organic-organic mixtures [Smitha *et al.*, 2004]. Among them, the dehydration of organic solvents is the best developed. Ethylene glycol is a widely used chemical in the manufacture of polyesters and as a non-volatile antifreeze. It is also commonly used as an inhibitor to gas hydrate formation in the natural gas industry. Currently, ethylene glycol is mainly produced by hydrolysis of ethylene oxide in the presence of a large excess of water, which needs to be removed eventually from the product. Ethylene glycol and water do not form an azeotrope over the entire composition range and can in principle be separated by multi-stage evaporation or distillation. However, the energy

* Portions of this work have been published in *J. Membr. Sci.*, 417-418 (2012) 34-44.

consumption of the thermal process is intensive because of the high boiling point (197.3℃) of ethylene glycol. On the other hand, pervaporation appears to be particularly attractive because it can operate at low temperatures and waste heat may be used as the energy source. The energy consumption for pervaporative separation of water from ethylene glycol is considerably low especially at feed water concentrations less than 30 wt% [Huang *et al.*, 2002].

Hydrophilic membranes are generally used for the dehydration of organic solvents because of the favorable solubility and diffusivity for selective permeation of water [Feng and Huang, 1997]. Considering the PVAm/PVA blend polymer is highly hydrophilic because of their amine and hydroxyl groups, PVAm/PVA blend is expected to favor preferential permeation of water molecules for dehydration of organic solvents by pervaporation. Moreover, by incorporating CNTs into the matrix of the polymer blend, not only will membranes swelling be constrained due to the interactions between the CNTs and the blend polymer, the CNTs are also expected to offer an additional passageway for the transport of water molecules. To our knowledge, PVAm/PVA blend membranes incorporated with CNTs for pervaporation separation are still lacking.

Therefore, the objective in this chapter is to study CNT-incorporated PVAm/PVA blend membranes for dehydration of ethylene glycol by pervaporation. This chapter reports the improved performance of such novel membranes based on the polymer blend and nanofillers, and elucidates how the nanotubes affect the mass transport. In order to achieve a good dispersion of CNTs in the polymer matrix, the CNTs were treated with strong acids (i.e., sulfuric acid and nitric acid) before being added to PVAm-PVA solutions for membrane fabrication. It may be mentioned that both dense films and composite membranes of PVAm-PVA/CNT were prepared. The dense films were used for characterization of the material properties (e.g., contact angle measurement and sorption uptake study), and composite membranes were used for pervaporation

separation where the asymmetricity was introduced to enhance permeation flux. The effects of feed water concentration, temperature and CNT content in the membrane on the performance of the membranes for ethylene glycol dehydration were investigated.

It needs to be pointed out that although there are a few reports on the use of carbon nanotubes to improve the performance of pervaporation membranes based on poly(vinyl alcohol) and chitosan, which are two widely used membrane materials for solvent dehydration, there appears to be an inconsistent trend in the effects of nanotubes on the membrane performance. For instance, there is an increase in the permeation flux and a decrease in the selectivity for ethanol dehydration when a small amount of multi-walled carbon nanotubes was incorporated into a poly(vinyl alcohol) membrane [Choi *et al.*, 2007, 2009], while the opposite can be observed for dehydration of isopropanol [Shirazi *et al.*, 2011]. Qiu *et al.* [2010] prepared chitosan membranes filled with CNTs for dehydration of 90 wt% ethanol and the degree of swelling of the membrane in the feed solution was reportedly increased with an increase in the CNT loading of the membrane, and an opposite trend was shown by Liu *et al.* [2009]. All these call for further studies to get an insight into the function of the nanotubes and what aspects the nanotubes affect with respect to pervaporative mass transport in the composite membranes. Therefore, in the present study, besides the membrane permselectivity, both the surface properties (i.e., the contact angle of the permeant on the membrane) and the bulk properties (sorption uptake of permeant in the membrane) were investigated as well in order to determine whether the improved separation performance of the membrane was due to enhanced membrane surface and/or bulk properties that directly affects the sorption aspect of the mass transport in pervaporation.

## 4.2 Experimental

### 4.2.1 Materials

Ethylene glycol was purchased from Fisher Scientific, and aqueous ethylene glycol solutions of different concentrations used in the pervaporation experiments were prepared by blending ethylene glycol and deionized water. Other materials were the same as used before.

### 4.2.2 Membrane preparation

The procedure for preparation of PVAm-PVA/CNT dense films and composite membranes was described in Chapter 3. The dense films were used for characterization of PVAm-PVA/CNT nanocomposite materials. During the preparation of PVAm-PVA/CNT composite membranes, the PVAm to PVA mass ratio in the coating solutions was the same as those used for preparing dense films (i.e., 60/40). However, a coating solution containing 6.53 wt% of the polymer (i.e., 3.92 wt% of PVAm and 2.61 wt% of PVA) was used for the first coat, and less viscous solutions containing 2.30 wt% of the polymer (i.e., 1.38 wt% of PVAm and 0.92 wt% of PVA) were used in subsequent two coatings. This was found to be effective to prepare defect-free membranes with only 2-3 coats. In both coating solutions, the polymer to MWNT ratio was maintained the same, and the MWNT content in the effective skin layer of the resulting membrane was determined by the MWNT to polymer mass ratio. In this chapter, two composite membranes were prepared, with one containing 0.5 wt% MWNTs and the other 2.0 wt% MWNTs. For a baseline comparison, a PVAm/PVA composite membrane containing no MWNTs was also prepared, and this membrane was designated as CNT 0.

### 4.2.3 Membrane characterization

The contact angles of water and ethylene glycol on the surface of PVAm-PVA/CNT nanocomposite membranes were measured using a contact angle meter (Cam-plus Micro, Tantec Inc.). The membrane samples were air dried at ambient temperature prior to the contact angle measurements. For each contact angle measurement, at least five readings from different surface locations were taken, and the contact angles reported here are the average values.

The sorption uptake measures the solubility characteristics of liquids in the membrane. The PVAm-PVA/CNT nanocomposite dense membranes were subjected to sorption measurements with water and ethylene glycol. The membrane was immersed in deionized water at room temperature to reach sorption equilibrium. Then the membrane was taken out of the water, and the membrane was weighed after excess surface water was quickly wiped out with Kimwipes. The membrane sample was then dried under vacuum at 80℃ for 1 day to determine the weight of the dry sample. The degree of swelling of the PVAm-PVA/CNT nanocomposite membrane in water was determined in terms of water sorption uptake in the membranes per g of the membrane:

$$Swelling\ degree = \frac{W_s - W_d}{W_d} \quad (4\text{-}1)$$

where $W_s$ and $W_d$ are the weights of the water-swollen and dry membranes, respectively. Similarly, the degrees of swelling of the membranes in ethylene glycol were also measured.

### 4.2.4 Pervaporation

The experimental setup for pervaporation experiments is schematically shown in Fig. 4-1. The membrane was mounted into a permeation cell, which had an effective surface area of 16.6 $cm^2$. Aqueous ethylene glycol solutions at different water concentrations were used as the feed.

The feed solution was circulated by a pump from the feed tank to the permeation cell, and the retentate was recycled back to the feed tank. The operating temperature was controlled using a thermal bath. On the permeate side, vacuum was applied to maintain a downstream pressure below 1 mmHg absolute. The vaporous permeate was condensed and collected in a cold trap immersed in liquid nitrogen. The permeation flux was determined from the weight of permeate sample collected over a given period of time, and the permeate composition was analyzed with a Hewlett-Packard 5890 (Series II) gas chromatography, equipped with a thermal conductivity detector and a Porapak Q column. The permeation was considered to have reached steady state when the permeation flux and permeate composition became constant. The permeation flux ($J$) and separation factor ($\alpha$) were used to measure the separation performance of the membrane:

$$J = \frac{Q}{A \cdot \Delta t} \tag{4-2}$$

$$\alpha = \frac{Y/(1-Y)}{X/(1-X)} \tag{4-3}$$

where $Q$ is the amount of permeate collected over a time interval $\Delta t$, $A$ is the effective membrane area, and $X$ and $Y$ are the mass fractions of water in the feed and the permeate, respectively. The partial permeation fluxes of ethylene glycol and water can be calculated easily from the total permeation flux and the permeate composition:

$$J_{water} = J \cdot Y;\ J_{EG} = J \cdot (1 - Y) \tag{4-4}$$

The pervaporation data reported here was averaged from at least two measurements and the experimental error in the measurement was shown to be less than 4%.

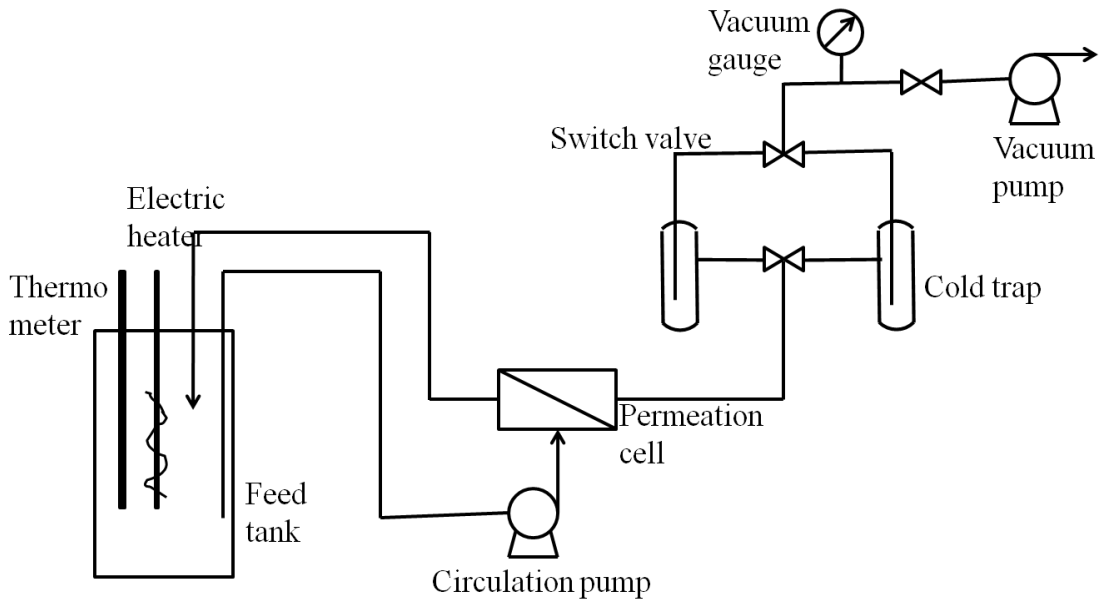


Fig. 4-1 Schematic diagram of pervaporation setup

## 4.3 Results and discussion

### 4.3.1 Membrane characterization

To consider the affinity of water and ethylene glycol to the surfaces of the PVAm-PVA/CNT nanocomposite films, the contact angles of both water and ethylene glycol on the membrane surface were measured. As shown in Fig. 4-2, water has a smaller contact angle than ethylene glycol for all the PVAm-PVA/CNT nanocomposite films, indicating that the nanocomposite films have a better affinity to water than ethylene glycol due to the presence of acid-treated MWNTs. This is understandable in view of the hydrophilic groups (-COOH) on the surface of MWNTs that will improve the hydrophilicity of the membrane surface. With an increase in the MWNT content, the contact angle of water on the film gradually decreases, suggesting that the acid-treated hydrophilic MWNTs incorporated into the membrane enhanced the surface hydrophilicity. Similar results can also be observed for MWNT-containing polyphenylene oxide and chitosan membranes [Tang *et al.*, 2009; Wu *et al.*, 2010]. The contact angle of ethylene

glycol was shown to decrease only slightly with an increase in the MWNT content in the film, presumably due to the hydrophobic carbon-carbon bonds of the molecule.

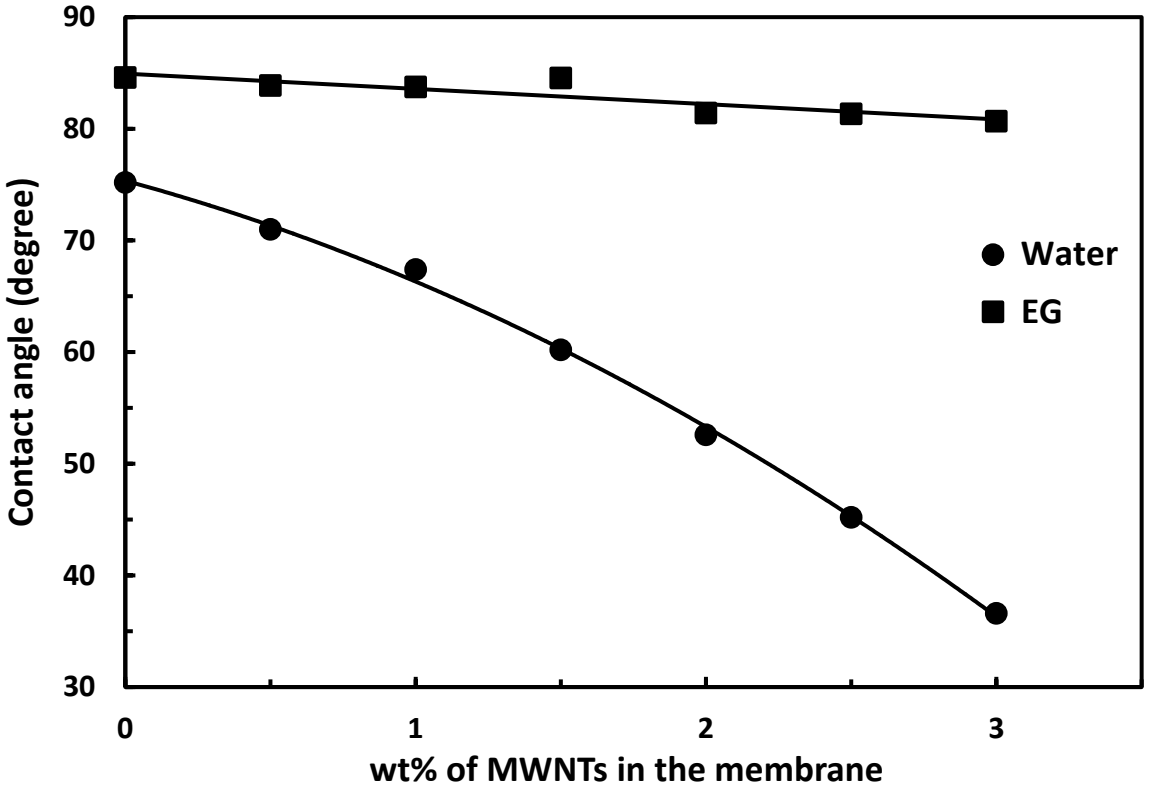


Fig. 4-2 Contact angles of water and ethylene glycol on PVAm-PVA/CNT nanocomposite membranes with different contents of CNTs

Table 4-1 shows the swelling degrees of the PVAm-PVA/CNT nanocomposite dense membranes in water and ethylene glycol. The sorption uptake of water in the membranes is approximately 10 times greater than the sorption uptake of ethylene glycol. This confirms the favorable solubility selectivity of the membranes for preferential removal of water from ethylene glycol. It is interesting to note that there were no considerable changes in the swelling degrees of the membranes when the MWNT contents in the membranes varied from 0 to 3 wt%. These results suggest that incorporation of MWNTs into the membrane, which showed an enhancement in the hydrophilicity of the membrane surface, did not result in a significant change in the liquid uptake, which is a bulk property of the membrane. This is understandable because a small

amount of MWNTs is insufficient to change the bulk property of the membrane significantly.

Table 4-1 Sorption uptake of water and ethylene glycol in PVAm-PVA/CNT nanocomposite membranes

| CNT content (wt%) | Degree of swelling in water (g water/g polymer) | Degree of swelling in ethylene glycol (g ethylene glycol/g polymer) |
|---|---|---|
| 0 | 2.3 | 0.23 |
| 0.5 | 2.2 | 0.22 |
| 1.0 | 2.3 | 0.21 |
| 1.5 | 2.2 | 0.19 |
| 2.0 | 2.5 | 0.21 |
| 2.5 | 2.5 | 0.20 |
| 3.0 | 2.4 | 0.21 |

### 4.3.2 Pervaporation performance of the membranes

In order to examine the impact of feed concentration on the performance of the PVAm-PVA/CNT composite membranes for the separation of water from ethylene glycol, pervaporation experiments were carried out at 38℃ for a feed water concentration ranging from 0.5 to 20 wt%. This concentration range is relevant to industrial applications, particularly in natural gas dehydration by ethylene glycol.

The water concentration in the permeate and the permeation flux as a function of feed water concentration are presented in Fig. 4-3 for a PVAm-PVA/CNT composite membrane containing 0.5 wt% of MWNTs. At a feed water concentration of 0.5 wt%, the water concentration in permeate reached 87 wt%. The permeate became substantially enriched with water (>95 wt%) at a feed water concentration greater than 3 wt%. On the other hand, the total permeation flux increased almost linearly with an increase in the feed water concentration. Similar trends were observed for ethylene glycol dehydration using some other hydrophilic membranes [Rao *et al.*, 2007; Xu *et al.*, 2010a]. An increase in feed water concentration not only represents an increase in the driving force for water permeation, it will also enhance the membrane swelling, thus making the permeant molecules to diffuse through the membrane more easily.

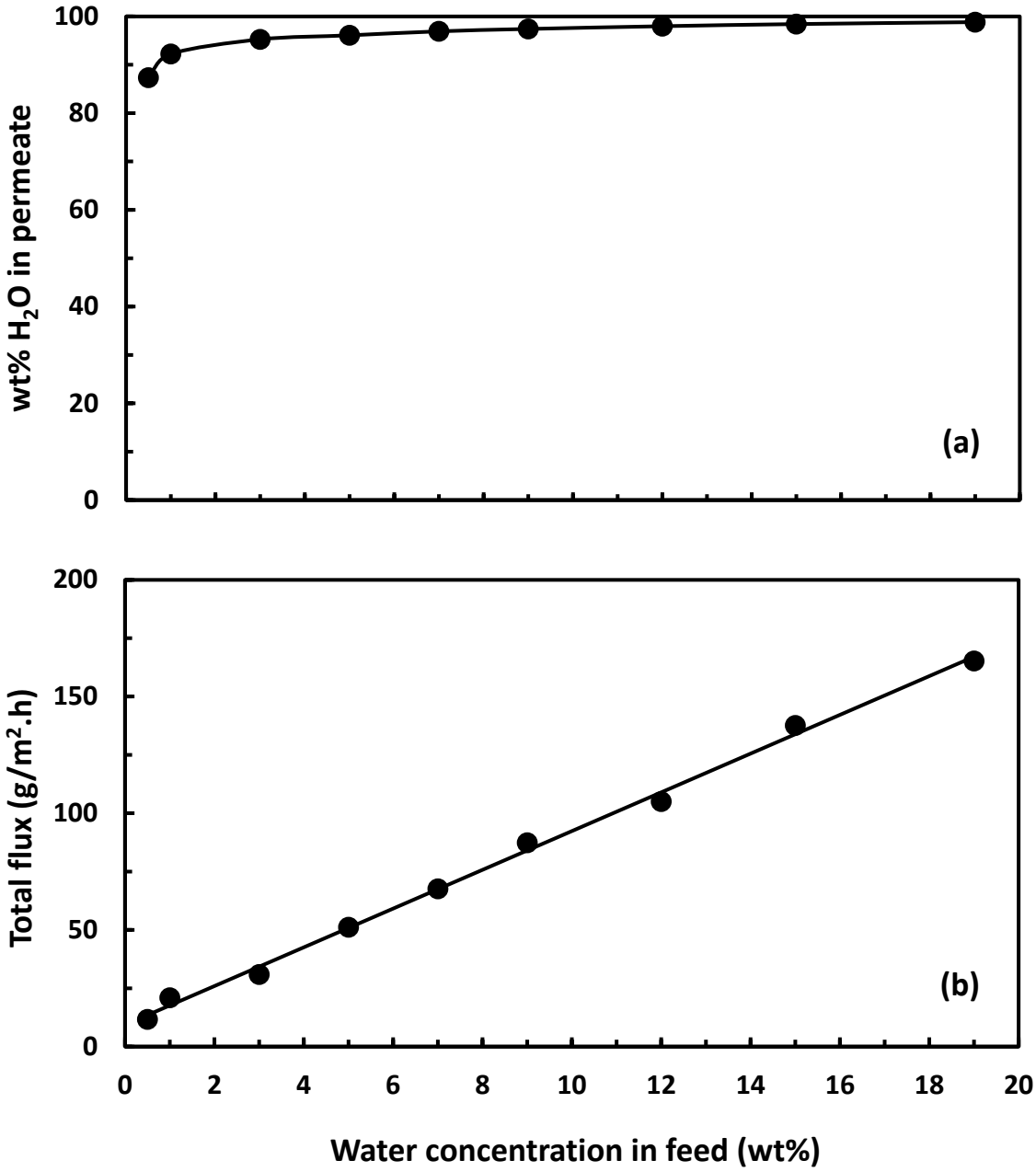


Fig. 4-3 Effects of water concentration in the feed on water concentration in permeate (a) and total permeation flux (b) through PVAm-PVA/CNT membrane (CNT 0.5). Temperature: 38 ℃.

The partial permeation fluxes of water and ethylene glycol with respect to feed water concentration are plotted in Fig. 4-4. The partial flux of water is approximately proportional to feed water concentration, while the permeation flux of ethylene glycol increased very slightly with the water concentration in feed. In the binary feed solutions, a higher feed water

concentration means a lower concentration of ethylene glycol and thus a lower driving force for ethylene glycol permeation. As shown by the sorption uptake data, water swells the membrane much more significantly than ethylene glycol. As the feed water concentration increases, the membrane will become more swollen, which favors the permeation of both water and ethylene glycol. The effect of feed water concentration on the permeation flux of ethylene glycol suggest that as feed water concentration increases, the enhanced permeability due to membrane swelling is more dominant over the decreased driving force for ethylene glycol permeation. Since the permeation flux of ethylene glycol is much lower than that of the water, the total permeation flux is mainly determined by the water flux. The high flux of water can be ascribed to both the relatively small sizes of water molecules and the stronger affinity between water and the membrane.

In general, an increase in permeation flux is often coupled with a reduction in the separation factor. The PVAm-PVA/CNT composite membranes also exhibited a similar trade-off relationship. As shown in Fig. 4-5, the separation factor of the PVAm-PVA/CNT composite membrane sharply decreased as the feed water concentration increased. However, the decrease in the separation factor is less significant at a higher water concentration in the feed, and the separation factor became essentially a constant over a feed water concentration in the range of 10 to 20 wt%. The PVAm-PVA/CNT composite membrane exhibited a very high separation factor for ethylene glycol dehydration at low feed water concentrations. For example, the membrane displayed a separation factor of 650, 1170 and 1370 at a feed water concentration of 3, 1 and 0.5 wt%, respectively. This is very favorable for practical applications from an energy consumption perspective as the membrane becomes more permselective when the feed is gradually depleted in water as pervaporation proceeds with time.

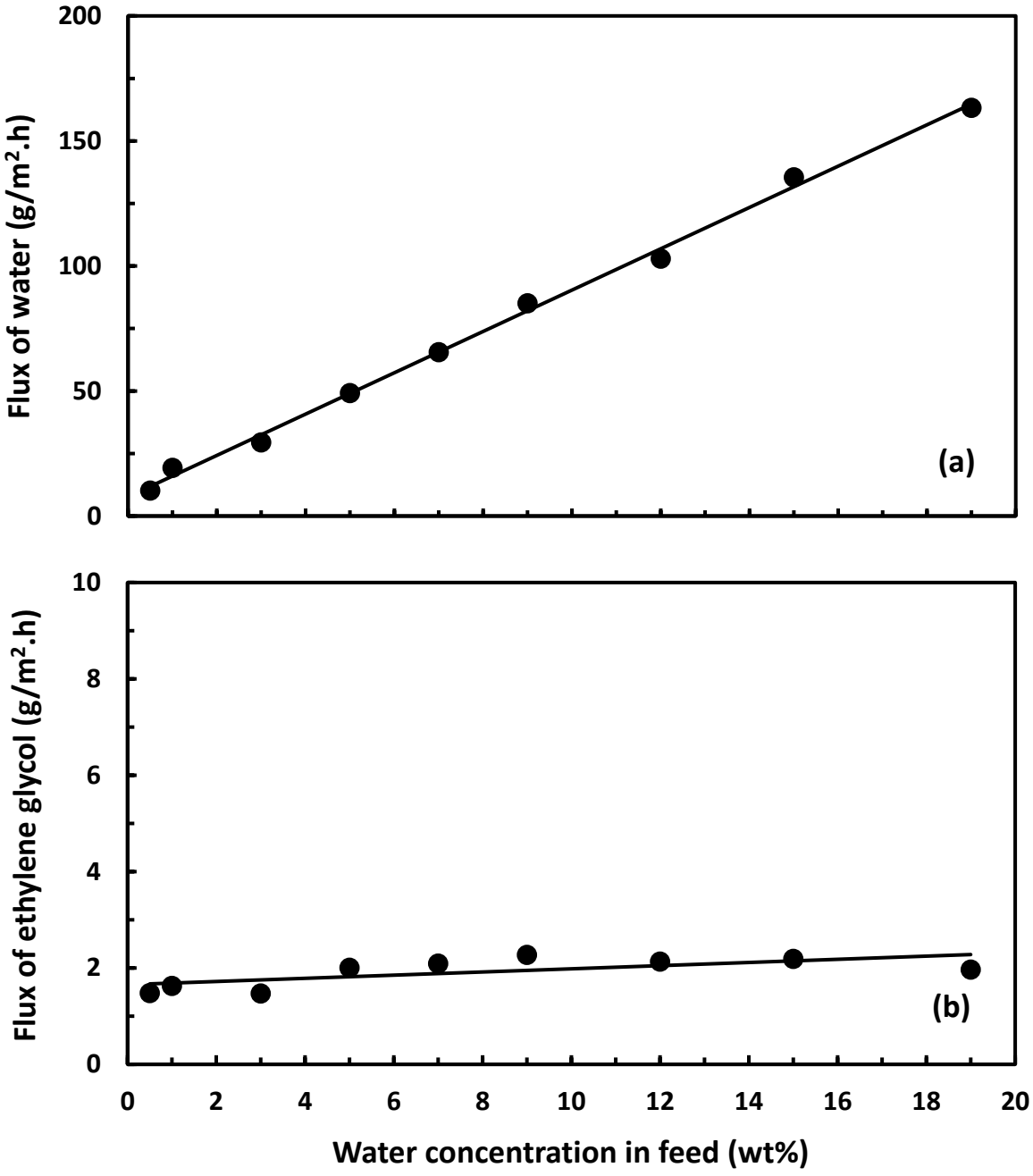


Fig. 4-4 Effects of feed water concentration on the partial permeation fluxes of water (a) and ethylene glycol (b) through PVAm-PVA/CNT membrane (CNT 0.5). Temperature: 38 ℃.

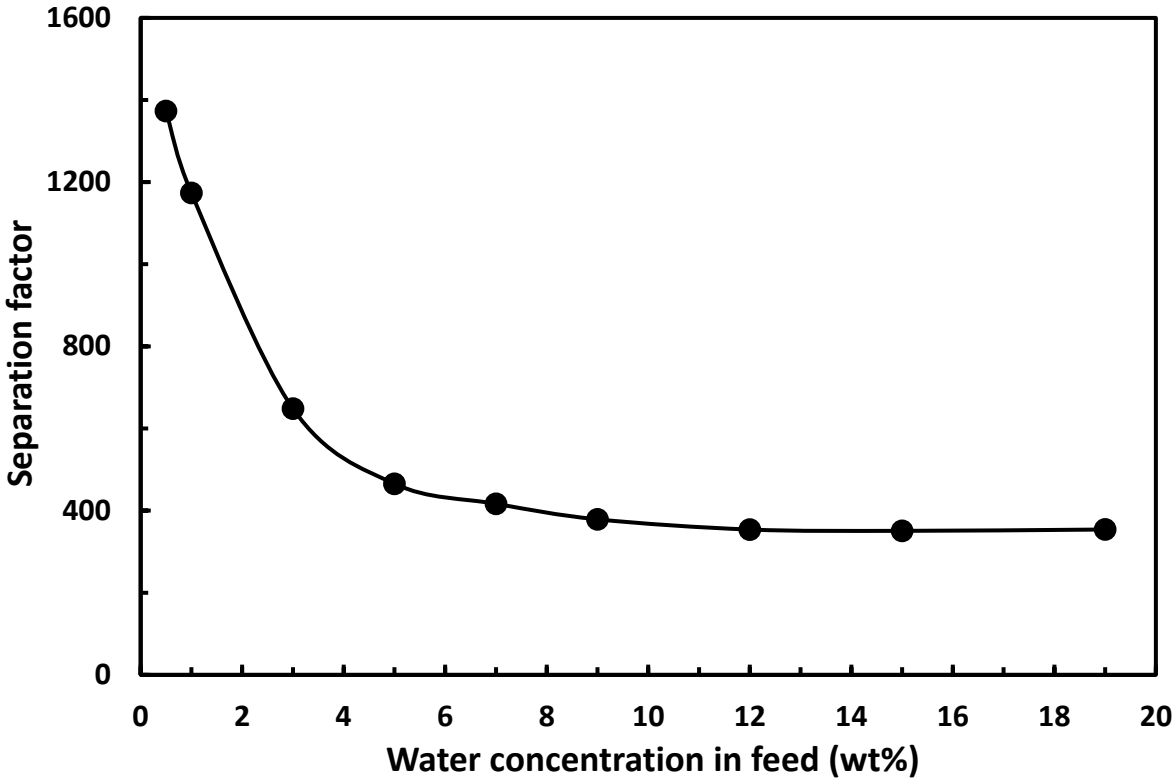


Fig. 4-5 Separation factor for dehydration of ethylene glycol using PVAm-PVA/CNT membrane (CNT 0.5). Temperature: 38 ℃.

Generally speaking, the operating temperature is an important operating parameter in pervaporation. Pervaporative dehydration of ethylene glycol using the PVAm-PVA/CNT composite membrane containing 0.5 wt% of MWNTs was conducted at various temperatures ranging from 30 to 70℃. Fig. 4-6 shows the partial permeation fluxes of water and ethylene glycol as a function of temperature, where the logarithmic fluxes were plotted against the reciprocal of temperature. Clearly, an increase in temperature resulted in an increase in both the partial permeation fluxes of water and ethylene glycol, and the temperature dependence of permeation flux followed an Arrhenius type of relation.

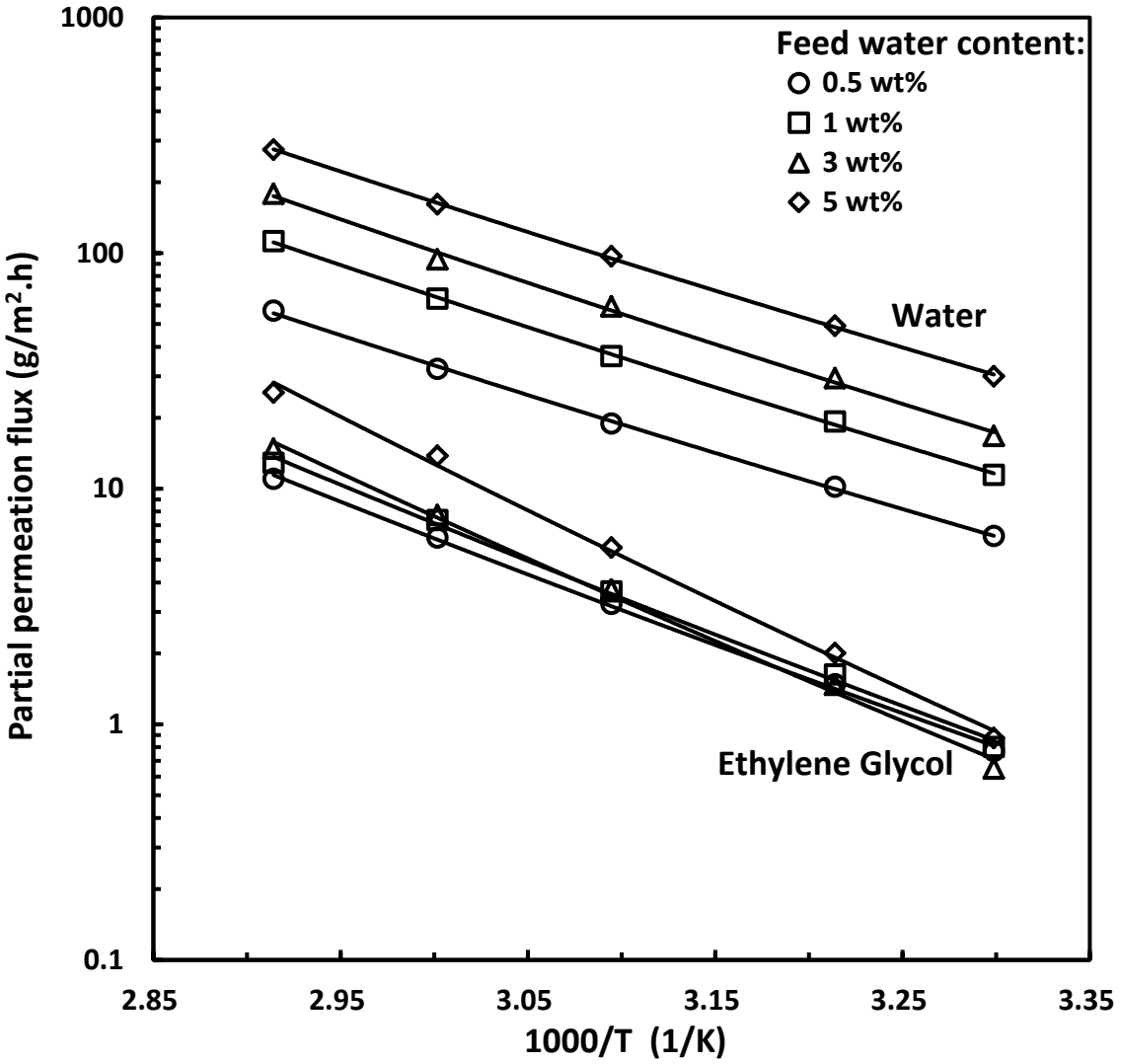


Fig. 4-6 Effects of temperature on partial permeation fluxes of water and ethylene glycol through PVAm-PVA/CNT membrane (CNT 0.5) at different feed water concentrations

It should be pointed out that the operating temperature affects permeation on two aspects: One is the driving force, and the other is the membrane permeability. When the temperature is increased, the saturated vapor pressures of both water and ethylene glycol are increased, leading to an increase in the driving force for mass transport through the membrane. On the other hand, based on the solution-diffusion model, the membrane permeability is determined by the diffusivity and solubility of the permeant in the membrane. With an increase in the temperature, the permeant becomes more energetic, and the segmental motion of the polymer chains is also

enhanced, leading to faster diffusion of the permeant in the membrane. However, sorption is generally an exothermic process, and the solubility of the permeant tends to decrease with an increase in temperature. Clearly, temperature has two opposite effects on the diffusivity and solubility. When the permeant diffusivity is sufficient to compensate the decrease in the permeant solubility, which is often the case for solvent dehydration with hydrophilic membranes, the permeability will increase as the temperature increases. The observed temperature dependence of the permeation flux reflects the combined effects of temperature on the driving force for permeation and the permeability of the permeant in the membrane.

The permeation of ethylene glycol appears to be influenced by the temperature more significantly than the permeation of water. For example, at a feed water concentration of 3 wt%, with an increase in temperature from 30 to 70℃, the water flux increased 10-fold from 16.7 to 179 g/($m^2$.h), while ethylene glycol experienced a 22-fold increase in its permeation flux, from 0.65 to 14.8 g/($m^2$.h). As a result, the separation factor decreased with an increase in temperature, as shown in Fig. 4-7. The temperature dependence of permeation flux can be measured quantitatively by the apparent activation energy for permeation, which can be determined from the slope of the Arrhenius plot based on,

$$J_i = J_{i0}\exp(-\frac{E_{Ji}}{RT}) \tag{4-5}$$

where $E_{Ji}$ is the apparent activation energy for component $i$ permeation. As shown in Fig. 4-8, the apparent activation energy for water permeation is essentially a constant at the feed concentrations studied here, while the activation energy for ethylene glycol permeation increases with an increase in the feed water concentration. As mentioned earlier, the apparent activation energy measures the overall effects of temperature on the permeation flux, which has accounted for the effect of temperature on the driving force. As a first approximation, the activation energy

that characterizes temperature dependence of membrane permeability is equal to the apparent activation energy minus the heat of evaporation of the permeant. At the feed concentrations studied here, the apparent activation energy is rather close to the heat of evaporation of the permeant, which is 40.7 and 53.2 kJ/mol for water and ethylene glycol [Perry and Green, 1999], respectively. This indicates that the increase in permeation flux with an increase in temperature is primarily due to increased driving force for the permeation.

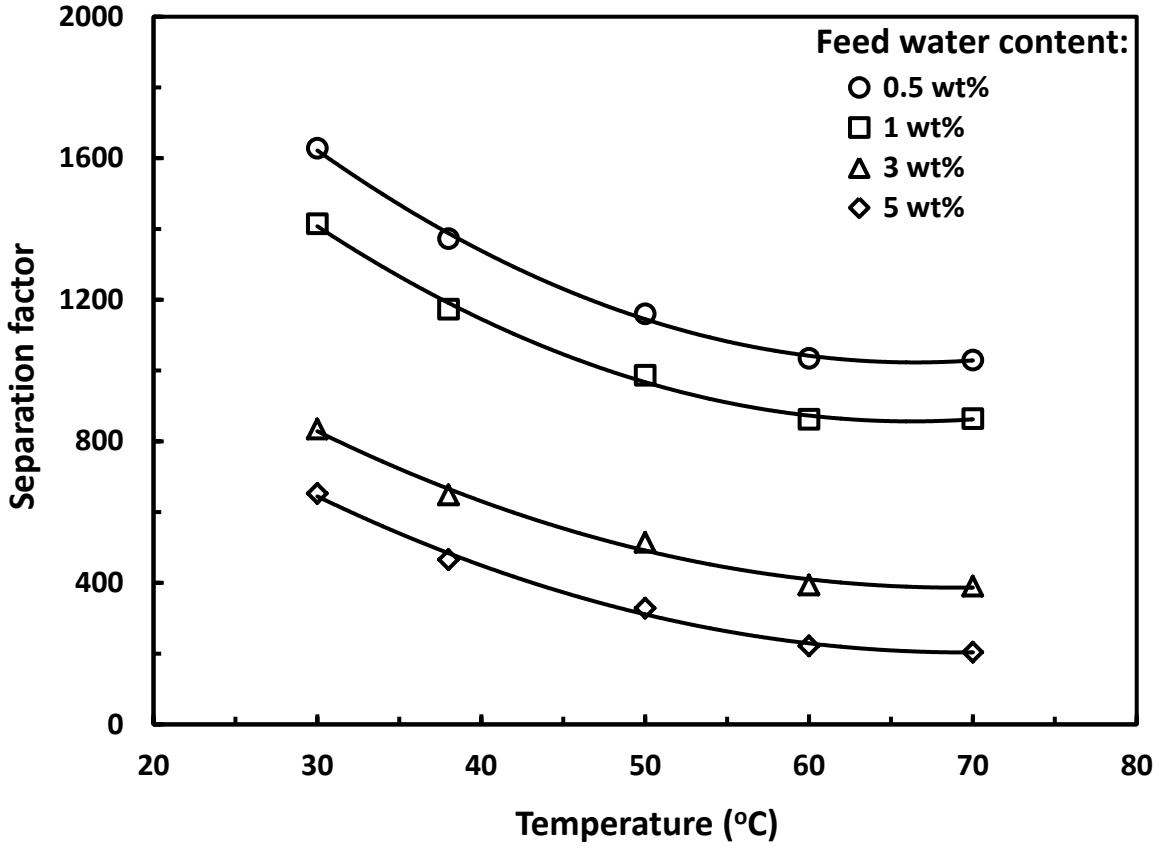


Fig. 4-7 Separation factor for dehydration of ethylene glycol at different temperatures using PVAm-PVA/CNT membrane (CNT 0.5)

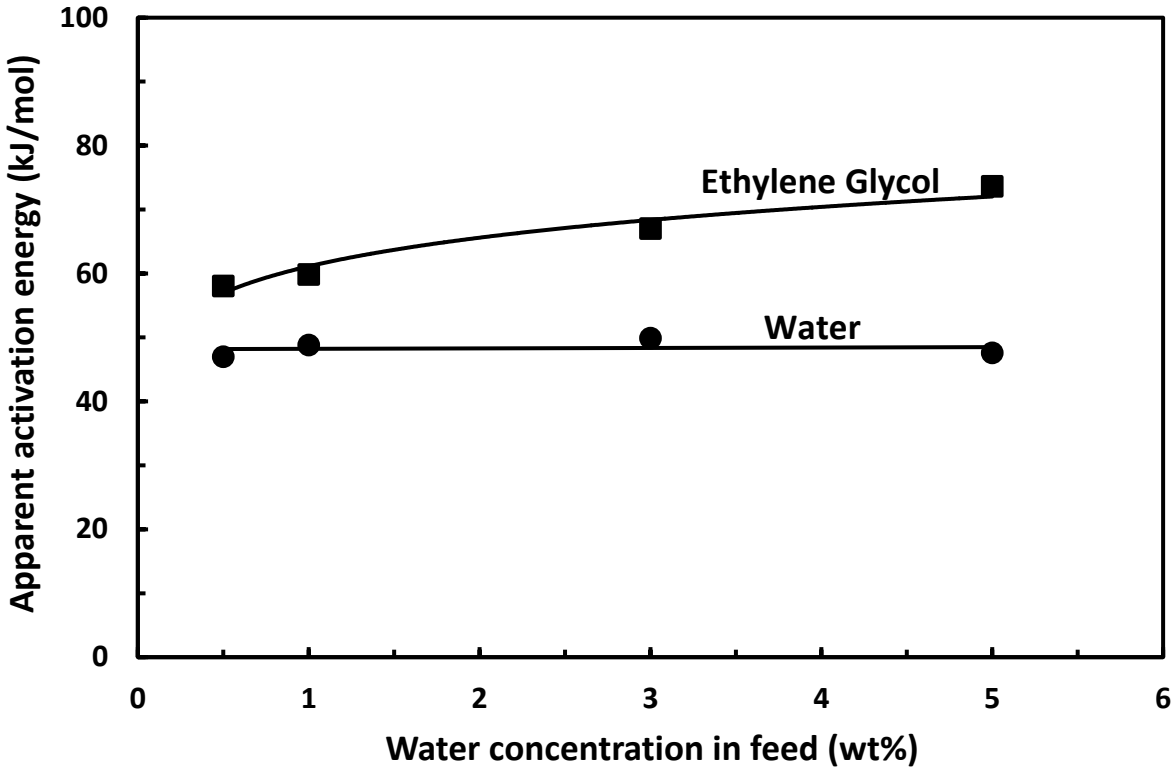


Fig. 4-8 Apparent activation energy for permeation through PVAm-PVA/CNT membrane (CNT 0.5)

Therefore, in order to separate the contribution of the intrinsic membrane property (i.e., membrane permeability) from that of the operating condition (i.e., driving force) to the permeation flux, the permeance of the membrane (i.e., the permeation flux normalized by the transmembrane driving force) was evaluated:

$$(P_i/l) = J_i/\left(p_i^s x_i \gamma_i - p_i^p y_i\right) \tag{4-6}$$

where $(P_i/l)$ is the membrane permeance, $p^s$ is the saturated vapor pressure which can be calculated from the Antoine equation [Yaws *et al.*, 2009], $\gamma$ is the activity coefficient in the liquid phase which can be calculated by the Wilson equation [Gmehling and Onken, 1977], $p^p$ is the permeate pressure, and subscript $i$ represents component $i$ in the feed. Fig. 4-9 shows the membrane permeance as a function of reciprocal temperature. It is apparent that the permeance of water is an order of magnitude higher than the permeance of ethylene glycol. The membrane permeance decreased with an increase in the temperature for water and, to a lesser extent,

ethylene glycol, suggesting that as the temperature increases, the increase in diffusivity is not sufficient to compensate the reduction in solubility, which results in a decrease in the membrane permeability. Thus, the observed increase in permeation flux is attributed to a large extent to the increase in the driving force. Similar results can be found for ethylene glycol dehydration by pervaporation using other hydrophilic membranes [Du *et al.*, 2008; Xu *et al.*, 2010a].

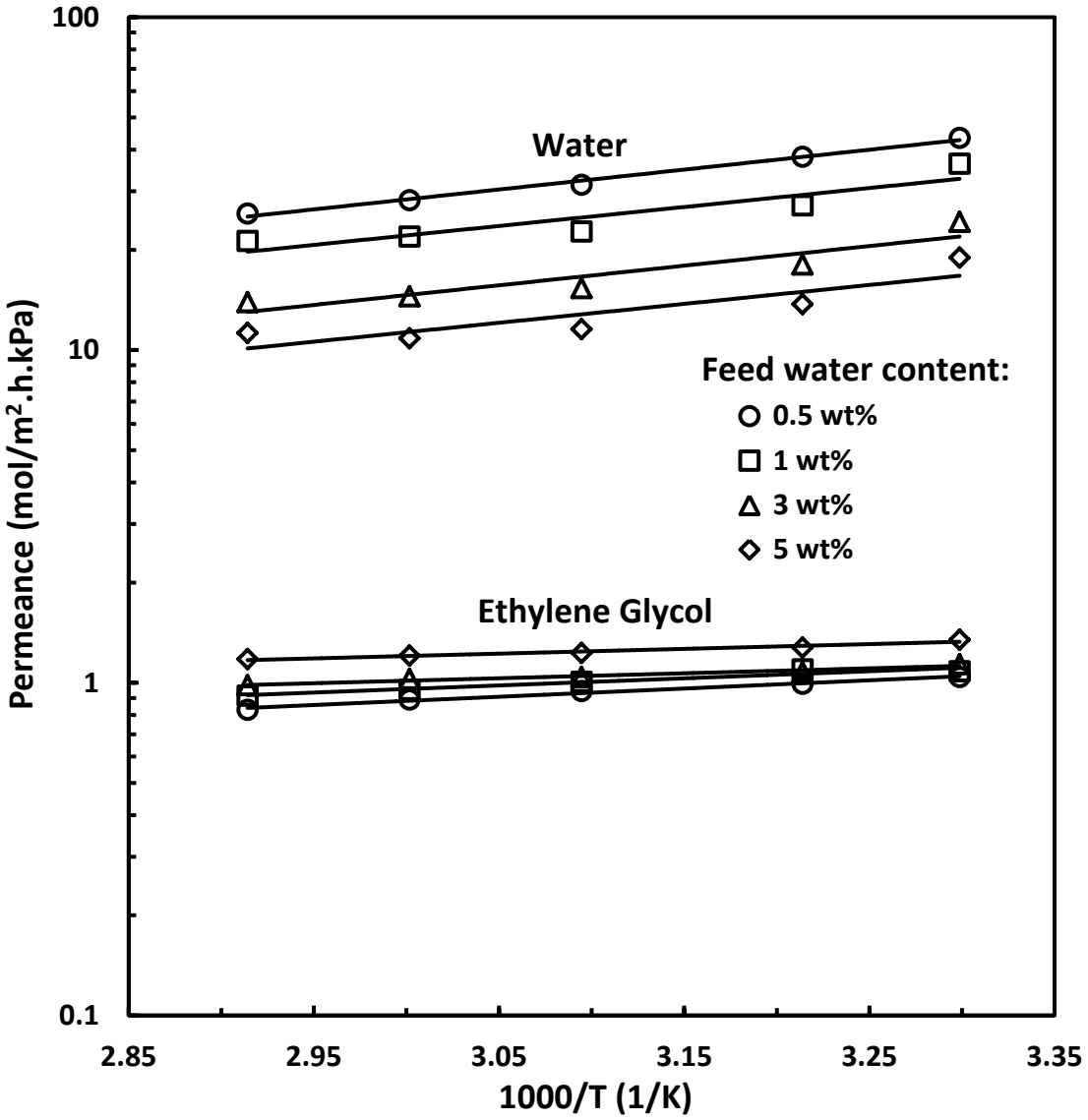


Fig. 4-9 Effects of temperature on the permeance of water and ethylene glycol through PVAm-PVA/CNT membrane (CNT 0.5) at different feed water concentrations

To study the effect of MWNT content in the membrane on the separation performance, the

PVAm-PVA/CNT composite membranes with different MWNT contents (i.e., CNT 0, CNT 0.5 and CNT 2) were tested for ethylene glycol dehydration at 38℃ with feed water concentrations ranging from 0.5 to 20 wt%. The results are shown in Fig. 4-10, where the vapor-liquid equilibrium (VLE) data for binary water/ethylene glycol mixtures [Perry and Green, 1999] are also plotted for comparison of the separation efficiency with conventional distillation. It is clear that pervaporation with these membranes are more selective than distillation for the dehydration of ethylene glycol, especially at relatively low feed water concentrations. In general, with the addition of MWNTs in the membrane, the permeate becomes more enriched with water and the permeation flux tends to be slightly higher. A close look of the partial permeation fluxes (Fig. 4-11) shows that at a given feed concentration, there is a slight increase in water flux with the addition of MWNTs in the membrane, whereas the opposite is true for the partial flux of ethylene glycol. While such changes in the partial fluxes may seem to be small, they are not insignificant at low feed water concentrations. This is shown more clearly in Fig. 4-12, where the addition of MWNTs in the membrane improved the separation factor considerably at a feed water concentration below 7 wt%. As shown before, although the presence of MWNTs in the membrane did not change the bulk water uptake in the membrane, it increased the surface hydrophilicity of membrane significantly. At low feed water concentrations, the water molecules are surrounded by ethylene glycol molecules, and the membrane surface is not readily accessible to water. Thus the enhanced hydrophilicity of the membrane surface becomes increasingly important for water sorption onto the membrane.

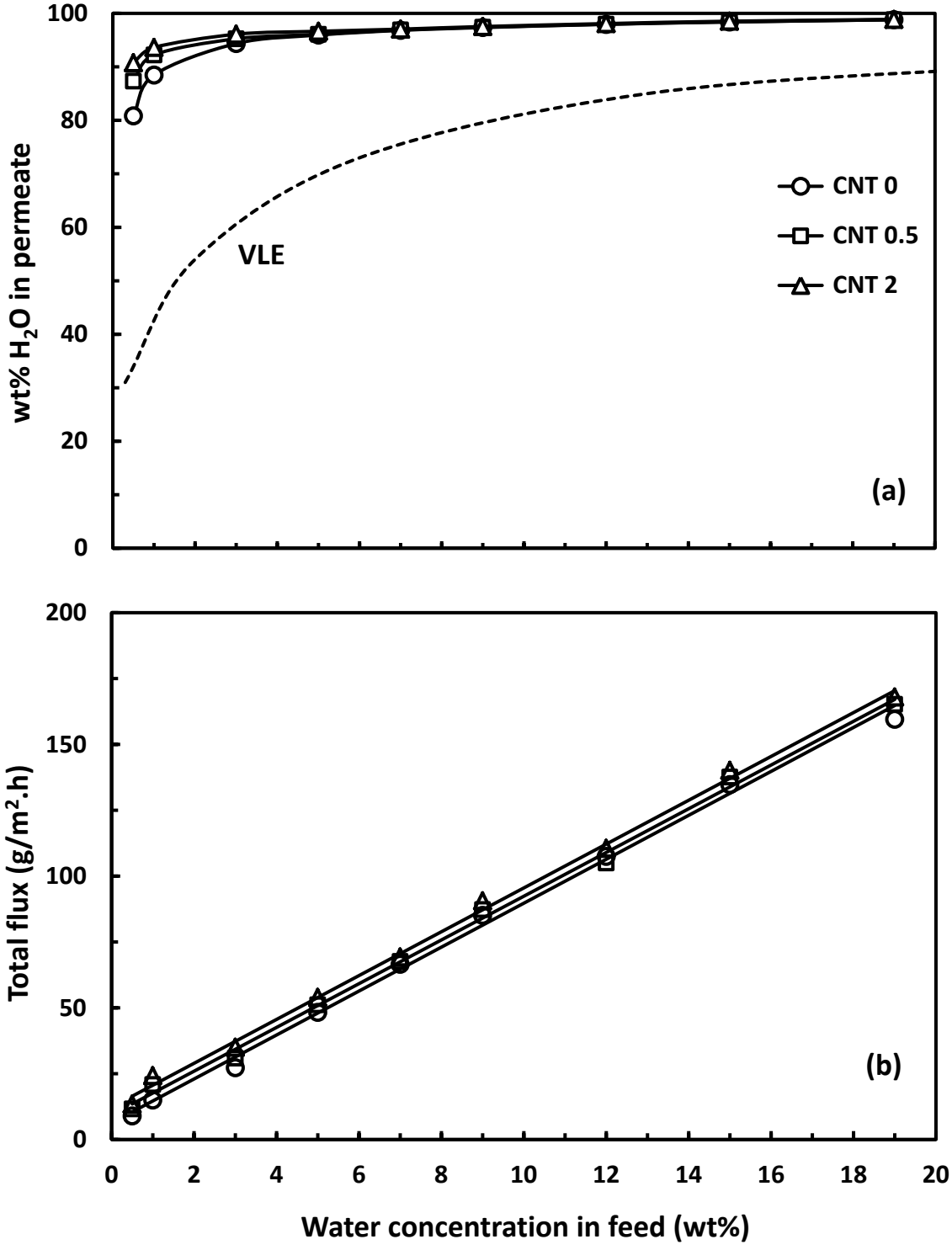


Fig. 4-10 Effect of CNT contents in the PVAm-PVA/CNT composite membranes on water concentration in permeate (a) and total permeation flux (b) at different feed water concentrations. Temperature: 38 ℃. The dotted line represents vapor-liquid equilibrium (VLE) data of binary ethylene glycol/water mixtures.

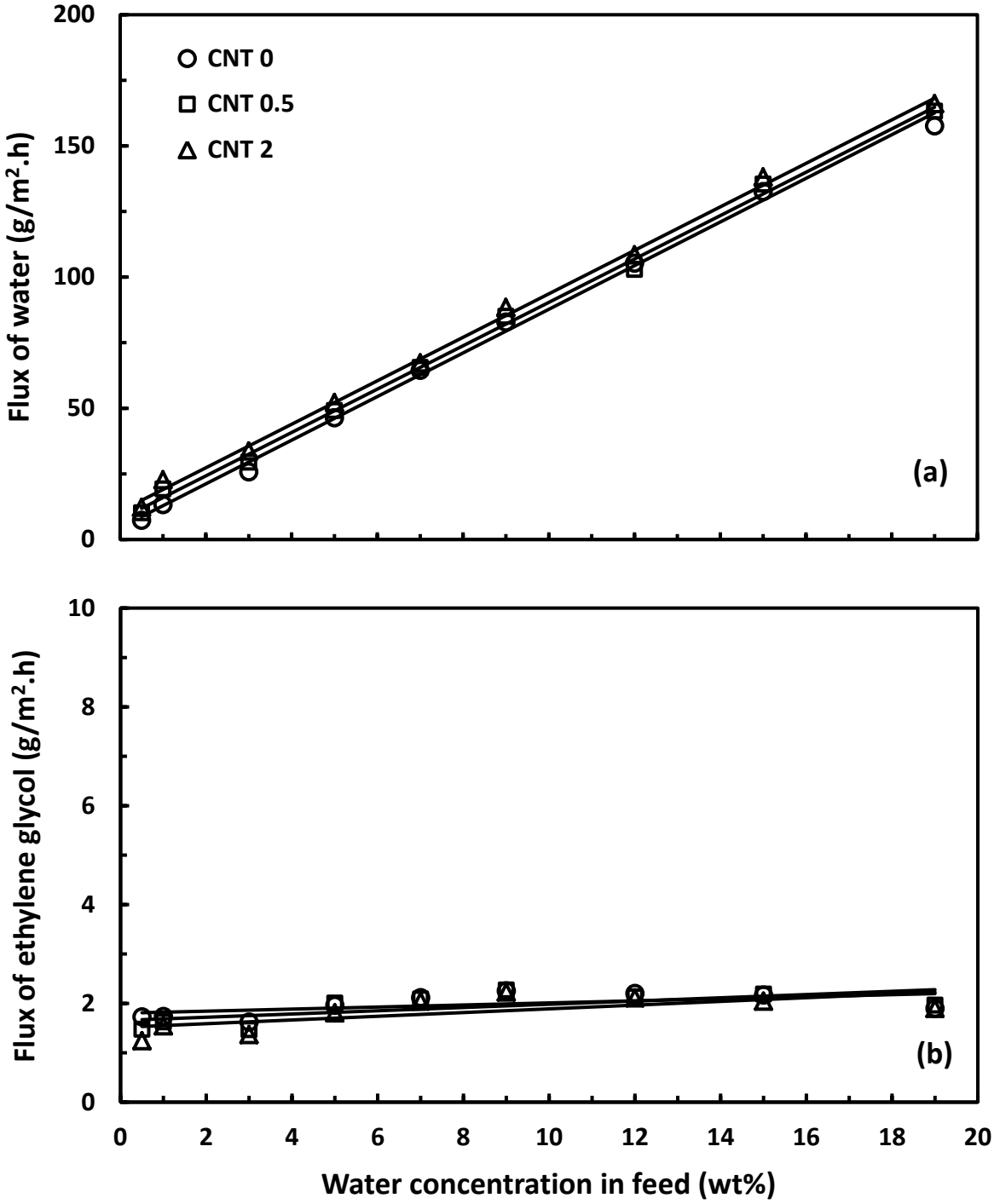


Fig. 4-11 Partial permeation fluxes of water (a) and ethylene glycol (b) through PVAm-PVA/CNT composite membranes with various CNT contents at different feed water concentrations. Temperature: 38 ℃.

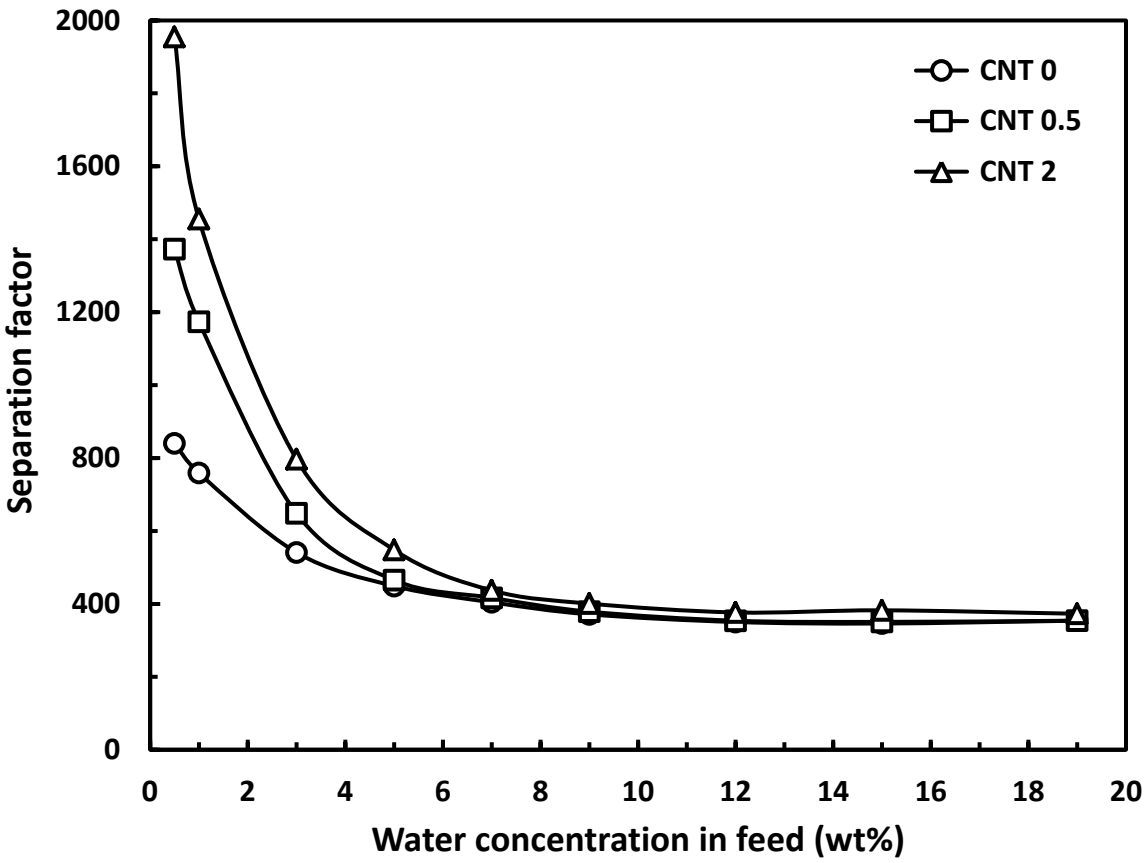


Fig. 4-12 Separation factor for dehydration of ethylene glycol using PVAm-PVA/CNT composite membranes with different CNT contents. Temperature: 38 ℃.

In order to further determine the effects of operating temperature on the separation performance of the MWNT-containing membranes, pervaporation experiments were carried out at different temperatures and at a water concentration of 1 wt% in the feed. The permeation fluxes of water and ethylene glycol and the separation factor are plotted in Fig. 4-13 and 4-14, respectively. At 30℃, the water permeation flux increased from 7.4 (with membrane CNT 0) to 11.5 (with membrane CNT 0.5) and 15.3 (with membrane CNT 2) g/($m^2$.h), and the separation factor also experienced an increase from 955 to 1410 and 1700, respectively. When the water concentration in the feed is sufficiently low, the permeation is more sensitive to the improved hydrophilicity caused by the addition of MWNTs, and thus an increase in water permeation flux and separation factor is expected. However, at a high feed water concentration for which a large

number of water molecules are readily available for sorption onto the membrane surface at the feed side, the increased surface hydrophilicity of the membrane due to the addition of MWNTs will not be as important to the preferential sorption of water onto the membrane surface, and the selective permeation of water would no longer be influenced significantly by the presence of MWNTs in the membrane.

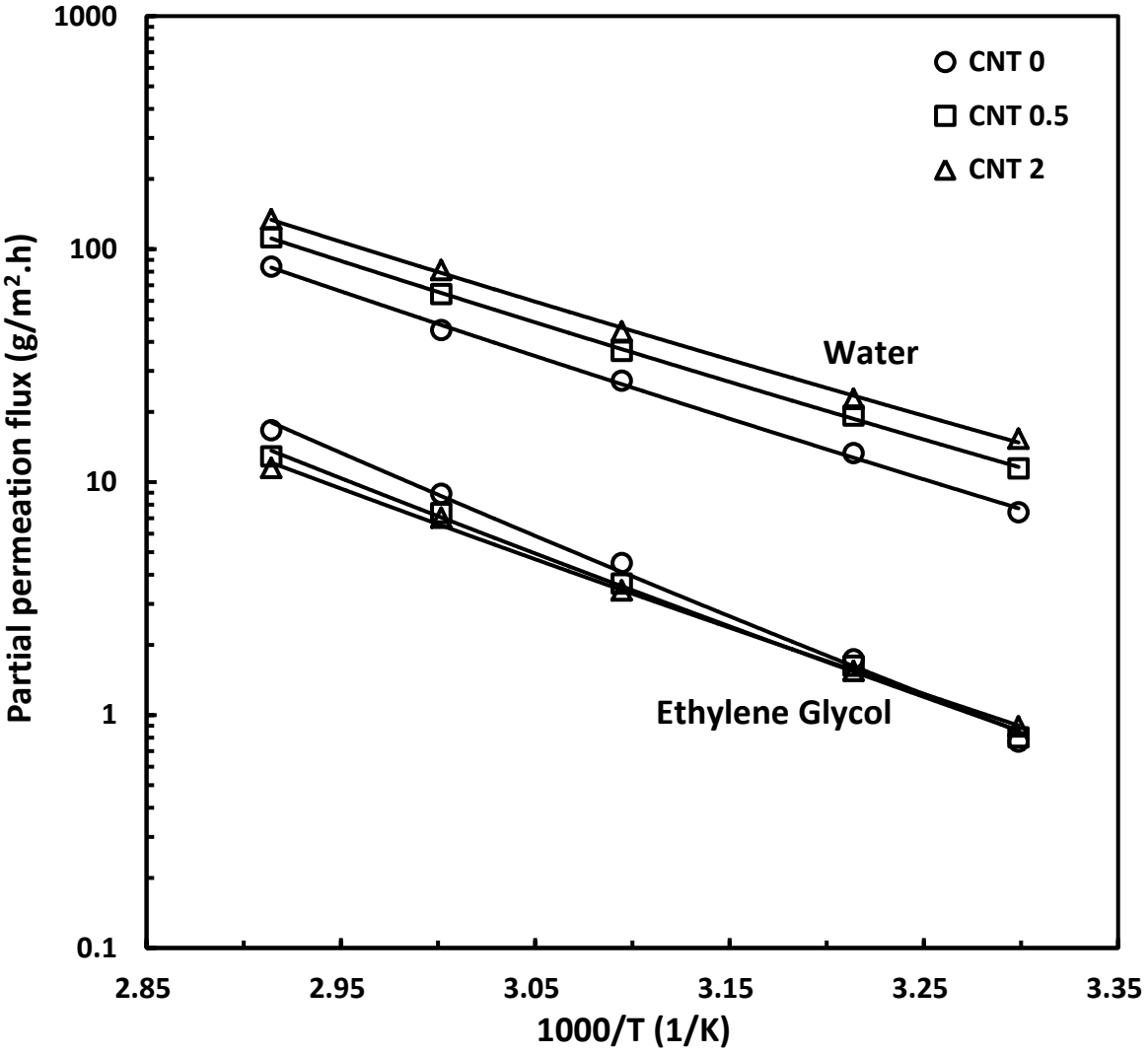


Fig. 4-13 Temperature dependence of permeation flux through PVAm-PVA/CNT composite membranes with different CNT contents. Feed water content: 1 wt%.

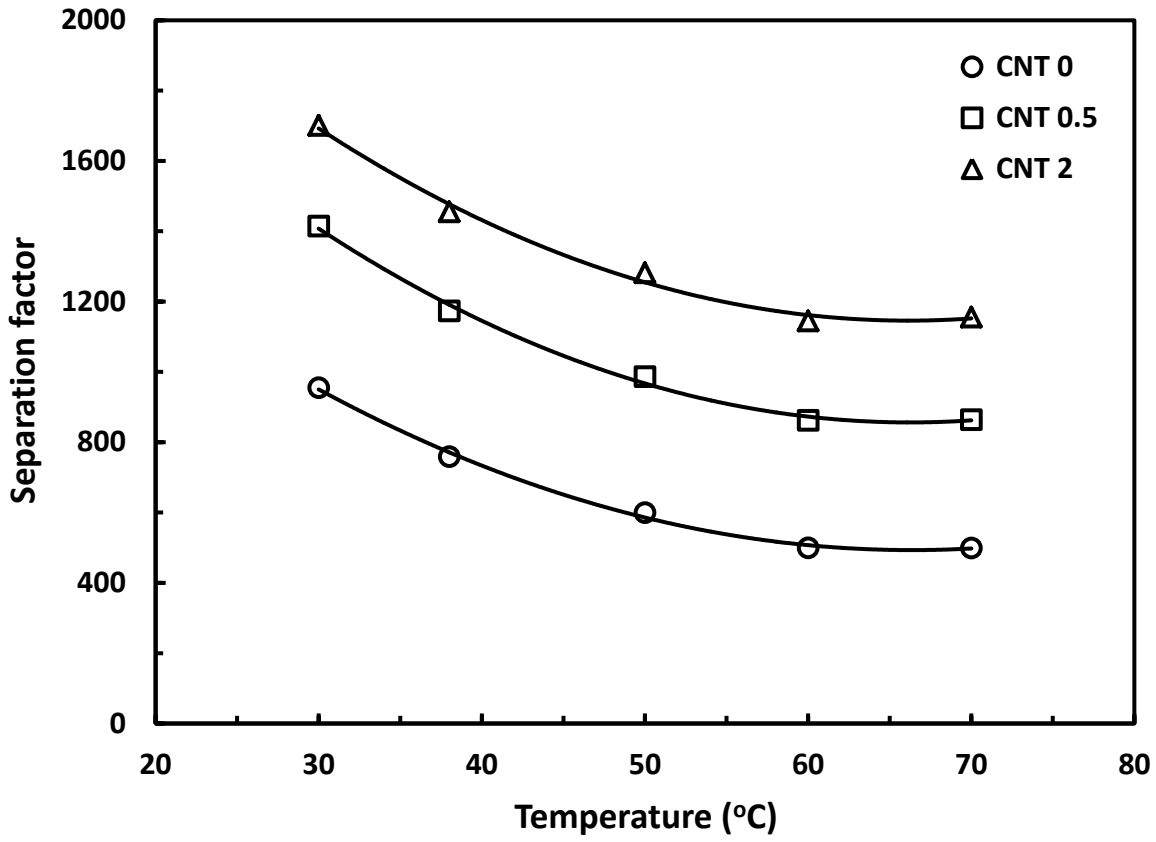


Fig. 4-14 Separation factor of PVAm-PVA/CNT composite membranes with different CNT contents for dehydration of ethylene glycol. Feed water content: 1 wt%.

Table 4-2 shows a ballpark comparison of the pervaporative performance of PVAm-PVA/CNT composite membrane developed in this study with other hydrophilic membranes reported in the literature. Ideally, the comparison should be done under identical operating conditions (i.e., feed composition, temperature), but it is difficult because of the lack of the performance data under same conditions. Nonetheless, these PVAm-PVA/CNT composite membranes are shown to compare favorably with other membranes for dehydration of ethylene glycol.

Table 4-2 Membrane performance for pervaporation

| Membrane | Feed mixture | Feed T (℃) | Feed water content (wt%) | Flux (g/m$^2$.h) | $\alpha$ | Reference |
|---|---|---|---|---|---|---|
| PAA-PEI polyelectrolytes on PA support | Water-EG | 40 | 3 | 400 | 340 | [Xu *et al.*, 2010a] |
| PVA on PES support | Water-EG | 80 | 17.5 | 231 | 402 | [Chen and Chen, 1996] |
| PVA/MPTMS | Water-EG | 70 | 20 | 67 | 311 | [Guo *et al.*, 2007] |
| PVA-GPTMS/TEOS | Water-EG | 70 | 20 | 60 | 714 | [Guo *et al.*, 2006] |
| PAA-PVA IPN | Water-EG | 30 | 20 | 480 | 196 | [Burshe *et al.*, 1998] |
| PAAM-PVA IPN | Water-EG | 30 | 20 | 140 | 96 | [Burshe *et al.*, 1998] |
| PVA/CNT (2 wt% CNTs) | Water-ethanol | 40 | 10 | 50 | 780 | [Choi *et al.*, 2009] |
| PVA/CNT (2 wt% CNTs) | Water-isopropanol | 30 | 10 | 79 | 1794 | [Shirazi *et al.*, 2011] |
| PVAm-PVA/CNT (2 wt% CNTs) on PSf support | Water-EG | 70 | 1 | 146 | 1156 | This study |
| PVAm-PVA/CNT (0.5 wt% CNTs) on PSf support | Water-EG | 70 | 3 | 194 | 391 | This study |
| PVAm-PVA/CNT (2 wt% CNTs) on PSf support | Water-EG | 38 | 19 | 168 | 373 | This study |

## 4.4 Conclusions

PVAm-PVA/CNT nanocomposite membranes were prepared for the dehydration of ethylene glycol. The nanocomposite was characterized by contact angle measurement and sorption uptakes using dense films. The pervaporation performance of PVAm-PVA/CNT composite membranes was investigated, and the following conclusions can be drawn:

(1) The incorporation of acid-treated CNTs in the membrane increased the surface hydrophilicity of the membrane, while there was no significant change in its bulk liquid sorption uptake, presumably due to the small loading of the CNTs in the membrane that was insufficient to cause a considerable change in permeant solubility in the membrane.

(2) The PVAm-PVA/CNT composite membranes were selective to water permeation in the range of the feed water concentrations (0-20 wt%) that are of the industrial interest. With an increase in the feed water concentration, the permeation flux increased and the separation factor decreased.

(3) The temperature dependence of the permeation flux followed an Arrhenius type of relationship, and the effect of temperature on the permeation flux is mainly derived from its effects on the driving force for permeation.

(4) Incorporation of MWNTs into the membrane increased the permeation flux and the separation factor, and the impact of the MWNTs on the separation performance was particularly significant at low feed water concentrations.

(5) At 70℃, a permeation flux of 146 g/($m^2$.h) and a separation factor of 1160 were achieved at 1 wt% water in feed using a PVAm-PVA/CNT composite membrane containing 2 wt% MWNTs. The membrane performance compared favorably with other membranes reported in the literature.

# Chapter 5

## PVAm-PVA composite membranes incorporated with molecular amines for $CO_2$ separation

---

### 5.1 Introduction

As stated before, facilitated transport membranes have demonstrated promising potential in separating $CO_2$ from its gas mixtures. The use of reactive carriers offers the membrane with a high permselectivity since they can react selectively and reversibly with $CO_2$ molecules in the membrane. The most commonly used carriers for $CO_2$ permeation are amines, including polyamines with functional amine groups and molecular amines [Francisco *et al.*, 2007, 2010; Du *et al.*, 2010b]. The amine groups in polyamines are fixed on the polymer chains, and their mobility is limited and the permeating component needs to "hop" towards the permeate side from one carrier site to the next. However, this helps retain a good stability of the membrane since the carriers are fixed. On the other hand, mobile carriers like molecular amines tend to have a much higher mobility since they can diffuse more freely in the membrane. Nevertheless, the membrane instability issue is also quite severe due to solvent loss and carrier washout under a transmembrane pressure. In light of the above, research efforts were devoted to improving the facilitated transport membranes by using both molecular amines as mobile carriers and polyamines as fixed carriers [Zou and Ho, 2006; Yuan *et al.*, 2011; Qiao *et al.*, 2013]. Not only is

the overall mobility of the carriers enhanced due to the inclusion of the mobile carriers, but the stability of the membrane is also improved because the intermolecular interactions between the mobile carriers and the polyamines help retain the mobile carriers in the membrane.

Several molecular amines used as carriers in facilitated transport of $CO_2$ from its mixtures have been investigated, including monoethanolamine (MEA) [Teramoto *et al.*, 1996; Francisco *et al.*, 2007; Gorji and Kaghazchi, 2008], diethanolamine (DEA) [Guha *et al.*, 1990; Saha and Chakma, 1995; Francisco *et al.*, 2010], ethylenediamine (EDA) [Yuan *et al.*, 2011] and piperazine (PZ) [Gorji and Kaghazchi, 2008; Qiao *et al.*, 2013]. PZ has two secondary amine groups attached to a heterocyclic and noncoplanar structure. The advantage of using a secondary amine as a facilitating agent is the ease of reversibility of the chemical reaction between secondary amine and $CO_2$ [Bao and Trachtenberg, 2006]. Although primary amines can react with $CO_2$ quickly, the binding constant is high and the dissociation to release $CO_2$ is difficult, whereas the reactions between tertiary amines and $CO_2$ are normally slow. Gorji and Kaghazchi [2008] prepared facilitated transport membranes containing aqueous MEA, DEA, EDA and PZ solutions to study the separation performance for $CO_2$ removal from $H_2$. PZ was shown to be the best facilitating agent among the four amines because of its moderate reaction equilibrium constant derived from both a high forward and reverse reaction rates. Moreover, crosslinked PVAm membranes containing piperazine were fabricated and investigated for $CO_2/N_2$ separation [Qiao *et al.*, 2013], and piperazine was shown to be well fixed in the membrane due to intermolecular hydrogen bonding between the secondary amine group of piperazine and the primary amine group in PVAm. The incorporation of piperazine in the membrane resulted in a large increase in the effective carrier concentration and low crystallinity, leading to a high $CO_2/N_2$ permselectivity.

Generally speaking, three major factors, including reaction rate, $CO_2$ loading capacity and ease of regeneration, should be considered to select a particular amine for facilitated transport of $CO_2$. Primary and secondary amines tend to react rapidly with $CO_2$ to form carbamates, but the $CO_2$ loading capacity is limited to 0.5 mol of $CO_2$ per mol of amine based on the overall reaction stoichiometry. Moreover, the heat of absorption related to the carbamate formation is high, which means it is difficult to dissociate for $CO_2$ release. On the other hand, because of the absence of hydrogen atom attached to the nitrogen atom in tertiary amines, the carbamate formation cannot take place, leading to a low reactivity with $CO_2$. Instead, tertiary amines facilitate the hydration of $CO_2$ in the presence of water and form bicarbonates. The heat of formation of bicarbonates is much lower than that of carbamate formation, and thus $CO_2$ release and solvent regeneration are easier to achieve. Moreover, tertiary amines have a high $CO_2$ loading capacity (i.e., 1 mol of $CO_2$ per mol of amine). In an attempt to improve the efficiency of facilitated transport of $CO_2$, mixed amine systems have attracted attention [Glasscock *et al.*, 1991; Al Marzouqi *et al.*, 2005; Vaidya and Kenig, 2007; Gorji and Kaghazchi, 2008]. The mixed amine systems are typically composed of a tertiary amine and a primary or secondary amine. It is thus expected that the mixed amine system will combine the higher reaction rates between $CO_2$ and primary or secondary amines and the higher $CO_2$ loading capacities and easier regeneration associated with the use of tertiary amines. It has been reported that the $CO_2$ absorption rates of tertiary amines can be enhanced by the addition of primary or secondary amines [Vaidya and Kenig, 2007]. Representative tertiary amines used in industries mainly include methyldiethanolamine (MDEA) and triethanolamine (TEA). The $CO_2$ absorption kinetics of the mixed amine solutions such as MEA/MDEA [Hagewiesche *et al.*, 1995; Mandal *et al.*, 2001], DEA/MDEA [Zhang *et al.*, 2002b], PZ/MDEA [Zhang *et al.*, 2001, 2003; Bishnoi and Rochelle, 2002] and MEA/TEA [Rangwala *et al.*, 1992;

Horng and Li, 2002] have been investigated. However, to our knowledge, facilitated transport membranes employing mixed amines for separating $CO_2$ are still lacking, needless to say the study of membranes consisting of polyamines combined with mixed molecular amines.

Thus, the objective of this chapter is to study facilitated transport membranes comprising of both polyamines (i.e., PVAm) and a single and mixed molecular amines (i.e., PZ, TEA and MDEA alone, as well as PZ/TEA and PZ/MDEA amine pairs) as carriers for $CO_2/N_2$ separation. First, PZ was incorporated into the PVAm/PVA polymer blends to prepare the PVAm-PVA/PZ composite membranes in view of the following: (1) the increase of the total carrier concentration and carrier mobility as the incorporation of PZ may increase the $CO_2$ permselectivity of the membrane; (2) the potential intermolecular hydrogen bonds formed between the secondary amine groups of PZ and primary amine groups of PVAm or hydroxyl groups of PVA may help densify the polymer matrix and retain the small molecular PZ within the polymer matrix, thereby maintaining a good stability of the membrane. Hence, the potential hydrogen bond formation between PZ and PVAm or PVA was characterized by attenuated total reflectance infrared (ATR-FTIR) spectroscopy. The morphology of the PVAm-PVA/PZ composite membranes was examined under scanning electron microscopy (SEM). The effects of PZ concentration in the membrane and polymer concentration in the coating solution on the separation performance of the composite membranes were studied for pure gas permeation. Then binary gas permeation, which is relevant to separation of gas mixtures, was conducted. The effect of feed $CO_2$ composition on the separation performance was investigated and the stability of the membrane for $CO_2/N_2$ separation was evaluated using a simulated flue gas containing 15.3 mol% $CO_2$ (balanced $N_2$). In addition, PVAm-PVA/PZ composite membranes were further modified by adding a tertiary amine (i.e., using mixed molecular amines, PZ/TEA and PZ/MDEA) in order to

study the effectiveness of using mixed secondary/tertiary amines. Therefore, the composite membranes with different mass ratios of PZ/TEA and PZ/MDEA were fabricated and tested for $CO_2/N_2$ separation based on pure gas and binary gas permeation.

## 5.2 Experimental

### 5.2.1 Materials

Piperazine (PZ), triethanolamine (TEA) and *N*-methyldiethanolamine (MDEA) with purities of 99% were supplied by Sigma Aldrich, BDH Chemicals and Acros Organics, respectively. The chemical structures of these molecular amines are shown in Fig. 5-1. Polyethersulfone (PES) ultrafiltration membrane with a molecular weight cutoff of 10,000 was provided by Sepro Membranes. Other materials were the same as used before.

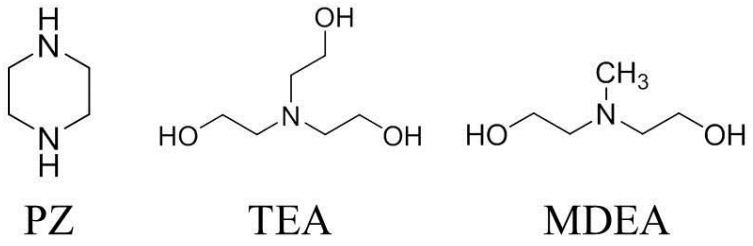


Fig. 5-1 Chemical structures of the molecular amines

### 5.2.2 Membrane preparation

The procedure for preparation of PVAm-PVA/amine composite membranes was similar to that described previously in Chapter 3 except that a PES ultrafiltration membrane was used as the substrate to form composite membranes in this part of the study. The mass ratio of PVAm to PVA in the membrane casting solution was kept at 60/40, and the overall polymer concentration was 5 wt% unless specified otherwise. Several single and mixed molecular amines (i.e., PZ, TEA, MDEA, PZ/TEA and PZ/MDEA) were used, and the mass ratio of amine to polymer was

varied: 20/100, 50/100, 100/100, 150/100 and 200/100. In the mixed amine case, the mass ratio of total amine (i.e., PZ plus TEA or PZ plus MDEA) to polymer was maintained at 100/100, and the mass ratios of PZ to TEA and PZ to MDEA were varied as follows: 80/20, 67/33, 50/50, 33/67 and 20/80. For the fabrication of all the PVAm-PVA/amine composite membranes, only one coat of the casting solution was found effective to prepare defect-free membranes.

### 5.2.3 Membrane characterization

The PVAm-PVA/PZ composite membranes with different PZ contents were characterized by attenuated total reflectance infrared (ATR-FTIR) spectroscopy (Bruker Tensor 27). Surface scanning electron microscopy (SEM) images of the PVAm-PVA/PZ composite membranes were examined using QUANTA 200, FEI COMPANY.

### 5.2.4 Gas permeation measurement

The experimental setup for binary gas mixture permeation experiments is shown in Fig. 5-2. The PVAm-PVA/amine composite membrane was mounted in the permeation cell with an effective permeation area of 22.90 $cm^2$. The feed gas, saturated with water vapor through a humidifier, was admitted to the permeation cell, and the residue stream was controlled by a needle valve. The permeate gas exited at atmospheric pressure. The operating temperature was kept at 24℃ unless specified otherwise. The feed gas mixture was prepared by using a dynamic gas blending system comprised of two Matheson mass flow controllers (Model 8270). To evaluate the effects of amine content in the membrane on the membrane performance as well as the membrane stability, a pre-mixed binary gas mixture containing 15.3% $CO_2$ (balanced $N_2$) supplied by Praxair was used as the feed. During the tests, a relatively high residue flow rate (about 200 $cm^3$(STP)/min) was used in order to minimize the concentration polarization. The

flow rates of the residue and permeate streams were measured by bubble flow meters. The compositions of the feed, residue and permeate streams were analyzed by an online Agilent gas chromatograph (Model 6890N) equipped with a Supelco packed column (60/80 mesh Carboxen-1000, 15′×1/8′) and a thermal conductivity detector. Quantitative evaluation was carried out by external calibration using standard samples of known concentrations. The permeance ($J_i$) of an individual component in the gas mixture through the membrane was given by:

$$J_i = \frac{Vy_i}{At\Delta p_i} = \frac{Vy_i}{At(p_f x_i - p_p y_i)} \tag{5-1}$$

where $V$ is the volume of the permeate collected (corrected to the standard state) over a period of time $t$, $A$ the effective area of the membrane, $x_i$ and $y_i$ the mole fraction of gas $i$ in the feed and the permeate, respectively, $p_f$ the feed pressure and $p_p$ the permeate pressure. The membrane selectivity was measured in terms of the $CO_2$ to $N_2$ permeance ratio. The permeation data reported here was averaged with replicate membrane samples from different batches, and the reproducibility was very good with a batch to batch variation within 8%.

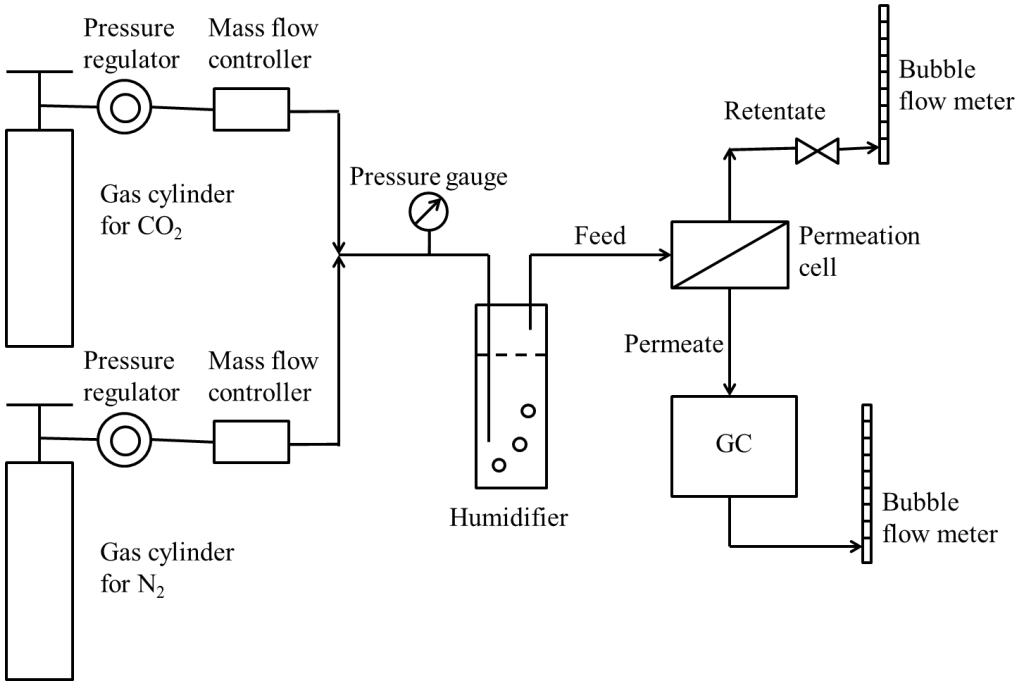


Fig. 5-2 Schematic diagram of experimental setup for binary gas permeation

## 5.3 Results and discussion

### 5.3.1 Membrane characterization

The structures of the PVAm-PVA/PZ composite membranes with different PZ contents were studied using ATR-FTIR and the spectra were shown in Fig. 5-3. It is clear that the characteristic band of PZ at around 996 $cm^{-1}$ ascribed to the C-N stretching vibration [Gunasekaran and Anita, 2008; Qiao *et al.*, 2013] appears in the spectra of PVAm-PVA/PZ membranes containing PZ. In addition, the intensity of this band increases accordingly with an increase in the PZ content in the membrane. Moreover, the band at 1585 $cm^{-1}$ (-$NH_2$ bending) [Deng *et al.*, 2009] shifts to lower wavenumbers with increasing the PZ content in the membrane, indicating that there are indeed intermolecular interactions between the polymer and the PZ molecules. Since there are no chemical reactions between the polymer (i.e., PVAm and PVA) and PZ, it can thus be deduced that the hydrogen bonds between primary amine groups from PVAm and secondary amine groups from PZ are formed and the intermolecular interactions become stronger at a higher PZ content in the membrane.

Fig. 5-4 displays the surface image of the PVAm-PVA/PZ composite membrane, and the surface of the composite membrane is smooth and defect-free.

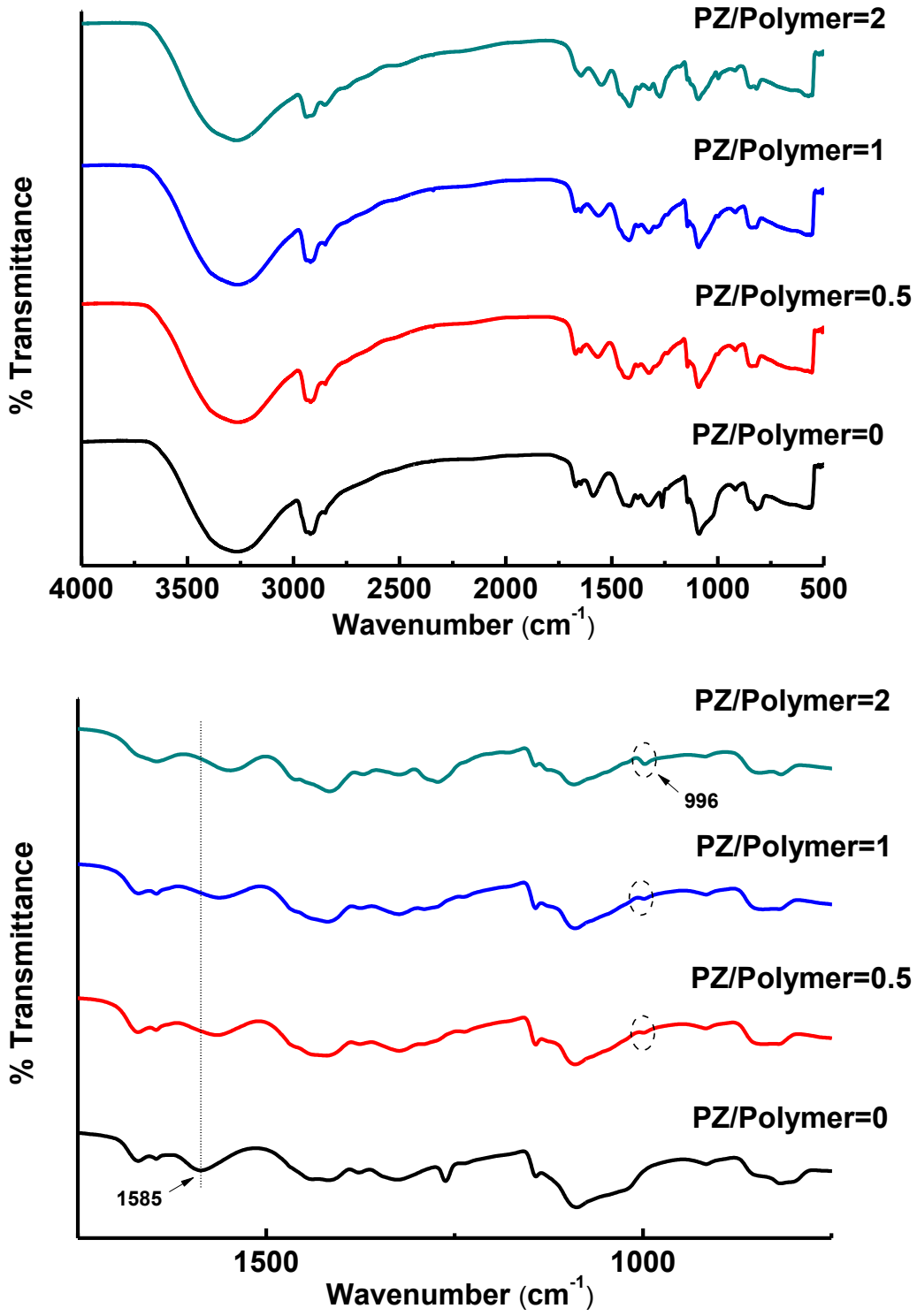


Fig. 5-3 ATR-FTIR spectra of PVAm-PVA/PZ composite membranes with different PZ contents (represented by the PZ/Polymer mass ratio)

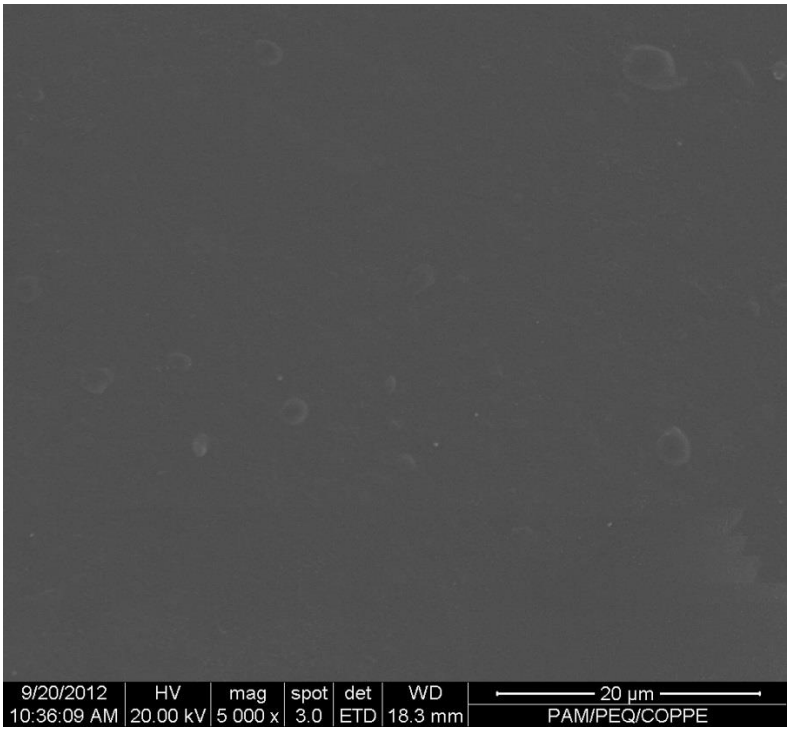


Fig. 5-4 SEM image of PVAm-PVA/PZ membrane surface. PZ content in the membrane: PZ/polymer mass ratio=1.

### 5.3.2 Gas transport facilitated by single amine

To verify the effectiveness of incorporating PZ into the membrane, pure gas permeation in the PVAm-PVA/PZ composite membranes with different mass ratios of PZ to polymer (i.e., PVAm plus PVA) were conducted. The $CO_2$ permeance, $N_2$ permeance and $CO_2/N_2$ selectivity of the membranes at different PZ contents are illustrated in Figs. 5-5 and 5-6.

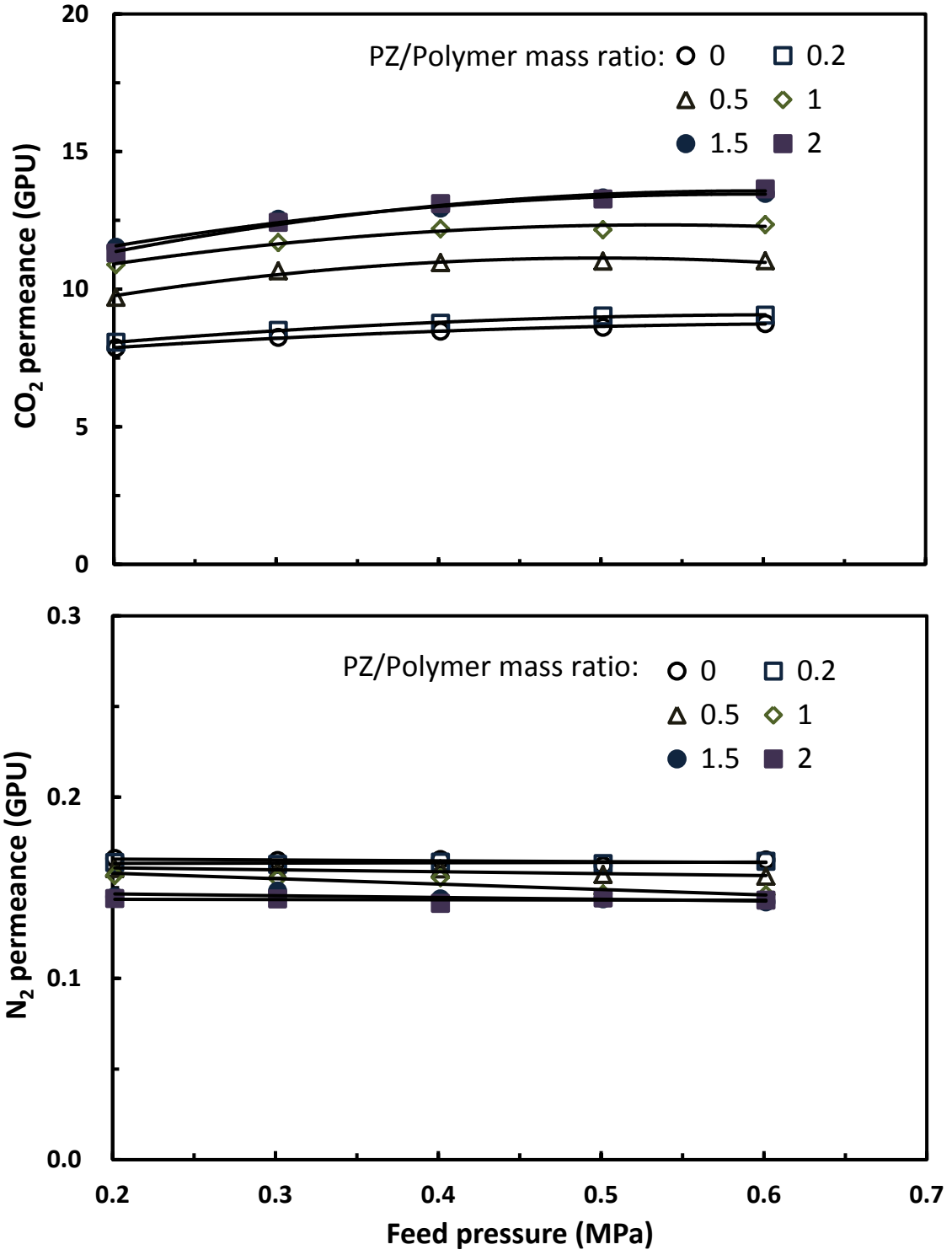


Fig. 5-5 Effect of PZ content (PZ/Polymer mass ratio) on the permeance of $CO_2$ and $N_2$ for pure gas permeation through PVAm-PVA/PZ composite membranes. Polymer concentration in the coating solution: 7.5 wt%.

As shown in Fig. 5-5, the $CO_2$ permeance of the membranes increases with the $CO_2$ pressure initially, and then levels off when the $CO_2$ pressure is high enough. However, the $N_2$

permeance is essentially independent of the gas pressure under the experimental conditions tested. This is understandable based on the following. On one hand, $N_2$ transports through the membrane via the physical solution-diffusion mechanism. Nevertheless, besides the simple molecular diffusion, $CO_2$ transport in the membrane also occurs in the carrier-mediated mode due to the amine groups acting as carriers to facilitate the $CO_2$ transport. On the other hand, water plays a key role in the gas transport [Liu *et al.*, 2008]. The permeation of a gas molecule through a water-swollen membrane normally includes two parts: one through polymer matrix and the other through water channels. It's expected that the transport of $CO_2$ facilitated by the amine carriers can be enhanced by the hydration of $CO_2$, and the transport of $CO_2$ through water channels can be improved by the amine carriers in the membrane. More importantly, these interactions are believed to be more significant for $CO_2$ permeation at higher concentrations [Du *et al.*, 2010b]. However, with an increase in $CO_2$ concentration, the amine carriers in the membrane will be gradually saturated with the $CO_2$ molecules, which in turn restrict them from further uptake of $CO_2$. Because there is no interactions between $N_2$ and amine carriers in the membrane, $N_2$ permeance remains unchanged with an increase in nitrogen pressure.

Fig. 5-5 shows that the permeance of $CO_2$ in the PVAm-PVA/PZ membranes is greater than that in the PVAm/PVA membranes containing no PZ, indicating that PZ does facilitate the transport of $CO_2$ in the membrane. However, the $CO_2$ permeance does not increase monotonically with an increase in the PZ content in the membrane. It increases up to some point and then levels off when the PZ content is high enough (i.e., PZ to polymer mass ratio above 1.5). This is not unexpected. Additional amine carriers from the molecular amines will enhance the solubility of $CO_2$ in the membrane, and the molecular amine carriers also tend to have a higher mobility than the polyamines, which help improve the diffusivity of $CO_2$-amine

complexes in the membrane. Thus, the PVAm-PVA/PZ membranes exhibited a higher $CO_2$ permeance than the PVAm/PVA membranes without PZ. With an increase in the PZ content in the membrane, more amine carriers will be available to facilitate transport of $CO_2$. On the other hand, in the reactions of $CO_2$ and amines, ionic species are formed (i.e., zwitterions, carbamates, bicarbonates or protonated amines). The ionic strength of the membrane increases with an increase in the PZ content in the membrane, which not only lowers the solubility of $CO_2$ due to the salting out effects but also decreases the diffusivity of $CO_2$-amine complexes in the membrane, leading to a reduction in the $CO_2$ permeance. These opposing effects determine whether the $CO_2$ permeance increases or decreases with an increase in the PZ content in the membrane. For the permeation of $N_2$, it is noticed that the $N_2$ permeance slightly decreases with an increase in the PZ content. Because of the small molecular size of PZ, the PZ molecules may occupy the space between the polymer chains, resulting in a reduction in the free volume of the polymer. In addition, the interactions between PZ and the polymer matrix due to hydrogen bonding may also densify the polymer matrix. Since $N_2$ does not interact with either amines or polymer matrix chemically, the densification of the polymer matrix will cause the reduction of $N_2$ permeance as well.

The variations in $CO_2$ and $N_2$ permeance with respect to feed pressure and PZ content in the membrane is reflected in the $CO_2/N_2$ selectivity, as illustrated in Fig. 5-6. All the membranes show a higher selectivity at a higher feed pressure. Furthermore, the PVAm-PVA/PZ composite membranes outperform the amine-free PVAm/PVA composite membranes in terms of the $CO_2/N_2$ selectivity, and a higher PZ content in the membrane tends to result in a better $CO_2/N_2$ selectivity.

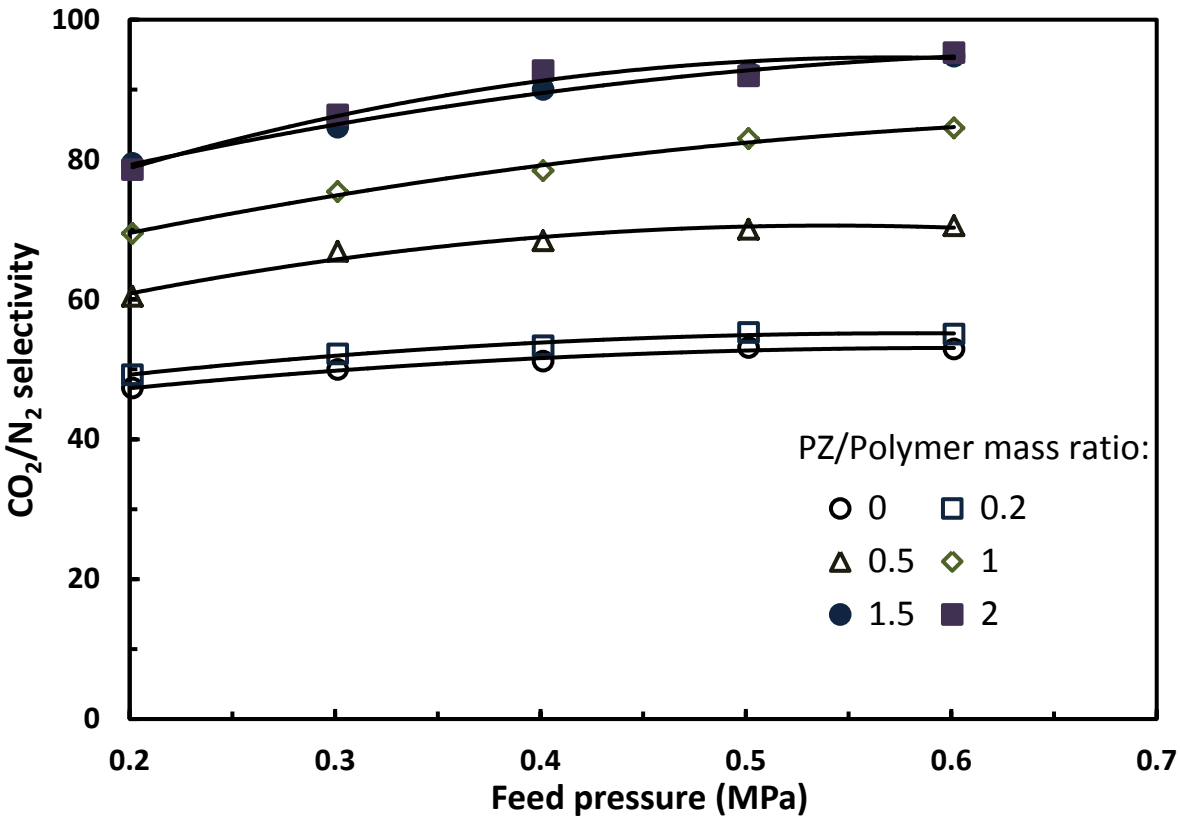


Fig. 5-6 Effect of PZ content (PZ/Polymer mass ratio) on $CO_2/N_2$ selectivity based on pure gas permeation. Polymer concentration in the coating solution: 7.5 wt%.

It should be noted that the PVAm-PVA/PZ composite membrane with a PZ to polymer mass ratio of 1 was used in subsequent investigations. The tertiary amines (i.e., TEA and MDEA) to be used in the mixed amine system are alkanolamines with both amine and hydroxyl groups, which are expected to have stronger interactions with PVAm-PVA polymer matrix than PZ, which contains only amine groups. Moderate interactions between molecular amines and the polymer matrix are desired to retain the small molecular amines in the polymer matrix to act as the $CO_2$ carriers properly. Nevertheless, if the interactions become too strong, the densification of the polymer matrix may become important, which may impose a negative impact on the gas permeance. Thus, based on the above considerations, the PVAm-PVA/PZ composite membrane with a PZ to polymer mass ratio of 1 was chosen for further studies.

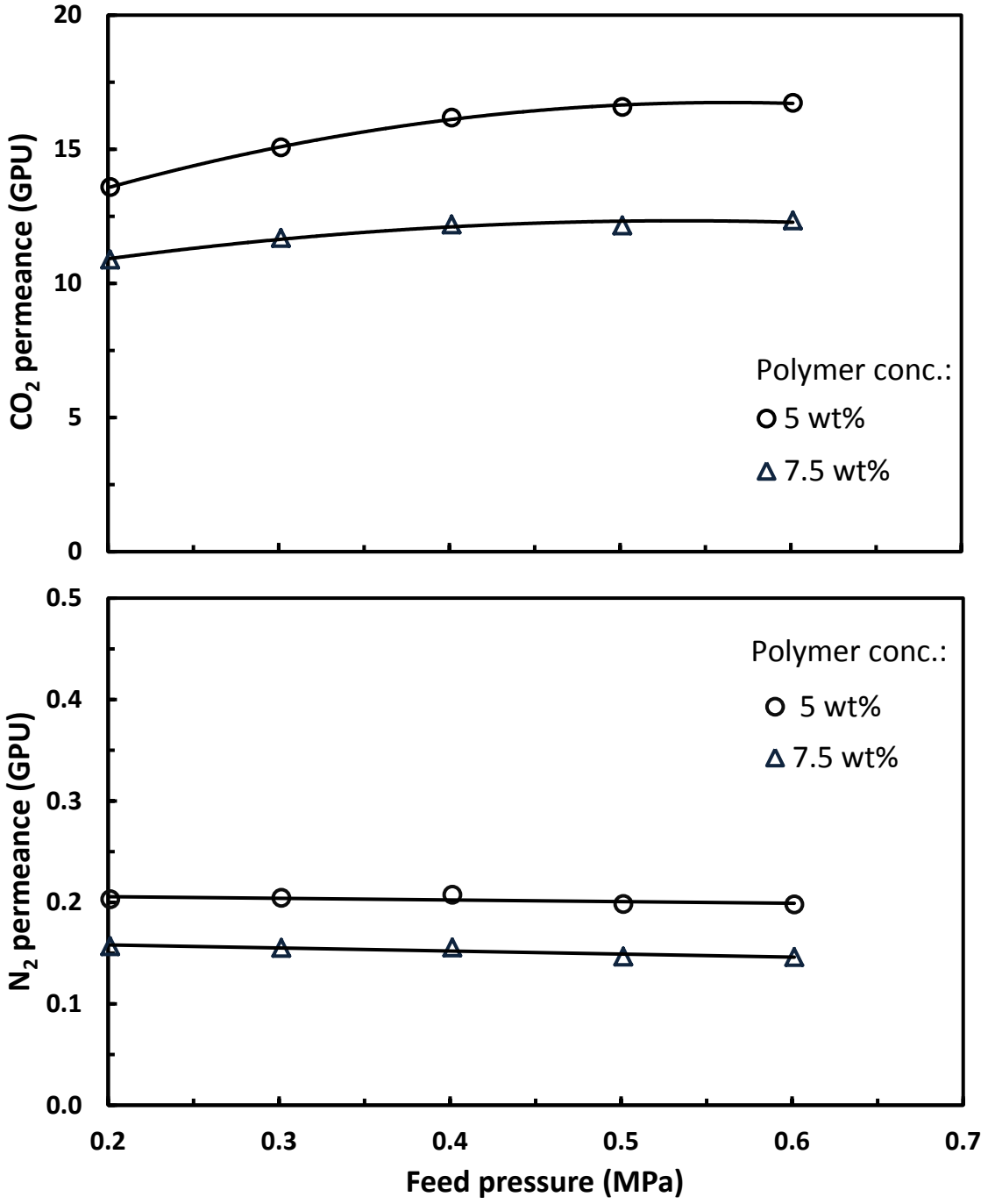


Fig. 5-7 Permeance of $CO_2$ and $N_2$ in PVAm-PVA/PZ composite membranes prepared using different polymer concentrations. PZ content in the membrane: PZ/polymer mass ratio=1.

In order to obtain a higher $CO_2$ permeance, the PVAm-PVA/PZ composite membrane with thinner selective layer was prepared by reducing the concentration of the polymer coating

solution. The thickness of the skin layer in the composite membrane is affected by the concentration of the coating solution. Hence, two polymer concentrations (i.e., 7.5 and 5 wt%) were used here. It's expected that the composite membrane prepared using a lower polymer concentration solution will have a higher gas permeance due to reduced thickness without compromising the $CO_2/N_2$ selectivity if the membrane remains defect-free.

Figs. 5-7 and 5-8 show the $CO_2$ permeance, $N_2$ permeance and $CO_2/N_2$ selectivity of the PVAm-PVA/PZ composite membranes (PZ/polymer mass ratio=1) fabricated using two different polymer concentrations in the coating solutions. It's obvious that both the $CO_2$ and $N_2$ permeance of the membrane prepared using a low polymer concentration are higher than the permeance of the membrane formed using a higher polymer concentration. Using the surface coating method, a lower polymer concentration will result in a thinner skin layer in the membrane and thus a higher gas permeance. However, if a membrane skin layer is very thin, defects are more likely to form on the membrane surface. Fig. 5-8 shows that the $CO_2/N_2$ selectivity of the two PVAm-PVA/PZ membranes formed using different polymer concentrations are essentially the same because both $CO_2$ and $N_2$ permeance experienced a 35% increase. This indicates that the PVAm-PVA/PZ composite membrane prepared by using a low polymer concentration solution (i.e., 5 wt%) is defect-free. This shows that the membrane permeance can be improved without compromising the membrane selectivity by properly controlling the membrane formation conditions.

It should be noted that the polymer concentration solution of 5 wt% was used to prepare the PVAm-PVA/PZ composite membranes in the following investigations unless otherwise specified.

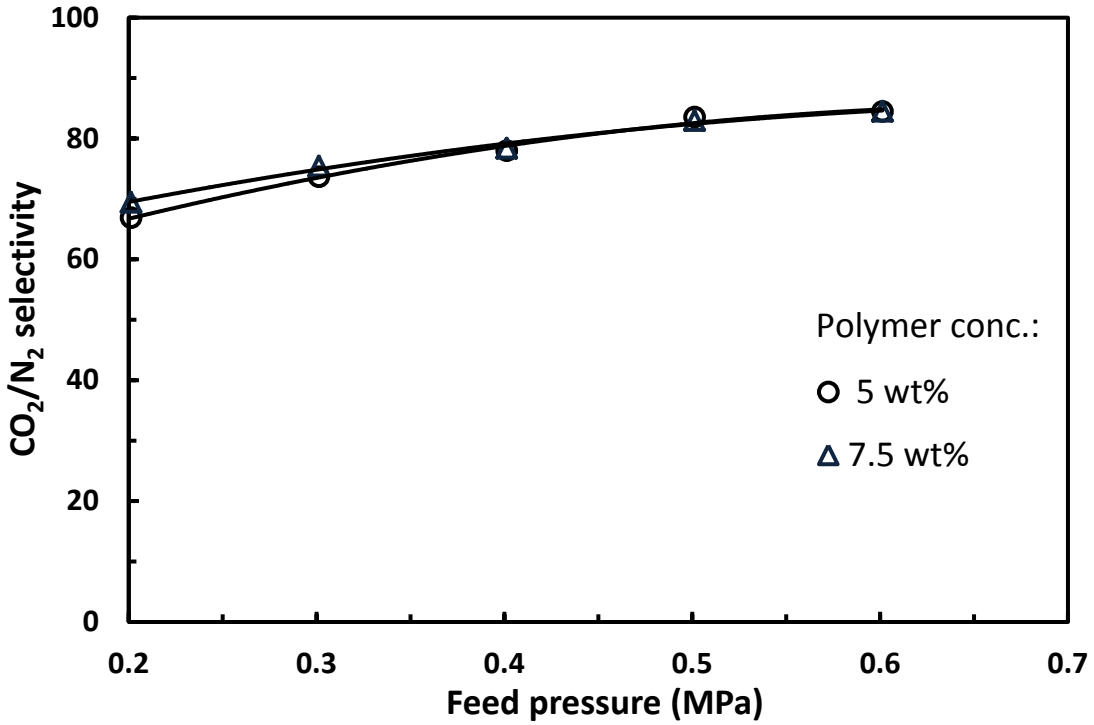


Fig. 5-8 $CO_2/N_2$ selectivity based on pure gas permeation in PVAm-PVA/PZ composite membranes prepared using two different polymer concentrations. PZ content in the membrane: PZ/polymer mass ratio=1.

To study the effect of temperature on the gas permeance and selectivity, the PVAm-PVA/PZ membrane was tested for $CO_2$ and $N_2$ permeation at temperatures ranging from 24 to 65 ℃ and transmembrane pressures from 0.1 to 0.5 MPa. The results are shown in Fig. 5-9. The permeance of both $CO_2$ and $N_2$ increases with an increase in temperature, and the temperature dependence of the permeance appears to follow an Arrhenius type of relationship. However, $N_2$ permeance is affected by temperature more significantly, resulting in a reduction in $CO_2/N_2$ selectivity when temperature increases, as shown in Fig. 5-10. The activation energies for $CO_2$ and $N_2$ permeation were calculated from the slopes of the straight lines in Fig. 5-9, and they are shown in Fig. 5-11. It is evident that the activation energy for $CO_2$ permeation decreases when the transmembrane pressure increases, whereas the activation energy for $N_2$ permeation is basically constant in the same pressure range. Furthermore, the activation energy for $CO_2$ permeation is lower than that for $N_2$ permeation, indicating that $CO_2$ can permeate through the membrane more easily.

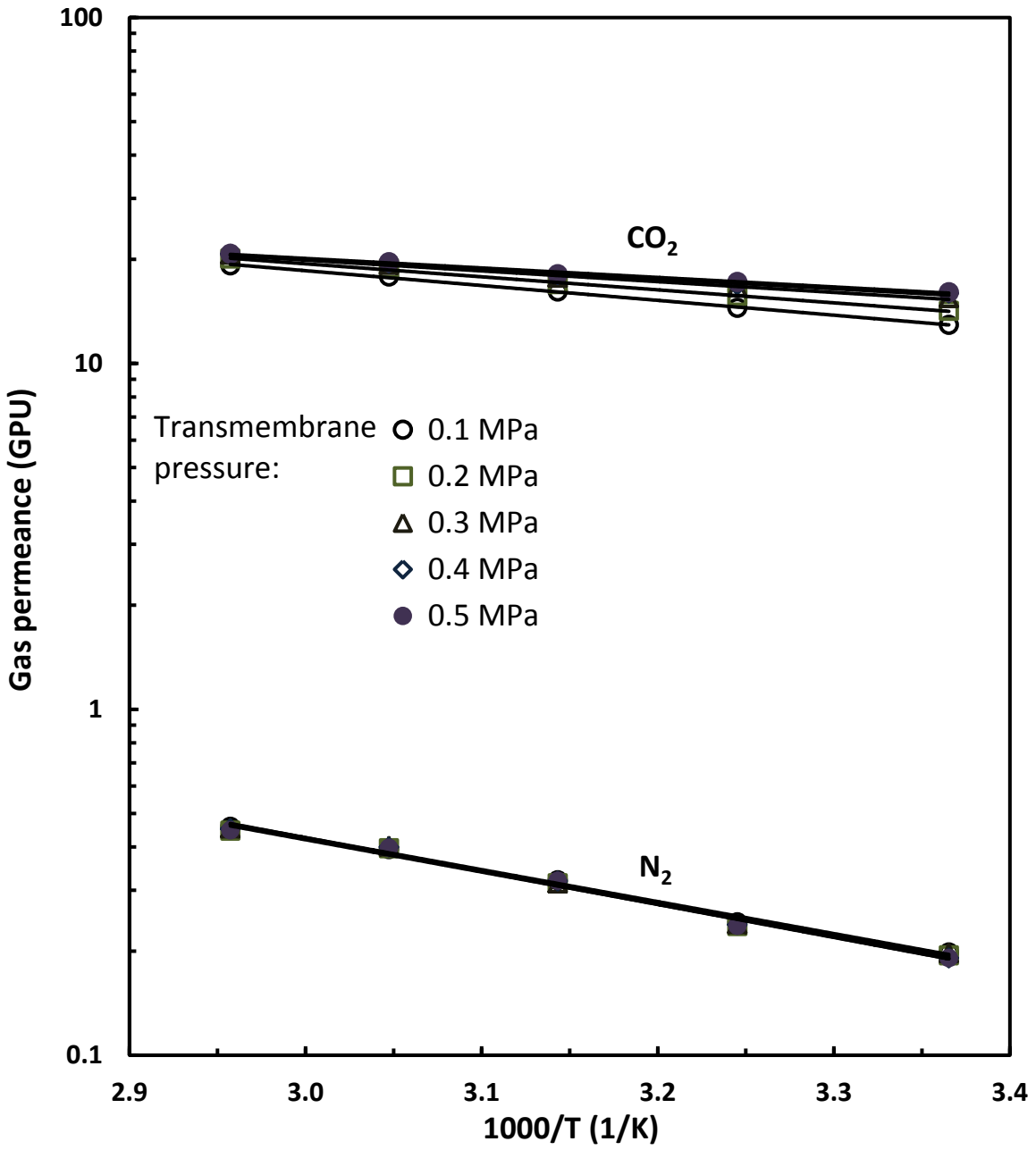


Fig. 5-9 Temperature dependence of the permeance of $CO_2$ and $N_2$ in PVAm-PVA/PZ composite membrane (prepared using a polymer concentration of 5 wt%). PZ content in the membrane: PZ/polymer mass ratio=1.

The solubility of $N_2$ in water is known to decrease with an increase in temperature, while the opposite holds for diffusivity. Since $N_2$ mainly transports through the membrane via physical solution-diffusion mechanism, the observed increase in $N_2$ permeance with an increase in temperature may suggest that the diffusivity is a stronger function of temperature than solubility,

which is in accordance with the temperature dependency of nitrogen solubility and diffusivity in water. For the permeation of $CO_2$ across the PVAm-PVA/PZ membrane, a chemical facilitation by the amine carriers occurs besides the physical solution-diffusion. Similarly, the solubility of $CO_2$ in water decreases and the diffusivity of $CO_2$ in water increases with an increase in temperature, and the temperature affects diffusivity more significantly than solubility. This means that the $CO_2$ permeance based on the physical solution-diffusion will increase as temperature increases. On the other hand, a higher temperature will also favor the facilitated transport of $CO_2$ not only because the enhanced reaction rate of $CO_2$-amine reactions but also due to increased diffusivity of the $CO_2$-amine complexes. However, in spite of the positive effects of temperature on both $CO_2$ and $N_2$ permeance, the temperature dependence of $N_2$ permeance is more pronounced, which in turn reduces the selectivity as temperature increases.

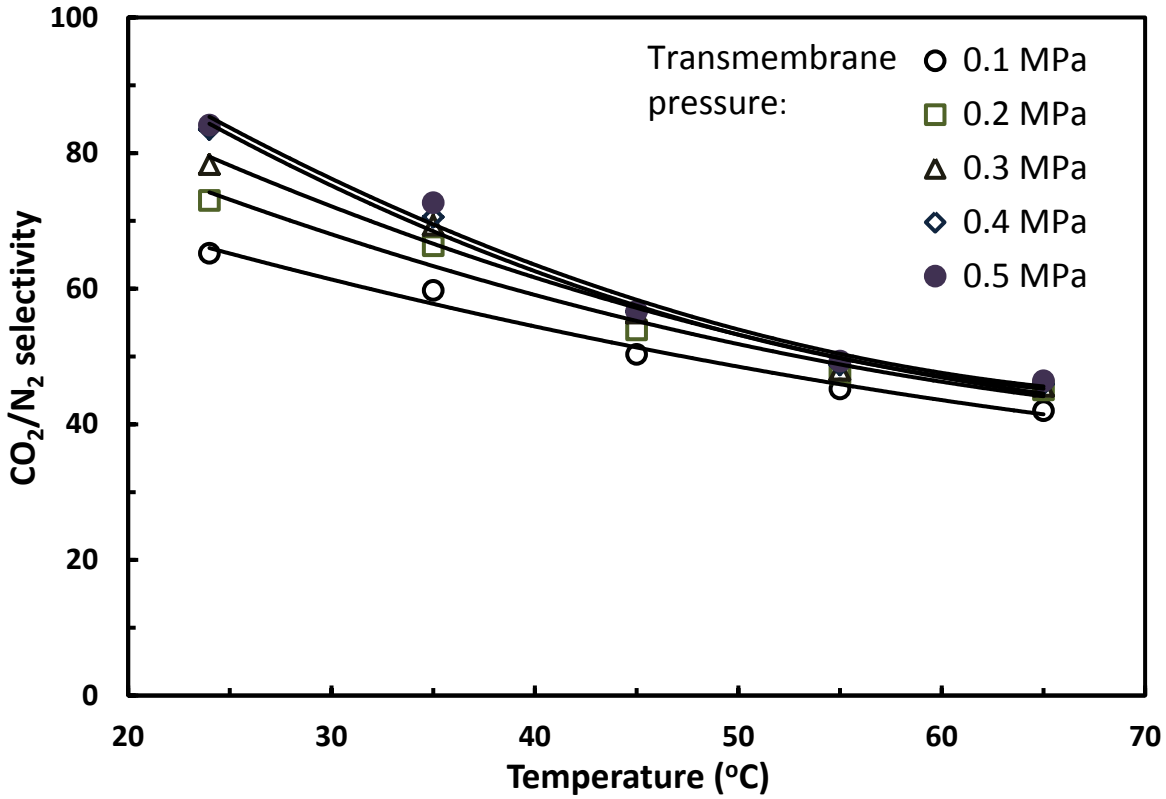


Fig. 5-10 Effect of temperature on $CO_2/N_2$ selectivity based on pure gas permeation through PVAm-PVA/PZ composite membrane

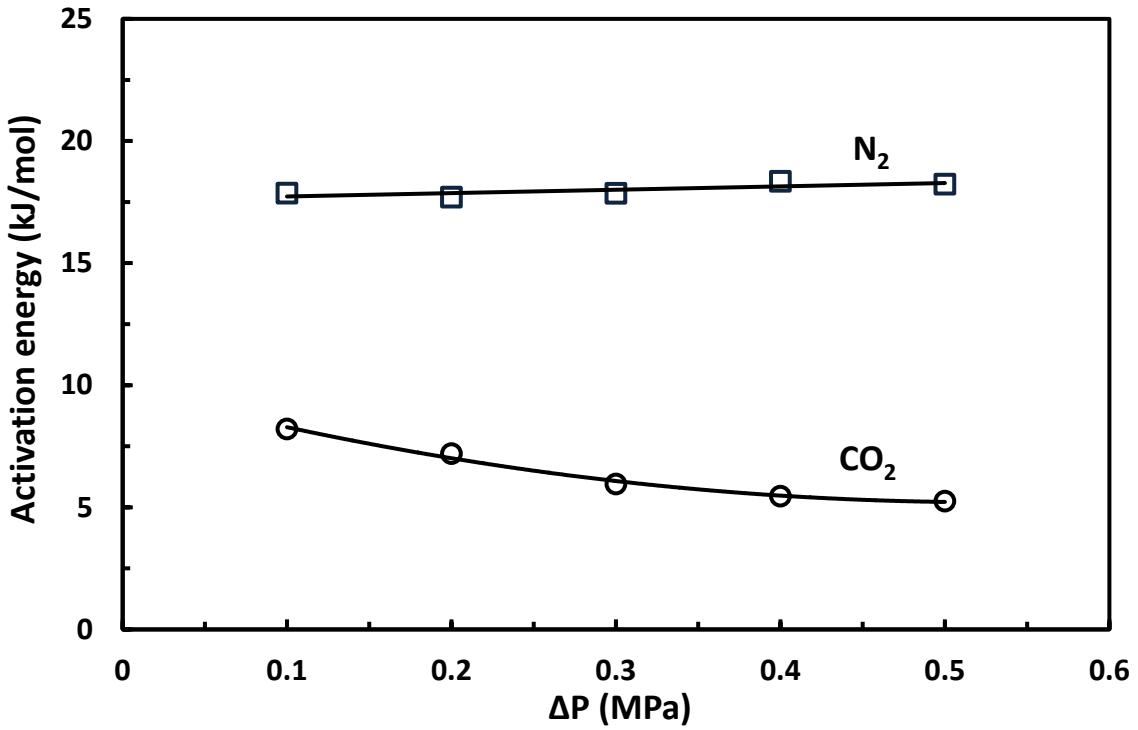


Fig. 5-11 Activation energies of permeation for $CO_2$ and $N_2$ in PVAm-PVA/PZ composite membrane

The PVAm-PVA/PZ composite membranes showed good $CO_2/N_2$ separation performance based on pure gas permeation tests. However, in practical applications, $CO_2$ needs to be separated from the gas mixtures, where there will be an interaction between the two permeants. Hence, in order to evaluate the applicability of the PVAm-PVA/PZ composite membranes for $CO_2/N_2$ separation, permeation experiments were conducted subsequently using binary gas mixtures.

The results for $CO_2/N_2$ binary mixture permeation at different feed compositions are shown in Fig. 5-12. The feed $CO_2$ compositions were varied in the entire concentration range; 0% $CO_2$ corresponds to pure $N_2$ and 100% $CO_2$ corresponds to pure $CO_2$. The feed pressure was kept constant at 281.3 kPa in all the measurements. The mole fraction of $CO_2$ in the permeate and the total permeation flux are plotted as a function of the mole fraction of $CO_2$ in feed. As expected, the concentration of $CO_2$ in permeate is always greater than that in feed, and it increases with an

increase in $CO_2$ concentration in the feed, indicating that $CO_2$ is preferentially transported through the membrane from the $CO_2/N_2$ binary mixtures regardless of the feed concentrations.

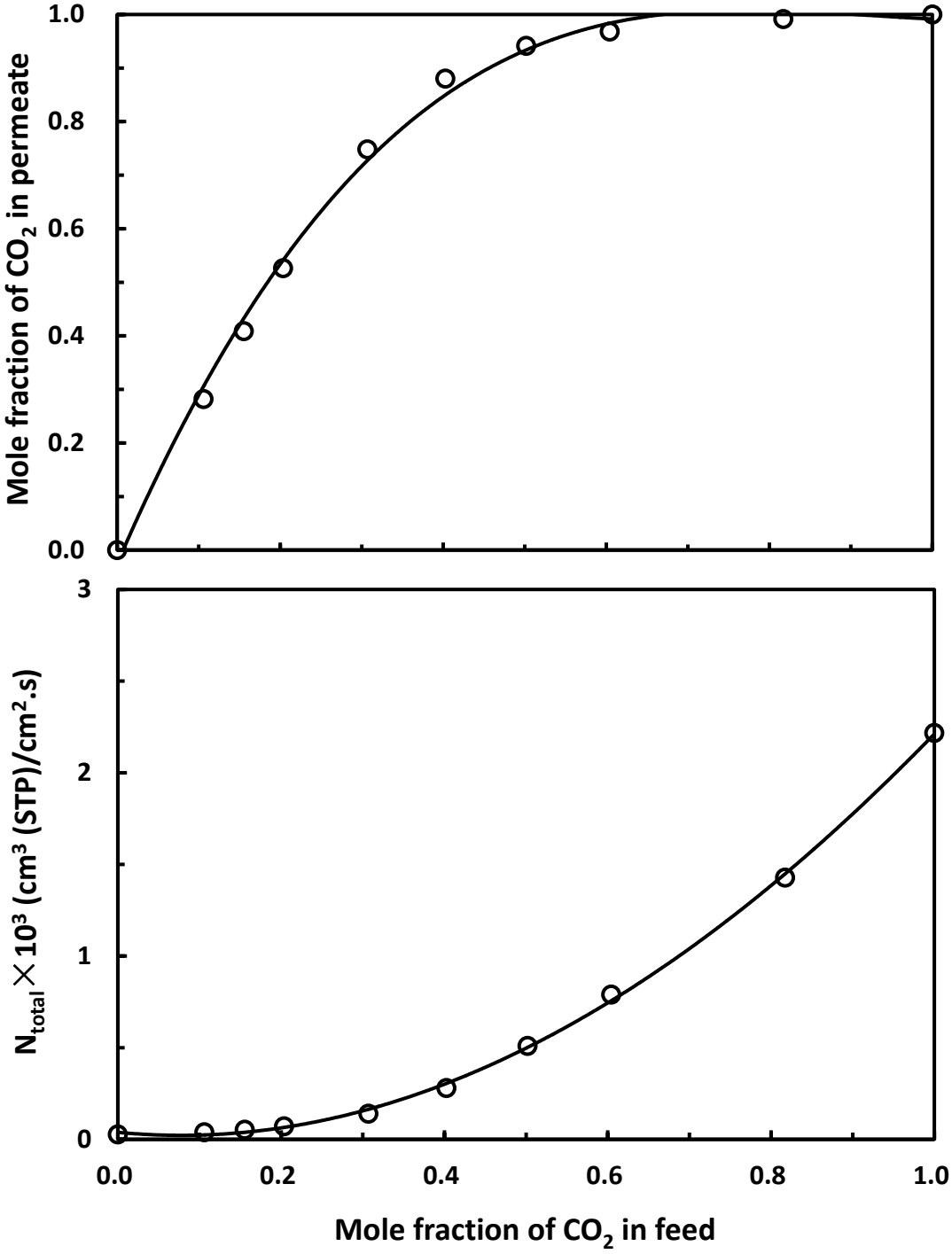


Fig. 5-12 Effect of feed composition on permeate concentration and total permeation flux for the permeation of $CO_2/N_2$ mixtures through PVAm-PVA/PZ composite membrane (polymer concentration in membrane coating solution, 5 wt%; PZ content in the membrane, PZ/polymer mass ratio=1). Feed pressure: 281.3 kPa.

The total permeation flux does not change linearly with the feed concentration, which can be explained from the individual permeation fluxes of the two components in the gas mixture, as plotted in Fig. 5-13. The dotted lines in the figures represent the ideal individual permeation flux if there are no interactions between the two permeating components, as determined from [Du *et al.*, 2010b]:

$$N_i^0 = J_i^0(p_f x_i - p_p y_i') \tag{5-2}$$

$$N_j^0 = J_j^0[p_f(1 - x_i) - p_p(1 - y_i')] \tag{5-3}$$

$$y_i' = \frac{N_i^0}{N_i^0 + N_j^0} \tag{5-4}$$

where subscripts $i$ and $j$ denote the fast component (i.e., $CO_2$) and the slow component (i.e., $N_2$) in the binary gas mixture, respectively, $J^0$ is the pure component permeance, and $N^0$ is the ideal permeation flux assuming the permeation of one component is not affected by the other component.

The $CO_2$ permeation flux is shown to increase with an increase in feed $CO_2$ concentration. However, the $CO_2$ permeation flux from the gas mixture is obviously lower than that based on pure gas permeation at the same $CO_2$ partial pressures, which means that $CO_2$ permeation is slowed down by the presence of $N_2$. In addition, it turns out that the $N_2$ permeation flux from the mixed gas is higher than the pure $N_2$ flux at pressures that are equal to the partial pressure difference in the mixture. Due to the presence of the strongly sorbing component (i.e., $CO_2$), $CO_2$-induced plasticization causes an increase in the local segmental motion of the polymer chains, leading to enhanced diffusivity of the membrane to all permeating components. Thus, the results suggest that the presence of $CO_2$ has enhanced the permeation of $N_2$.

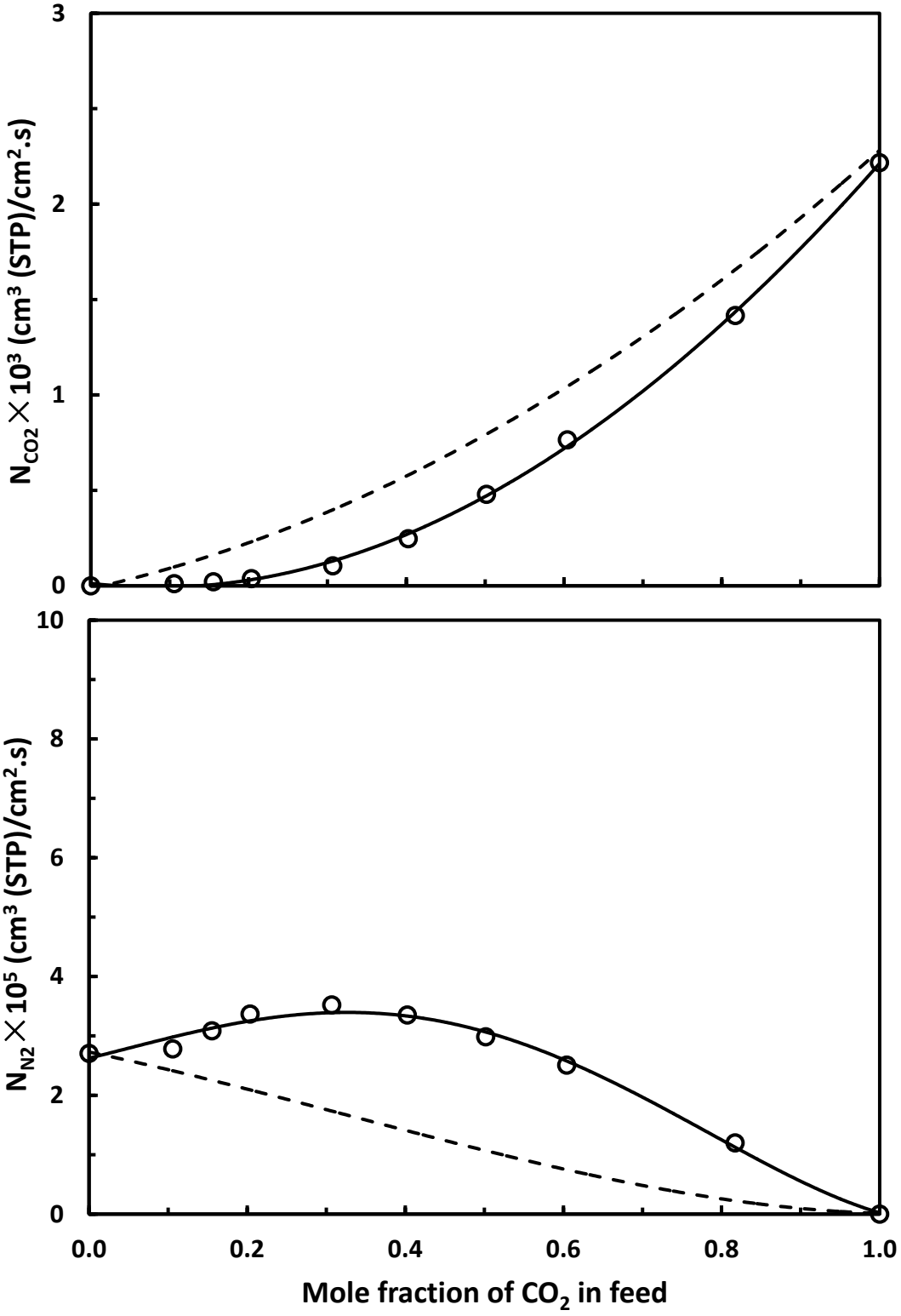


Fig. 5-13 Effect of feed composition on partial permeation fluxes of $CO_2$ and $N_2$ for the permeation of $CO_2/N_2$ mixtures through PVAm-PVA/PZ composite membrane (polymer concentration in membrane coating solution, 5 wt%; PZ content in the membrane, PZ/polymer mass ratio=1). Feed pressure: 281.3 kPa.

Fig. 5-14 shows the permeance of $CO_2$ and $N_2$ for permeation of the $CO_2/N_2$ mixtures at different compositions. It's clear that the permeance of both $CO_2$ and $N_2$ increases with an increase in feed $CO_2$ concentration. The $CO_2$ permeation through the PVAm-PVA/PZ composite membranes, which is facilitated by the amine, is dependent on the concentrations of $CO_2$ and $CO_2$-amine complexes across the membrane. The $CO_2$-amine complexes include zwitterions, carbamates, bicarbonates and protonated amines. The higher the concentration of $CO_2$ dissolved in the membrane, the greater the rate of formation of $CO_2$-amine complexes, and thus a higher $CO_2$ permeance. However, when the $CO_2$ concentration in the membrane is sufficiently high, a further increase in $CO_2$ concentration in the membrane will not continue to increase $CO_2$ permeance significantly since the available amine carriers are gradually exhausted once occupied by the $CO_2$ molecules. On the other hand, the ionic species formed during the reactions between $CO_2$ and amines will cause a "salting out effect" [Matsuyama *et al.*, 1999] on the transport of $CO_2$ through the membrane, which decreases the solubility of $CO_2$ in the membrane and results in a reduction in the diffusivity of $CO_2$-amine complexes and physically dissolved $CO_2$ molecules since part of the polymer chains are surrounded by these ions. For $N_2$ permeation, due to the $CO_2$-induced plasticization effect, when the feed $CO_2$ content increases, the $N_2$ permeance will also increase. The membrane selectivity for binary $CO_2/N_2$ permeation at different feed $CO_2$ concentrations is shown in Fig. 5-15. An increase in feed $CO_2$ concentration reduces the selectivity at a relatively low feed $CO_2$ concentration, and a constant selectivity was observed at higher feed $CO_2$ concentrations. The $CO_2$-induced plasticization effect is more significant at higher feed $CO_2$ concentration, and as a result, the membrane selectivity decreases with an increase in the mole fraction of $CO_2$ in feed.

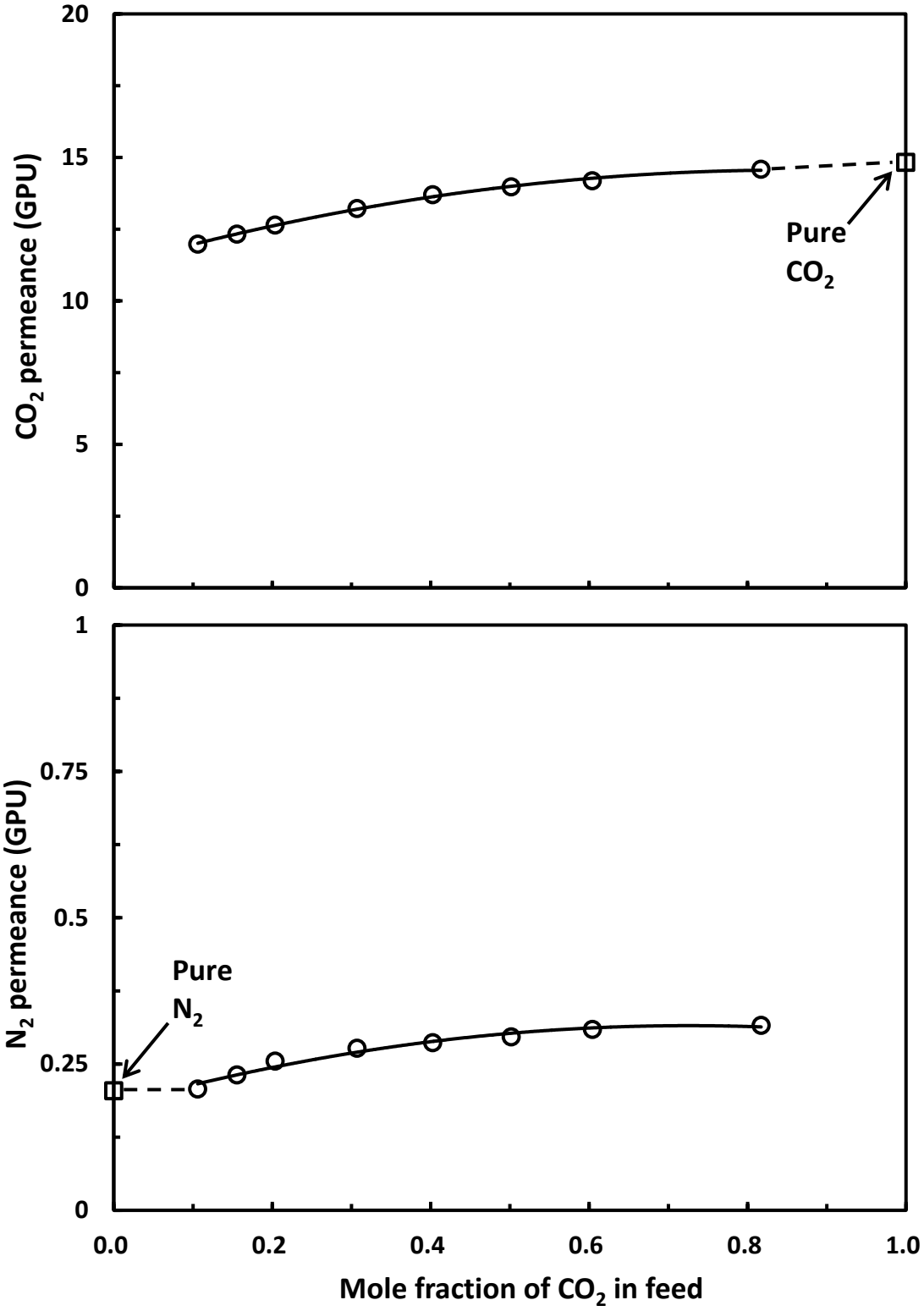


Fig. 5-14 Effect of feed composition on the permeance of $CO_2$ and $N_2$ for permeation of $CO_2/N_2$ mixtures through PVAm-PVA/PZ composite membrane (polymer concentration in membrane coating solution, 5 wt%; PZ content in the membrane, PZ/polymer mass ratio=1). Feed pressure: 281.3 kPa.

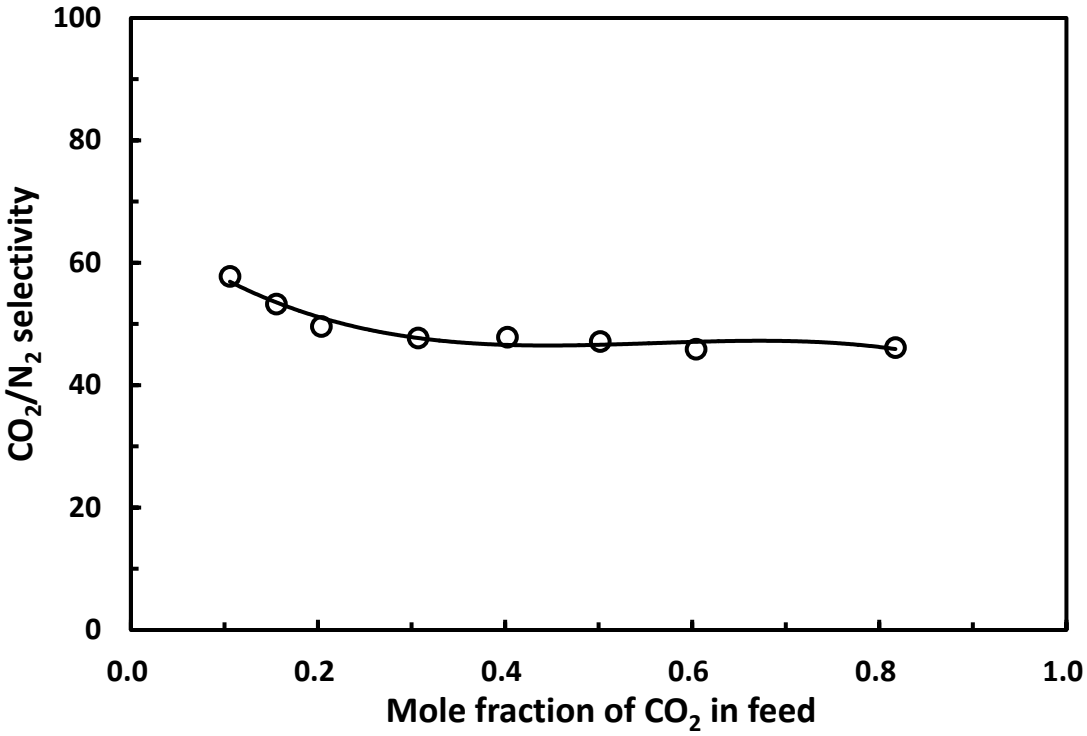


Fig. 5-15 Effect of feed composition on $CO_2/N_2$ selectivity for the permeation of $CO_2/N_2$ mixtures through PVAm-PVA/PZ composite membrane (polymer concentration in membrane coating solution, 5 wt%; PZ content in the membrane, PZ/polymer mass ratio=1). Feed pressure: 281.3 kPa.

The membrane stability, which is always a key issue to the viability of the membrane for practical uses, was evaluated in this chapter using a simulated flue gas containing 15.3 mol% $CO_2$ (balanced $N_2$) at feed pressures varying periodically between 0.3 and 0.6 MPa, and the results are shown in Fig. 5-16 and 5-17. The feed gas was saturated with water to keep a constant level of swelling of the membrane throughout the experiments. As stated before, the $CO_2$ permeance of the membrane increases as the feed pressure increases, whereas the $N_2$ permeance basically keeps at a constant level when varying the feed pressure. Because of the distinct behavior of $CO_2$ and $N_2$ with varying feed pressure, the corresponding $CO_2/N_2$ selectivity also changes. The membrane was shown to be stable, and no reduction in the membrane permeance was observed during the course of continuous permeation for a period of more than 7 weeks. The results also indicate that the PZ is well retained in the PVAm-PVA/PZ composite membrane during the $CO_2$ separation process.

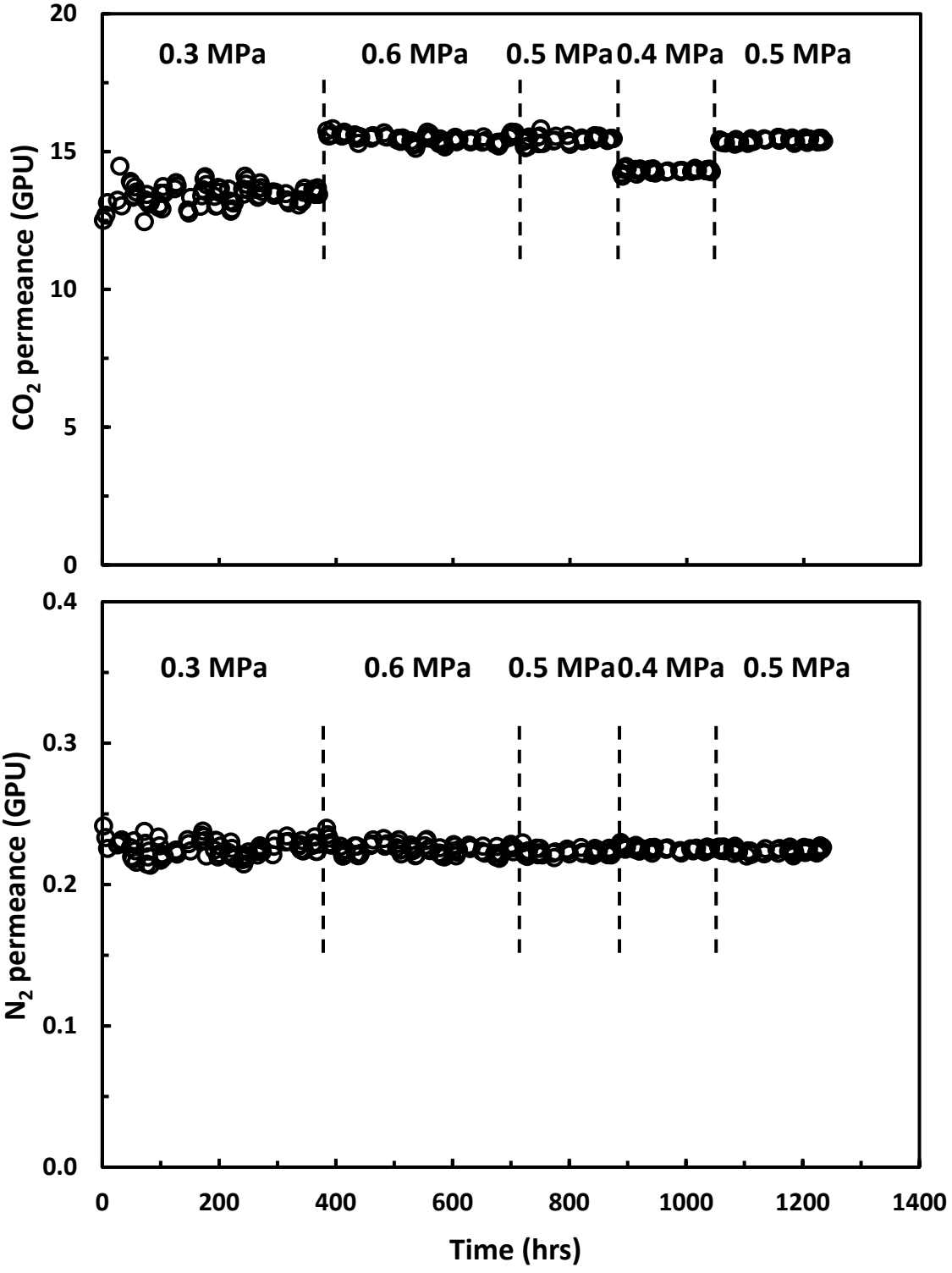


Fig. 5-16 Stability of PVAm-PVA/PZ composite membrane for continuous permeation over more than 7 weeks. Polymer concentration for membrane fabrication, 5 wt%; PZ content in the membrane, PZ/polymer mass ratio=1. Feed $CO_2$ concentration, 15.3 mol%; temperature, 298 K.

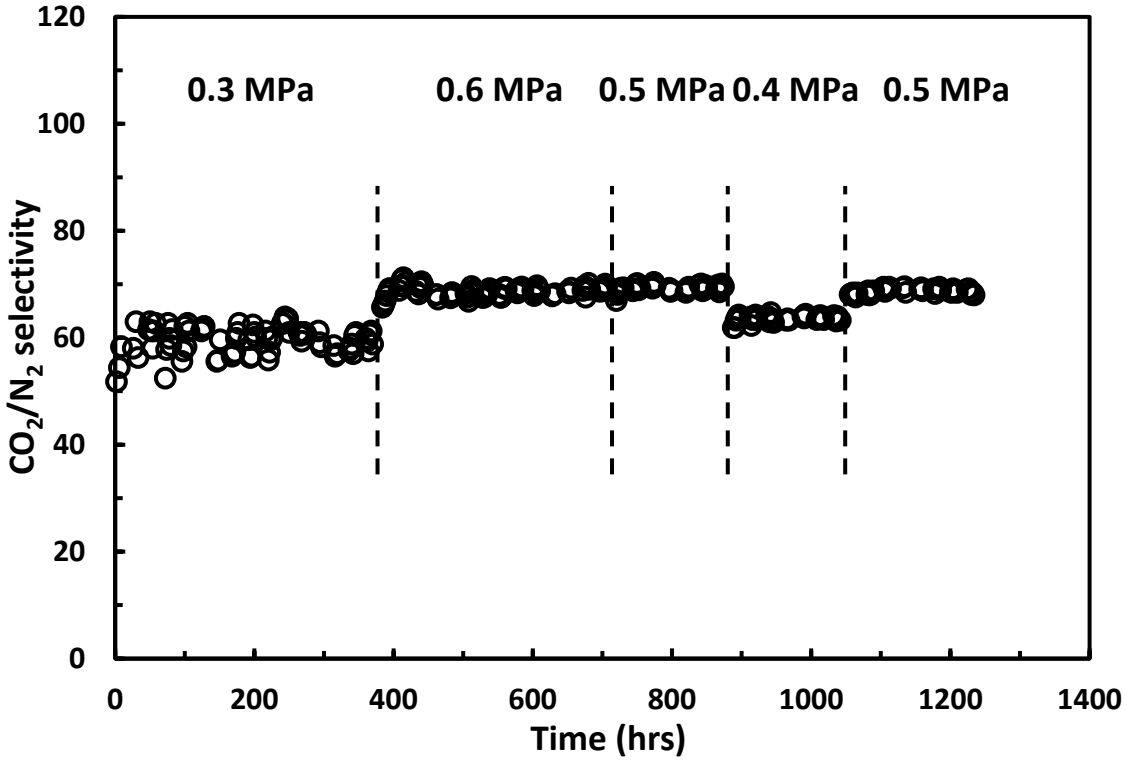


Fig. 5-17 $CO_2/N_2$ selectivity of PVAm-PVA/PZ composite membrane for continuous separation over more than 7 weeks. Polymer concentration for membrane fabrication, 5 wt%; PZ content in the membrane, PZ/polymer mass ratio=1. Feed $CO_2$ concentration, 15.3 mol%; temperature, 298 K.

### 5.3.3 Mixed amine systems

Since the PVAm-PVA composite membranes incorporated with secondary amine piperazine have shown good separation performance for separating $CO_2$ from $N_2$, as discussed earlier, the membranes containing mixed amines (i.e., PZ+TEA and PZ+MDEA) are expected to have better performance for $CO_2$ separation due to the simultaneous uses of secondary and tertiary amines. In the following, PVAm-PVA/amine composite membranes at different PZ/TEA and PZ/MDEA ratios were tested for both pure gas (e.g., $CO_2$, $N_2$ and He) and binary gas (e.g., $CO_2/N_2$ mixture) permeation. For easy comparison, the amine content in the membrane was kept at a mass ratio of amine to polymer of 1 (where the amine represents the total amount of PZ+TEA or PZ+MDEA), and the concentration of the polymer in the coating solution was 5 wt%.

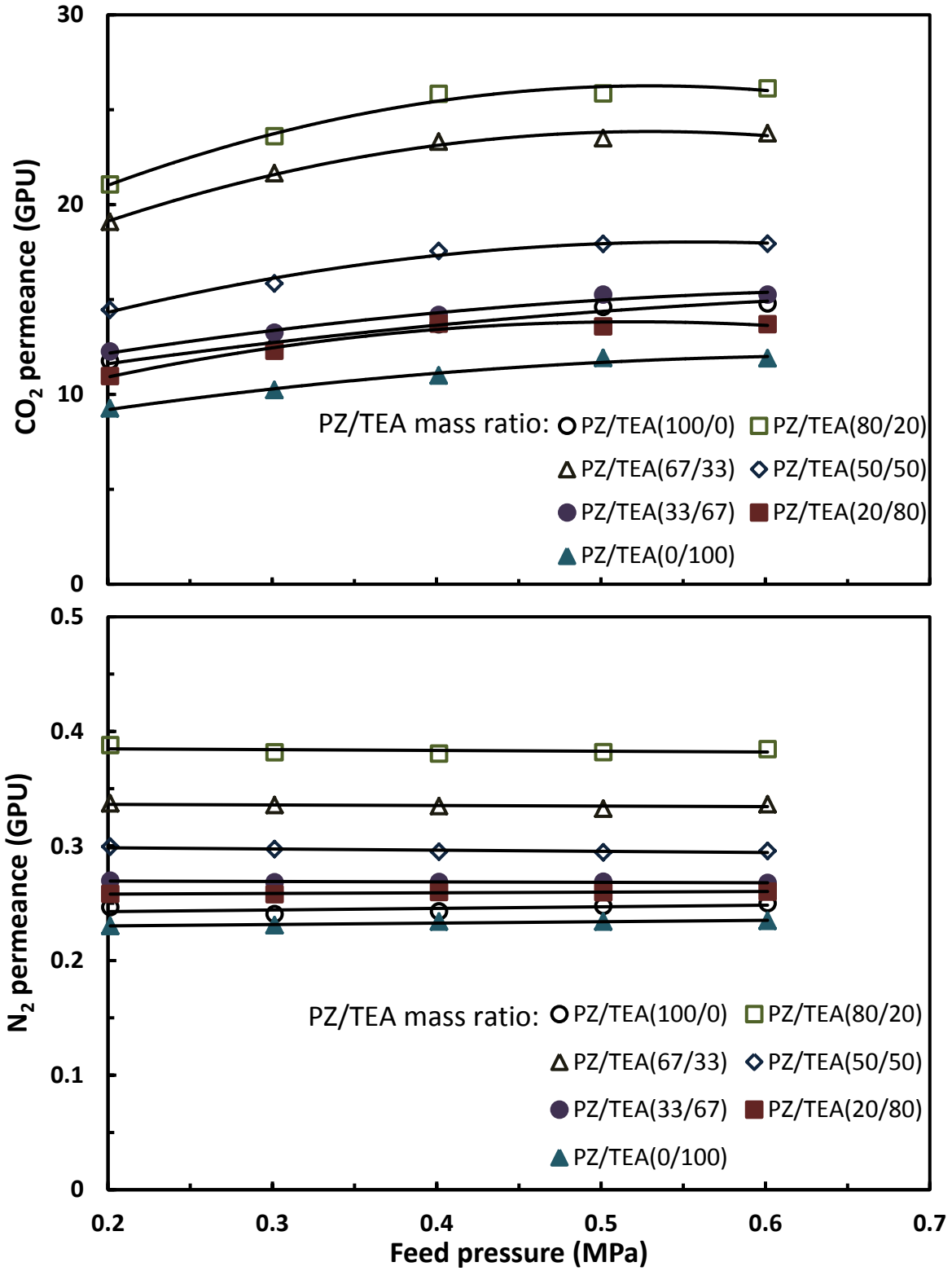


Fig. 5-18 Effect of PZ/TEA mass ratio in the membrane on the permeance of $CO_2$ and $N_2$ for the permeation of $CO_2/N_2$ mixtures. Polymer concentration in the coating solution, 5 wt%; amine content in the membrane, amine/polymer mass ratio=1. Feed $CO_2$ concentration, 15.3 mol%; temperature, 298 K.

Figs. 5-18 and 5-19 show the membrane permeance and $CO_2/N_2$ selectivity of PVAm-PVA composite membranes containing mixed amines of PZ and TEA at different PZ/TEA mass ratios for separating $CO_2/N_2$ mixture. It appears that all the membranes with a PZ/TEA mass ratio greater than or equal to 1 show a higher $CO_2$ permeance than the membranes with a PZ/TEA mass ratio less than 1. In addition, the composite membranes with a PZ/TEA mass ratio of 80/20 and 67/33 outperform the membranes that contain either PZ or TEA alone in terms of $CO_2$ permeance and $CO_2/N_2$ selectivity.

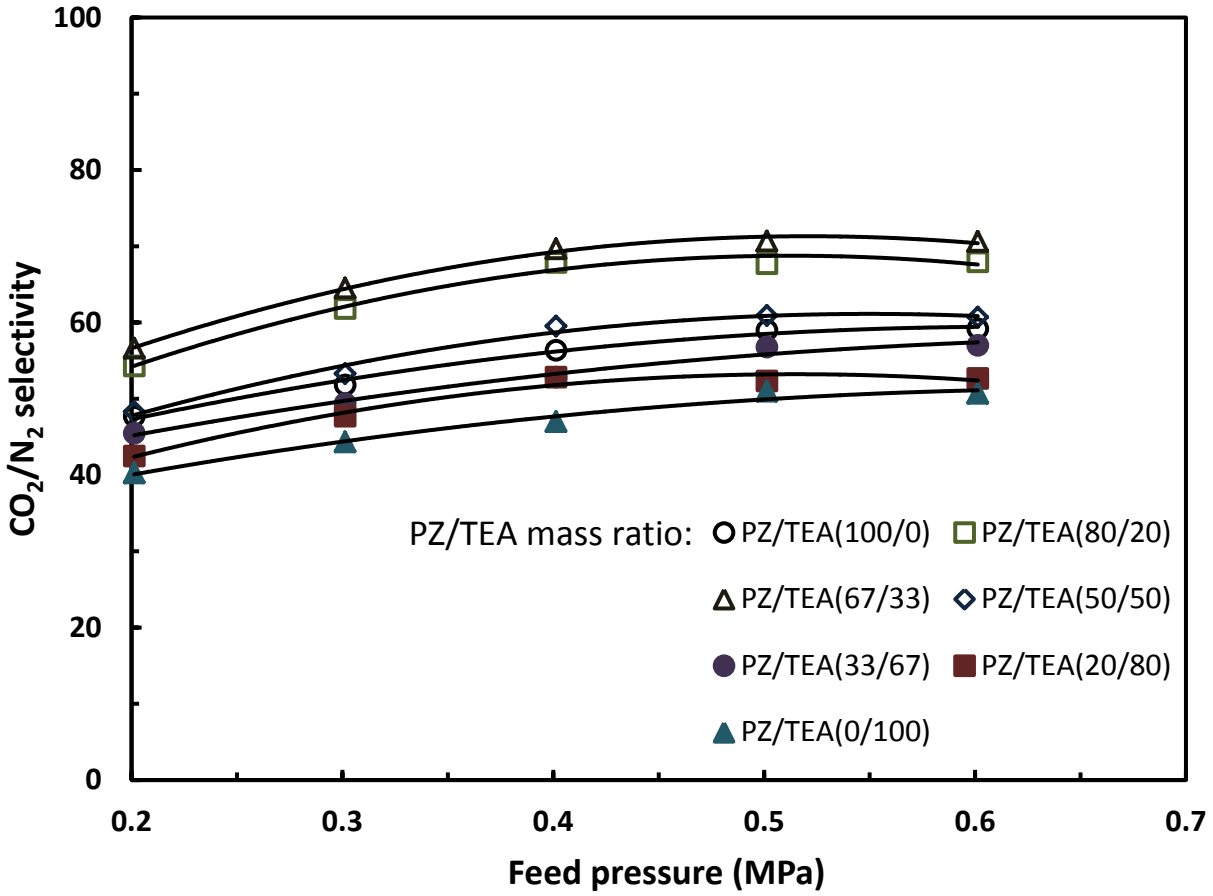


Fig. 5-19 Effect of PZ/TEA mass ratio in the membrane on $CO_2/N_2$ selectivity. Polymer concentration in the coating solution, 5 wt%; amine content in the membrane, amine/polymer mass ratio=1. Feed $CO_2$ concentration, 15.3 mol%; temperature, 298 K.

As can be seen from Table 5-1, PZ has a much higher $k_1$ value and a higher $k_r$ value than TEA, indicating that both the forward and reverse reactions for the $CO_2$-PZ system are fast.

Hence, the PVAm-PVA/amine composite membrane containing only PZ tends to have a higher $CO_2$ permeance than the composite membrane containing only TEA. Furthermore, PZ was suggested to contribute to absorption of $CO_2$ and enhance the overall rate of absorption even when a small amount of PZ was added into an aqueous tertiary amine solution according to absorption kinetics studies [Zhang *et al.*, 2001; Horng and Li, 2002; Vaidya and Kenig, 2007]. A substantially high absorption rate of $CO_2$ was reported at a high PZ concentration in the mixed amine [Vaidya and Kenig, 2007]. In the PZ-tertiary amine mixed system, in addition to carbamate formation, PZ can transfer the absorbed $CO_2$ to tertiary amine rapidly [Zhang *et al.*, 2001], thus promoting the $CO_2$ absorption. As a result, part of PZ may facilitate the $CO_2$ transport via the carbamate reaction, and the other may help enhance the $CO_2$ absorption in the tertiary amine. On the other hand, the tertiary amine may also function as a catalyst to facilitate the $CO_2$ hydration reaction as indicated previously [Yu *et al.*, 2010]. Therefore, the composite membranes containing mixed amines are expected to display a higher $CO_2$ permeance than the composite membranes containing either amine alone. With an increase in the PZ/TEA mass ratio, more PZ are available for carbamate formation and promotion of $CO_2$ absorption in combination with TEA. Since PZ alone is more effective in facilitating $CO_2$ transport than TEA alone, composite membranes with a PZ/TEA mass ratio of greater than or equal to 1 are more $CO_2$-selective. However, they also have a higher permeance to $N_2$ than the composite membranes with a PZ/TEA mass ratio less than 1. TEA has one tertiary amine and three hydroxyl groups in its molecular structure, the intermolecular interactions between PVAm-PVA and the mixed amines are much stronger than that between PVAm-PVA and PZ alone, which may change the bulk solution properties and densify the polymer matrix, affecting the resulting membrane thickness. The composite membranes with a PZ/TEA mass ratio of 80/20 and 67/33 show good $CO_2/N_2$

selectivity.

Table 5-1 Physicochemical properties of $CO_2$-amine systems at 298 K

| Amine | $k_1\ (cm^3/(mol \cdot s))$ | $K_{eq}\ (cm^3/mol)$ | $k_r = k_1/K_{eq}\ (s^{-1})$ |
|---|---|---|---|
| PZ[a] | $7 \times 10^7$ | $8 \times 10^7$ | 0.875 |
| TEA[b] | $3.74 \times 10^3$ | $2.38 \times 10^4$ | 0.157 |
| MDEA[b] | $5.1 \times 10^3$ | $1.91 \times 10^5$ | 0.0267 |

[a] Taken from [Derks *et al.*, 2006].

[b] Taken from [Teramoto *et al.*, 1997].

Parameters $k_1$, $k_2$ and $k_3$ are the rate constants for $CO_2$-amine reactions shown in Equations (2-3), (2-4) and (2-7). $K_{eq}$ is the equilibrium constant, which is equal to $(k_1k_3)/(k_2k_4)$ for primary and secondary amines and $(k_1/k_2)$ for tertiary amines.

To further understand the permeation behavior of gases in the membranes with different PZ/TEA mass ratios, pure gas permeation tests with $CO_2$, $N_2$ and He were also conducted, and the results are presented in Figs. 5-20 to 5-22.

The variations in $CO_2$ permeance and $N_2$ permeance with respect to the PZ/TEA mass ratio in the membranes for pure gas permeation are very similar to binary mixture permeation, except that the membrane exhibited a higher permeance to $CO_2$ and a lower permeance to $N_2$ for the pure gas permeation. Thus, the ideal $CO_2/N_2$ selectivity based on pure gas permeation is higher than the selectivity for mixture gas permeation. This can be attributed to the coupling effects between permeating components in mixture permeation, which reduces the permeance of the more permeable component and increases the permeance of the less permeable one. Furthermore, the composite membranes showing a higher $N_2$ permeance in $CO_2/N_2$ gas mixture permeation (for example, with a PZ/TEA mass ratio of 80/20 and 67/33) also have a higher $N_2$ permeance in pure $N_2$ permeation. This can be explained from the following two aspects. First, as the PZ/TEA mass ratio of the PVAm-PVA/mixed amine solution increases, the viscosity of the coating solution decreases when the polymer concentration of the coating solution and the mass ratio of amine to polymer are fixed. Though both PZ and TEA are small molecular amines, the interactions between the polymer matrix and the amines PZ and TEA can be strong enough to

alter the bulk solution properties (e.g., viscosity). In addition, TEA tends to have stronger interactions with the polymer matrix via hydrogen bonding because of the presence of three hydroxyl groups per molecule. Thus, at a higher PZ/TEA ratio, the polymer-amine interactions are weaker and the membrane coating solutions are less viscous, resulting in a thinner skin layer and thus a higher gas permeance. On the other hand, the weaker interactions between the polymer matrix and amines will produce a less densified polymer network, which also helps increase the gas permeance. Since $N_2$ mainly transports through the membrane via the physical solution-diffusion mechanism, these two effects will determine how the $N_2$ permeance changes with varying the PZ/TEA ratio of the membrane. To further verify this, pure helium permeation in these membranes was also tested because helium is an inert gas. As shown in Fig. 5-21, the He permeance follows exactly the same trend as $N_2$ permeance when the PZ/TEA ratio was varied. This suggests that the thickness of the skin layer and densified polymer matrix are the main causes that determine the permeation behavior of non-reactive component (e.g., $N_2$ and He) in the composite membrane.

The $CO_2/N_2$ selectivity for gas mixture permeation and $CO_2/N_2$ ideal selectivity based on pure gas permeation in the PVAm-PVA/PZ-TEA composite membranes were compared, as plotted in Fig. 5-23. Both the $CO_2/N_2$ selectivity and $CO_2/N_2$ ideal selectivity have the same trend with varying PZ/TEA ratios. A PZ/TEA mass ratio of 67/33 or 80/20 in the PVAm-PVA/PZ-TEA composite membrane is appropriate as far as the $CO_2/N_2$ separation performance is concerned.

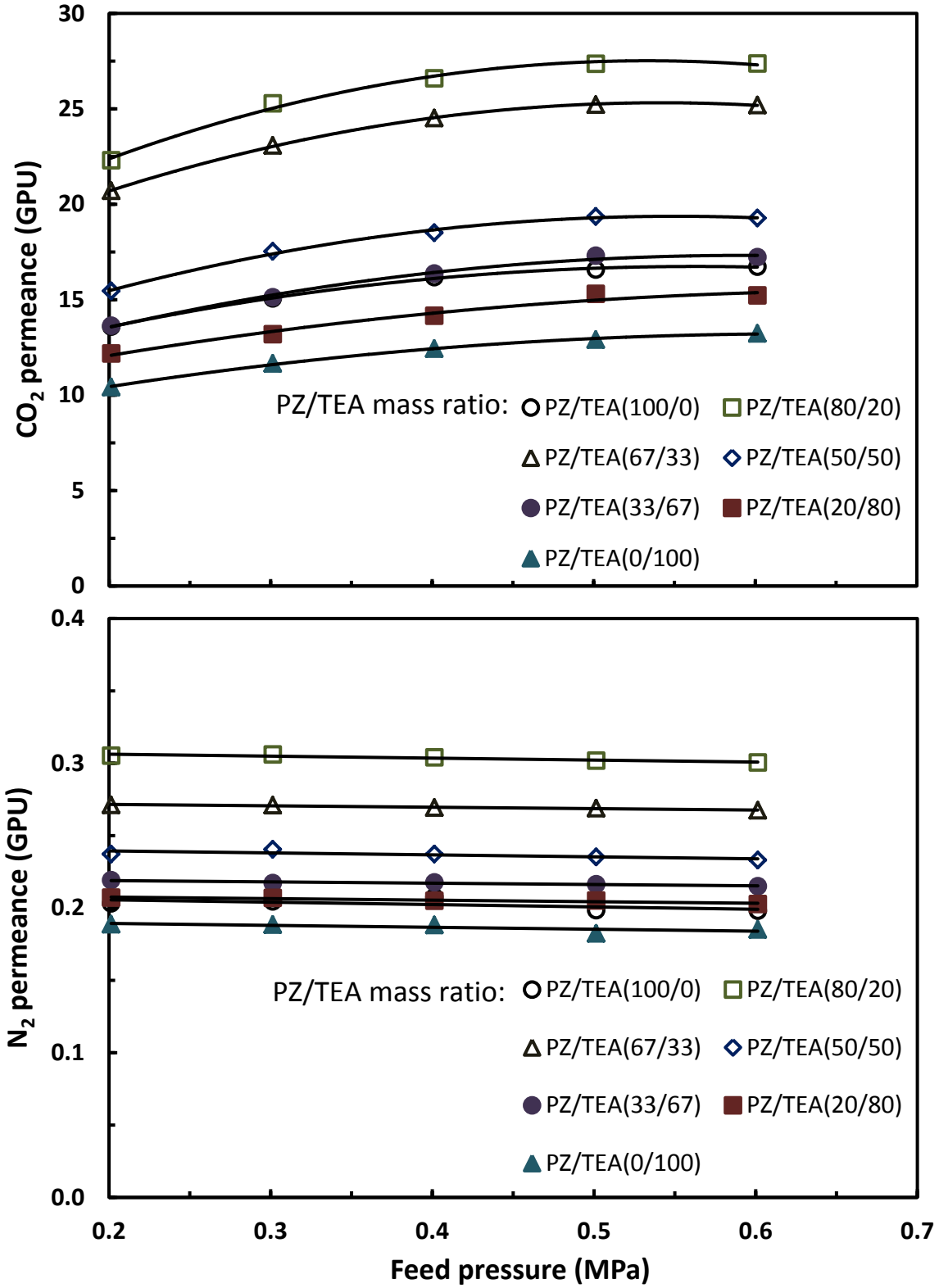


Fig. 5-20 Effect of PZ/TEA mass ratio in the membrane on the permeance of $CO_2$ and $N_2$ for pure gas permeation through PVAm-PVA/PZ-TEA composite membranes. Polymer concentration in the coating solution, 5 wt%; amine content in the membrane, amine/polymer mass ratio=1. Temperature, 298 K.

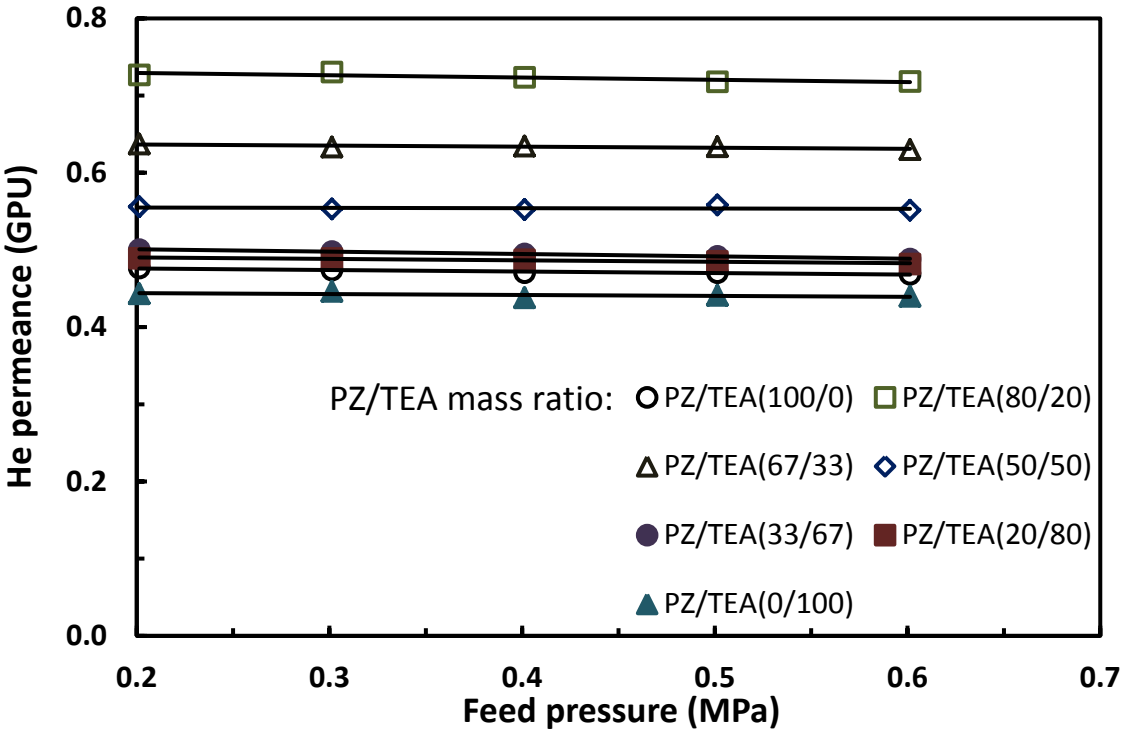


Fig. 5-21 Effect of PZ/TEA mass ratio in the membrane on He permeance for pure gas permeation through PVAm-PVA/PZ-TEA composite membranes. Polymer concentration in the coating solution, 5 wt%; amine content in the membrane, amine/polymer mass ratio=1. Temperature, 298 K.

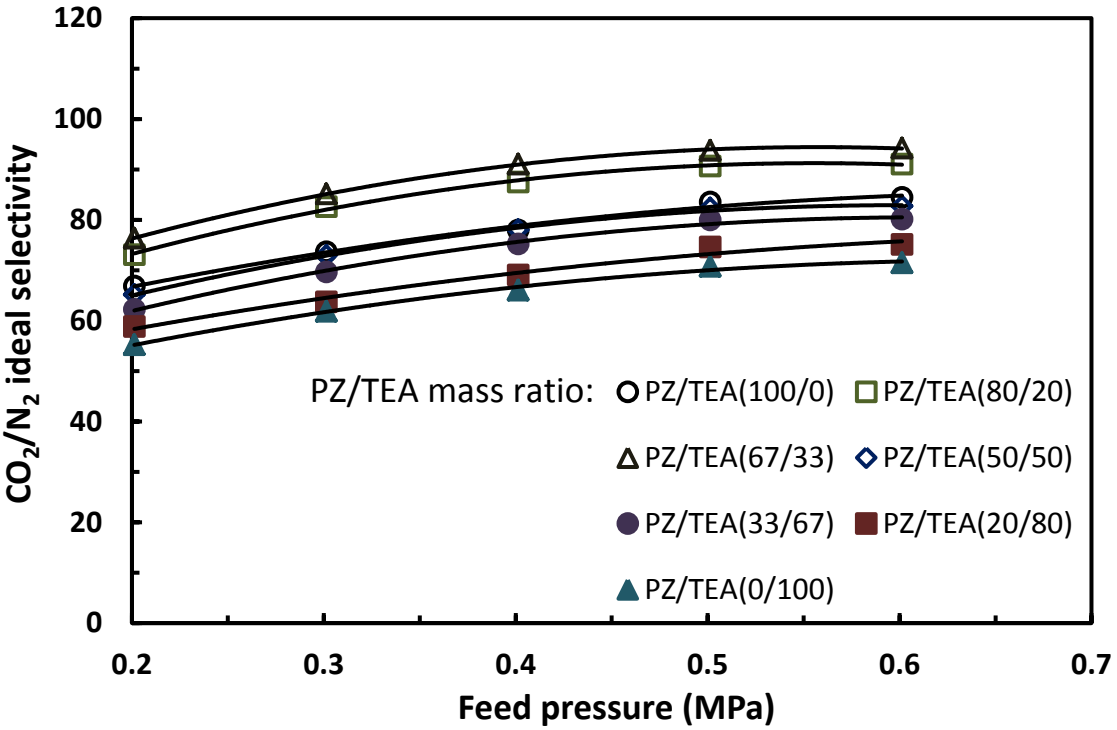


Fig. 5-22 Effect of PZ/TEA mass ratio in the membrane on $CO_2/N_2$ ideal selectivity for pure gas permeation through PVAm-PVA/PZ-TEA composite membranes. Polymer concentration in the coating solution, 5 wt%; amine content in the membrane, amine/polymer mass ratio=1. Temperature, 298 K.

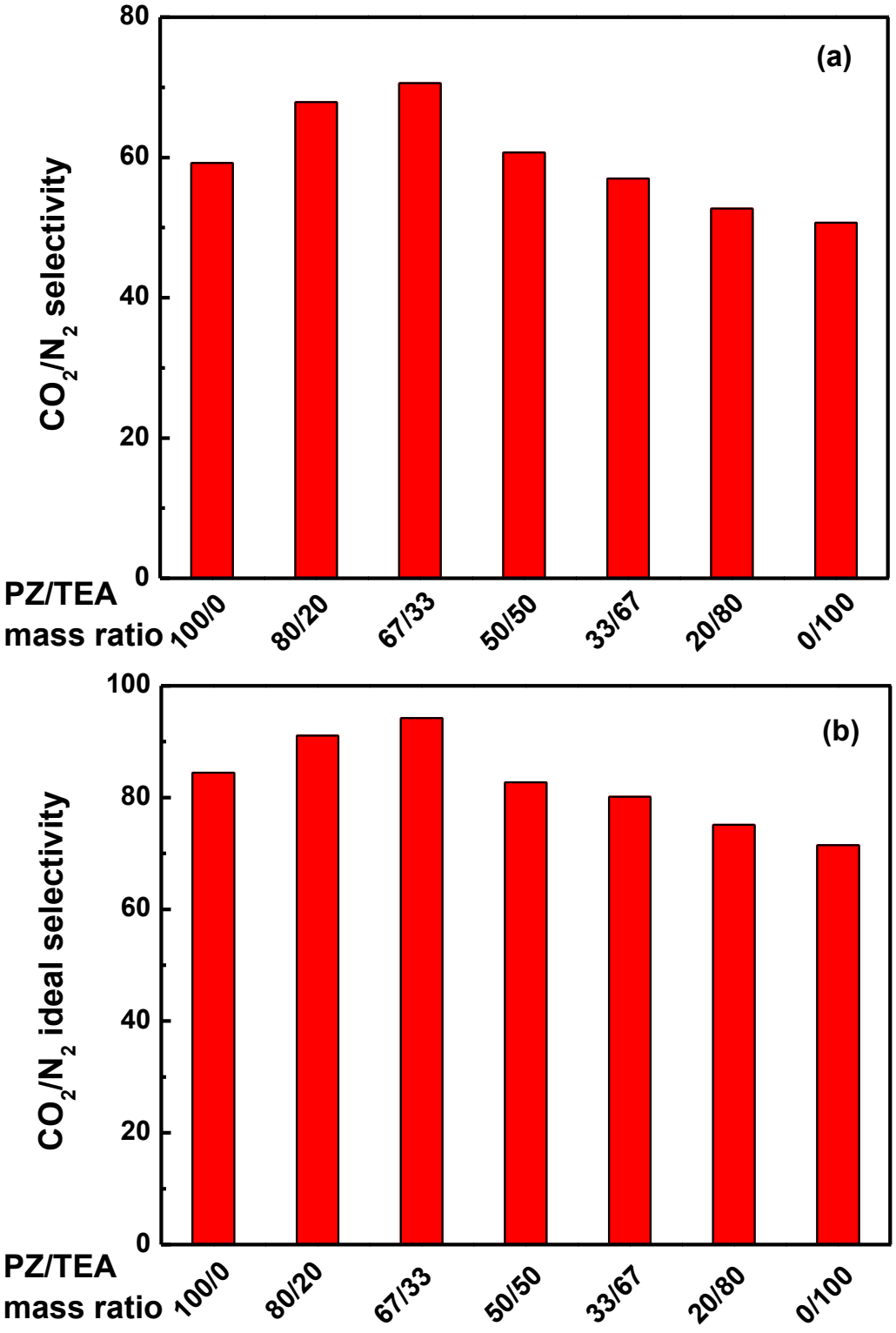


Fig. 5-23 A comparison of (a) $CO_2/N_2$ selectivity for binary $CO_2/N_2$ mixture (15.3 mol% $CO_2$) permeation and (b) $CO_2/N_2$ ideal selectivity based on pure gas permeation for PVAm-PVA/PZ-TEA composite membranes at different PZ/TEA mass ratios. Polymer concentration in the coating solution, 5 wt%; amine content in the membrane, amine/polymer mass ratio=1. Feed pressure, 601.3 kPa; temperature, 298 K.

Besides TEA, MDEA is another important tertiary alkanolamine to be used in industries. Therefore, the PVAm-PVA composite membranes containing mixed amines of PZ and MDEA were also fabricated and tested for separating $CO_2/N_2$ gas mixtures. The gas permeance and selectivity of the membranes with different PZ/MDEA mass ratios for gas mixture permeation are shown in Figs. 5-24 and 25.

It turns out that the membranes containing PZ alone or MDEA alone have similar $CO_2$ permeance, and that membranes containing mixed amines have a higher $CO_2$ permeance than the membranes containing either amine alone. In addition, membranes with a PZ/MDEA ratio of greater than or equal to 1 have a higher $CO_2$ permeance than the membranes with PZ/MDEA ratios less than 1. In general, membranes with a PZ/MDEA mass ratio of 80/20 and 67/33 yield the best $CO_2$ permeance and $CO_2/N_2$ selectivity.

Similar to the case for mixed amines of PZ and TEA, the presence of PZ in the PZ-MDEA mixture can facilitate the $CO_2$ transport via carbamate formation and enhance the absorption of $CO_2$ to MDEA. Combined with the $CO_2$ hydration facilitated by MDEA, the composite membranes with mixed amines of PZ and MDEA tend to have a higher $CO_2$ permeance than membranes with either PZ or MDEA alone. Generally, amines with moderate $K_{eq}$ and large $k_1$ values are desirable to have high $CO_2$ permeance [Teramoto *et al.*, 1997]. As shown in Table 5-1, the equilibrium constant for $CO_2$ reaction with MDEA is large compared to that for $CO_2$ reaction with TEA, but the opposite holds for the reverse reaction rate constant. The low rate constant of the reverse reaction makes it hard for $CO_2$ to desorb and release at the permeate side of the membrane. However, MDEA has a slightly larger $k_1$ value than TEA. Thus, in consideration of the steps involved in $CO_2$ transport facilitated by amines (that is, absorption of $CO_2$ with amines at the feed side, diffusion of the $CO_2$-amine complexes across the membrane,

and desorption of $CO_2$ from the complexes at the permeate side), the efficiency of using MDEA and TEA to facilitate the $CO_2$ transport could be similar. On the other hand, the molecular structure of MDEA and TEA is slightly different (Fig. 5-1). Because of the extra hydroxyl group of TEA compared to MDEA, the intermolecular interactions between TEA and the polymer may be stronger than that between MDEA and the polymer, resulting in a more densely packed polymer network. This will affect the gas permeance negatively. Thus, the membrane containing MDEA alone displays a slightly higher $CO_2$ permeance than membrane containing TEA alone. Similarly, the membranes containing mixed amines of PZ and MDEA all show an increased $CO_2$ permeance compared to membranes containing mixed amines of PZ and TEA at the same PZ/tertiary amine mass ratio. For example, at a PZ/tertiary amine mass ratio of 67/33, the membrane containing mixed amines of PZ and MDEA showed a $CO_2$ permeance of 27.7 GPU, while the membrane containing mixed amines of PZ and TEA showed a $CO_2$ permeance of 23.8 GPU at a feed pressure of 0.6 MPa for separating a $CO_2/N_2$ binary mixture containing 15.3 mol% $CO_2$.

As for $N_2$ permeation, the membranes with PZ/MDEA mass ratio of 80/20 and 67/33, which have a higher $CO_2$ permeance, also have a higher $N_2$ permeance than other membranes. This can also be ascribed to the thinner skin layer and less densely packed polymer matrix with increasing the PZ/MDEA ratio in the membranes.

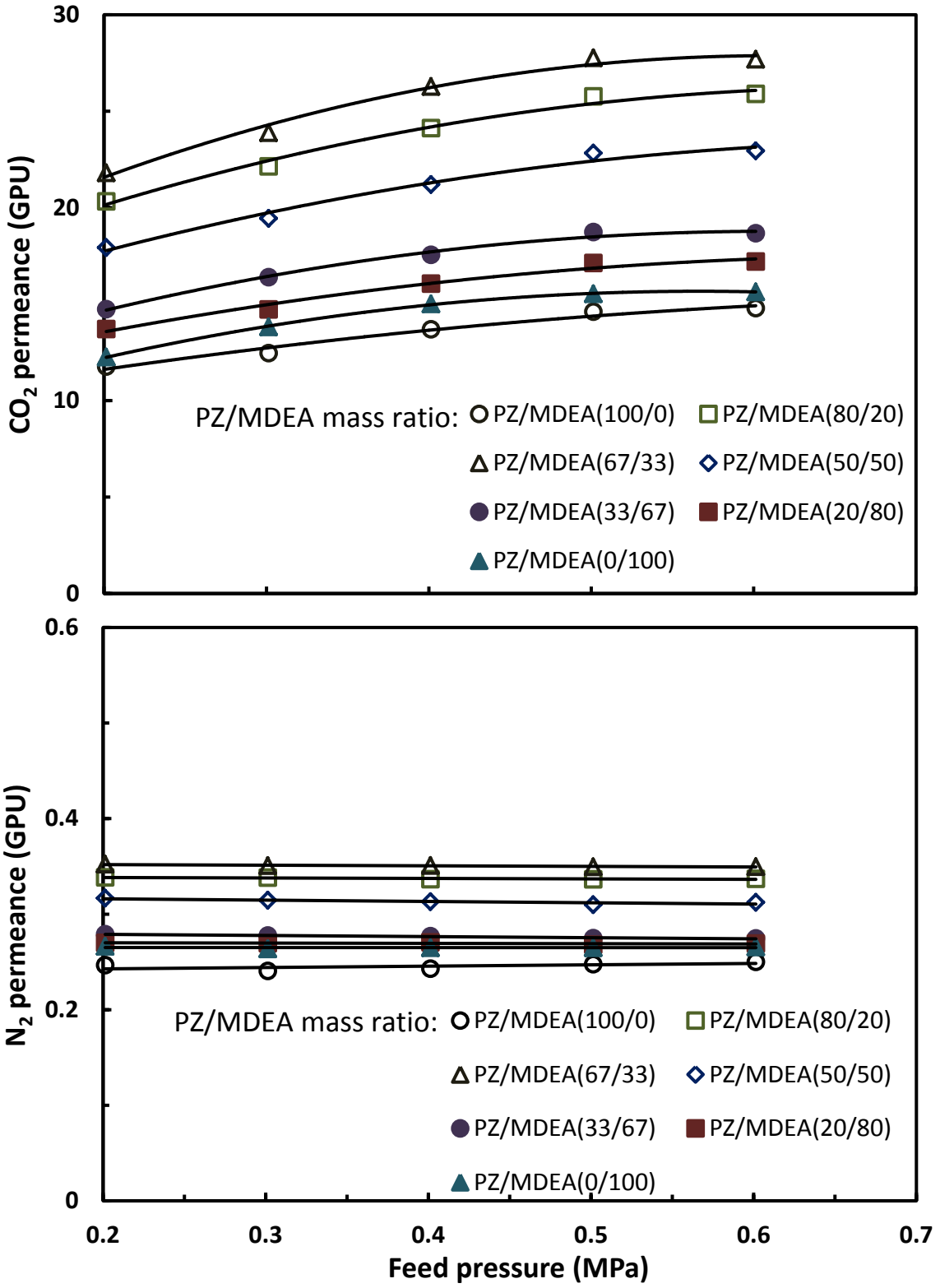


Fig. 5-24 Effect of PZ/MDEA mass ratio in the membrane on the permeance of $CO_2$ and $N_2$ for permeation of $CO_2/N_2$ mixtures. Polymer concentration in the coating solution, 5 wt%; amine content in the membrane, amine/polymer mass ratio=1. Feed $CO_2$ concentration, 15.3 mol%; temperature, 298 K.

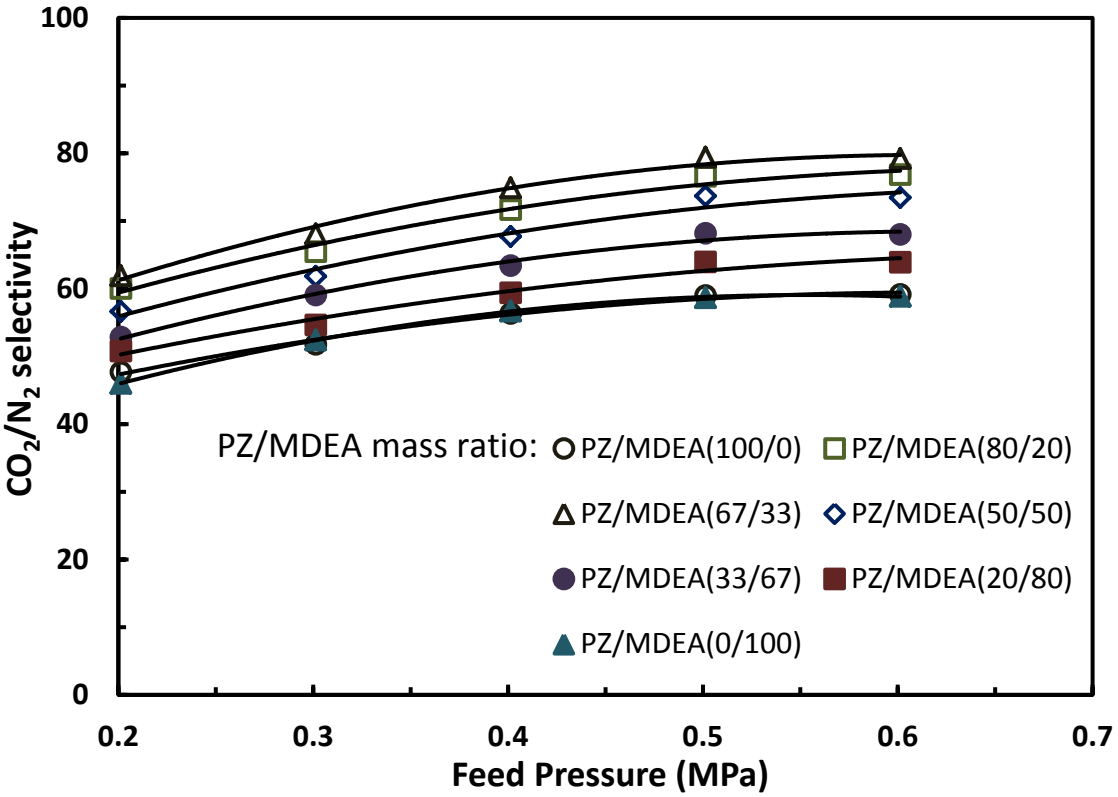


Fig. 5-25 Effect of PZ/MDEA mass ratio in the membrane on $CO_2/N_2$ selectivity for permeation of $CO_2/N_2$ mixtures. Polymer concentration in the coating solution, 5 wt%; amine content in the membrane, amine/polymer mass ratio=1. Feed $CO_2$ concentration, 15.3 mol%; temperature, 298 K.

The separation performance of PVAm-PVA composite membranes containing mixed amines of PZ and MDEA at different PZ/MDEA ratios was also evaluated with pure gas permeation tests using $CO_2$, $N_2$ and He and the data are plotted in Figs. 5-26 to 5-28.

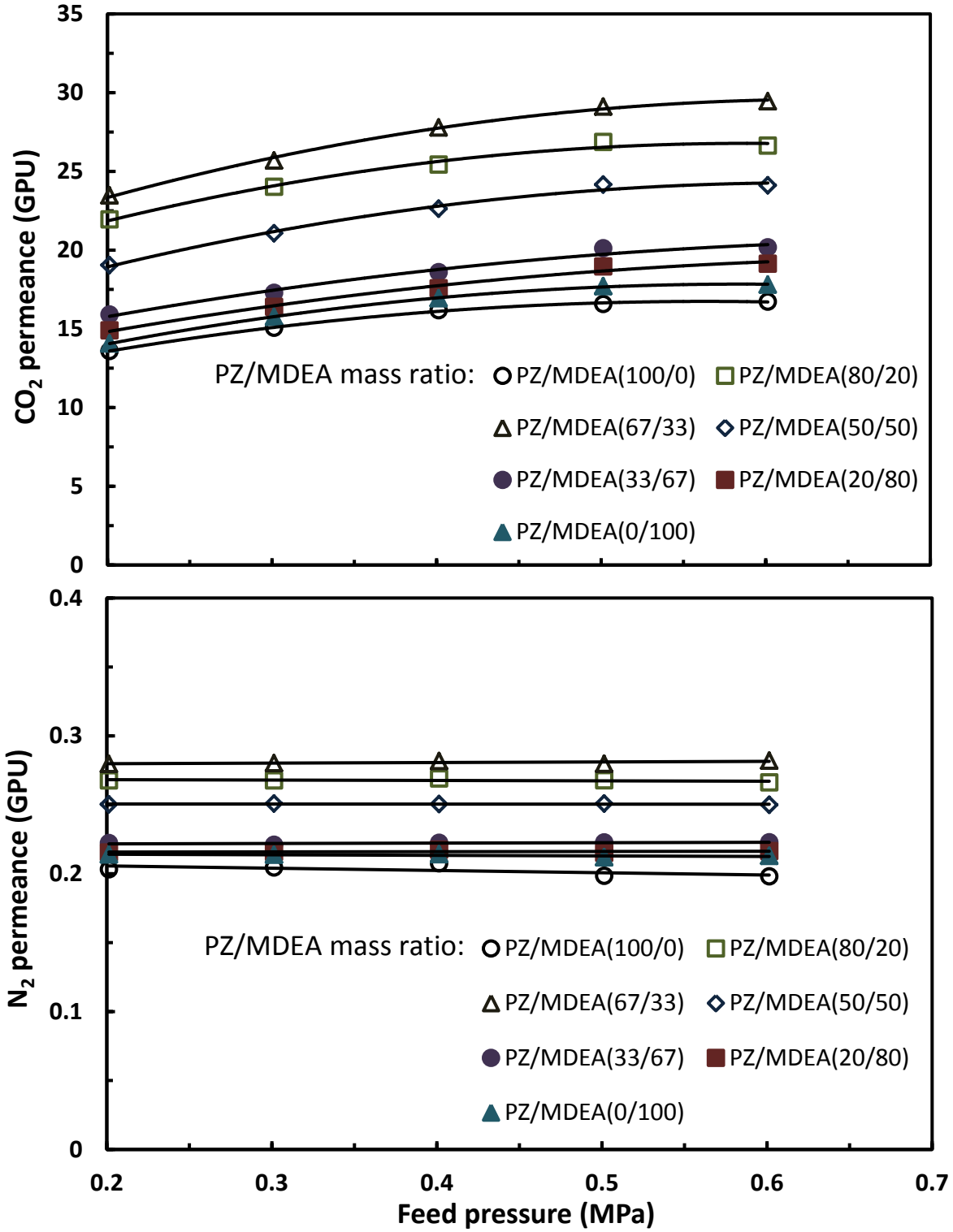


Fig. 5-26 Effect of PZ/MDEA mass ratio in the membrane on the permeance of $CO_2$ and $N_2$ for pure gas permeation through PVAm-PVA/PZ-MDEA composite membranes. Polymer concentration in the coating solution, 5 wt%; amine content in the membrane, amine/polymer mass ratio=1. Temperature, 298 K.

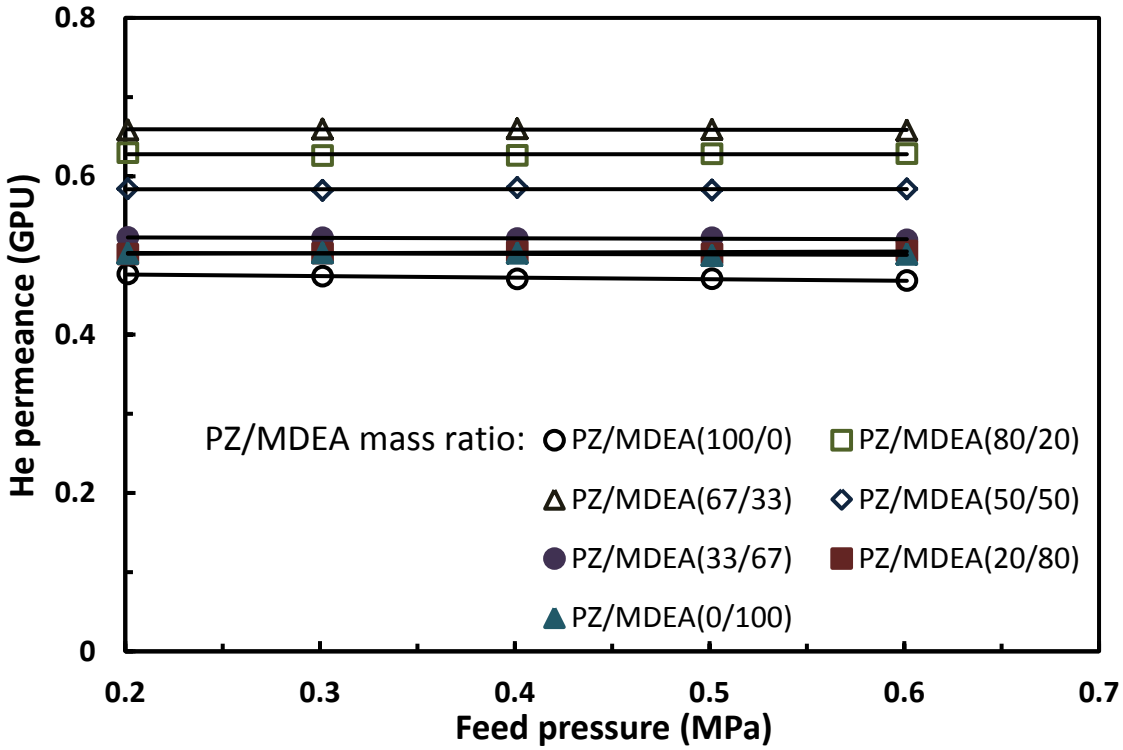


Fig. 5-27 Effect of PZ/MDEA mass ratio in the membrane on He permeance for pure gas permeation through PVAm-PVA/PZ-MDEA composite membranes. Polymer concentration in the coating solution, 5 wt%; amine content in the membrane, amine/polymer mass ratio=1. Temperature, 298 K.

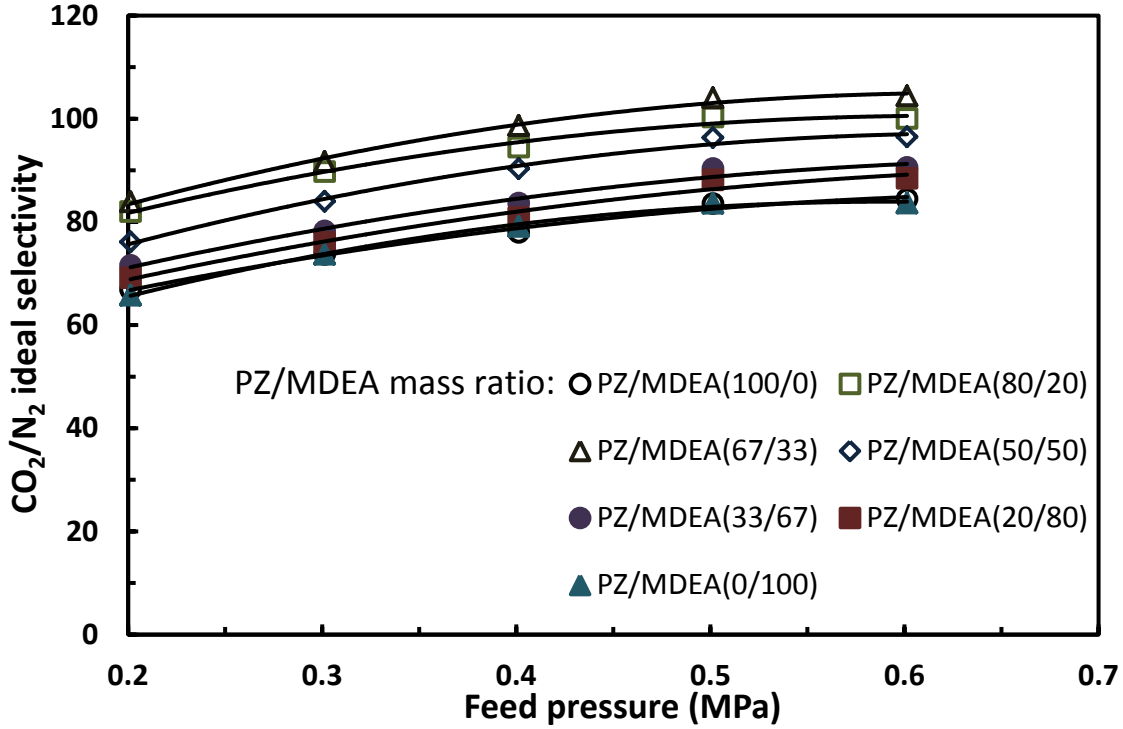


Fig. 5-28 Effect of PZ/MDEA mass ratio in the membrane on $CO_2/N_2$ ideal selectivity for pure gas permeation through PVAm-PVA/PZ-MDEA composite membranes. Polymer concentration in the coating solution, 5 wt%; amine content in the membrane, amine/polymer mass ratio=1. Temperature, 298 K.

The pure $CO_2$ permeance is greater than the $CO_2$ permeance for gas mixture permeation, whereas the opposite is true for $N_2$ permeance at a given PZ/MDEA ratio in the membrane. Thus, the $CO_2/N_2$ ideal selectivity based on the pure gas permeation is higher than the $CO_2/N_2$ selectivity based on the binary gas permeation. The results of pure helium permeation tests of the membranes also indicate the same trend with varying the PZ/MDEA ratios as for pure nitrogen permeation. In general, the membranes containing PZ/TEA behaved similarly to the membranes containing PZ/MDEA.

The $CO_2/N_2$ selectivity for gas mixture permeation and $CO_2/N_2$ ideal selectivity based on pure gas permeation for PVAm-PVA/PZ-MDEA composite membranes at different PZ/MDEA ratios were compared in Fig. 5-29. Both the $CO_2/N_2$ selectivity and $CO_2/N_2$ ideal selectivity of the PVAm-PVA/PZ-MDEA membranes are slightly greater than those of the PVAm-PVA/PZ-TEA membranes at the same PZ/tertiary amine mass ratio. A PZ/MDEA mass ratio of 67/33 or 80/20 appears to be appropriate to prepare a PVAm-PVA/PZ-MDEA composite membrane with improved $CO_2/N_2$ separation performance.

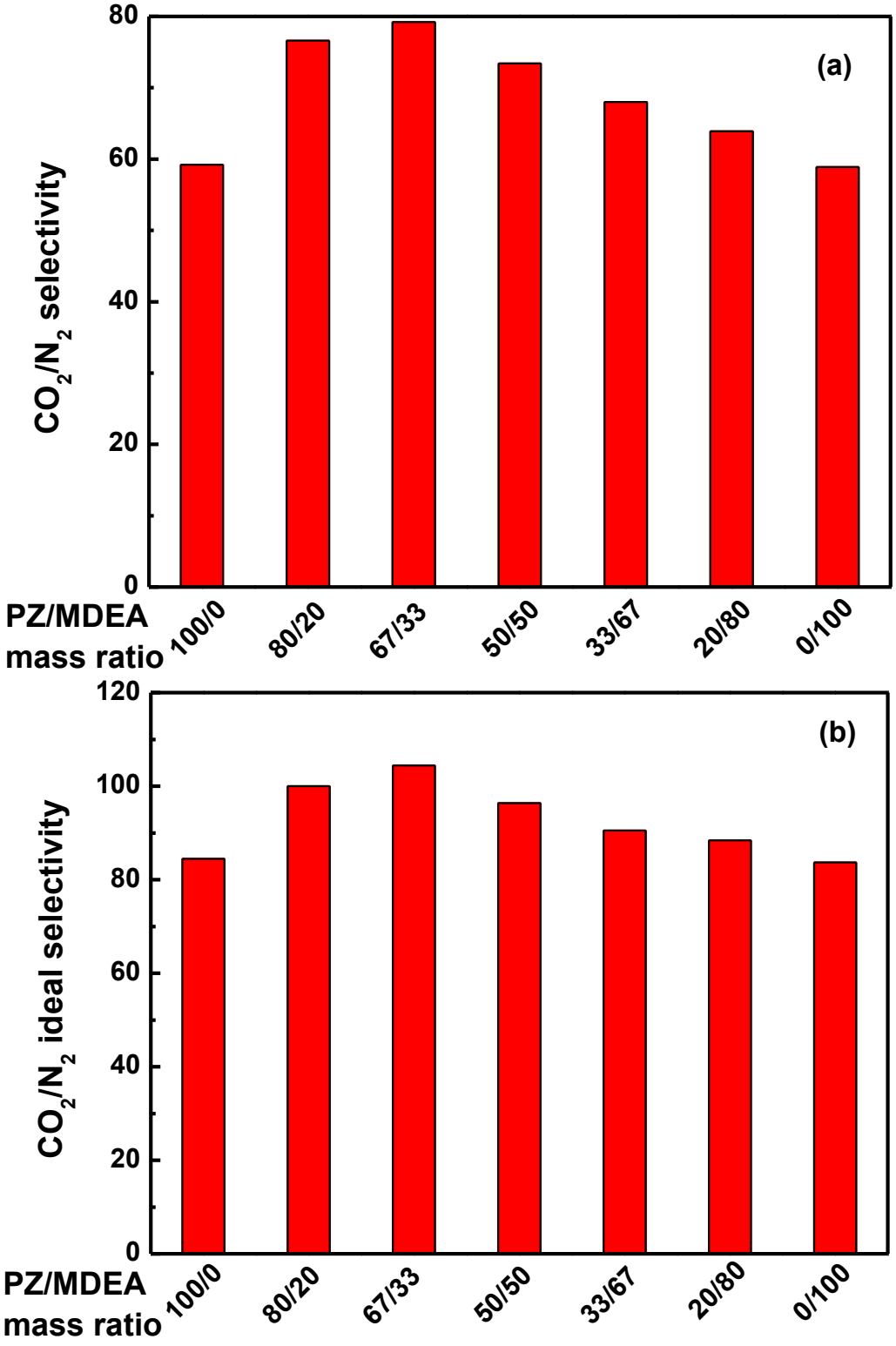


Fig. 5-29 A comparison of (a) $CO_2/N_2$ selectivity for binary $CO_2/N_2$ mixture (15.3 mol% $CO_2$) permeation and (b) $CO_2/N_2$ ideal selectivity based on pure gas permeation for PVAm-PVA/PZ-MDEA composite membrane at different PZ/MDEA mass ratios. Polymer concentration in the coating solution, 5 wt%; amine content in the membrane, amine/polymer mass ratio=1. Feed pressure, 601.3 kPa; temperature, 298 K.

## 5.4 Conclusions

PVAm-PVA composite membranes containing a molecular amine (i.e., PZ) and mixed molecular amines (i.e., PZ/TEA and PZ/MDEA) were developed and studied for $CO_2/N_2$ separation. The following conclusions can be drawn:

(1) The ATR-FTIR spectra confirmed the formation of hydrogen bonds between PVAm and PZ.

(2) The $CO_2$ permeance of PVAm-PVA/PZ membranes was shown to increase with an increase in the PZ concentration in the membrane or a decrease in the polymer concentration in the coating solution.

(3) The separation performance of PVAm-PVA/PZ membranes was investigated under various operating conditions (i.e., feed pressure, temperature and composition). The facilitation in $CO_2$ transport was more significant with higher $CO_2$ partial pressures.

(4) The stability of PVAm-PVA/PZ membranes was demonstrated for separating a $CO_2/N_2$ gas mixture continuously over a period of more than 7 weeks, and no deterioration in the membrane performance was observed.

(5) The PVAm-PVA membranes were incorporated with mixed amines of (PZ+TEA) or (PZ+MDEA) at different PZ/TEA and PZ/MDEA ratios. The membranes with a PZ/TEA or PZ/MDEA mass ratio of greater or equal to 1 were shown to have improved $CO_2/N_2$ permselectivity as compared to membranes containing either of the amine component alone (i.e., PZ, TEA or MDEA). A PZ/tertiary amine mass ratio of 67/33 or 80/20 in the membrane appeared to be appropriate for improved membrane permselectivity.

# Chapter 6

## PVAm-PVA composite membranes incorporated with diethylenetriamine and triethylenetetramine for $CO_2$ separation

---

### 6.1 Introduction

The incorporation of molecular amines into the PVAm-PVA composite membranes was shown to improve the $CO_2/N_2$ separation performance. Nevertheless, considering the ease of preparation and operation, one category of molecular amines with multi-amino functionalities appear to be more desirable than the aqueous amine blends. They contain two or more amino groups within a single molecule and thus possess a high affinity to $CO_2$. Diethylenetriamine (DETA) and triethylenetetramine (TETA), both of which are the derivatives of ethyleneamine products, are two such molecular amines that have been investigated extensively [Alper and Bouhamra, 1994; Al Marzouqi *et al.*, 2005; Amann and Bouallou, 2009; Hartono and Svendsen, 2009; Hartono *et al.*, 2009; Schaffer *et al.*, 2012].

DETA has three amino functionalities - two primary amino groups ($-NH_2$) and one secondary amino group (-NH), whereas TETA has four functional groups - two primary and two secondary amino groups, suggesting that both DETA and TETA may have a high capacity for binding $CO_2$ and a high absorption rate. Several amines (including DETA) were used as immobilized liquids in a facilitated transport membrane for selective removal of $CO_2$ and the

membrane containing DETA showed the highest $CO_2$ permeance and $CO_2/CH_4$ selectivity [Al Marzouqi *et al.*, 2005]. This is presumably due to the highest number of nitrogen atoms per amine molecule of DETA among the amines used, which can be correlated to its high loading capacity and large amine reactivity with $CO_2$. Another kinetic study [Schaffer *et al.*, 2012] of $CO_2$ absorption from flue gas also confirmed that TETA outperformed MEA in terms of $CO_2$ loading capacity. Furthermore, the amines with multi-amino functionalities were shown to have favorable reaction rates, in addition to enhanced loading capacity, because of the multi-amino sites [Alper and Bouhamra, 1994].

The main reaction of $CO_2$ with primary and secondary amines is the carbamate formation, which can take place by either the zwitterion mechanism or termolecular mechanism. The two-step zwitterion mechanism suggests that the reaction between $CO_2$ and an amine (denoted here as AmH) proceeds through the formation of a zwitterion as an intermediate (reaction 6-1), and the subsequent deprotonation of the zwitterion by a base B (reaction 6-2), forming carbamate ions [Vaidya and Kenig, 2007].

$$CO_2 + AmH \rightleftharpoons AmH^+COO^- \tag{6-1}$$

$$AmH^+COO^- + B \rightarrow AmCOO^- + BH^+ \tag{6-2}$$

On the other hand, the termolecular mechanism [Hartono *et al.*, 2009; Vaidya and Kenig, 2010] assumes that an amine reacts with $CO_2$ and the base simultaneously. The reaction occurs in a single step via a loosely bound encounter complex as the intermediate instead of a zwitterion (reaction 6-3).

$$CO_2 + AmH \cdots B \rightleftharpoons AmCOO^- \cdots BH^+ \tag{6-3}$$

Most of these complexes can break up to produce the reagent molecules (i.e., $CO_2$ and amine), whereas a few could react with a second molecule of amine or a molecule of water to form ionic

products (carbamate). Based on the kinetic studies, many reaction systems (including single and mixed amines, amines with multi-amino functionalities) could be well represented and interpreted by the zwitterion and termolecular mechanism [Vaidya and Kenig, 2010]. The kinetic study of $CO_2$ absorption in an aqueous solution of DETA gave identical results when fitting of experimental data to both of these models [Hartono *et al.*, 2009].

The presence of multi-amino groups in DETA and TETA makes the reaction system more complicated than a single amine system. Theoretically, one molecule with n amino groups can form polycarbamates composed of a maximum of n molecules of $CO_2$ bound as carbamate [Schaffer *et al.*, 2012]. Earlier NMR analysis of DETA-$CO_2$-$H_2O$ system [Hartono *et al.*, 2007] didn't reveal polycarbamate species where all 3 amino groups are present as carbamates, but happened to detect the presence of dicarbamate. Furthermore, the two primary amino groups of DETA were found to react with $CO_2$ at low amine loadings, before the secondary amino group began to react. The TETA-$CO_2$-$H_2O$ system showed similar results [Schaffer *et al.*, 2012].

The purpose of this chapter is to develop a novel facilitated transport membrane containing both PVAm as fixed carriers and DETA or TETA as mobile carriers in a PVAm/PVA blend polymer matrix for $CO_2$ removal from flue gas. It may be noted that DETA is reported to have a high rate of degradation, which may be an issue for long term use in conventional absorption applications [Davis and Rochelle, 2008]. However, the potential interactions between the amino groups of DETA (so as TETA), the amino groups of PVAm and the hydroxyl groups of PVA may help retain the DETA in the polymer network and thus enhance the membrane stability. First, the effect of amine content (DETA and TETA) in the membrane was examined, and the mixed gas and pure gas permeation was carried out. The effects of temperature and feed $CO_2$ content on the separation performance were also studied for $CO_2$ separation with the PVAm-PVA/DETA and

PVAm-PVA/TETA membranes.

## 6.2 Experimental

Diethylenetriamine (DETA) and triethylenetetramine (TETA) were supplied by Sigma Aldrich with purities of 99% and 60%, respectively. Other materials used were the same as described before. The procedure for preparation of PVAm-PVA/DETA and PVAm-PVA/TETA composite membranes was similar to that described in chapter 5. The mass ratio of PVAm to PVA in the membrane casting solution was kept at 60/40, and the overall polymer concentration was 5 wt%. The mass ratio of amine (i.e., DETA or TETA) to polymer was varied as follows: 20/100, 50/100, 100/100, 150/100, 200/100 and 250/100. For the fabrication of all the PVAm-PVA/amine composite membranes, only one coat of the casting solution was found effective to prepare defect-free membranes.

The experimental setup and procedure for binary gas mixture permeation experiments have been described in chapter 5. The operating temperature was 25℃ unless specified otherwise. The permeation tests were repeated several times with replicate membrane samples, and the reproducibility of the membranes was found to be within 12%.

## 6.3 Results and discussion

### 6.3.1 Effect of amine content

Facilitated transport membranes containing PVAm as fixed carriers and DETA or TETA as mobile carriers in a PVAm/PVA blend polymer matrix were fabricated and the effects of amine content (i.e., DETA and TETA) in the membrane on the membrane performance were examined for $CO_2/N_2$ separation. Both mixed gas and pure gas permeation tests were conducted for

purpose of comparison. In the mixed gas test, a pre-mixed $CO_2/N_2$ gas containing 15.3 mol% $CO_2$ (balanced $N_2$) was used as the feed.

Figs. 6-1 and 6-2 show the effects of amine content in the membrane on the membrane permeance to $CO_2$ and $N_2$. As shown in these figures, for a given membrane, the $CO_2$ permeance increases with an increase in the feed pressure initially and then reaches a constant when the feed pressure is high enough, whereas the $N_2$ permeance seems to be independent of the feed pressure within the pressure range tested. The different trends in $CO_2$ and $N_2$ permeance with respect to the feed pressure observed here may be attributed to the following: because of the presence of amino groups from PVAm and DETA or TETA, $CO_2$ transport across the membrane occurs in two modes: one is carrier-mediated transport and the other free molecular diffusion. For the carrier-mediated transport, the free amino carriers are bound with $CO_2$ molecules to form $CO_2$-carrier complexes at the feed side of the membrane, which diffuse across the membrane down the concentration gradient to the permeate side, where $CO_2$ molecules and carriers are liberated. In addition, $CO_2$ transport through the membrane may also be conveyed in the form of $HCO_3^-$ and diffuse as ions in water [Deng *et al.*, 2009; Deng and Hagg, 2010]. Increasing $CO_2$ partial pressure will enhance the rate of reaction between $CO_2$, water and the carriers, leading to an increase in the $CO_2$ permeance. However, when the $CO_2$ partial pressure becomes increasingly high, the limited carrier sites in the membrane are gradually exhausted and no longer be available for additional $CO_2$ molecules, thereby preventing further uptake of $CO_2$ molecules. This is often the case for the so-called "carrier saturation", which yields a constant $CO_2$ permeance. On the other hand, the $CO_2$ partial pressure has little effect on the $CO_2$ permeability coefficient due to physical solution-diffusion. Consequently, the trend of $CO_2$ permeance due to carrier-mediated transport with respect to pressure determines the overall pressure dependence of $CO_2$ permeance.

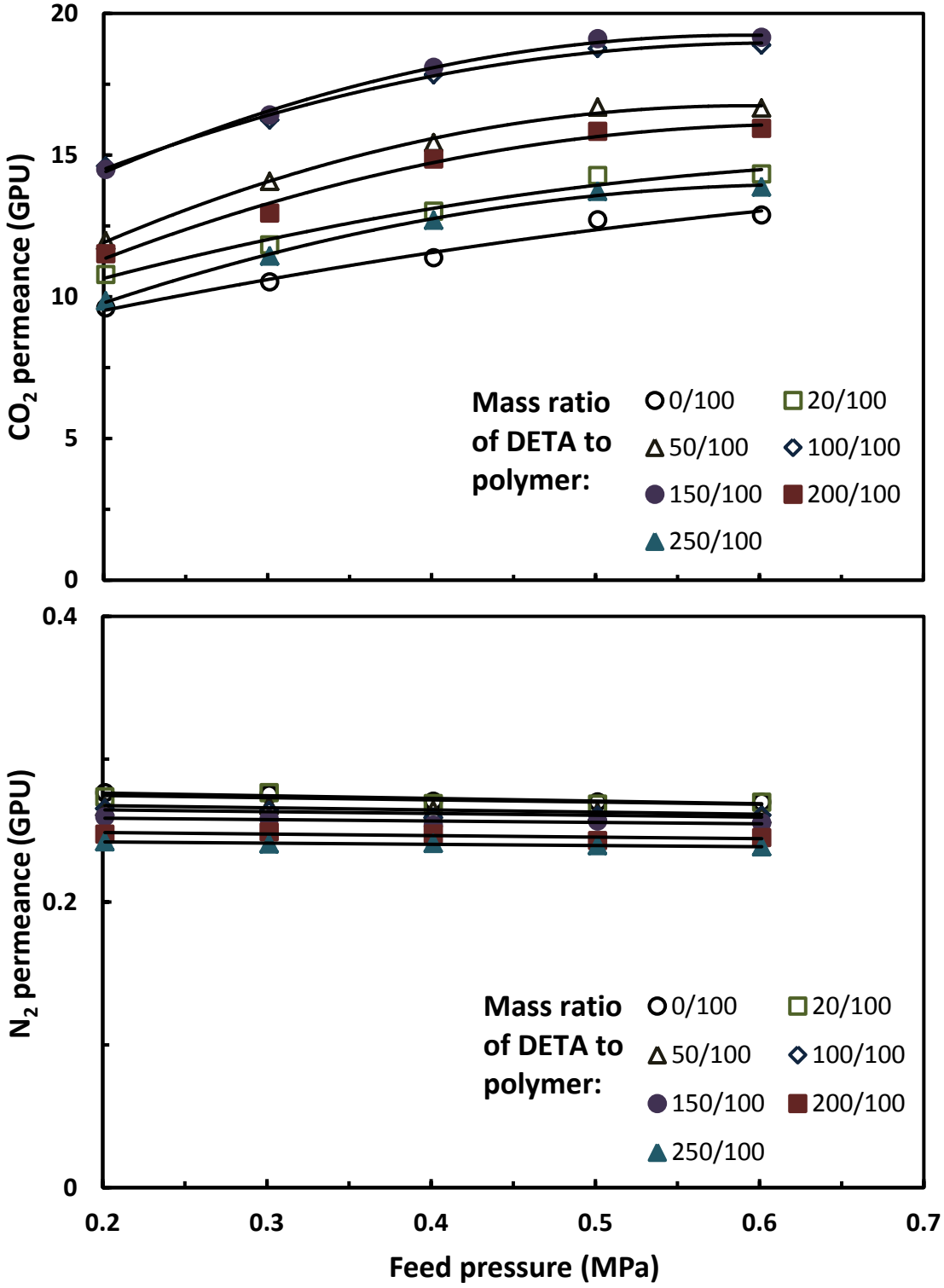


Fig. 6-1 Effect of DETA content (mass ratio of DETA to polymer) in the membrane on permeance of $CO_2$ and $N_2$ for binary $CO_2/N_2$ permeation through PVAm-PVA/DETA membranes. Polymer concentration in the coating solution, 5 wt%. Feed $CO_2$ content: 15.3 mol%; temperature, 298 K.

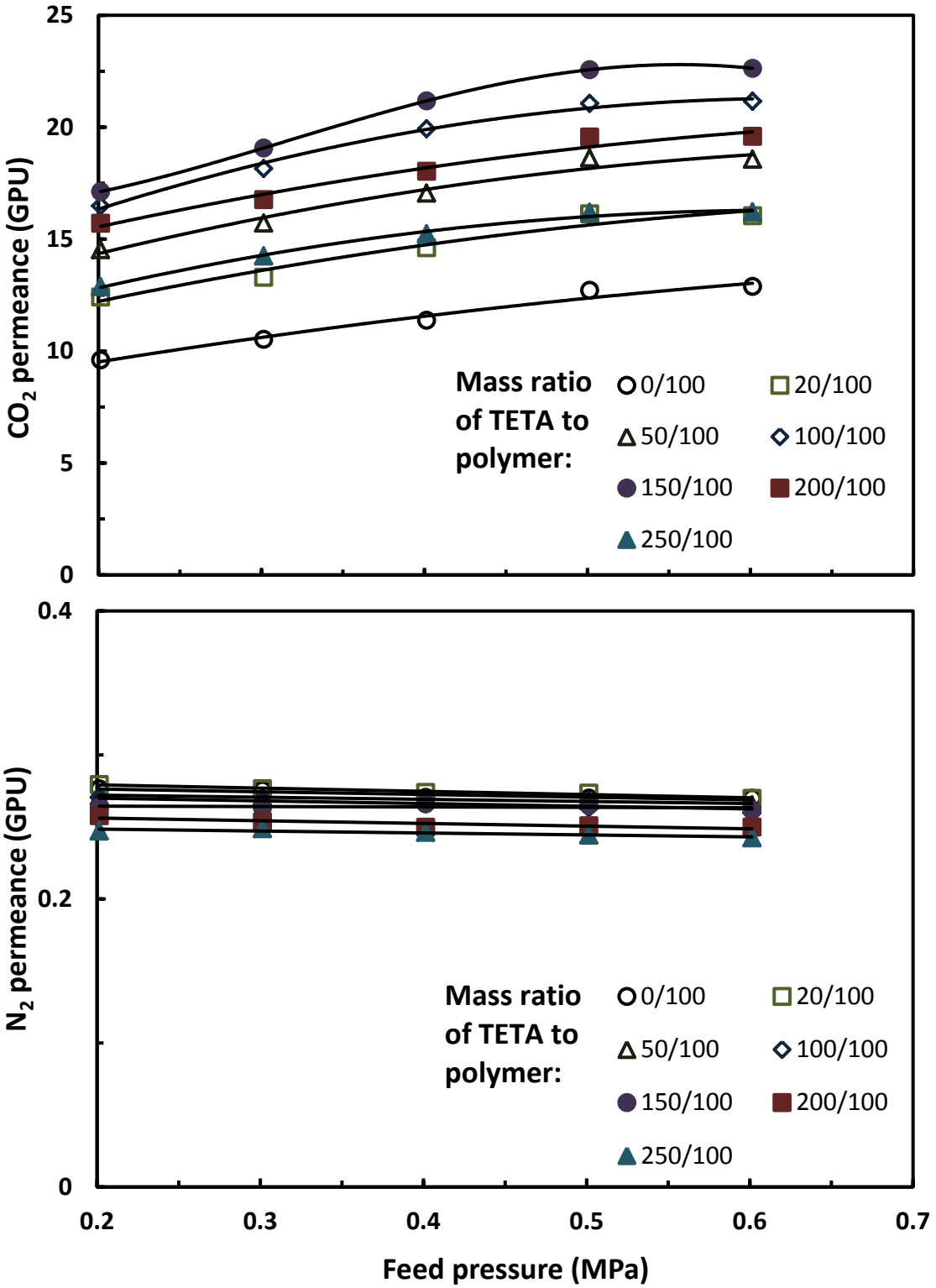


Fig. 6-2 Effect of TETA content (mass ratio of TETA to polymer) in the membrane on permeance of $CO_2$ and $N_2$ for binary $CO_2/N_2$ permeation through PVAm-PVA/TETA membranes. Polymer concentration in the coating solution, 5 wt%. Feed $CO_2$ content: 15.3 mol%; temperature, 298 K.

However, since amino carriers don't react with $N_2$, $N_2$ transport through the membrane follows the simple physical solution-diffusion model. Therefore, the $N_2$ permeance remains unchanged when changing the feed pressure.

Comparing to the PVAm/PVA membrane without amines, both the PVAm-PVA/DETA and PVAm-PVA/TETA membranes showed a greater $CO_2$ permeance, as seen in Figs. 6-1 and 6-2, indicating the effectiveness of using the amines to facilitate $CO_2$ transport by exploiting fixed and mobile carriers. This observation is easily understood: the addition of DETA or TETA as mobile carriers increases the total amount of free carriers in the membrane, which favors the transport of $CO_2$ and thus enhances the $CO_2$ permeance of the membrane. Thus, with an increase in the amount of DETA or TETA in the membrane, the $CO_2$ permeance of the membrane increases accordingly. However, when the mass ratio of DETA to polymer exceeds a certain point (i.e., 150/100), it turns out that the $CO_2$ permeance of the membrane begins to drop with a further increase of DETA content in the membrane. The PVAm-PVA/TETA membrane also exhibited a similar trend with increasing TETA content in the membrane. A similar TETA to polymer mass ratio of 150/100 was found to correspond to the turning point at which the $CO_2$ permeance begins to decrease when additional TETA is incorporated into the membrane. As stated previously, the addition of DETA or TETA as mobile carriers increases the total number of carriers in the membrane, which results in an increase of $CO_2$ solubility; furthermore, the mobile nature of DETA and TETA molecules can enhance the diffusivity of $CO_2$-carrier complexes in the membrane. Both of these aspects contribute to a higher $CO_2$ permeance. On the other hand, the reactions between $CO_2$ and amino carriers will inevitably produce ionic species according to either the zwitterion mechanism or termolecular mechanism. These ionic species (including carbamate and polycarbamate ions) can potentially reduce the $CO_2$ solubility in the membrane

due to the salting out effects, which makes it hard for $CO_2$ molecules to access the amino carriers, resulting in a decrease in the diffusivities of $CO_2$ molecules and $CO_2$-carrier complexes. Both of these may lead to a lower $CO_2$ permeance. These opposite effects from carrier content and ionic species with increasing amine content in the membrane determine the overall trend of $CO_2$ permeance with the addition of DETA or TETA in the membrane.

The intermolecular interactions via hydrogen bonding between the amino groups of PVAm, hydroxyl groups of PVA and the amino groups of DETA or TETA may be stronger with increasing the content of small molecules DETA or TETA in the membrane and result in a more densely packed polymer matrix, which leads to a reduction in the gas diffusivity. Since $N_2$ does not involve in chemical reaction with carriers, the reduction in the diffusivity will slightly reduce $N_2$ permeance, as displayed in these figures.

Fig. 6-3 illustrates the variation of $CO_2/N_2$ selectivity with respect to the DETA and TETA content in the membrane at different feed pressures. Both the PVAm-PVA/DETA and PVAm-PVA/TETA membranes show a higher selectivity than the PVAm-PVA membranes containing no small molecules DETA or TETA. At a feed pressure of 0.6 MPa, the highest $CO_2/N_2$ selectivity observed was 75 with a PVAm-PVA/DETA membrane and 86.5 with a PVAm-PVA/TETA membrane at an amine/polymer mass ratio of 150/100.

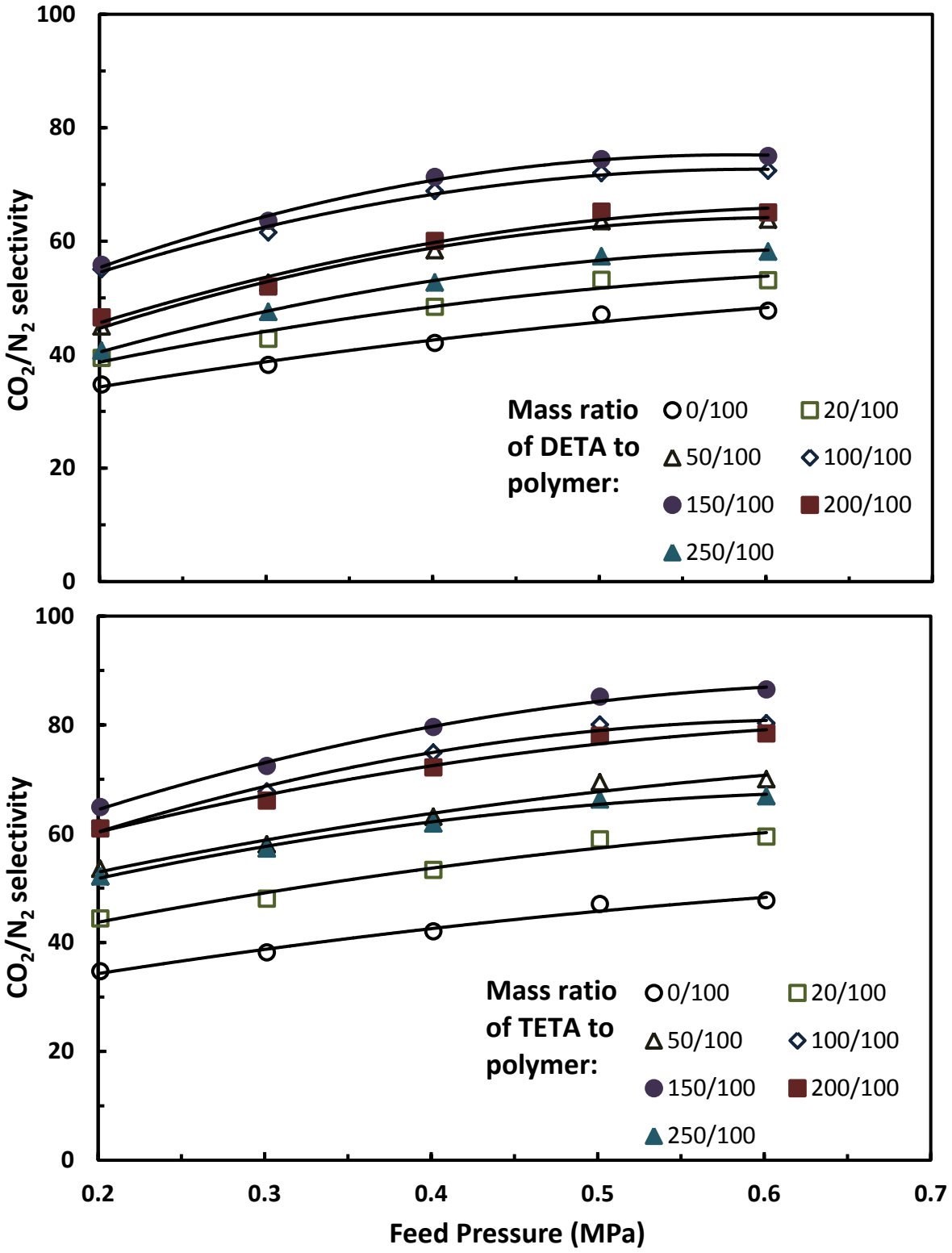


Fig. 6-3 Effect of amine content (mass ratio of amine to polymer) in the membrane on $CO_2/N_2$ selectivity for binary $CO_2/N_2$ permeation through PVAm-PVA/amine membranes. Amine used: DETA and TETA. Polymer concentration in the coating solution, 5 wt%. Feed $CO_2$ content, 15.3 mol%; temperature, 298 K.

From the experimental data presented here, one may notice that the PVAm-PVA membranes containing TETA have shown a slightly higher $CO_2$ permeance and $CO_2/N_2$ selectivity than the membranes containing DETA at the same amine/polymer ratio in the membrane. TETA molecule has one more secondary amino group than DETA, which will help make it more effective to facilitate $CO_2$ transport as previous studies show that the reaction rates increase with increasing number of amine functionalities in the molecule [Al Marzouqi *et al.*, 2005; Hartono *et al.*, 2009]. Nevertheless, the difference in the gas permeance in these membranes containing DETA and TETA is not very significant. This is because the primary amino groups are expected to react first with $CO_2$ before the reaction between the secondary amino groups and $CO_2$. The reaction rate of the primary amino groups with $CO_2$ is reported to be faster that the reaction between the secondary amino groups and $CO_2$ [Schaffer *et al.*, 2012].

To further look into the trends of how the membrane permeability and selectivity vary with DETA and TETA contents in the membrane, pure $CO_2$ and $N_2$ permeation tests were conducted, and the results are presented in Figs. 6-4 to 6-6.

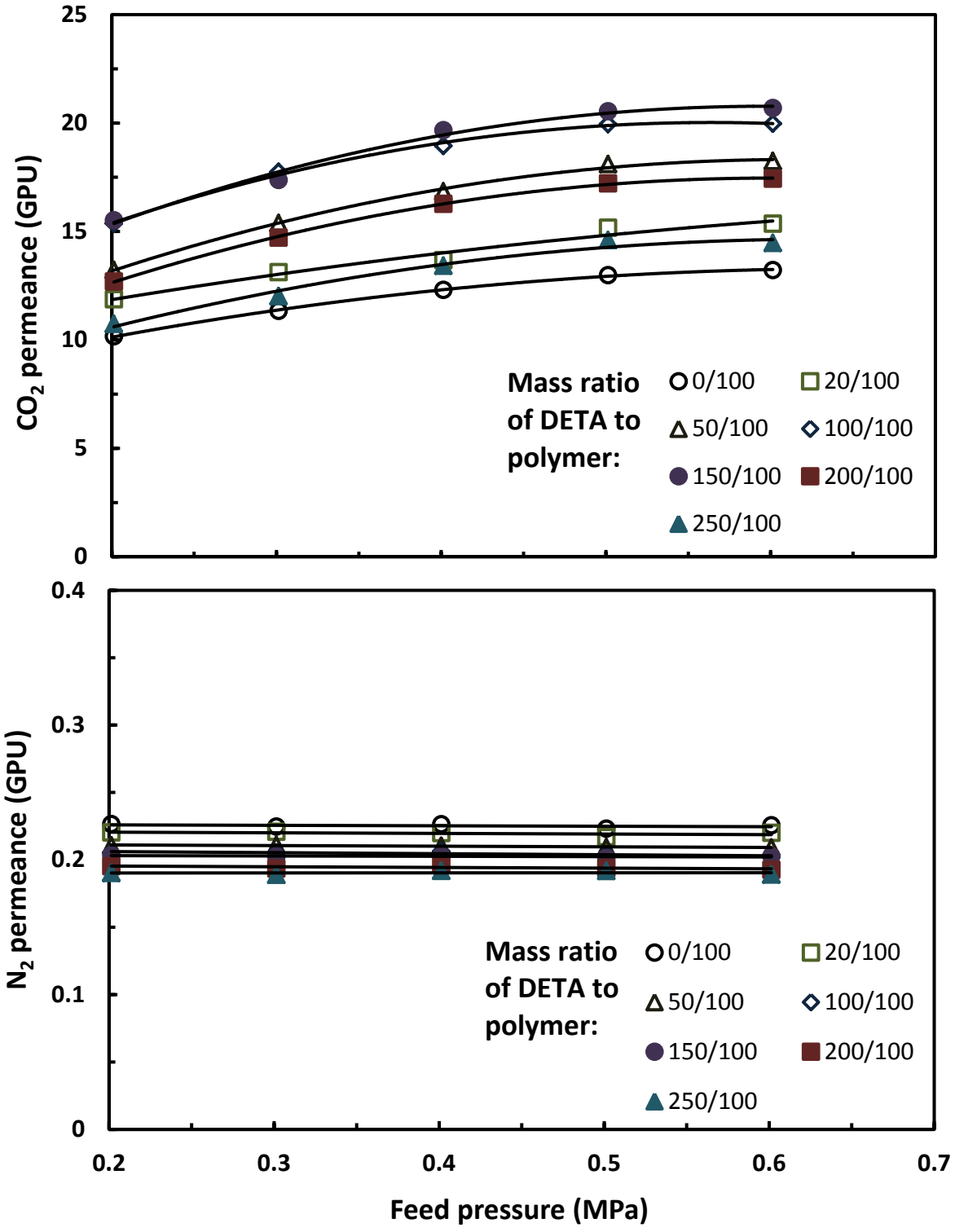


Fig. 6-4 Effect of DETA content (mass ratio of DETA to polymer) in the membrane on the permeance of $CO_2$ and $N_2$ for pure $CO_2$ and $N_2$ permeation through PVAm-PVA/DETA membrane. Polymer concentration in the coating solution, 5 wt%. Temperature, 298 K.

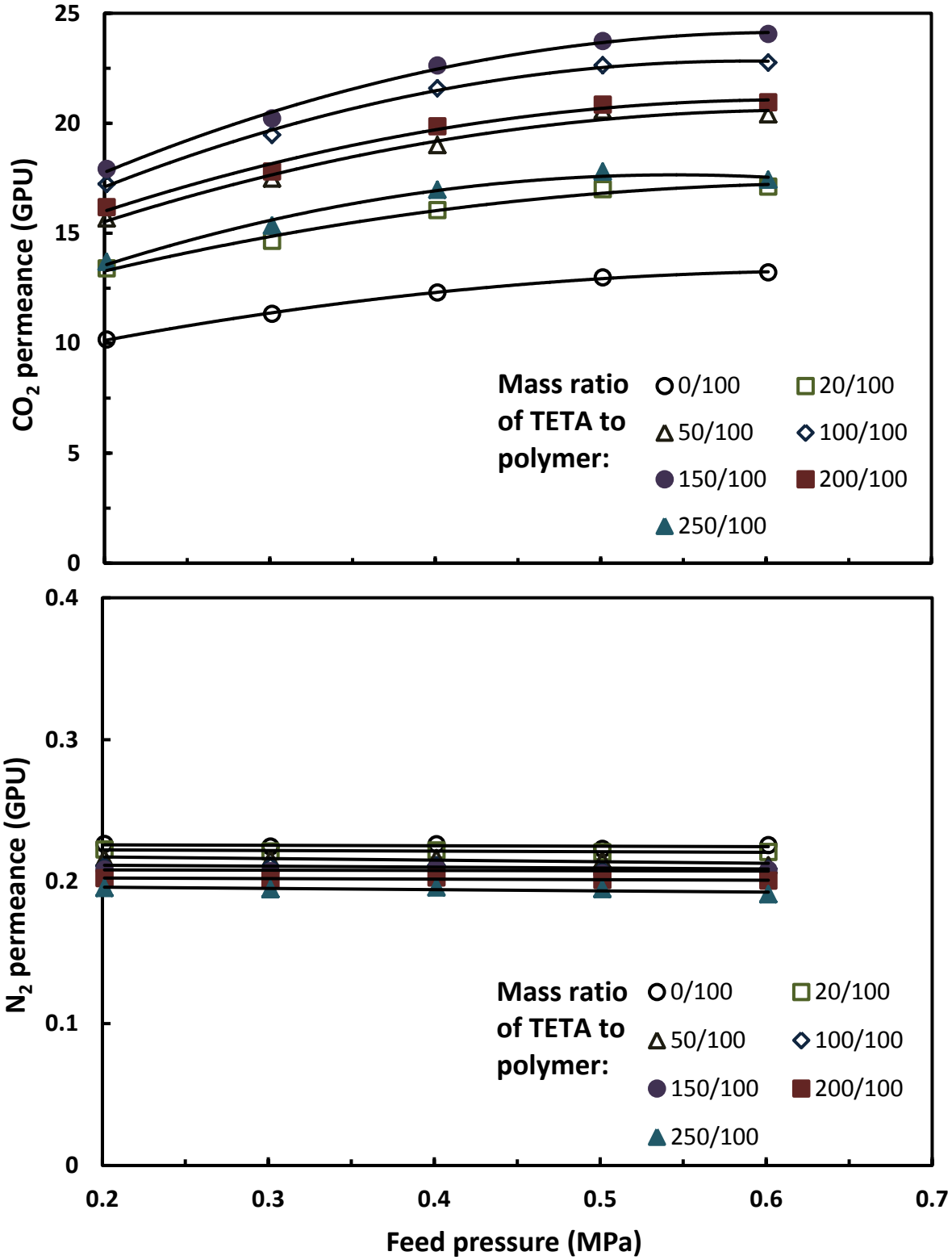


Fig. 6-5 Effect of TETA content (mass ratio of TETA to polymer) in the membrane on the permeance of $CO_2$ and $N_2$ for pure $CO_2$ and $N_2$ permeation through PVAm-PVA/TETA membrane. Polymer concentration in the coating solution, 5 wt%. Temperature, 298 K.

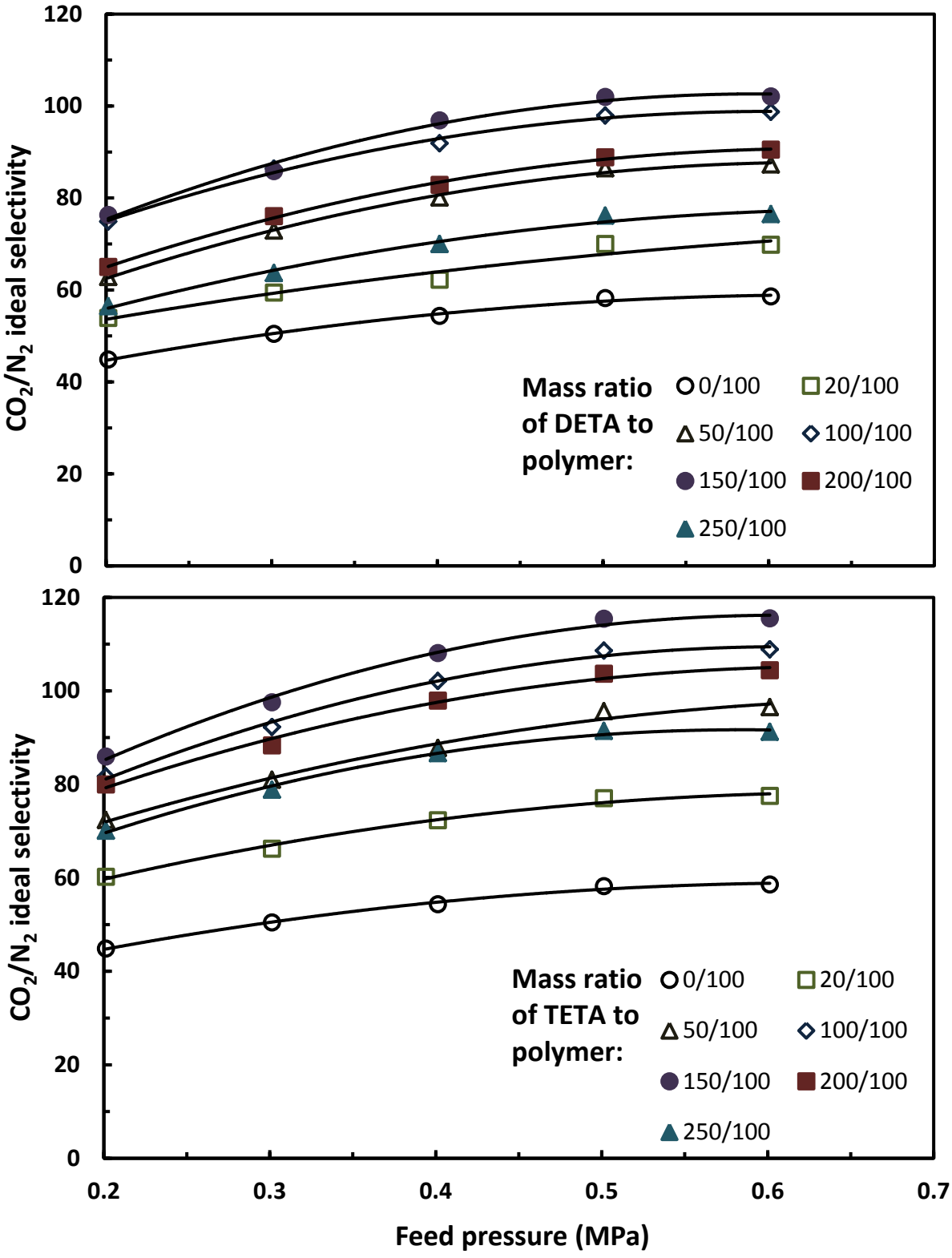


Fig. 6-6 Effect of amine content (mass ratio of amine to polymer) in the membrane on $CO_2/N_2$ ideal selectivity for pure $CO_2$ and $N_2$ permeation through PVAm-PVA/amine membrane. Amine used: DETA and TETA. Polymer concentration in the coating solution, 5 wt%. Temperature, 298 K.

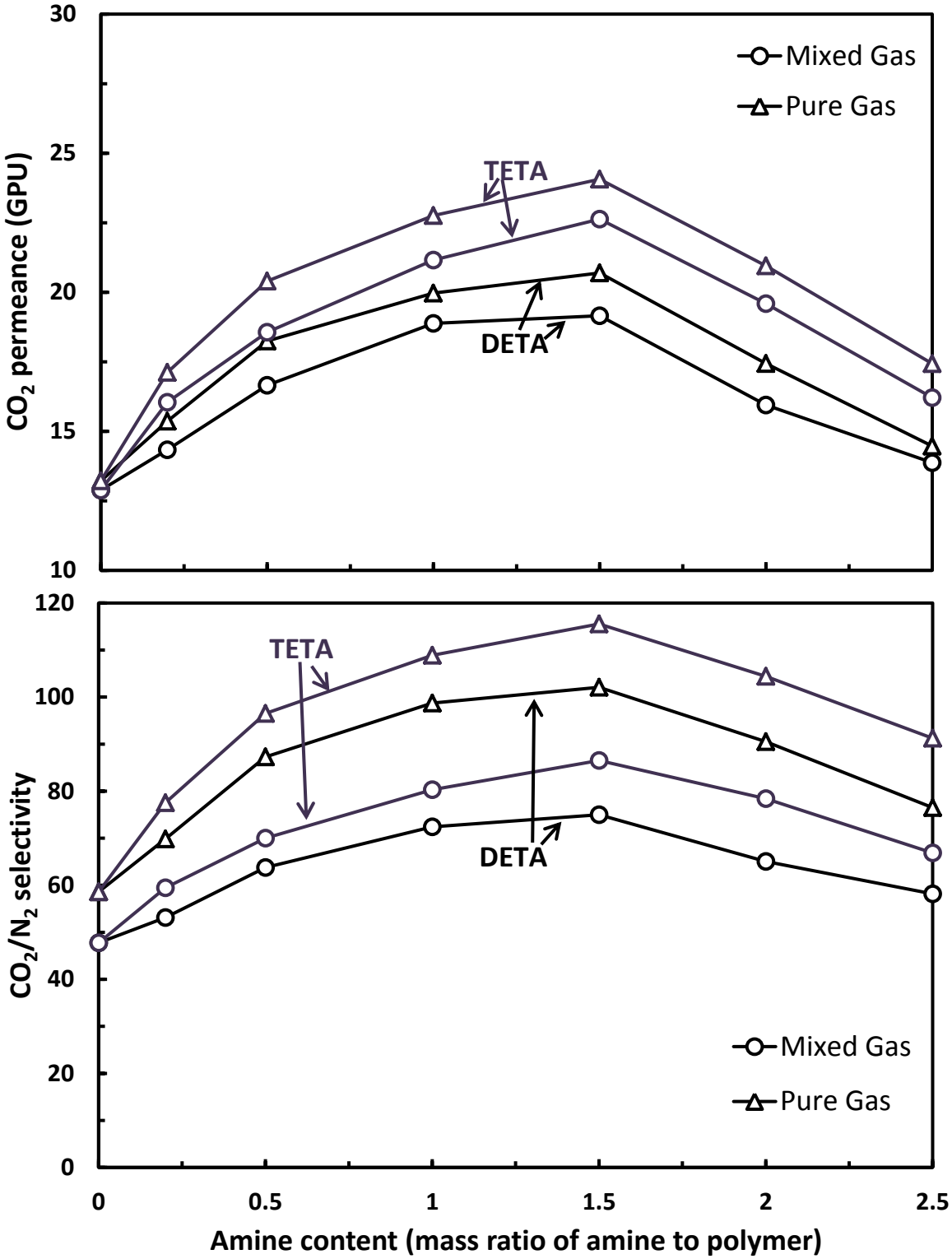


Fig. 6-7 A comparison of $CO_2$ permeance and $CO_2/N_2$ selectivity for pure and mixed gas permeation through PVAm-PVA/amine membranes at different amine content. Amine used: DETA and TETA. Polymer concentration in the coating solution, 5 wt%. Feed $CO_2$ concentration in $CO_2/N_2$ mixed gas, 15.3 mol%. Feed pressure, 601.3 kPa; temperature, 298 K.

It's obvious that the variations in $CO_2$ permeance, $N_2$ permeance and $CO_2/N_2$ selectivity with respect to DETA or TETA content in the membrane for pure gas permeation have the same fashion as in the case of $CO_2/N_2$ mixed gas separation. Both the pure $CO_2$ permeance and $CO_2/N_2$ ideal selectivity increase with an increase in the amine content in the membrane, and then start to decrease when the amine/polymer ratio is beyond certain point (i.e.,150/100), no matter whether DETA or TETA is used. The pure $N_2$ permeance slightly decreases with an increase in the amine content. Compared to pure gas permeation, the $CO_2$ permeance of the membranes for mixed gas permeation is slightly lower and the $N_2$ permeance is higher, resulting in a lower $CO_2/N_2$ selectivity than the $CO_2/N_2$ ideal selectivity based on the pure gas permeation. This trend is more clearly shown in Fig. 6-7, and this may be attributed to the coupling effects between permeating species in mixed gas permeation, which reduce the permeance of the more permeable component (i.e., $CO_2$) and increase the permeance of the less permeable one (i.e., $N_2$). The differences of pure and mixed gas permeation will be further investigated and discussed in details later in evaluating effects of feed $CO_2$ concentration on the membrane performance. Particularly, the PVAm-PVA/DETA membrane with a DETA to polymer mass ratio of 150/100 shows a $CO_2/N_2$ selectivity of 102 at a feed pressure of 0.6 MPa, and the PVAm-PVA/TETA membrane at the same TETA to polymer mass ratio displays a $CO_2/N_2$ selectivity as high as 115. Similarly, the PVAm-PVA/TETA membranes also show better $CO_2$ permeance and $CO_2/N_2$ permeance ratio than PVAm-PVA/DETA membranes based on the pure gas permeation data.

### 6.3.2 Effect of temperature

Pure gas permeation was conducted at different temperatures and at a fixed feed pressure of 0.6 MPa. The effects of temperature on the gas permeance of the PVAm/PVA membranes incorporated with different amounts of DETA and TETA were investigated, and the results were

shown in Figs. 6-8 to 6-10. Fig. 6-8 shows that regardless of the DETA content in the membrane, both $CO_2$ and $N_2$ permeance increases with an increase in the temperature, and the temperature dependence of the permeance appears to follow an Arrhenius type of relationship. Similar pattern was also observed for PVAm-PVA/TETA membranes with different TETA content in the membrane, as shown in Fig. 6-9. Further, the temperature tends to affect the $N_2$ permeance more significantly than $CO_2$ permeance, and thus there is a reduction in $CO_2/N_2$ ideal selectivity as temperature increases, which is shown in Fig. 6-10.

For gases such as $N_2$ following the simple solution-diffusion mechanism when transporting through the membrane, the diffusivity in the membrane is expected to increase with an increase in temperature, whereas the opposite holds for the solubility. The temperature often affects the diffusivity of permanent gases more significantly than the solubility. Hence, the $N_2$ permeance is shown to increase with increasing temperature. However, for $CO_2$ permeation, the carrier-mediated transport also occurs in addition to the simple molecular diffusion. From the solution-diffusion perspectives, a higher $CO_2$ permeance is expected when increasing the temperature. On the other hand, since the $CO_2$ molecules react with amino carriers, an increase in temperature will result in an enhanced reaction rate and increased diffusivity of the $CO_2$-carrier complexes simultaneously, which are favorable for $CO_2$ transport. These aspects seem to be more significant at higher amine loadings in the membrane. Thus, from Figs. 6-8 and 6-9, one can easily see that the $CO_2$ permeance tends to increase more dramatically with increasing temperature at higher amine content in the membrane. However, the increase in $CO_2$ permeance with temperature is still less pronounced than that of $N_2$ permeance, as reflected by the lowering of $CO_2/N_2$ permeance ratio (i.e., ideal selectivity) as temperature increases.

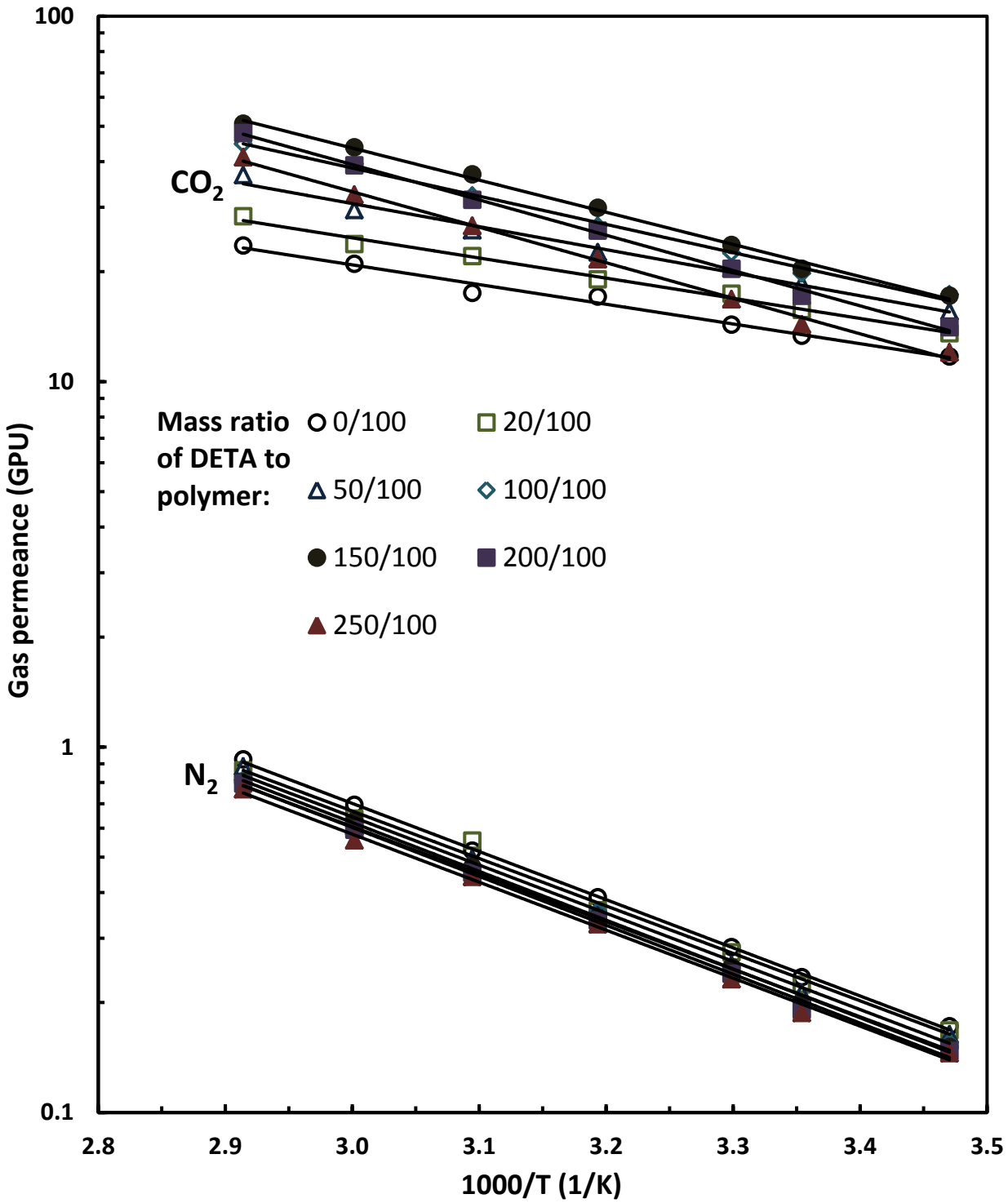


Fig. 6-8 Effect of temperature on the permeance of $CO_2$ and $N_2$ for pure $CO_2$ and $N_2$ permeation through PVAm-PVA/DETA membranes at different DETA content. Polymer concentration in the coating solution, 5 wt%. Feed pressure, 601.3 kPa.

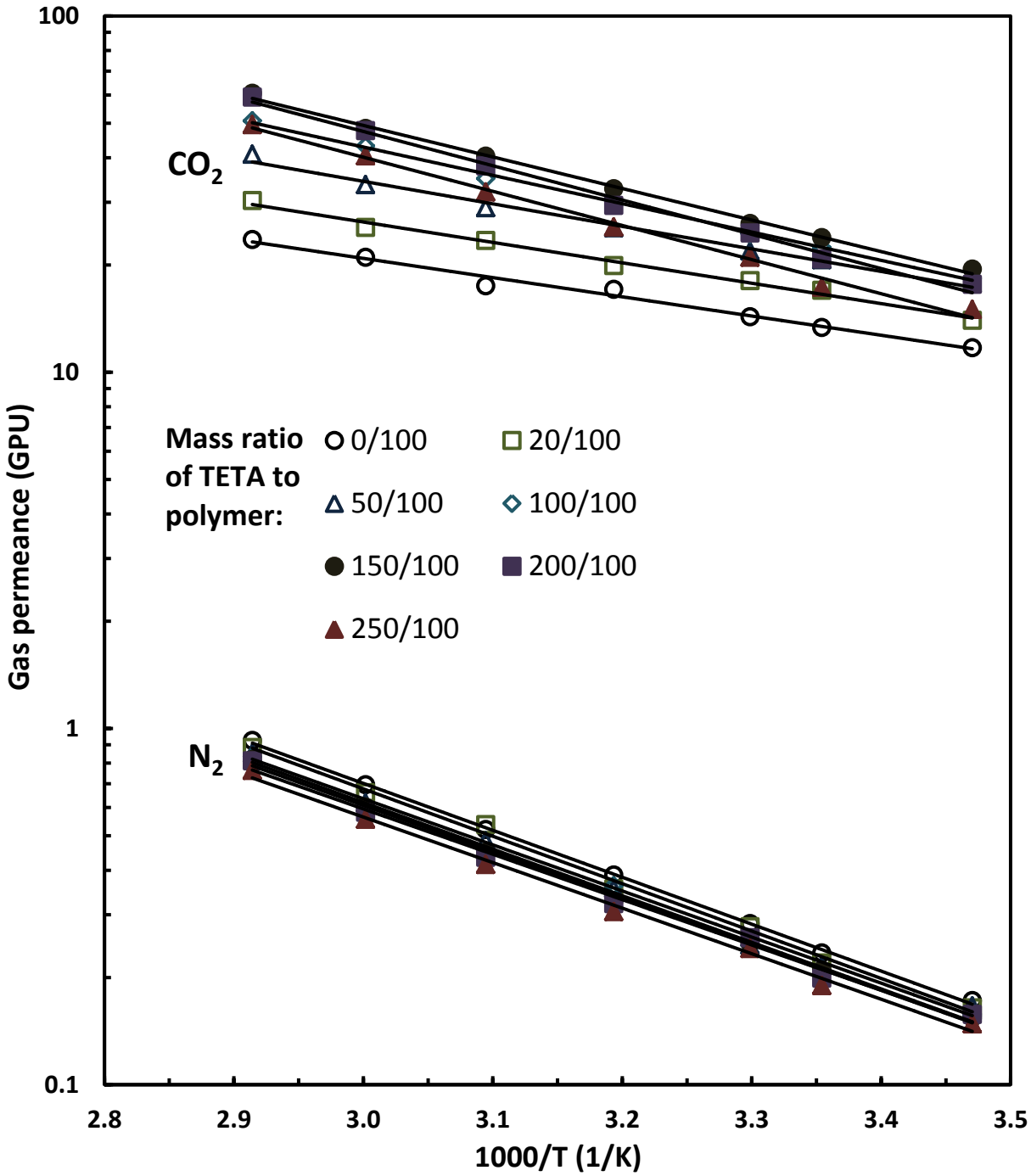


Fig. 6-9 Effect of temperature on the permeance of $CO_2$ and $N_2$ for pure $CO_2$ and $N_2$ permeation through PVAm-PVA/TETA membranes at different TETA content. Polymer concentration in the coating solution, 5 wt%. Feed pressure, 601.3 kPa.

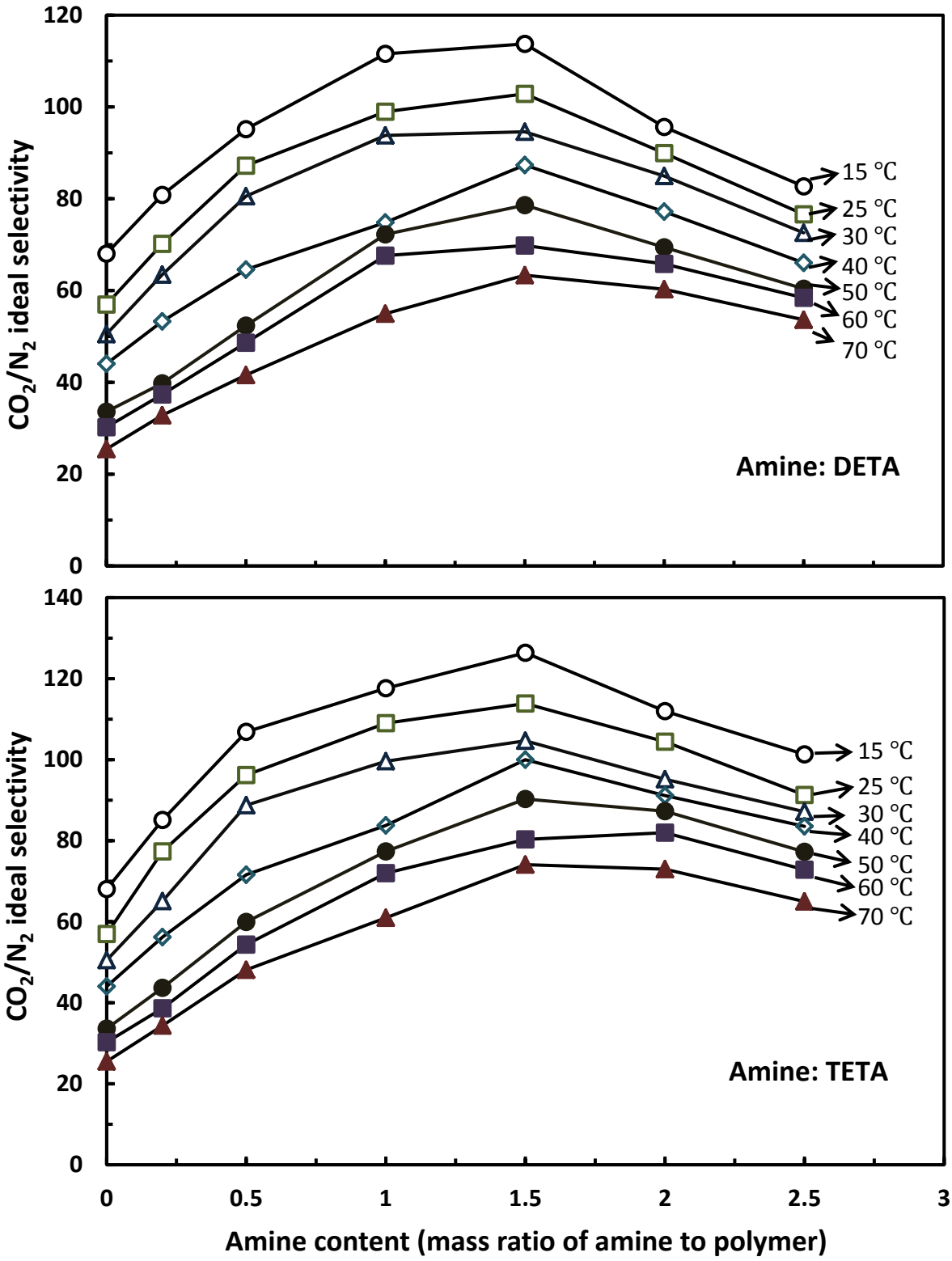


Fig. 6-10 Effect of amine content (mass ratio of amine to polymer) in the membrane on $CO_2/N_2$ ideal selectivity for pure $CO_2$ and $N_2$ permeation through PVAm-PVA/amine membranes at different temperatures. Amine used: DETA and TETA. Polymer concentration in the coating solution, 5 wt%. Feed pressure, 601.3 kPa.

The activation energy of permeation for $CO_2$ and $N_2$ at different DETA and TETA contents was then calculated from the experimental data, as shown in Fig. 6-11. A lower value of activation energy of permeation for $CO_2$ indicates $CO_2$ permeation through the membrane more easily. However, the activation energy of $CO_2$ increases with the addition of DETA and TETA in the membrane, while the activation energy of $N_2$ seems to be independent of DETA and TETA contents in the membrane. Recall that the enhanced reaction rates and increased diffusivity of the $CO_2$-carrier complexes at higher temperatures will increase the $CO_2$ permeance, and these effects are more significant at higher DETA and TETA loadings. On the other hand, the ionic strength of $CO_2$-amine reaction products in the membrane will become stronger at higher amine content as temperature increases, and the salting-out effects due to the ionic species will reduce the $CO_2$ permeance. Hence, the activation energy for $CO_2$ permeation begins to level off when the DETA and TETA content in the membrane is sufficiently high. The increased activation energy for $CO_2$ permeation at higher amine contents in the membrane is consistent with the activation energy of the reaction for the observed kinetics rate constants with respect to DETA concentration reported by Hartono *et al.* [2009], as shown in Table 6-1.

Table 6-1 Comparison of activation energy between literature and this study

| | | | | | | | | |
|---|---|---|---|---|---|---|---|---|
| DETA concentration ($kmol/m^3$) | 1 | 1.5 | 2 | 2.5 | 2.9 | | | [Hartono et al., 2009] |
| Activation energy of rate constant (kJ/mol) | 28.33 | 31.50 | 32.05 | 35.06 | 33.62 | | | |
| Mass ratio of DETA to polymer | 0 | 0.2 | 0.5 | 1 | 1.5 | 2 | 2.5 | This study |
| Activation energy of $CO_2$ (kJ/mol) | 10.33 | 10.55 | 12.07 | 14.77 | 16.83 | 18.50 | 18.62 | |

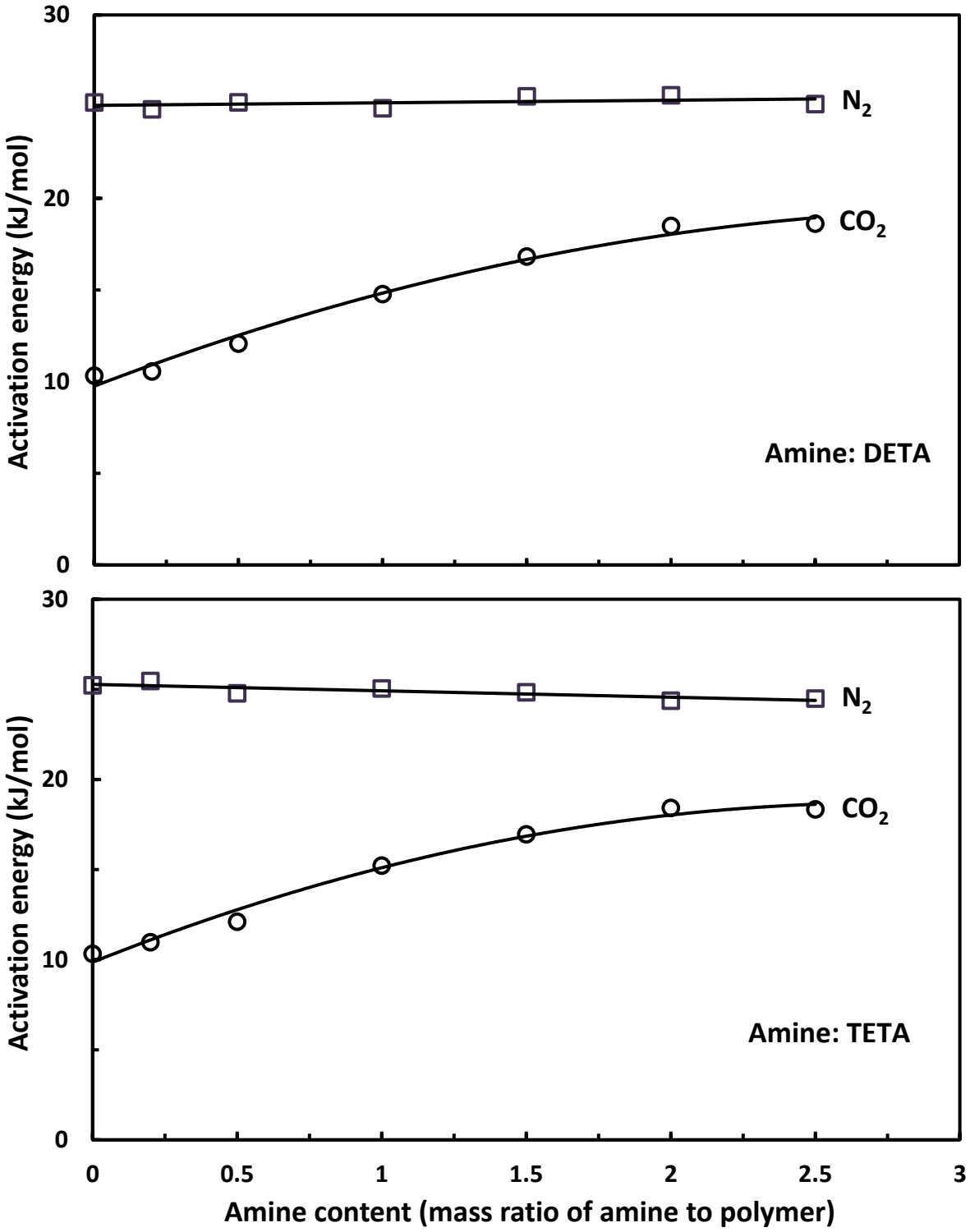


Fig. 6-11 Activation energies of permeation for $CO_2$ and $N_2$ in PVAm-PVA/amine membranes at different amine contents. Amine used: DETA and TETA. Polymer concentration in the coating solution, 5 wt%.

### 6.3.3 Effect of feed $CO_2$ concentration

The effects of feed $CO_2$ content on the performance of PVAm-PVA/DETA and PVAm-PVA/TETA membranes were investigated in order to determine the effects of interactions between the permeating components in the gas mixture on membrane performance. Membranes with DETA or TETA to polymer mass ratio of 150/100 were chosen because of their good permselectivity. The feed $CO_2$ content was varied from 3 mol% to 80 mol% $CO_2$, and the pure $N_2$ (i.e., 0 mol% $CO_2$) and pure $CO_2$ (i.e., 100 mol% $CO_2$) data was also included for comparisons. The feed pressure was kept constant at 351.3 kPa, while the permeate pressure was at 101.3 kPa in all the measurements. The $CO_2$ mole fraction in the permeate and total permeation flux through the membrane are plotted as a function of feed $CO_2$ content for the PVAm-PVA/DETA and PVAm-PVA/TETA membranes, as shown in Figs. 6-12 and 6-13, respectively. The mole fraction of $CO_2$ in permeate is always greater than that in the feed and increases with an increase in feed $CO_2$ content because $CO_2$ is preferentially transported from the $CO_2/N_2$ binary mixture through the membrane.

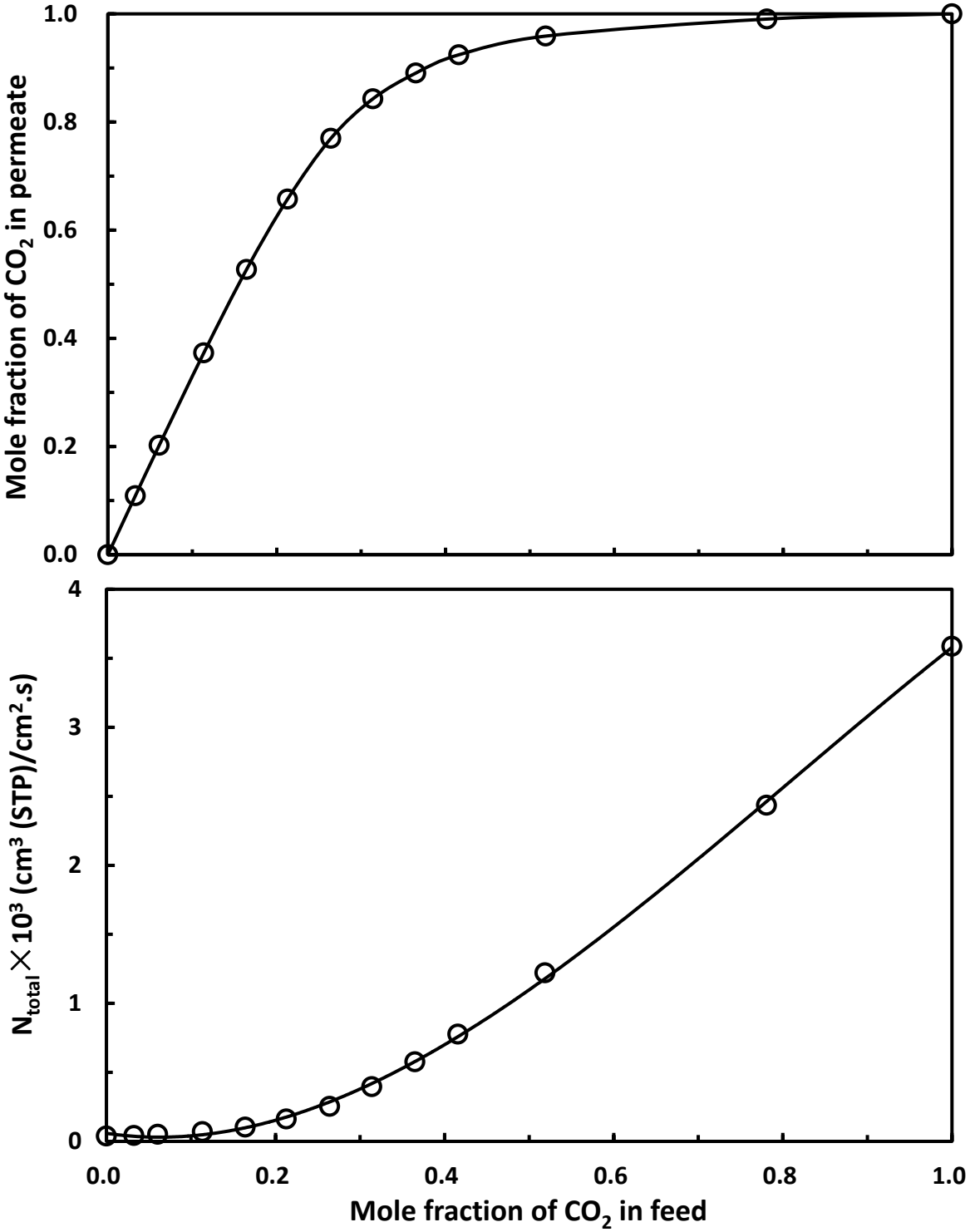


Fig. 6-12 Effect of feed $CO_2$ content on permeate concentration and total permeation flux for binary $CO_2/N_2$ permeation through PVAm-PVA/DETA membranes. DETA content in the membrane, DETA/polymer mass ratio=150/100. Feed pressure, 351.3 kPa; temperature, 298 K.

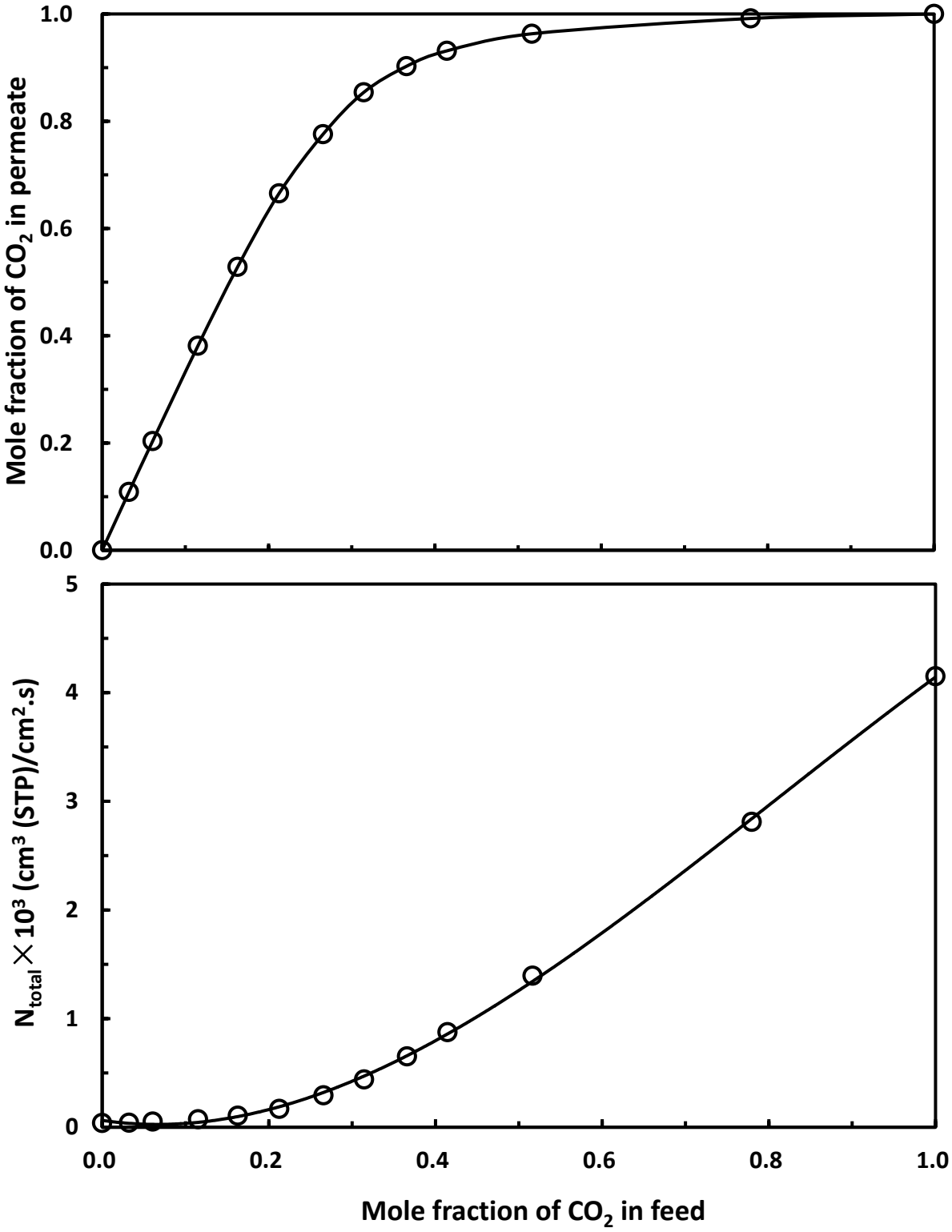


Fig. 6-13 Effect of feed $CO_2$ content on permeate concentration and total permeation flux for binary $CO_2/N_2$ permeation through PVAm-PVA/TETA membranes. TETA content in the membrane, TETA/polymer mass ratio=150/100. Feed pressure, 351.3 kPa; temperature, 298 K.

The permeance of the membrane to individual permeating component at different feed $CO_2$ concentrations is shown in Fig. 6-14. Both $CO_2$ and $N_2$ permeance increase with an increase in feed $CO_2$ content, and the increase in $N_2$ permeance is more significant for both PVAm-PVA/DETA and PVAm-PVA/TETA membranes. That is to say, the fast permeating component $CO_2$ is slowed down by the presence of $N_2$, and the transport of slow permeating $N_2$ is enhanced by the presence of $CO_2$. When the feed $CO_2$ content increases, the strong sorbing $CO_2$ in the membrane will make the polymer chains more flexible, allowing the gas molecules to diffuse through the membrane more easily. The gas molecules with a bigger kinetic diameter (e.g., $N_2$) will benefit more from the increased diffusivity than the one with smaller kinetic diameter (e.g., $CO_2$). On the other hand, the ionic species formed in the $CO_2$-amine reactions will reduce the solubility of $N_2$ in the membrane due to the salting-out effects. It appears that increased $N_2$ diffusivity can compensate for the reduction in its solubility with an increase in feed $CO_2$ content, resulting in a higher $N_2$ permeance. Because of the strong interactions between $CO_2$ and the membrane, the $CO_2$ permeance experiences only a slight increase when the feed $CO_2$ content increases. With an increase in feed $CO_2$ concentration, the amine carriers in the membrane available to shuttle additional $CO_2$ molecules become increasingly limited due to carrier saturation. As a result, the $CO_2/N_2$ selectivity drops with an increase in feed $CO_2$ concentration when the feed $CO_2$ content is low and levels off at higher feed $CO_2$ contents, as shown in Fig. 6-15. In general, both PVAm-PVA/DETA and PVAm-PVA/TETA membranes show a similar trend in $CO_2/N_2$ selectivity with feed $CO_2$ content, and the latter membrane is more permselective to $CO_2$ separation from $N_2$.

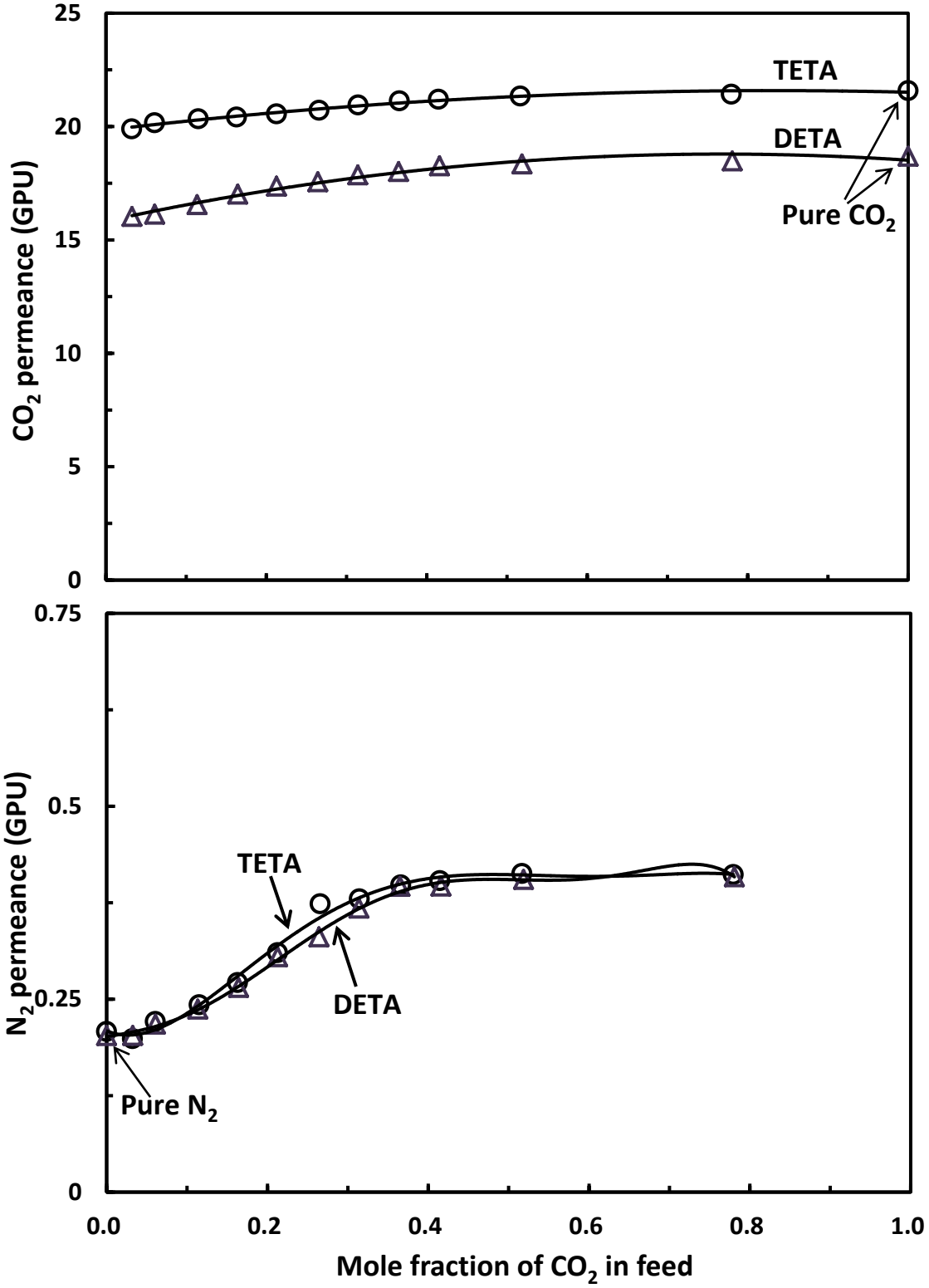


Fig. 6-14 Effect of feed $CO_2$ content on the permeance of $CO_2$ and $N_2$ for binary $CO_2/N_2$ permeation through PVAm-PVA/DETA and PVAm-PVA/TETA membranes. Amine content in the membrane, amine/polymer mass ratio=150/100. Feed pressure, 351.3 kPa; temperature, 298 K.

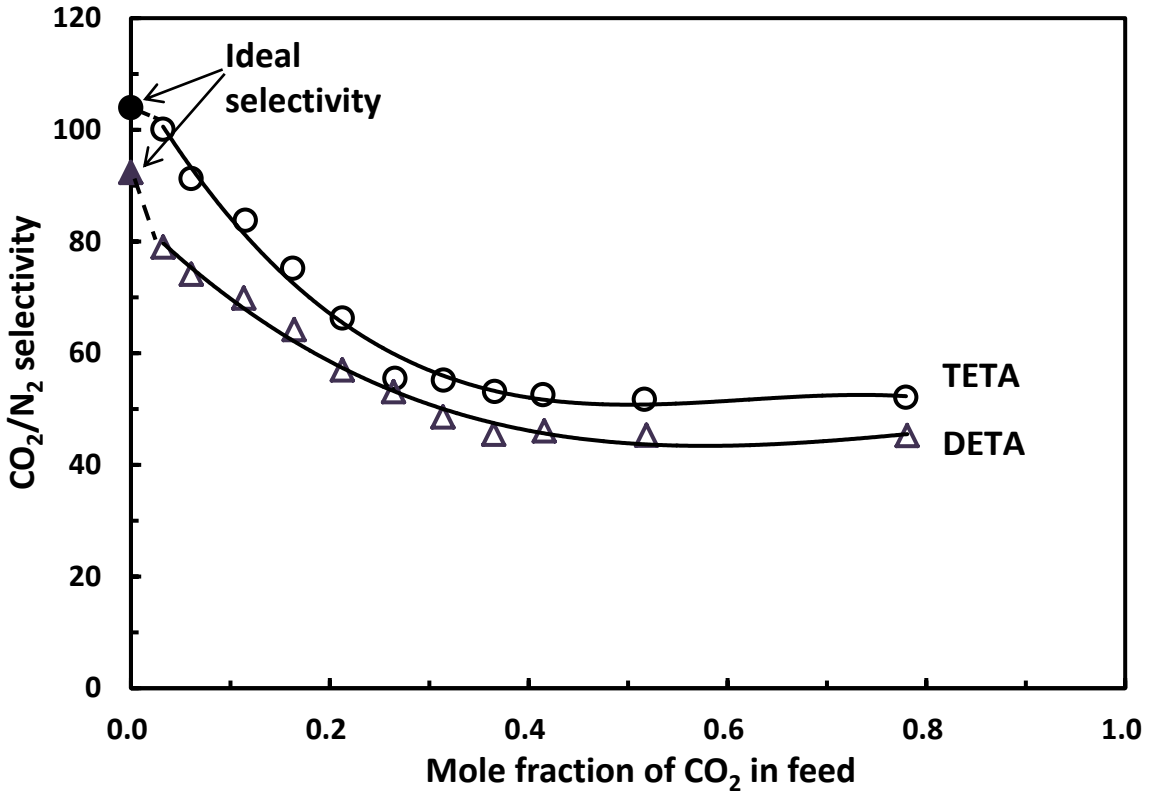


Fig. 6-15 Effect of feed $CO_2$ content on $CO_2/N_2$ selectivity for binary $CO_2/N_2$ permeation through PVAm-PVA/DETA and PVAm-PVA/TETA membranes. Amine content in the membrane, amine/polymer mass ratio=150/100. Feed pressure, 351.3 kPa; temperature, 298 K.

## 6.4 Conclusions

Novel facilitated transport membranes containing both PVAm as fixed carriers and DETA or TETA as mobile carriers in a PVAm/PVA blend polymer structure were prepared and studied for $CO_2$ removal from flue gas. The effects of DETA and TETA content in the membrane on the separation performance of the membranes were examined using both mixed gas and pure gas permeation. The effects of feed temperature and $CO_2$ content in the feed on the membrane performance were also investigated. The following conclusions can be drawn:

(1) The $CO_2$ permeance increased with an increase in the DETA and TETA content in the membrane, and then began to decrease with a further increase in the amine content if the

amine content was high enough. TETA was shown to be more effective in facilitating $CO_2$ transport than DETA in terms of $CO_2$ permeance and $CO_2/N_2$ selectivity.

(2) Activation energies for $CO_2$ and $N_2$ permeation through membranes with different DETA and TETA contents were determined, and the activation energy for $CO_2$ permeation increased with an increase in the amine content in the membrane, whereas the activation energy for $N_2$ permeation didn't change significantly.

# Chapter 7

## $H_2$ purification using PVAm-PVA/TETA composite membranes

---

### 7.1 Introduction

Hydrogen has attracted great interest for uses in petrochemical and fuel cells industries. Currently, the dominant process for $H_2$ production is steam reforming of hydrocarbons (mainly $CH_4$), which yields CO and $H_2$, followed by a water gas shift reaction, to produce additional $H_2$ through the conversion of CO to $CO_2$ [Hagg and Quinn, 2006; Zhao *et al.*, 2008b; Chen and Chung, 2012]. Therefore, a cost-effective removal of $CO_2$ from $H_2$ is essential to the downstream chemical operations requiring high purity $H_2$. Considering the huge demands for $H_2$ usage, considerable capital and energy savings can be expected with even a moderate improvement in $H_2$ purification.

Generally speaking, polymeric membranes used for $H_2$ purification can be $H_2$-selective or $CO_2$-selective [Shao *et al.*, 2009b]. $H_2$ has a smaller kinetic diameter and thus a higher diffusivity than $CO_2$, while $CO_2$ has a higher solubility due to its higher condensability. Thus, these counter-balance characteristics make it a challenging task to separate $H_2$ from $CO_2$ since gas transport through conventional polymeric membranes follows the solution-diffusion mechanism and the permeability is a product of its diffusivity and solubility in the membrane. For those polymeric membranes made of glassy polymers with strong size-sieving properties (i.e., high diffusivity

selectivity), $H_2$ will preferentially permeate through the membranes to make the membranes $H_2$-selective since the diffusivity selectivity dominates the overall selectivity [Chung *et al.*, 2006; Zou and Ho, 2006]. However, the $H_2$-selective membranes have some serious drawbacks: 1) the need to recompress the permeate $H_2$ stream after separation for future use, which is quite energy consuming and diminishes the energy efficient advantage of membrane separation over other separation techniques [Reijerkerk *et al.*, 2011b]; 2) since $CO_2$ is typically the minor component in the $CO_2$ stream to be purified, a large membrane area is often required to remove $H_2$ from the $H_2/CO_2$ gas mixture, which obviously offsets the cost savings advantage of membrane separation [Xing and Ho, 2011]. However, these unfavorable aspects can be avoided by using $CO_2$-selective membranes for $H_2$ purification, which eliminates expensive recompression of $H_2$ since the $H_2$-rich retentate is obtained at a pressure close to feed pressure and the minor component $CO_2$ preferentially permeates through the membrane.

For polymeric membranes to be $CO_2$-selective for $H_2$ purification, it is important to maximize the solubility selectivity while minimizing the size exclusion ability [Lin *et al.*, 2006a]. Recently, polymers containing ethylene oxide (EO) units have received attention for this application. The polar ether moieties in EO units included on the backbones or in linkages along the polymer chain can be used to promote favorable chemical interactions with $CO_2$ molecules, thereby producing high solubility selectivity and facilitating molecular transport of $CO_2$ [Patel *et al.*, 2003, 2004]. On the other hand, polymers containing EO units are normally highly flexible, resulting in weak size discrimination ability and thus high diffusivity [Lin *et al.*, 2006a]. Both of these contribute to a high $CO_2$ permeability and high $CO_2/H_2$ selectivity. By preparing a highly permeable poly(ethylene oxide) based multi-block copolymer membrane, Reijerkerk *et al.* [2011b] achieved a $CO_2$ permeability of 470 Barrer and a $CO_2/H_2$ selectivity of 9 at a $CO_2$ partial

pressure of 4 bar at 35℃ for binary $CO_2/H_2$ separation. Thin film composite membranes containing EO groups were also fabricated via interfacial polymerization with trimesoyl chloride and diamines and they exhibited a $CO_2$ permeance of 815 GPU and a $CO_2/H_2$ selectivity of 10 at a feed pressure of 0.11 MPa for separating a $CO_2/H_2$ gas mixture [Li *et al.*, 2013].

Though polymeric membranes containing EO units have demonstrated good separation performance for the removal of $CO_2$ from $H_2$, a further improvement in permeability/selectivity is still needed. Especially, the acquired $CO_2/H_2$ selectivity of these membranes is not good enough to compete with the current separation techniques. Nevertheless, facilitated transport membranes containing both mobile and fixed carriers may offer an attractive method of obtaining a high selectivity without compromising permeability. Ho and coworkers [Tee *et al.*, 2006; Zou and Ho, 2006; Bai and Ho, 2009; Xing and Ho, 2011] have fabricated a series of facilitated transport membranes containing amino acid salts as mobile carriers and polyamines as fixed carriers. For example, a membrane containing both AIBA-K and $K_2CO_3$-$KHCO_3$ as the mobile carriers, and poly(allylamine) as the fixed carriers in a crosslinked poly(vinyl alcohol) network showed a $CO_2$ permeability of 6500 Barrer and a $CO_2/H_2$ selectivity as high as 210 at a $CO_2$ partial pressure of 0.25 atm at 100℃ for a ternary gas mixture ($CO_2/H_2/N_2$, 20/40/40, vol%) [Zou and Ho, 2006]. Bai and Ho [2009] also reported a membrane containing AIBA-K as the mobile carrier and polyethylenimine as the fixed carrier in a sulfonated polybenzimidazole copolymer matrix which showed a $CO_2/H_2$ selectivity of 64.9 and a $CO_2$ permeance of 70.5 GPU at 100℃ when the membrane composition was optimized. In addition, Wang and coworkers [Yuan *et al.*, 2011; Qiao *et al.*, 2013] have also fabricated polyvinylamine-based facilitated transport membranes containing small molecule amines (such as ethylenediamine and piperazine) for $CO_2/N_2$ separation.

In chapters 5 and 6, PVAm-PVA composite membranes incorporated with PZ, DETA and TETA were developed and then investigated for the removal of $CO_2$ from $N_2$. Among the amines tested, TETA was shown to be the most effective one in facilitating $CO_2$ transport in terms of $CO_2/N_2$ permselectivity. Therefore, PVAm-PVA/TETA membranes were used for $H_2$ purification in this chapter. TETA has multi-amino functionalities - two primary amino groups ($-NH_2$) and two secondary amino groups (-NH-). This implies that TETA has four possible reaction sites to interact with $CO_2$. Previous kinetic studies of TETA for $CO_2$ absorption have demonstrated a high $CO_2$ loading capacity in TETA [Schaffer *et al.*, 2012]. Moreover, Matsuyama *et al.* [1996] prepared ion exchange membranes employing TETA as the carriers by plasma grafting polymerization, and the membranes showed an unusually high $CO_2$ permselectivity under a very small $CO_2$ partial pressure for $CO_2/N_2$ separation. However, to the best of our knowledge, polyamine based membranes incorporated with TETA has not been attempted to remove $CO_2$ from $H_2$ for $H_2$ purification.

Therefore, the objective of this chapter was to investigate the applicability of using PVAm-PVA composite membranes incorporated with TETA for $CO_2/H_2$ separation. First, the effect of TETA content in the membrane on the separation performance of the composite membranes was examined for pure $CO_2$ and $H_2$ permeation. Then the effects of feed pressure, feed $CO_2$ content and temperature on the separation performance of the PVAm-PVA/TETA composite membranes were investigated. Finally, the stability of the membrane for continuous separation of $CO_2/H_2$ was evaluated using a simulated syn gas containing 20 mol% of $CO_2$ (balanced $H_2$).

## 7.2 Experimental

The materials and procedure for preparation of PVAm-PVA/TETA composite membranes

were the same as described in chapter 5. The mass ratio of PVAm to PVA in the membrane casting solution was kept at 60/40, and the overall polymer concentration was 5 wt%. The mass ratio of TETA to polymer was varied as follows: 20/100, 50/100, 100/100, 150/100, 200/100 and 250/100. For the fabrication of all the PVAm-PVA/TETA composite membranes, only one coat of the casting solution was found effective to prepare defect-free membranes.

The experimental setup and procedure for binary gas mixture permeation experiments have been described in chapter 5.

## 7.3 Results and discussion

### 7.3.1 Effect of TETA content in the membrane

The effectiveness of improving the permselectivity of PVAm-PVA composite membranes by incorporating a molecular amine - TETA was verified first by measuring the pure gas (i.e., $CO_2$ and $H_2$) permeance of the PVAm-PVA/TETA membranes containing different TETA contents. The $CO_2$ permeance, $H_2$ permeance and $CO_2/H_2$ ideal selectivity of the membranes with different TETA contents are shown in Figs. 7-1 and 7-2.

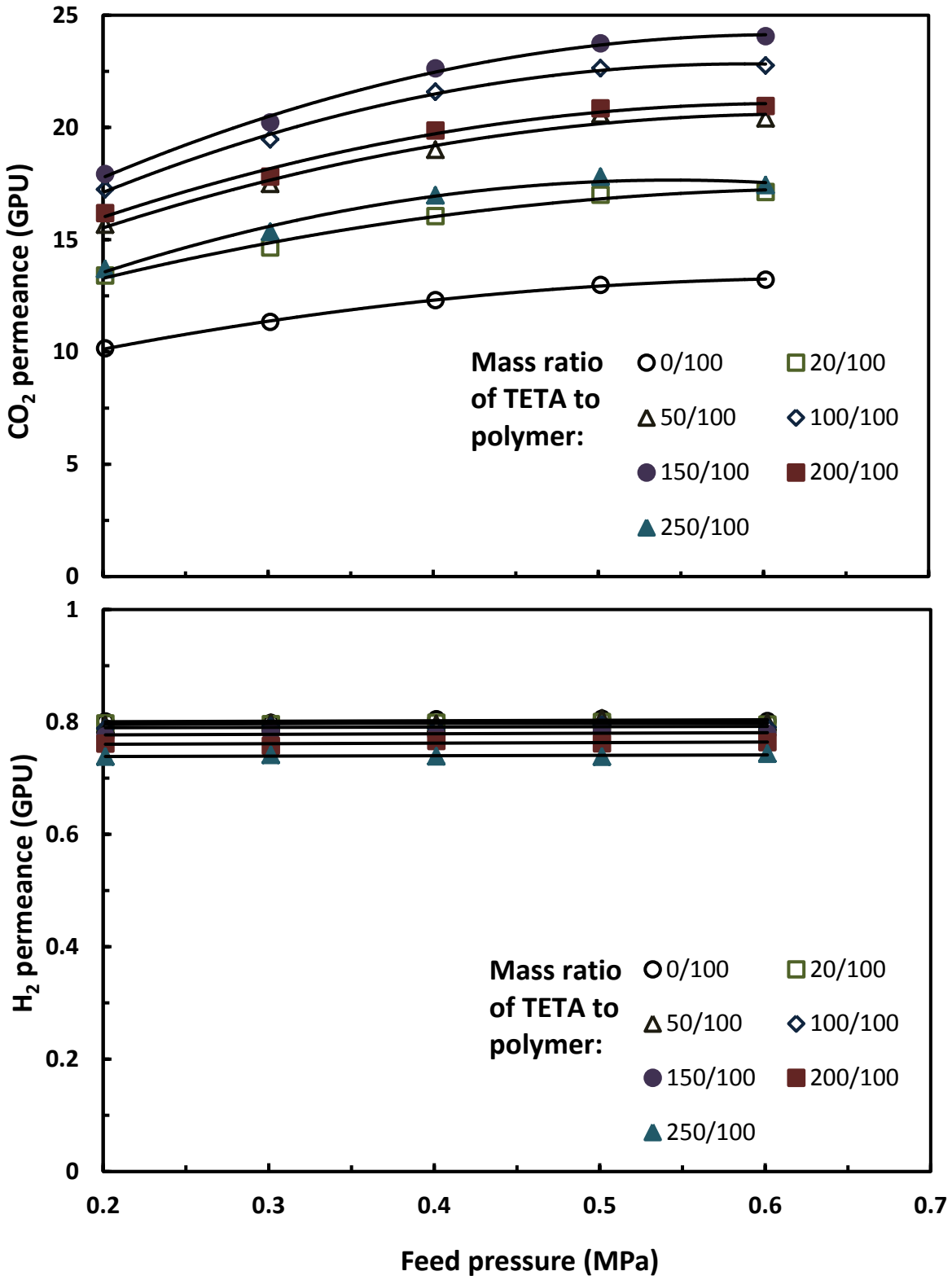


Fig. 7-1 Effect of TETA content (the mass ratio of TETA to polymer) in the membrane on the permeance of $CO_2$ and $H_2$ for pure $CO_2$ and $H_2$ permeation through PVAm-PVA/TETA membranes. Temperature, 298 K.

As shown in Fig. 7-1, the PVAm-PVA/TETA composite membranes have shown greater $CO_2$ permeance than the PVAm-PVA composite membrane without TETA, indicating enhancement in membrane permeability by incorporating TETA into PVAm-PVA matrix for removal of $CO_2$ from $H_2$. Due to the presence of amino carriers contained in the membrane, there're two modes of gas transport behavior for $CO_2$ molecules. One is the physical solution-diffusion mode, and the other carrier-mediated transport mode. In the latter case, $CO_2$ molecules are bound to the carriers to form $CO_2$-carrier complexes, which diffuse across the membrane and then $CO_2$ molecules are released on the permeate side of the membrane, thereby facilitating $CO_2$ transport through the membrane. PVAm has abundant primary amino groups on its backbone, which are readily available to facilitate $CO_2$ transport. However, these amino groups are limited to certain sites along the polymer chain and have limited mobility. With the addition of molecular TETA that has several amine functionalities per molecule, not only is the total number of available amino carriers increased, thereby increasing the solubility of $CO_2$ in the membrane, but the higher mobility of the carriers derived from the molecular TETA will also result in a higher diffusivity of the $CO_2$-amine complexes in the membrane. Both of these contribute to a higher $CO_2$ permeance in the membranes containing TETA. However, the $CO_2$ permeance of the PVAm-PVA/TETA membranes cannot increase monotonically as the TETA content increases in the membrane; it initially increases until reaching a certain point (i.e., TETA to polymer mass ratio of 150/100) and then begins to drop with a further increase in the TETA content, as shown in Fig. 7-1. This is similar to the case of $CO_2/N_2$ separation using PVAm-PVA/TETA membranes. On one hand, as stated before, the additional amino carriers from TETA favor $CO_2$ transport when TETA content increases. On the other hand, the reactions between primary and secondary amines and $CO_2$ molecules, which are usually described by the zwitterion mechanism via

carbamate formation, will produce several ionic species. The ionic strength of the membrane thus increases as the TETA content in the membrane increases, which will not only reduce the solubility of $CO_2$ but also negatively affect the diffusivity of $CO_2$-amine complexes in the membrane, resulting in a lower $CO_2$ permeance. These opposite effects will determine whether the TETA content in the membrane will increase or decrease the $CO_2$ permeance.

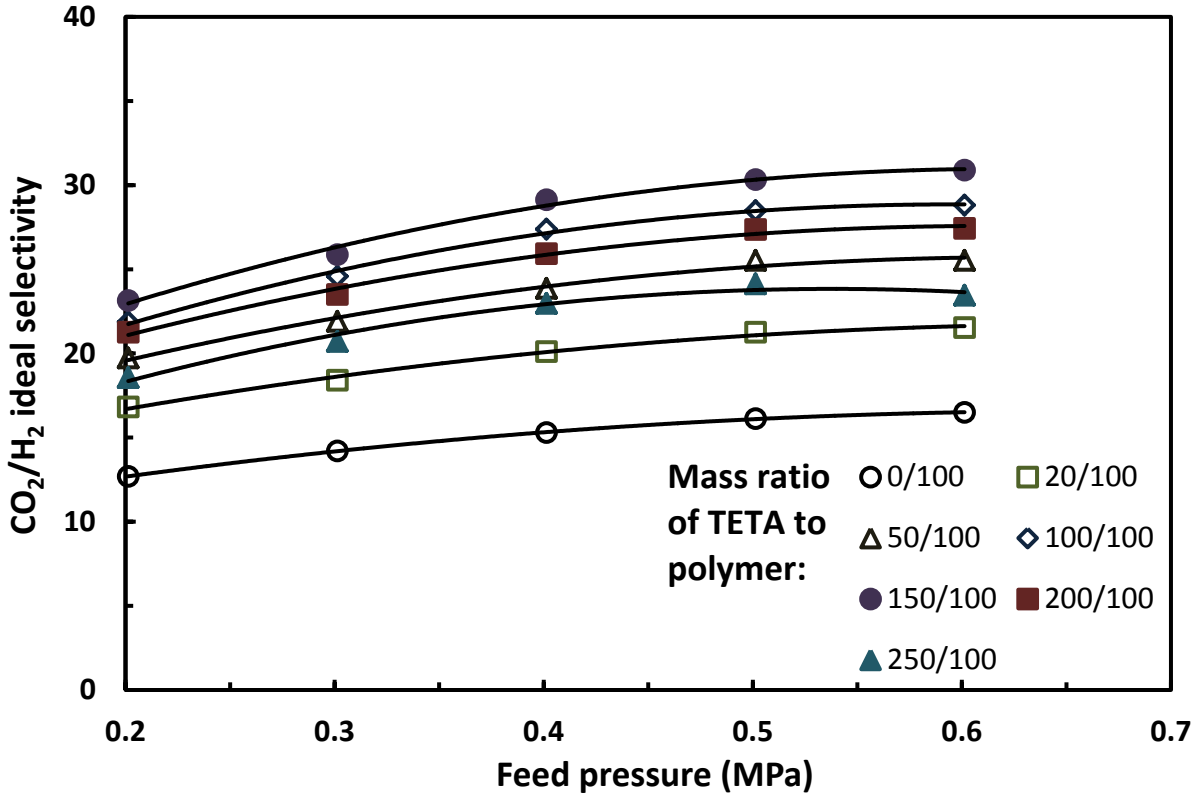


Fig. 7-2 Effect of TETA content (the mass ratio of TETA to polymer) on $CO_2/H_2$ ideal selectivity for pure $CO_2$ and $H_2$ permeation through PVAm-PVA/TETA membrane. Temperature, 298 K.

$H_2$ does not react with amino carriers, and $H_2$ permeation follows the simple molecular diffusion via solution-diffusion mechanism. However, the primary and secondary amine groups of TETA can interact with the primary amine groups of PVAm and hydroxyl groups of PVA via intermolecular hydrogen bonding. The more the TETA content in the membrane, the stronger the hydrogen bonding effect will be. Thus, the intermolecular interaction will cause a more densely packed polymer network, leading to a reduction in the diffusivities of the permeant. Therefore, a

slight reduction in $H_2$ permeance with an increase in the TETA content in the membrane was observed, as indicated in Fig. 7-1.

The variation of $CO_2$ and $H_2$ permeance with respect to the TETA content in the membrane is reflected in the $CO_2/H_2$ ideal selectivity, as shown in Fig. 7-2. The PVAm-PVA/TETA composite membranes tend to have a higher selectivity than the PVAm-PVA membrane without TETA. The composite membrane with a TETA to polymer mass ratio of 150/100 displayed the best $CO_2/H_2$ ideal selectivity among all the membranes studied here, reaching 30 at a feed pressure of 0.6 MPa.

### 7.3.2 Effect of feed pressure

Among all the PVAm-PVA/TETA composite membranes tested, the one with a TETA to polymer mass ratio of 150/100 showed the best $CO_2/H_2$ selectivity and permeability. Thus, this membrane was chosen to investigate the effects of other operating parameters on the performance of the PVAm-PVA/TETA membranes in the following.

Fig. 7-3 shows the effects of feed pressure on $CO_2$ and $H_2$ permeance at different feed $CO_2$ contents ranging from 10 to 70 mol%, and the pure $CO_2$ and $H_2$ permeance data is also plotted in this figure for a comparison. As shown in this figure, the $CO_2$ permeance increases as the feed pressure increases, and then levels off when the feed pressure is high enough; whereas the $H_2$ permeance remains unchanged in the entire range of the feed pressures tested. These observations are further confirmed in Fig. 7-4, where the $CO_2$ and $H_2$ permeance are plotted against their average pressures. The average pressure is taken as the average of the upstream and downstream partial pressures of each component (i.e., $CO_2$ and $H_2$) in the mixture.

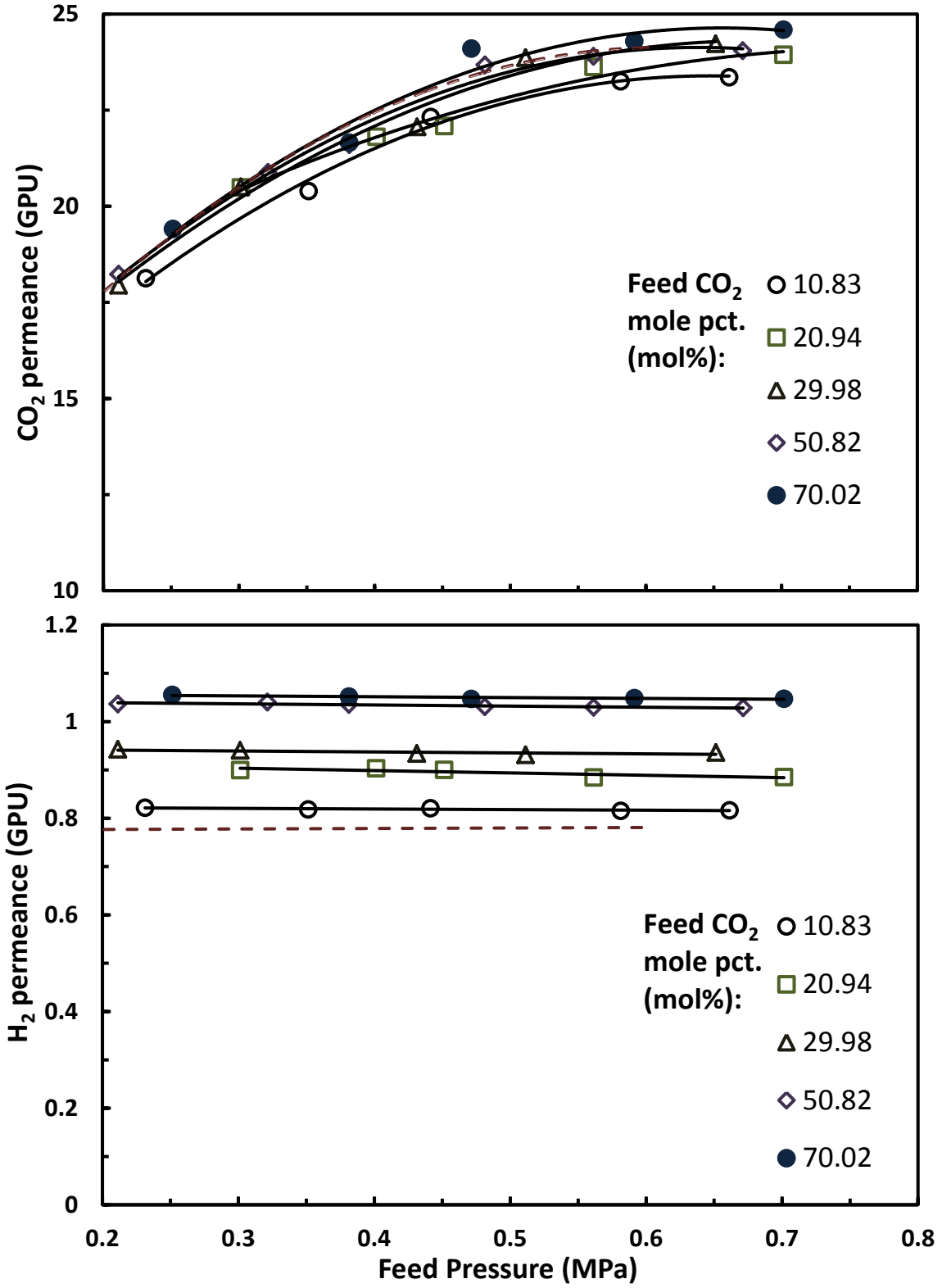


Fig. 7-3 Effect of feed pressure on the permeance of $CO_2$ and $H_2$ for binary $CO_2/H_2$ permeation at different feed $CO_2$ contents through PVAm-PVA/TETA membrane. TETA content in the membrane, TETA/polymer mass ratio=150/100. Temperature, 298 K. The dotted line represents pure $CO_2$ and $H_2$ permeance.

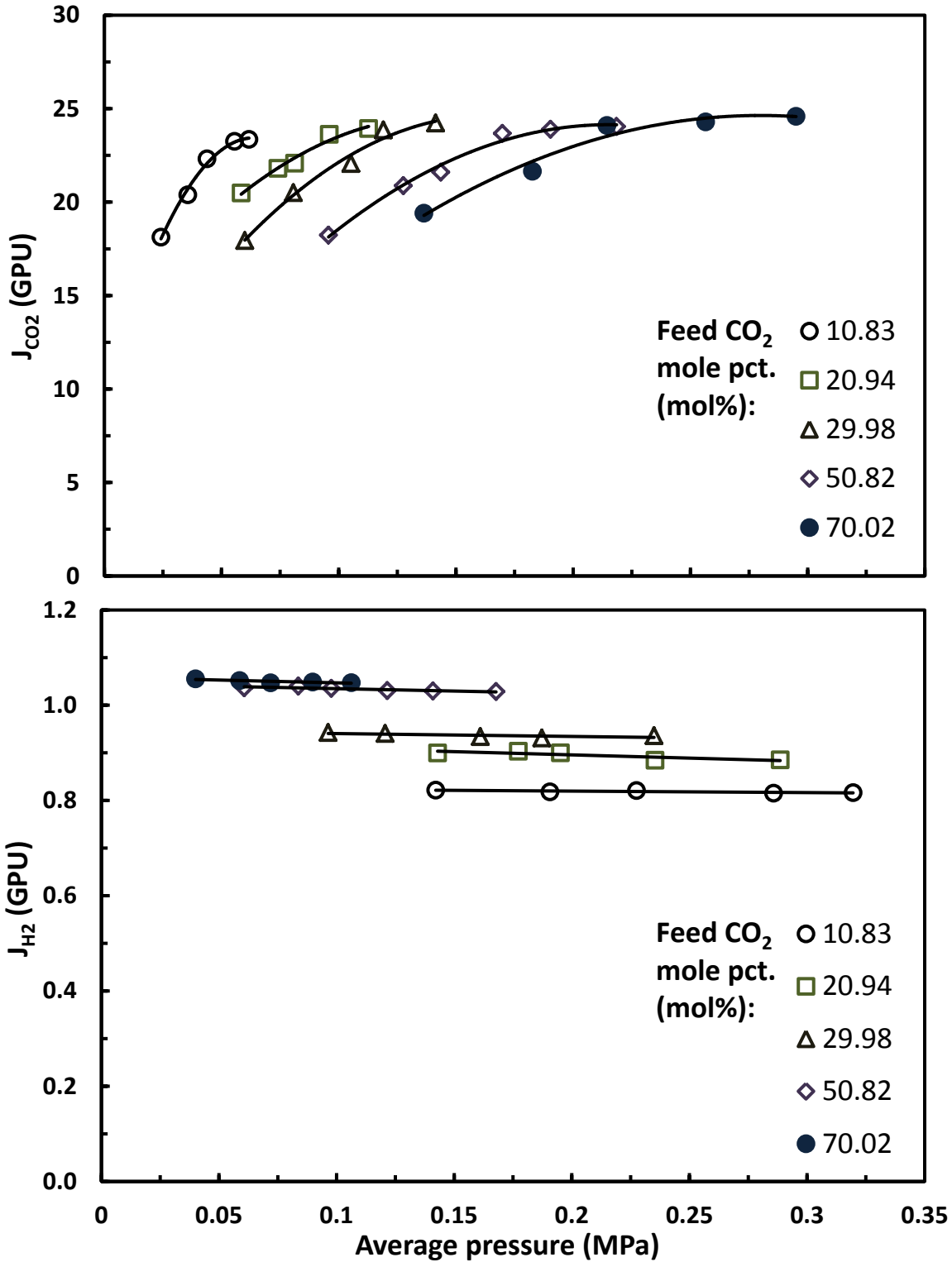


Fig. 7-4 Effect of average pressure on $CO_2$ and $N_2$ permeance for binary $CO_2/H_2$ permeation at different feed $CO_2$ contents through PVAm-PVA/TETA membrane. TETA content in the membrane, TETA/polymer mass ratio=150/100. Temperature, 298 K. The average pressure is taken as the average of the upstream and downstream partial pressures of each component in the mixture.

As mentioned previously, two transport mechanisms occur simultaneously for $CO_2$ permeation in the membrane: molecular diffusion and carrier-mediated transport. In addition, water also plays an important role in the gas transport since it can interact with $CO_2$ molecules to form bicarbonate ions. Du *et al.* [2010b] investigated a humidified poly(*N,N*-dimethylaminoethyl methacrylate) membrane and concluded that facilitated transport of $CO_2$ along the amino groups in the polymer matrix and the water passageways take place simultaneously. The facilitated transport of $CO_2$ by the amino carriers is expected to be improved by the hydration of $CO_2$, and similarly, the transport of $CO_2$ in the water passageways is believed to be enhanced by the amino carriers in the membrane. Moreover, these interactions can be more significant for $CO_2$ transport at higher concentrations. Thus, the $CO_2$ permeance is shown to increase with an increase in the average pressure of $CO_2$. However, with an increase in the $CO_2$ pressure, the carrier sites in the membrane will be gradually occupied by the $CO_2$ molecules, which in turn restrict them from further taking up additional $CO_2$ molecules. Thus, the $CO_2$ permeance due to the carrier-mediated transport will reach a constant when $CO_2$ pressure is sufficiently high. Consequently, the overall $CO_2$ permeance approaches constant. Unlike $CO_2$ permeation, $H_2$ transport in the membrane occurs mainly in the simple molecular diffusion mode, and it's not surprising to observe a constant $H_2$ permeance, regardless of feed pressure or average pressure of $H_2$.

The $CO_2/H_2$ selectivity also increases with an increase in the feed pressure, and then levels off at high feed pressures, as shown in Fig. 7-5. At a feed $CO_2$ content of 10 mol%, the composite membrane yielded a $CO_2/H_2$ selectivity of 28.5.

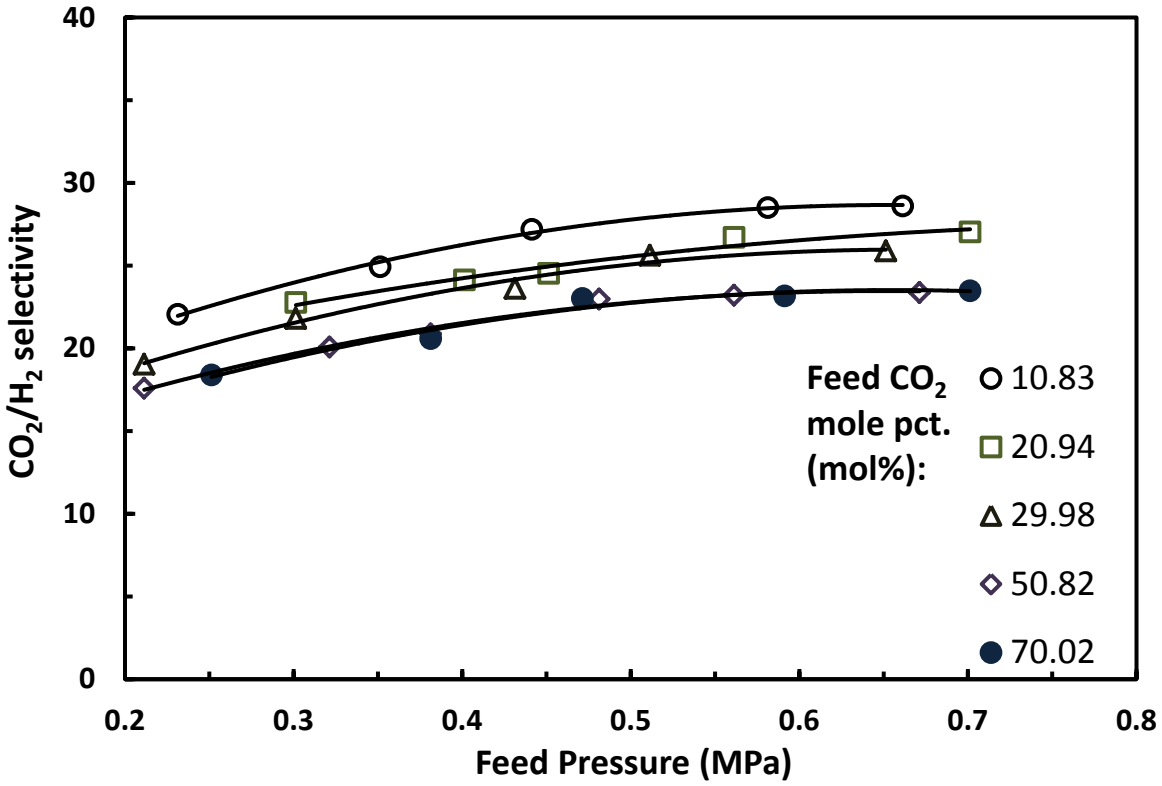


Fig. 7-5 Effect of feed pressure on $CO_2/H_2$ selectivity for binary $CO_2/H_2$ permeation at different feed $CO_2$ contents through PVAm-PVA/TETA membrane. TETA content in the membrane, TETA/polymer mass ratio=150/100. Temperature, 298 K.

From Fig. 7-3, the PVAm-PVA/TETA composite membranes display a $CO_2$ permeance that is not affected significantly by the feed $CO_2$ content, and even pure $CO_2$ permeance is close to these values. However, the $H_2$ permeance appears to increase with increasing the feed $CO_2$ content. Based on these observations, one may perceive that the presence of $H_2$ in the binary gas mixture does not affect the transport of $CO_2$ significantly, whereas the presence of $CO_2$ enhances the transport of slow permeating $H_2$. This will be further examined in the following tests by varying feed $CO_2$ contents at different feed pressures.

### 7.3.3 Effect of feed $CO_2$ content

The effects of feed $CO_2$ content on the separation performance of PVAm-PVA/TETA composite membranes at given pressures were examined. The feed $CO_2$ concentration was varied

from 6 to 90 mol% $CO_2$, and the pure $N_2$ (i.e., 0% $CO_2$) and pure $CO_2$ (i.e., 100% $CO_2$) permeance data was also included for comparison. Two feed pressures were used in the experiments, 0.35 and 0.7 MPa.

Fig. 7-6 shows the mole fraction of $CO_2$ in permeate and total permeation flux of the membrane as a function of feed $CO_2$ content. The mole fraction of $CO_2$ in permeate is always greater than that in the feed, and it increases with an increase in feed $CO_2$ content because $CO_2$ is preferentially transported from the $CO_2/H_2$ mixture through the membrane. At a given feed $CO_2$ content, both the mole fraction of $CO_2$ in permeate and the total permeation flux increase when a higher feed pressure is used, which is consistent with the previous results about the effects of feed pressure.

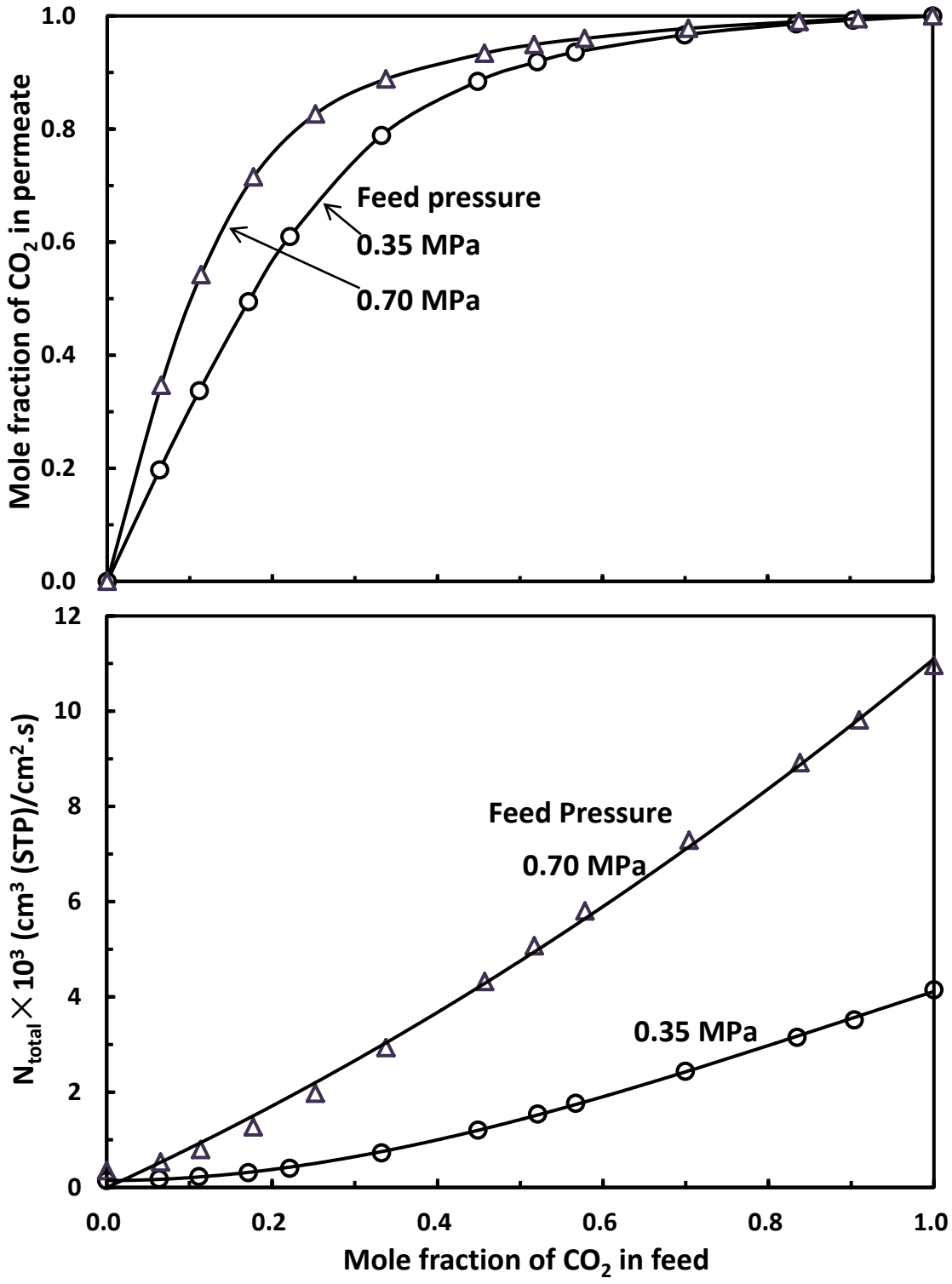


Fig. 7-6 Effect of feed $CO_2$ content on permeate concentration and total permeation flux for binary $CO_2/H_2$ permeation at different feed pressures through PVAm-PVA/TETA membrane. TETA content in the membrane, TETA/polymer mass ratio=150/100. Temperature, 298 K.

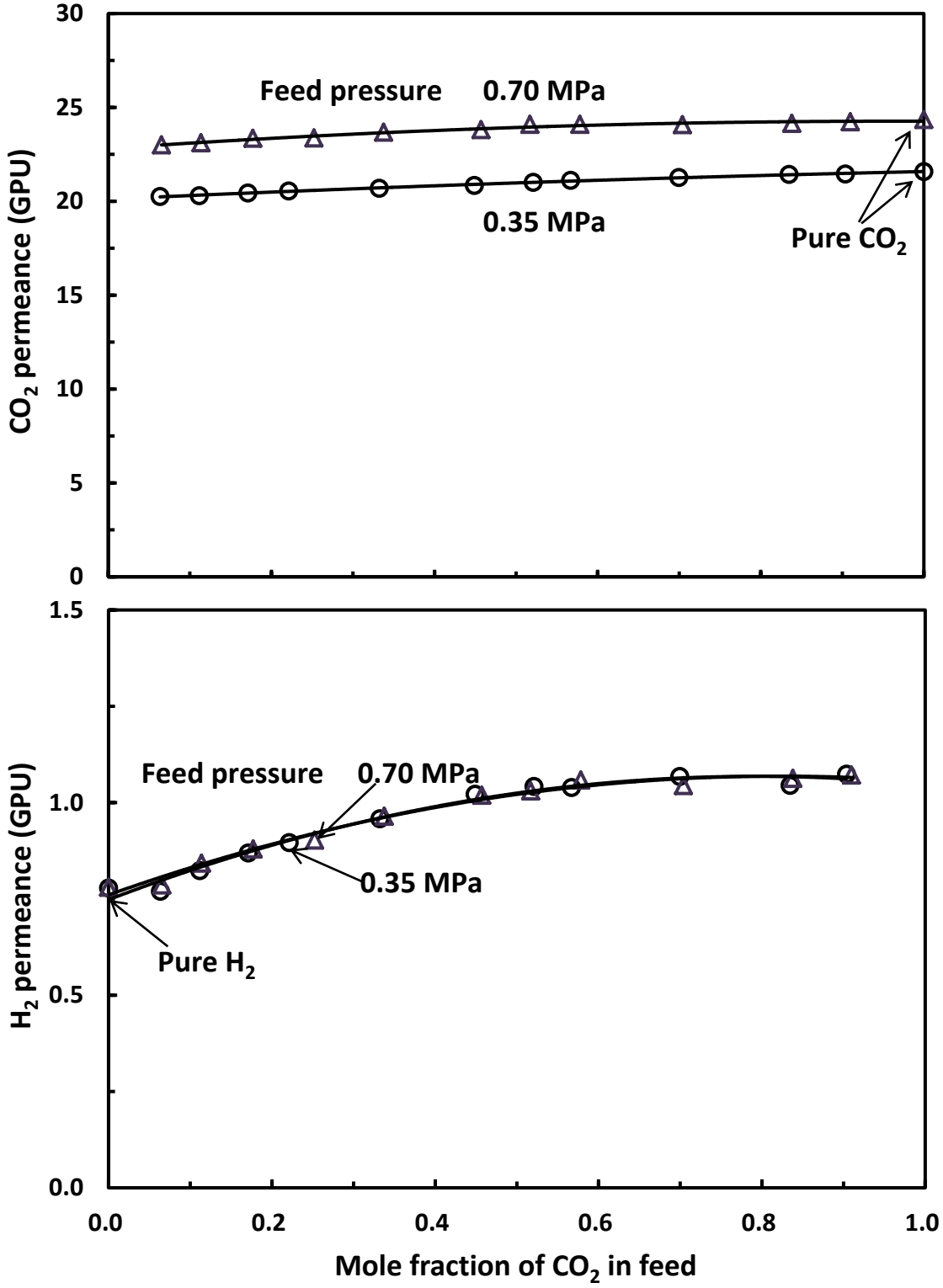


Fig. 7-7 Effect of feed $CO_2$ content on the permeance of $CO_2$ and $H_2$ for binary $CO_2/H_2$ permeation at different feed pressures through PVAm-PVA/TETA membrane. TETA content in the membrane, TETA/polymer mass ratio=150/100. Temperature, 298 K.

The permeance of the membrane to individual permeant component is shown in Fig. 7-7. At a given feed $CO_2$ content, the $CO_2$ permeance is higher at a higher feed pressure, while the $H_2$ permeance remains the same. At a given feed pressure, the $CO_2$ permeance does not change significantly with feed composition, whereas the $H_2$ permeance increases more significantly. In other words, the fast permeating $CO_2$ has a positive effect on the transport of $H_2$, while the slow permeating $H_2$ has little influence on the transport of $CO_2$, which is in accordance with the trend observed in a study with polyamine based membranes [Du *et al.*, 2010b]. The presence of $H_2$ has little impact on the permeation of $CO_2$ presumably due to strong interactions between $CO_2$ and the membrane. As mentioned earlier, $CO_2$ molecules can interact with amine carriers and water in the membrane to form several ionic species such as carbamates and bicarbonate ions, and this will decreases the solubility of $H_2$ in the membrane due to the salting-out effect, eventually leading to a reduction in $H_2$ permeance. On the other hand, the strong sorbing $CO_2$ in the membrane will swell the membrane and make the polymer chains more flexible when the concentration of $CO_2$ dissolved on the feed side of the membrane increases, which permits the permeant to diffuse through the membrane more easily. Recall that $H_2$ has a low solubility in the membrane due to its low condensability, but with a high diffusivity in the membrane because of its small molecular size. Thus, the increase in $H_2$ diffusivity can compensate for the reduction in its solubility when feed $CO_2$ content increases. When the feed $CO_2$ content is sufficiently high, because of gradual carrier saturation, the membrane will not be able to take additional $CO_2$ molecules effectively. Thus, the increasing diffusivity of permeants induced by dissolved $CO_2$ will gradually diminish. As a result, the $H_2$ permeance does not change significantly when the feed $CO_2$ content is high enough. Accordingly, the $CO_2/H_2$ selectivity decreases with increasing feed $CO_2$ content and eventually approaches a constant when the feed $CO_2$ content is sufficiently

high, as shown in Fig. 7-8. At a given feed $CO_2$ content, the PVAm-PVA/TETA membrane shows a higher $CO_2/H_2$ selectivity at a higher feed pressure.

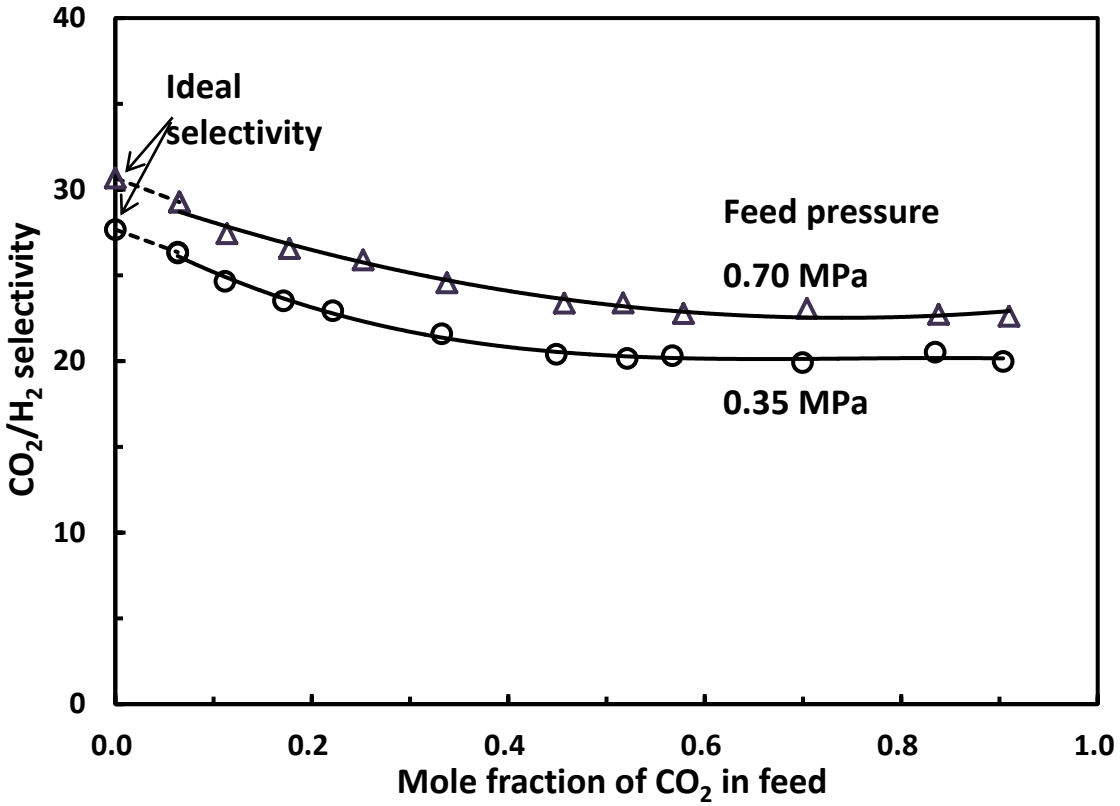


Fig. 7-8 Effect of feed $CO_2$ content on $CO_2/H_2$ selectivity for binary $CO_2/H_2$ permeation at different feed pressures through PVAm-PVA/TETA membrane. TETA content in the membrane, TETA/polymer mass ratio=150/100. Temperature, 298 K.

### 7.3.4 Effect of temperature

Figs. 7-9 and 7-10 present the results of the effects of operating temperature on the membrane permselectivity of PVAm-PVA/TETA composite membranes at different feed $CO_2$ contents. The experiments were carried out in a temperature range of 15-70℃ at a fixed feed pressure of 0.4 MPa. Binary gas mixtures containing 10, 20 and 50 mol% $CO_2$ (balanced $H_2$) were used as the feed in the tests. As shown in Fig. 7-9, both the $CO_2$ and $H_2$ permeance increase with an increase in temperature, and the temperature dependence of the permeance follows an Arrhenius type of relationship. Furthermore, the temperature seems to have a more significant

effect on $H_2$ permeation than $CO_2$, resulting in a reduction in $CO_2/H_2$ selectivity when temperature elevates, as shown in Fig. 7-10. Activation energies for $CO_2$ and $H_2$ permeation were calculated to be 18.2 and 32.2 kJ/mol, respectively. The feed $CO_2$ content was found to have little impact on the activation energy for both $CO_2$ and $H_2$. The lower value of activation energy for permeation of $CO_2$ suggests that $CO_2$ permeate through the membrane more easily than $H_2$.

Since the transport of $H_2$ through the membrane mainly follows the physical solution-diffusion mechanism, the solubility of $H_2$ in the polymeric membrane decreases and the diffusivity of $H_2$ increases with an increase in the temperature. The diffusivity aspect normally affects the permeability more significantly than the solubility aspect for gases with low condensabilities, thus the $H_2$ permeance is enhanced when increasing the temperature. However, for the permeation of $CO_2$ in the membrane, besides simple dissolution and diffusion, there're reactions between $CO_2$ molecules and carriers. From the solution-diffusion perspective, the solubility of $CO_2$ in the membrane reduces while the diffusivity increases when temperature increases. From the chemical facilitation perspective, increasing temperature could enhance the reaction rate of $CO_2$-carrier reactions and the diffusivity of the $CO_2$-carrier complexes simultaneously, but the release of $CO_2$ from the membrane on the permeate side will be negatively affected. Nonetheless, the $CO_2$ permeance is shown to increase with temperature, though its temperature dependence is less significant than $H_2$. As the activation energy values suggested, the increase in $H_2$ permeance is more pronounced than that of $CO_2$ permeance with an increase in temperature, which reduces the corresponding $CO_2/H_2$ selectivity at higher temperatures, as shown in Fig. 7-10.

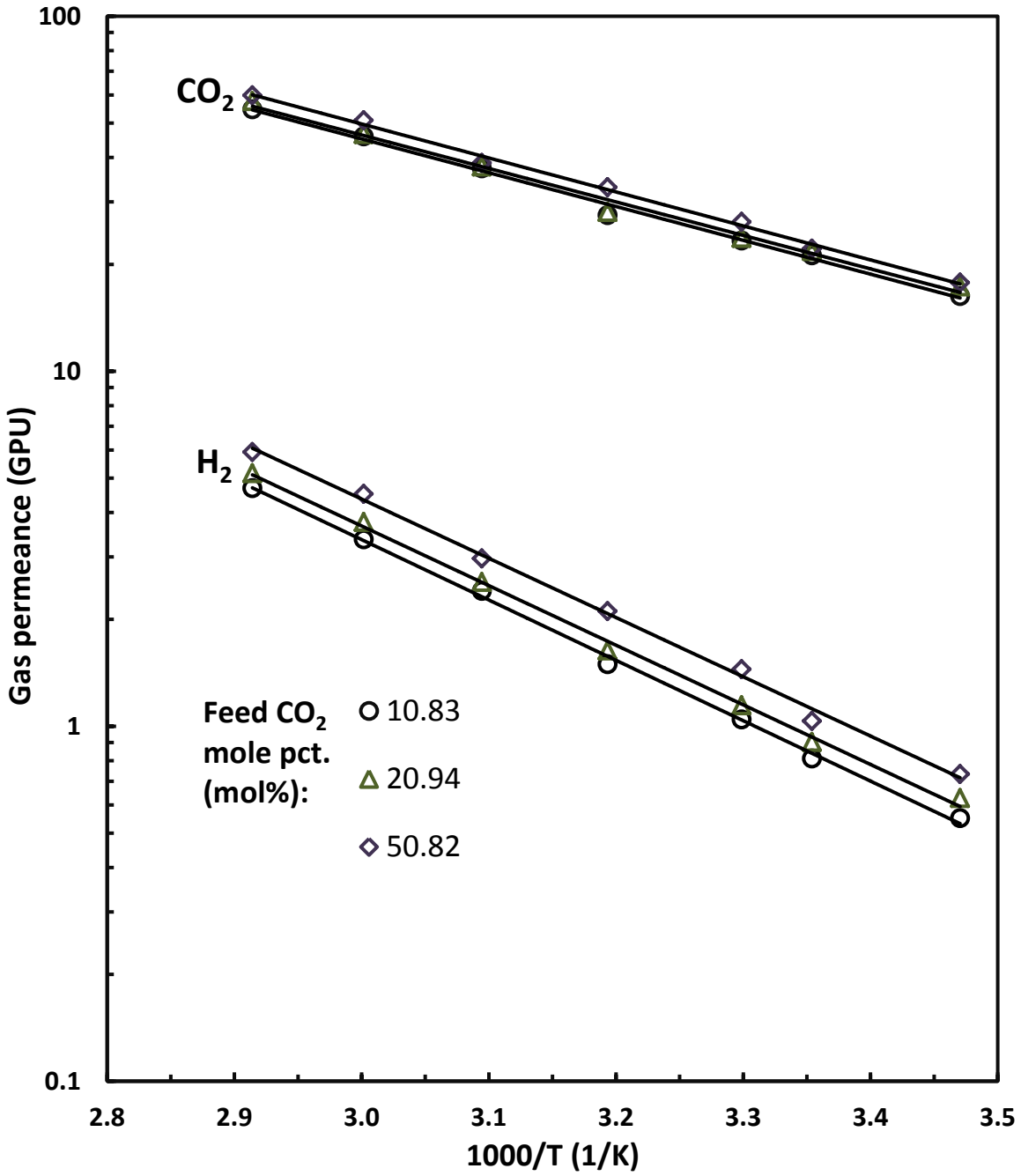


Fig. 7-9 Effect of temperature on the permeance of $CO_2$ and $H_2$ for binary $CO_2/H_2$ permeation at different feed $CO_2$ contents through PVAm-PVA/TETA membrane. TETA content in the membrane, TETA/polymer mass ratio=150/100. Feed pressure, 0.4 MPa.

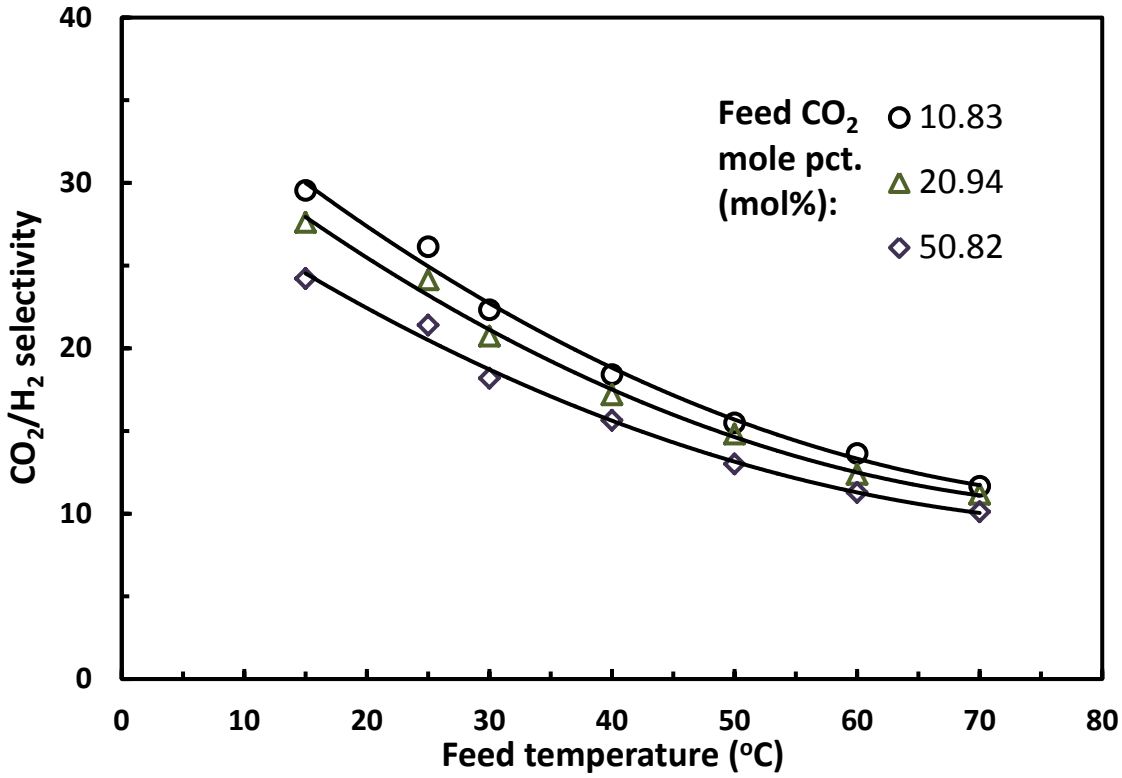


Fig. 7-10 Effect of temperature on $CO_2/H_2$ selectivity for binary $CO_2/H_2$ permeation at different feed $CO_2$ contents through PVAm-PVA/TETA membrane. TETA content in the membrane, TETA/polymer mass ratio=150/100. Feed pressure, 0.4 MPa.

### 7.3.5 Membrane stability

Good stability of membranes is an important criterion for practical applications. However, little work is available in the literature that deals with the membrane stability in $H_2$ purification. Due to potential intermolecular hydrogen bonding between TETA and the polymers, the PVAm-PVA/TETA membranes are expected to be stable since the small TETA molecules with a high boiling point (206.9℃) can be encapsulated and retained in the polymer network. Thus, the membrane stability was evaluated using a simulated syn gas containing 20 mol% $CO_2$ (balanced $H_2$) at feed pressures of 0.3 and 0.6 MPa.

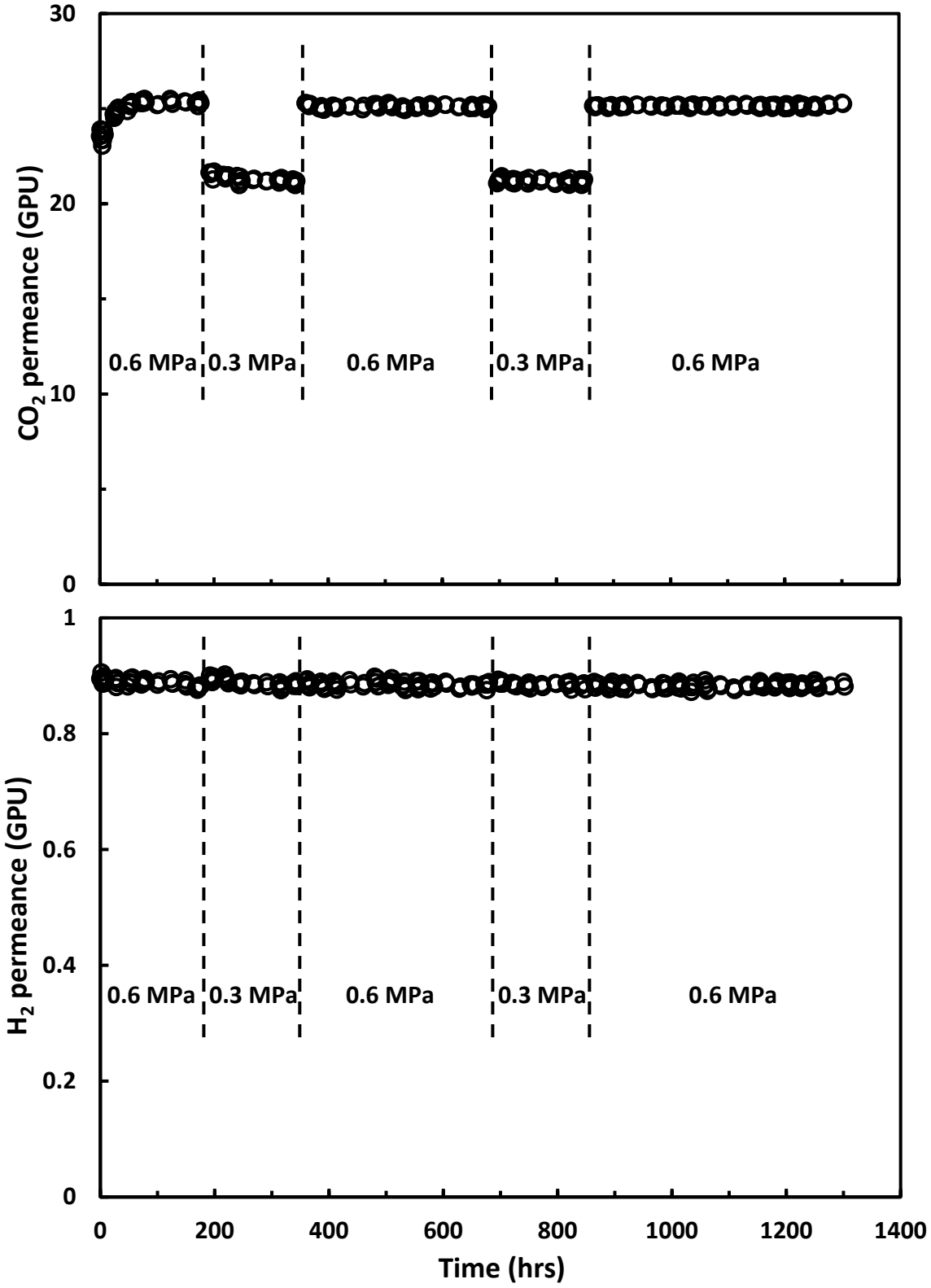


Fig. 7-11 Stability of PVAm-PVA/TETA membrane for continuous permeation of $CO_2/H_2$ gas mixture close to 2 months. TETA content in the membrane, TETA/polymer mass ratio=150/100. Feed $CO_2$ concentration, 20 mol%; temperature, 298 K.

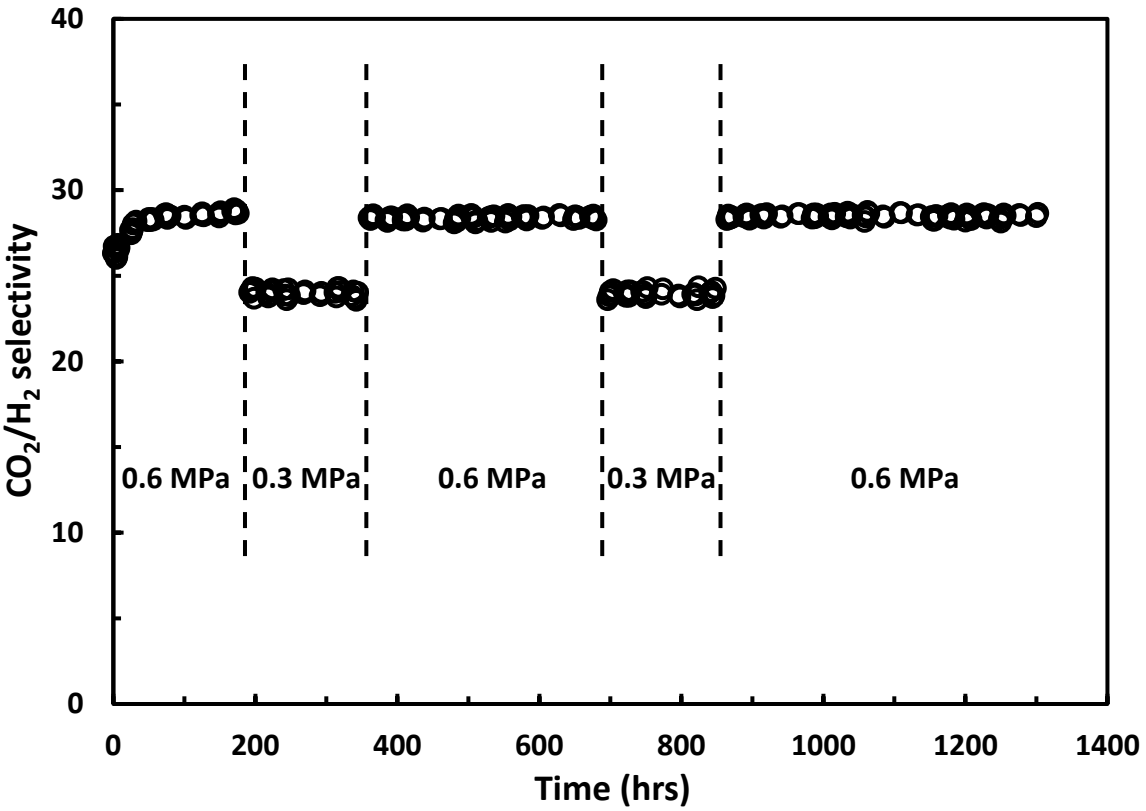


Fig. 7-12 $CO_2/H_2$ selectivity of PVAm-PVA/TETA membrane for continuous permeation of $CO_2/H_2$ gas mixture close to 2 months. TETA content in the membrane, TETA/polymer mass ratio=150/100. Feed $CO_2$ concentration, 20 mol%; temperature, 298 K.

The results of the performance stability tests with the PVAm-PVA/TETA membranes are shown in Figs. 7-11 and 7-12. The feed gas was saturated with water to keep a constant level of swelling of the membrane throughout the experiments. As stated before, the membrane tend to have a higher $CO_2$ permeance and $CO_2/H_2$ selectivity at higher feed pressures for a given feed $CO_2$ content, while the $H_2$ permeance is independent of feed pressure. It was observed that the $CO_2$ permeance indeed decreases when a lower feed pressure is applied, but it increases back to the original level once switched to the higher feed pressure again. The $CO_2/H_2$ selectivity followed a similar trend. The PVAm-PVA/TETA composite membrane is shown to be fairly stable and no deterioration in the membrane performance was observed during the course of continuous permeation for a period of time close to 2 months. The results also confirm that the

molecular TETA is well retained in the membrane without loss at extended period of time.

Table 7-1 lists the $CO_2$ separation performance of PVAm-PVA/TETA composite membranes developed in this study and other related membranes reported in the literature for $CO_2/H_2$ separation, including polymeric membranes based on EO units [Reijerkerk *et al.*, 2010; Chen and Chung, 2012; Li *et al.*, 2013] and facilitated transport membranes [Quinn and Laciak, 1997; Du *et al.*, 2006; Bai and Ho, 2009; Zhao *et al.*, 2008b]. It should be noted that no data on PVAm based facilitated transport membranes for $CO_2/H_2$ separation is available for inclusion in this table since PVAm based membranes reported are mainly focused on $CO_2/N_2$ and $CO_2/CH_4$ separations. A few studies reported the ideal $CO_2/H_2$ selectivity based on the pure $CO_2$ and $H_2$ permeation data (i.e., pure $CO_2$ and $H_2$ permeance ratio) [Du *et al.*, 2006; Zhao *et al.*, 2008b; Reijerkerk *et al.*, 2010], which is known to be different from the actual membrane selectivity for gas mixture permeation [Quinn and Laciak, 1997; Bai and Ho, 2009; Chen and Chung, 2012; Li *et al.*, 2013]. In addition, a few studies [Zhao *et al.*, 2008b; Reijerkerk *et al.*, 2010; Chen and Chung, 2012] reported only $CO_2$ permeability instead of the $CO_2$ permeance, and the thickness of the membranes was not provided. This makes it difficult to evaluate the gas permeance which is a more useful parameter if membrane area is to be calculated for a given separation. Moreover, in some other studies, feed gases were supplied at very low pressures or the permeate side was purged with a sweep gas [Bai and Ho, 2009; Chen and Chung, 2012; Li *et al.*, 2013]. It's quite difficult to directly compare the results obtained at different conditions. However, the table is served to give us an overview of membrane performance for $H_2$ purification.

The membranes developed in this study work well at a feed pressure from 0.2 to 0.7 MPa and at a temperature up to 70℃, while the permeate stream is at atmospheric pressure. For instance, a $CO_2$ permeance of 23.3 GPU and a $CO_2/H_2$ selectivity of 28.5 were obtained at a feed

pressure of 580 kPa for separating $CO_2$ from a $CO_2/H_2$ mixture containing 10 mol% $CO_2$.

Table 7-1 Membrane performance for $H_2$ purification

| Membrane | System ($CO_2$ vol.%) | Feed pressure (kPa) | Permeate pressure (kPa) | Temp. (K) | $\alpha_{CO_2/H_2}$ | $P_{CO_2}$ (Barrer) | $J_{CO_2}$ (GPU) | Reference |
|---|---|---|---|---|---|---|---|---|
| PDMAEMA on PS support | Pure $CO_2$ and $H_2$ | 412 | 101.3 | 296 | 6 | - | 30 | [Du *et al.*, 2006] |
| PDMAEMA-PEGMEMA | Pure $CO_2$ and $H_2$ | 253.3 | 101.3, sweep gas | 308 | 7.3 | 112.8 | - | [Zhao *et al.*, 2008b] |
| Pebax/PDMS-PEG | Pure $CO_2$ and $H_2$ | 400 | vacuum | 308 | 10.6 | 532 | - | [Reijerkerk *et al.*, 2010] |
| PSHM/PEGDME | $CO_2/H_2$ (50%) | 1013.2 | 101.3, sweep gas | 308 | 9.4 | 680 | - | [Chen and Chung, 2012] |
| PVBTAF | $CO_2/H_2$ (30.6%) | 520 | 101.3, sweep gas | 296 | 43 | - | 3 | [Quinn and Laciak, 1997] |
| DGBAmE-TMC on PS support | $CO_2/H_2$ (40%) | 500 | 101.3, sweep gas | 295 | 6.5 | - | 340 | [Li *et al.*, 2013] |
| AIBA-K/PEI/SPBI | $CO_2/H_2/N_2$ (20%) | 206.8 | 101.3, sweep gas | 373 | 64.9 | - | 70.5 | [Bai and Ho, 2009] |
| PVAm-PVA/TETA on PES support | $CO_2/H_2$ (10%) | 580 | 101.3 | 298 | 28.5 | - | 23.3 | This study |
| PVAm-PVA/TETA on PES support | $CO_2/H_2$ (50%) | 560 | 101.3 | 298 | 23.2 | - | 23.9 | This study |

## 7.4 Conclusions

Facilitated transport membranes containing PVAm as fixed carriers and TETA as mobile carriers in a crosslinked PVAm-PVA network were fabricated for the removal of $CO_2$ from $H_2$. The effect of TETA content in the membrane on the permselectivity of the PVAm-PVA/TETA membranes was examined using pure $CO_2$ and $H_2$ permeation. The separation performance of the membranes was also investigated under various operating conditions (i.e., feed pressure, feed $CO_2$ content and temperature). The following conclusions can be drawn:

(1) The $CO_2$ permeance was shown to increase with an increase in the TETA content in the membrane and then decrease with a further increase in the TETA content.

(2) At a given feed $CO_2$ content, the $CO_2$ permeance was shown to increase with an increase in

the feed pressure and then level off when the feed pressure is high enough, while the $N_2$ permeance remained unchanged. At a given feed pressure, the $CO_2$ permeance didn't change significantly with increasing the feed $CO_2$ content, whereas the $H_2$ permeance slightly increased.

(3) An increase in temperature resulted in an increase in both $CO_2$ and $H_2$ permeance, and the temperature affects $H_2$ permeance more significantly than $CO_2$, resulting in a reduction in the $CO_2/H_2$ selectivity.

(4) The stability of the membrane was evaluated for separating a $CO_2/H_2$ gas mixture on a continuous permeation basis for nearly 2 months, and no reduction in the membrane performance was observed.

# Chapter 8

## $CO_2$ separation from ethanol fermentation off gas using PVAm-PVA/TETA composite membranes

---

### 8.1 Introduction

As the energy crisis is imminent to the society, efforts have been devoted to finding renewable fuels to replace the non-renewable petroleum-based fuels. Moreover, renewable fuels are estimated to minimize the $CO_2$ emissions compared to the fossil based energy. Since $CO_2$ emissions from combustion of fossil fuels account for the major part of $CO_2$ in the atmosphere, the use of renewable fuels appears promising to reduce $CO_2$ emissions and help mitigate the severe environmental problems due to global warming caused by greenhouse gases (e.g., $CO_2$).

The need to find an alternative renewable energy fuel source has triggered the fast growing interests in ethanol production. Pure ethanol is rarely used as a fuel for internal combustion, and it's now generally used as an additive to gasoline and diesel. Ethanol is produced via fermentation of various grains and sugar crops, with $CO_2$ being a by-product. For example, in corn ethanol production, to produce one gallon of ethanol will produce 6.29 lbs of $CO_2$ [Rosentrater, 2006]. The amount of $CO_2$ produced from fermentation currently is not significant compared to the large volume of $CO_2$ released from fossil fuel uses. Nevertheless, as ethanol

industry continues to expand, the issue of $CO_2$ emission from fermenters will need to be considered.

The $CO_2$ generated from ethanol fermentation processes is at a high purity on a dry basis (i.e., ~99%), at a low to atmospheric pressure [Mollersten *et al.*, 2003; Yu and Lin, 2012]. The impurities mainly include ethanol, methanol and water vapors. Therefore, it's apparent that the capture process of ethanol fermentation $CO_2$ is quite simple and cost-effective, compared to other $CO_2$ streams such as flue gas from power plants where the $CO_2$ concentration is typically in the range of 10-12%. The only required separation process to capture $CO_2$ from fermentation is the removal of water vapor and ethanol vapor [Xu *et al.*, 2010b]. The residual water vapor can be removed from the gas stream to prevent potential corrosion of $CO_2$ pipelines. Membrane process can thus be used to capture $CO_2$ and eliminate the water vapor simultaneously. When the $CO_2$ stream exiting fermentation broth passes through a membrane unit, water will preferentially permeate through the membrane, and dried $CO_2$ stream is thus retained and captured in the retentate.

To date, not much information on $CO_2$ dehydration from ethanol fermentation off gas is available. In this chapter, $CO_2$ dehydration through PVAm-PVA/TETA composite membranes was studied considering that this membrane was shown to have the best performance for $CO_2$ separation among the various membranes studied in the thesis work. First of all, simplified binary systems (i.e., $CO_2$-$H_2O$ and $CO_2$-EtOH) were used to verify the effectiveness of using PVAm-PVA/TETA membranes for $CO_2$ dehydration and dealcoholization. Further, considering that in ethanol fermentation the $CO_2$ stream contains saturated water and ethanol vapors, the $CO_2$ stream containing both $H_2O$ and EtOH vapors was used as the feed to investigate the $CO_2$

dehydration performance. The effects of operating parameters (e.g., feed composition, temperature) on the membrane performance for $CO_2$ purification were examined.

## 8.2 Experimental

### 8.2.1 Materials

Ethanol was purchased from Fisher Scientific. Other materials used were the same as before. The membrane preparation process was the same as described in chapter 5. The mass ratio of PVAm to PVA in the membrane casting solution was kept at 60/40, and the overall polymer concentration was 5 wt%. A TETA to polymer mass ratio of 150/100 was used to prepare the PVAm-PVA/TETA membranes based on the previous investigations on $CO_2/N_2$ and $CO_2/H_2$ separations in chapters 6 and 7. For the fabrication of the composite membranes, only one coat of the casting solution was found effective to prepare defect-free membranes.

### 8.2.2 Permeation test for gas dehydration

The schematic diagram of the experimental setup for gas dehydration is shown in Fig. 8-1. The PVAm-PVA/TETA membrane was mounted in the permeation cell, which had an effective permeation area of 22.9 $cm^2$. A stream of carbon dioxide gas was bubbled through a solvent bubbling tank (which may contain pure water, pure ethanol or water-ethanol liquid mixtures with given compositions), and this stream was optionally mixed with a stream of dry carbon dioxide to change the feed composition if needed. The flow rates of both gas streams were controlled by mass flow controllers (Matheson Gas, Model 8270), and the inlet vapor composition to the membrane was controlled by adjusting the flow rates of the two streams. The feed gas mixture was admitted to the permeation cell continuously at a flow rate of 200 sccm. The operating

temperature was at 25℃ unless otherwise specified. In studying temperature dependence of membrane performance, the operating temperature was varied in the range of 25 to 65℃ by using a thermal bath. The feed and residual vapor compositions were determined using an online Agilent gas chromatograph (Model 6890N) equipped with a Supelco packed column (60/80 mesh Carboxen-1000, 15′×1/8′) and a thermal conductivity detector. The feed side was maintained at atmospheric pressure, while the permeate side was kept at vacuum (3.3 kPa) using a vacuum pump. The water or ethanol vapor that permeated through the membrane was condensed in a cold trap immersed in liquid nitrogen, and their permeation rates were determined by weighing the permeate collected in the condenser for a given period of time. For permeate samples containing both water and ethanol, their composition was determined using a refractometer (ATAGO 3T, Japan).

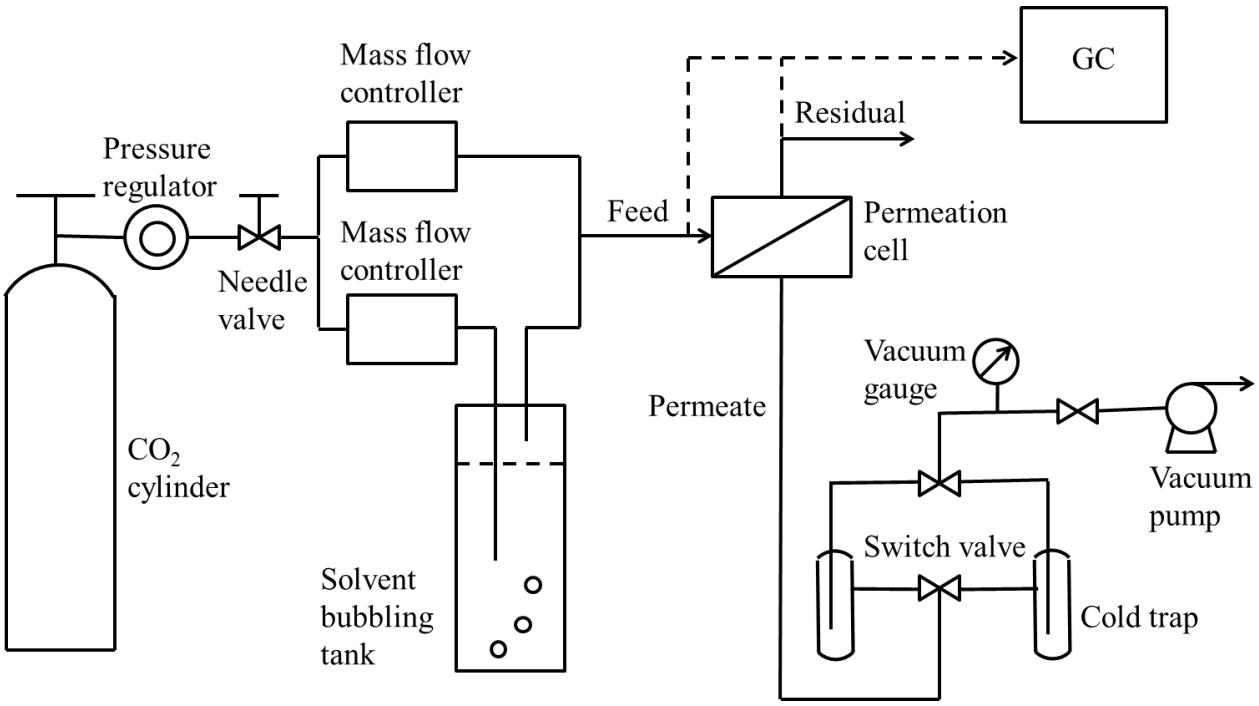


Fig. 8-1 Schematic diagram of experimental setup for $CO_2$ separation from ethanol fermentation off gas

For $CO_2$-$H_2O$ binary system, the permeance of water vapor was calculated based on the following equations:

$$Q_{H_2O} = AJ_{H_2O}\left(p_f X - p_p Y\right) \quad (8\text{-}1)$$

$$Q_{CO_2} = AJ_{CO_2}\left[p_f(1-X) - p_p(1-Y)\right] \quad (8\text{-}2)$$

$$Y = \frac{Q_{H_2O}}{Q_{H_2O}+Q_{CO_2}} \quad (8\text{-}3)$$

where $Q$ is the permeation rate ($cm^3(STP)/s$), $J$ is the permeance ($cm^3(STP)/cm^2 \cdot s \cdot cmHg$) ($1\ cm^3(STP)/cm^2 \cdot s \cdot cmHg = 10^6\ GPU$). $A$ is the effective membrane area for permeation ($cm^2$), and $X$ and $Y$ are the concentrations (mole fraction) of water vapor on the feed and permeate sides, respectively. Because of the high selectivity to water vapor permeation, the water concentration at the residual side was lower than the feed inlet, and thus $X$ was taken as an average of the water concentration. $p_f$ and $p_p$ are the feed and permeate pressures ($cmHg$), respectively. Looking at Eqs. (8-1)-(8-3), $A$, $p_f$, $p_p$, $Q_{H2O}$ and $X$ are the known quantities from the experiment, and the $CO_2$ permeance $J_{CO2}$ has been determined previously. Therefore, water vapor permeance $J_{H2O}$ and the other two unknown quantities (i.e., $Q_{CO2}$ and $Y$) can be determined from the above three equations. Similarly, the permeance of ethanol vapor for $CO_2$-EtOH binary system can also be calculated in the same manner.

It should be pointed out that based on $CO_2$ permeance of the PVAm-PVA/TETA membrane with a TETA to polymer mass ratio of 150/100 at different feed pressures (see Fig. 6-5), the $CO_2$ permeance of this membrane at $\sim 1\ atm$ was estimated to be 14.4 GPU. On the other hand, the $CO_2$ permeance was known to change slightly with the mole fraction of $CO_2$ in the feed in $CO_2/N_2$ and $CO_2/H_2$ separation in previous studies. Thus, to verify whether the $CO_2$ permeance is a constant in the $CO_2$-$H_2O$ and $CO_2$-EtOH streams with different feed $CO_2$ concentrations (in the range of 90 to 100 mol%), an experiment was conducted by bubbling dry $CO_2$ through either a water or ethanol tank, and the gas mixture was admitted to the permeation cell, while the permeate side was kept at vacuum. The schematic diagram of this experiment is shown in Fig. 8-

2. After the water vapor (or ethanol vapor) was saturated in $CO_2$ stream under room temperature, the $CO_2$ flow was closed. Then the permeation rate of $CO_2$ through the membrane was determined by a bubble flow meter on the retentate side. Based on the experimental data, a $CO_2$ permeance at $\sim 1\ atm$ was determined to be 14.2 (for $CO_2$-$H_2O$ system) or 14.1 (for $CO_2$-EtOH system) GPU. Therefore, the $CO_2$ permeance was assumed to be the same (i.e., 14.4 GPU) in the entire $CO_2$ dehydration experiments unless the temperature was changed.

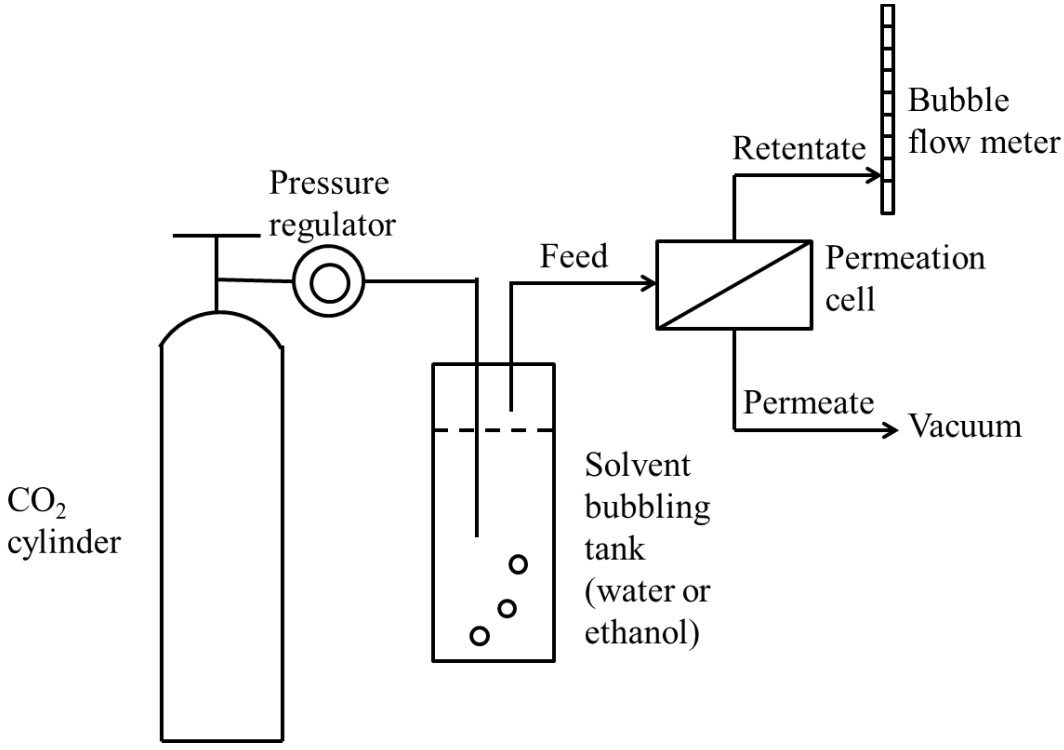


Fig. 8-2 Schematic diagram of verification experiment

Furthermore, in order to mimic a representative gas stream released from a fermenter, carbon dioxide was bubbled through a tank of ethanol and water mixtures to produce a ternary $CO_2$-$H_2O$-EtOH gas mixture. The permeances of water and ethanol vapor were then determined using the following equations:

$$Q_{H_2O} = AJ_{H_2O}\left(p_f X_{H_2O} - p_p Y_{H_2O}\right) \tag{8-4}$$

$$Q_{CO_2} = AJ_{CO_2}\left(p_f X_{CO_2} - p_p Y_{CO_2}\right) \tag{8-5}$$

$$Q_{EtOH} = AJ_{EtOH}\left[p_f\left(1 - X_{H_2O} - X_{CO_2}\right) - p_p\left(1 - Y_{H_2O} - Y_{CO_2}\right)\right] \quad (8\text{-}6)$$

$$Y_{H_2O} = \frac{Q_{H_2O}}{Q_{H_2O}+Q_{CO_2}+Q_{EtOH}} \quad (8\text{-}7)$$

$$Y_{CO_2} = \frac{Q_{CO_2}}{Q_{H_2O}+Q_{CO_2}+Q_{EtOH}} \quad (8\text{-}8)$$

where $X$ and $Y$ are the concentrations of corresponding components on the feed and permeate sides, and subscripts $H_2O$, $CO_2$ and $EtOH$ represent water vapor, $CO_2$ and ethanol vapor, respectively. In Eqs. (8-4)-(8-8), $A$, $p_f$, $p_p$, $Q_{H_2O}$, $Q_{EtOH}$, $X_{H_2O}$ and $X_{CO_2}$ are the known quantities from the experiment, and $J_{CO_2}$ is also available. Thus, water vapor permeance $J_{H_2O}$, ethanol vapor permeance $J_{EtOH}$, and the other three unknown quantities (i.e., $Q_{CO_2}$, $Y_{H_2O}$ and $Y_{CO_2}$) can be determined from the above five equations.

## 8.3 Results and discussion

### 8.3.1 $CO_2$-$H_2O$ and $CO_2$-EtOH binary systems

To evaluate the $CO_2$ separation performance of PVAm-PVA/TETA membranes used for ethanol fermentation, separations of $CO_2$-$H_2O$ and $CO_2$-EtOH binary mixtures were first examined. Fig. 8-3 shows the results of the $CO_2$ dehydration experiments at an operating temperature of 25 ℃ when the water vapor in feed concentration varied from 0.5 to 2.5 mol%.

As shown in Fig. 8-3(a), the water vapor is substantially enriched in the permeate stream, and the water vapor concentration in permeate increases with an increase in feed water vapor concentration. For example, the permeate vapor concentration reaches over 70 mol% when the water vapor concentration in feed is 2.5 mol%. Since water vapor can interact strongly with the hydrophilic polymer via hydrogen bonding, a high solubility and diffusivity of water vapor are generally observed in hydrophilic polymeric materials, compared to permanent gases. The

PVAm-PVA/TETA membranes developed in this study contain abundant hydrophilic groups, i.e., primary, secondary amino groups and hydroxyl groups. This membrane displayed an outstanding selectivity to water vapor. In Fig. 8-3(b), the water flux is shown to experience a progressive increase with an increase in the feed water concentration. This is understandable considering the strong interaction between water and the polymer.

Similarly, permeation of binary $CO_2$-EtOH system was also investigated using the PVAm-PVA/TETA membrane for a feed ethanol concentration of 1.4 to 7 mol%. Fig. 8-4 shows that ethanol vapor is also enriched in the permeate stream, however, to a lesser extent as compared to water vapor. The ethanol concentration reached 44 mol% at a feed ethanol concentration of 7 mol%. Similar to water permeation, ethanol can also interact with the hydrophilic polymer via hydrogen bonding, resulting in preferential permeation of ethanol over $CO_2$ in the PVAm-PVA/TETA membrane. Further, the ethanol flux is shown to increase with an increase in the ethanol content in feed.

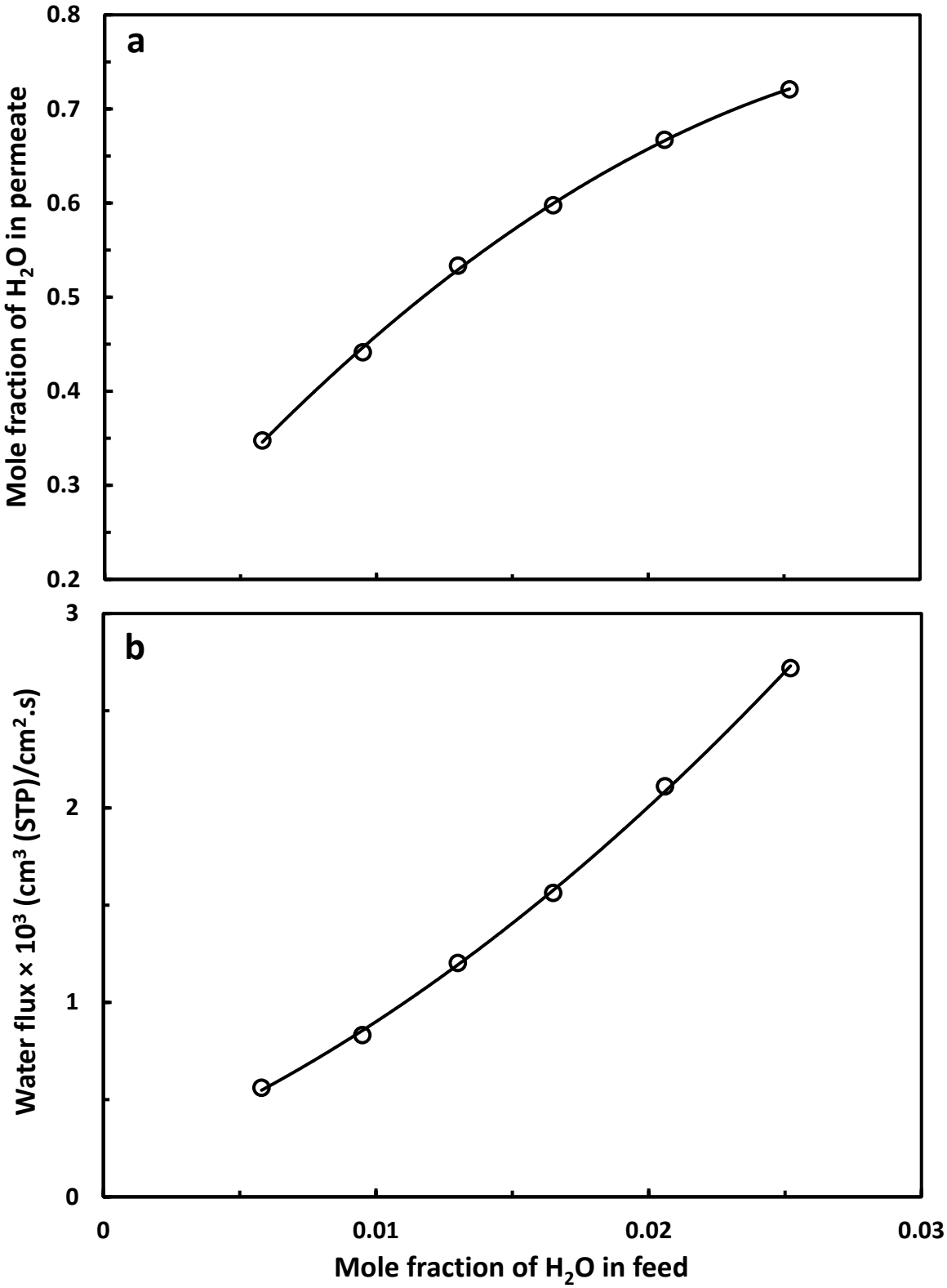


Fig. 8-3 Effect of water vapor concentration in feed on (a) permeate concentration and (b) water permeation flux. Operating temperature: 25 ℃.

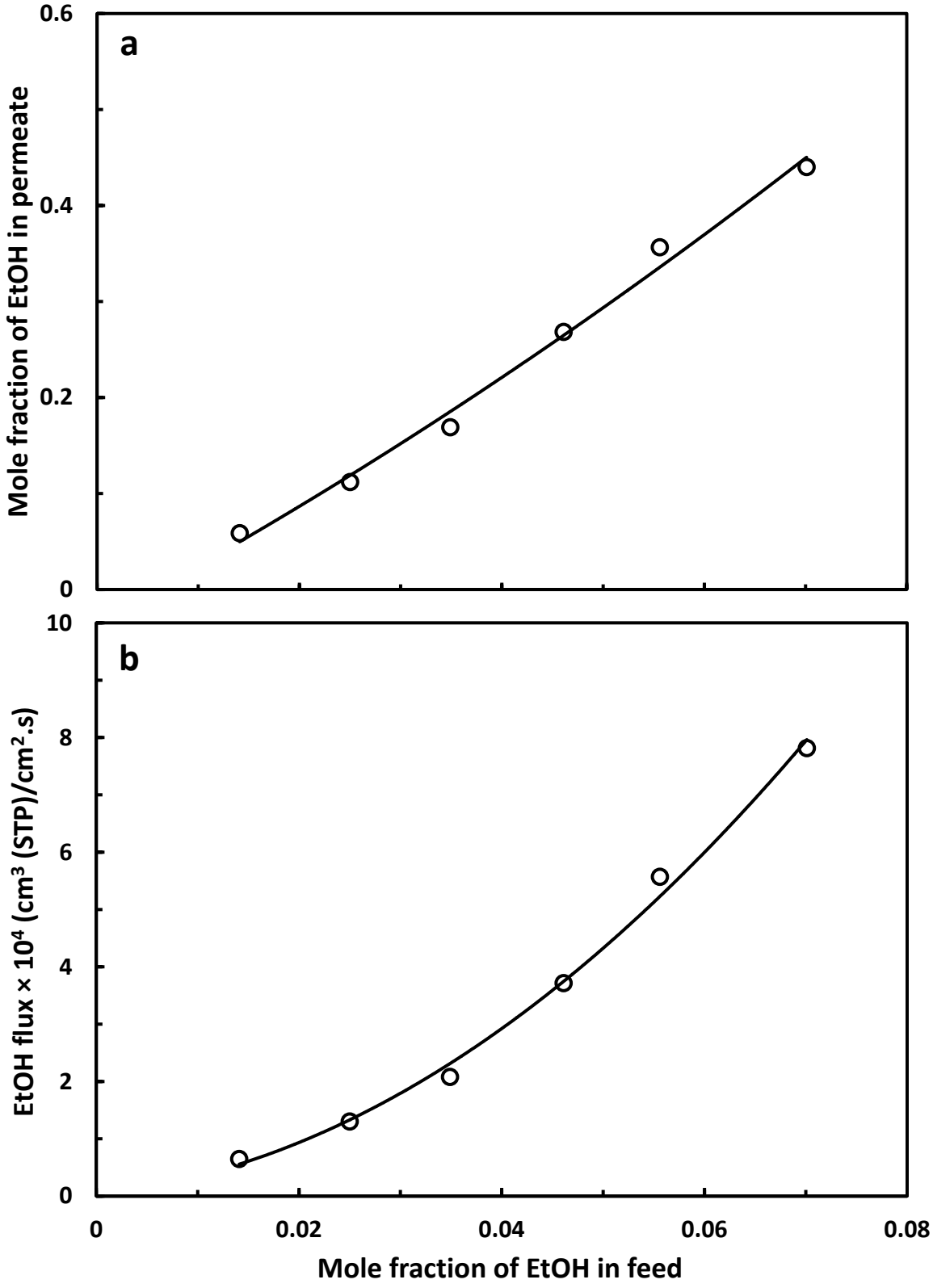


Fig. 8-4 Effect of ethanol vapor concentration in feed on (a) permeate concentration and (b) ethanol permeation flux. Operating temperature: 25 ℃.

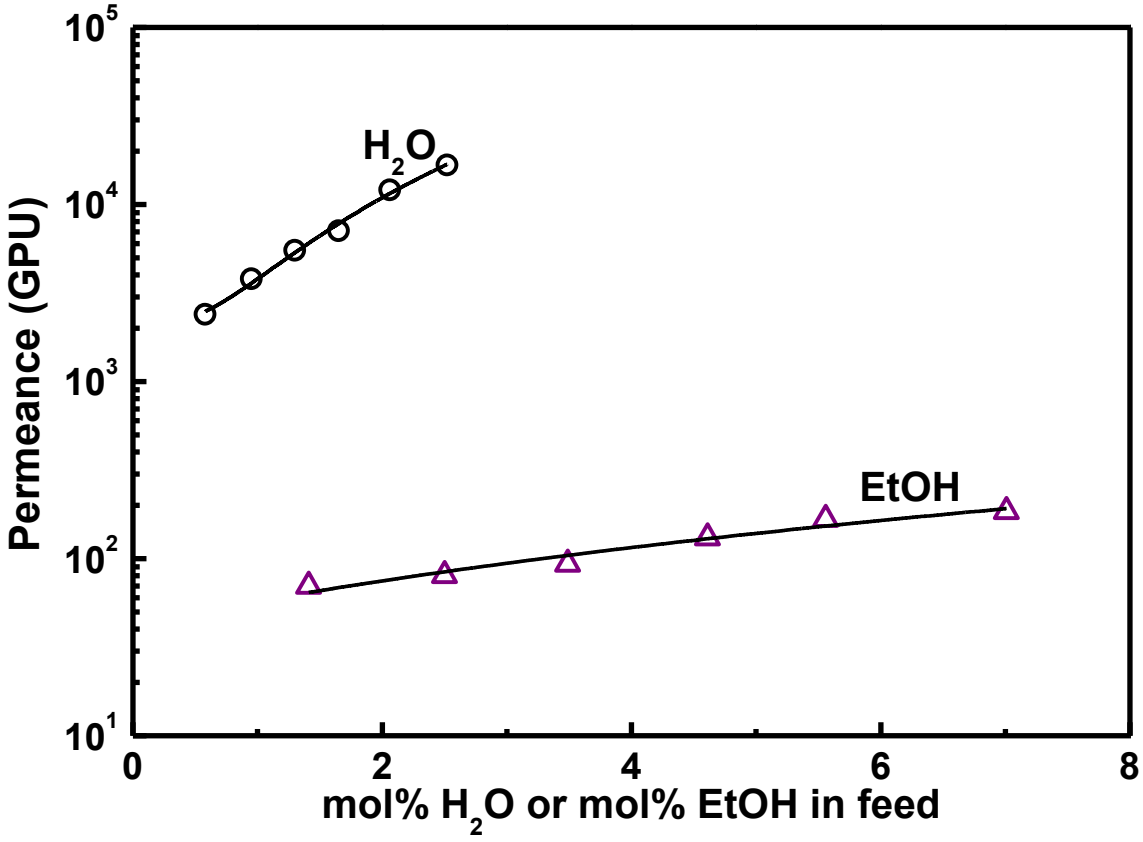


Fig. 8-5 Effect of water or ethanol vapor concentration in feed on water vapor and ethanol vapor permeance. Operating temperature: 25 ℃.

Figs. 8-5 and 8-6 show the permeance of water vapor and ethanol vapor for binary $CO_2$-$H_2O$ and $CO_2$-EtOH permeation in the membrane with respect to water vapor or ethanol vapor concentration in feed and percentage saturation with water or ethanol in feed, respectively. The percentage saturation with water or ethanol in feed was calculated as the feed water or ethanol vapor concentration divided by the saturated water or ethanol vapor concentration at 25℃. The water vapor permeance is found to increase significantly with the water vapor concentration in the feed, and could reach as high as 16700 GPU at a 2.5 mol% feed water concentration or a 81% saturation with water in feed. The selectivity of water vapor over $CO_2$ is more than 1000. The ethanol permeance also increases significantly with ethanol concentration in the feed, but the highest ethanol permeance recorded in the experiments was only 185 GPU at a feed ethanol concentration of 7 mol% or a 91% saturation with ethanol in feed, two orders of magnitudes less

than the water vapor permeance. The selectivity of ethanol vapor to $CO_2$ is found to be a little higher than 10.

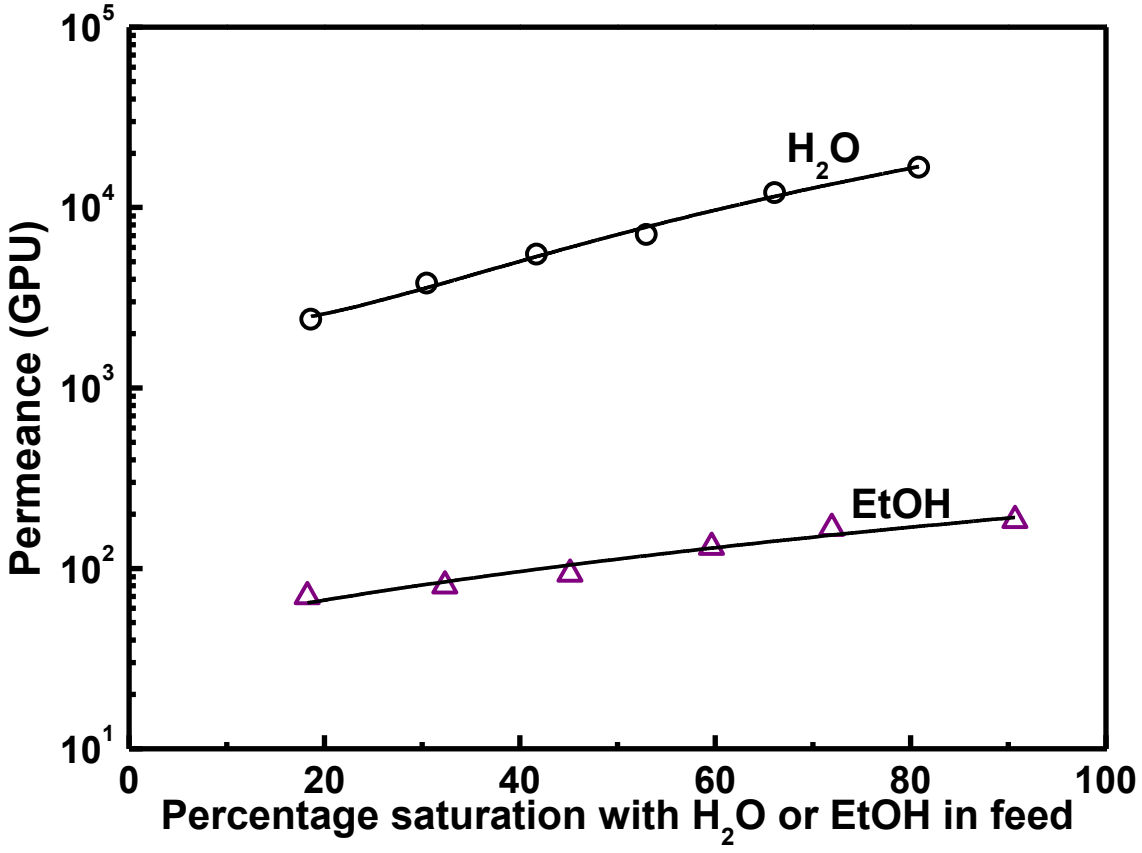


Fig. 8-6 Effect of percentage saturation with $H_2O$ or EtOH in feed on water vapor and ethanol vapor permeance. Operating temperature: 25 ℃.

The effects of temperature on the permeance of water vapor, ethanol vapor and $CO_2$ through the PVAm-PVA/TETA membranes for both $CO_2$-$H_2O$ (2.5 mol% $H_2O$) and $CO_2$-EtOH (7 mol% EtOH) binary mixtures are shown in Figs. 8-7 and 8-8. Note that the $CO_2$-$H_2O$ and $CO_2$-EtOH systems were saturated with water and ethanol, respectively. With an increase in temperature, despite the increased fluxes of water and ethanol, a decreasing trend of water and ethanol concentration in the permeate is observed for both binary systems, as shown in Figs. 8-7 and 8-8.

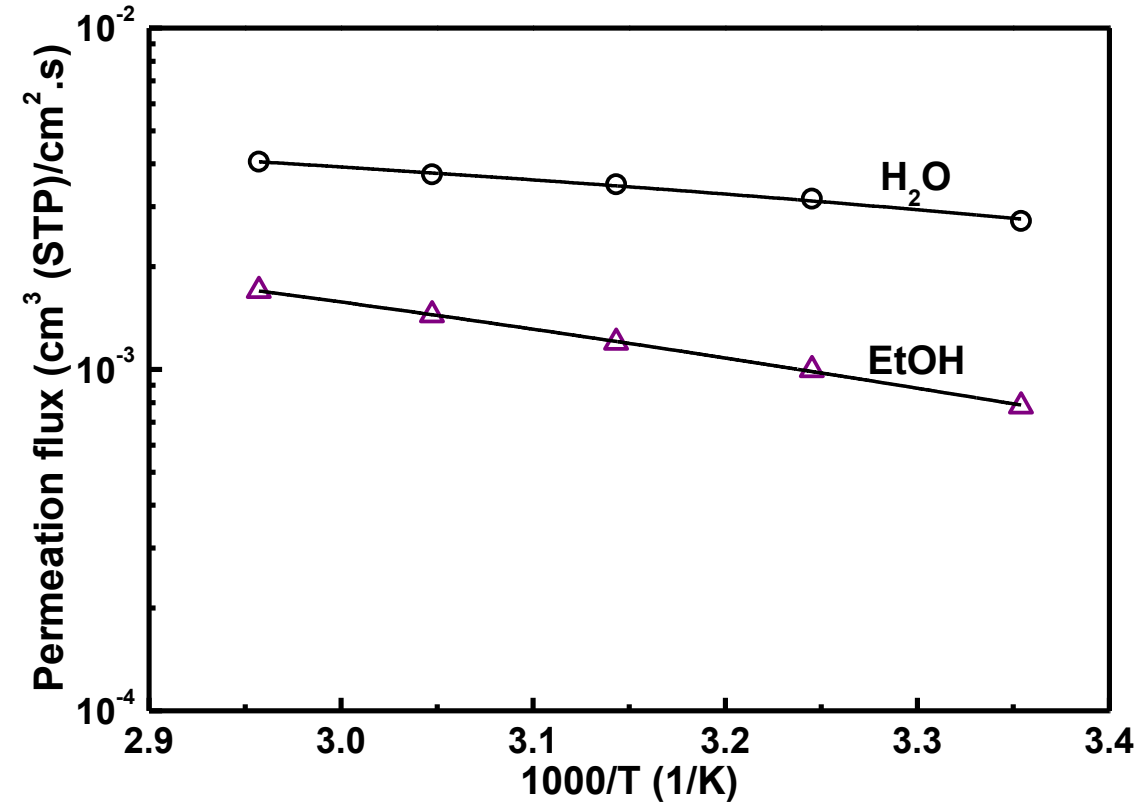


Fig. 8-7 Temperature dependence of water and ethanol flux for permeation of $CO_2$-$H_2O$ and $CO_2$-EtOH binary systems, respectively

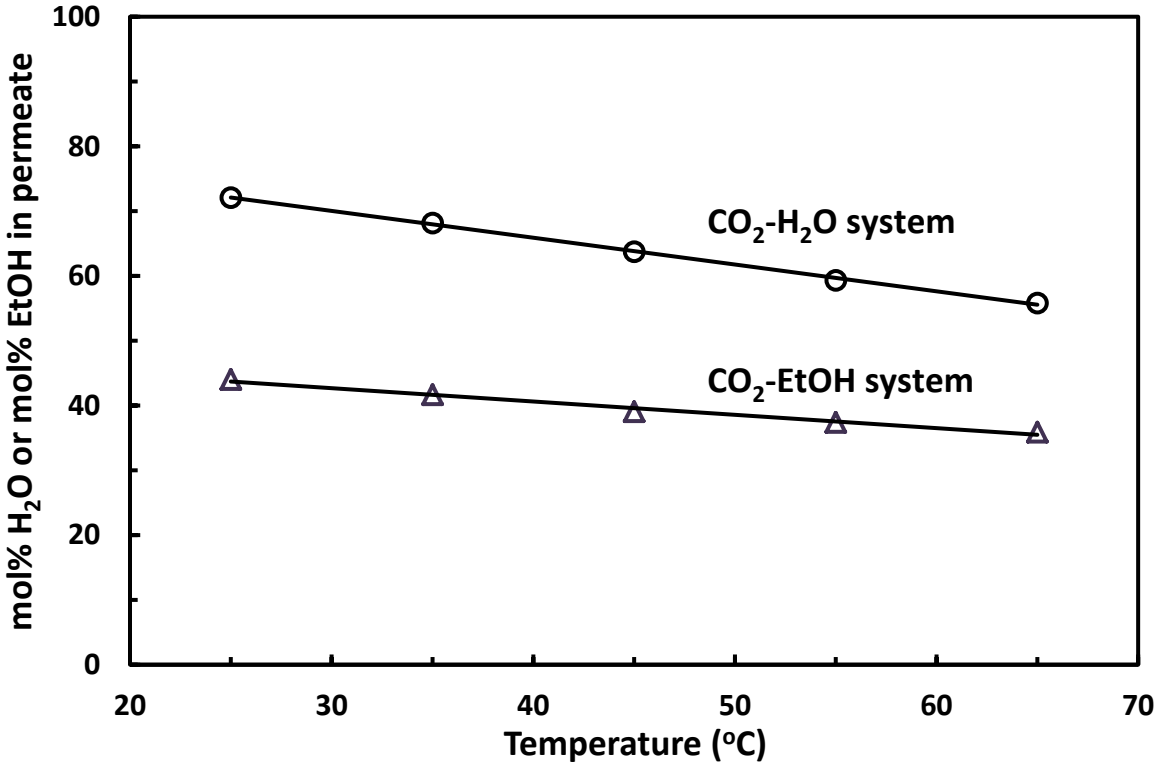


Fig. 8-8 Permeate concentration versus operating temperature for $CO_2$-$H_2O$ and $CO_2$-EtOH binary systems

Fig. 8-9 shows the permeance of water vapor, ethanol vapor and $CO_2$ against the reciprocal of temperature on a semi-logarithmic scale. The permeance of $CO_2$ and ethanol increase with an increase in temperature, and their temperature dependencies follow an Arrhenius type of relation. The apparent activation energies for $CO_2$ and ethanol permeation were calculated to be 23.5 and 15.2 kJ/mol, respectively. The water vapor permeance, on the other hand, decreases when the operating temperature increases. This can be explained qualitatively in the following. According to the solution-diffusion mechanism, the permeability is determined by the solubility and diffusivity of the permeant in the membrane, and the overall temperature dependence of permeability (which is characterized by the activation energy for permeation $E_P$) is the sum of the activation energy of diffusion ($E_D$) and the heat of sorption ($\Delta H_S$) [Du *et al.*, 2008; 2010a]:

$$E_P = E_D + \Delta H_S \tag{8-9}$$

The diffusivity generally increases with an increase in temperature, and the activation energy for diffusion is always positive. The heat of sorption for gases in polymers normally has a small negative value, and thus the overall gas permeability tends to increase with temperature. This is found to be the case for $CO_2$ permeation through the membrane. Ethanol permeation also showed a similar result. Nevertheless, water vapor is a much more condensable permeant, and its heat of sorption will be more pronounced and may become dominant over the activation energy of diffusion, causing a negative temperature dependence of permeability. A similar observation of negative temperature dependence of water permeability was made using PDMAEMA/PAN membrane in natural gas dehydration [Du *et al.*, 2010a].

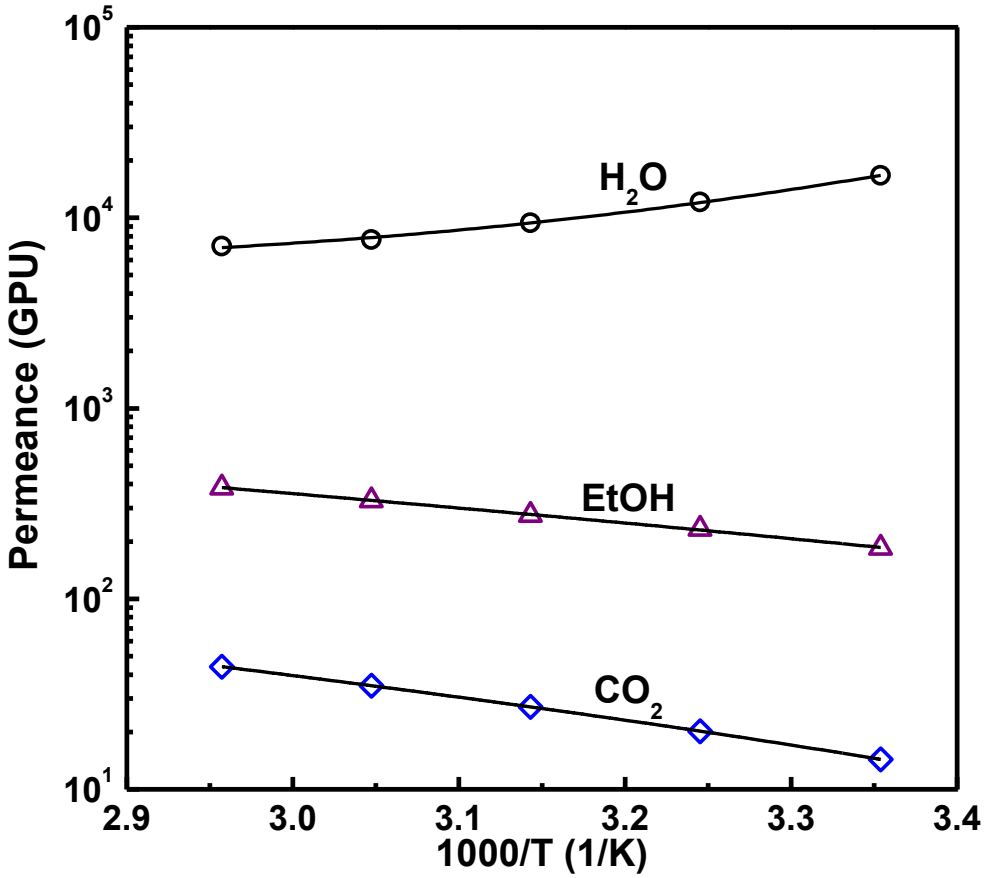


Fig. 8-9 Permeance of $CO_2$, water and ethanol vapor at different temperatures

### 8.3.2 $CO_2$-$H_2O$-EtOH ternary system

Considering enzymic ethanol fermentation, the major components in overhead gas phase are $CO_2$, water and ethanol vapors. Because most of the yeasts have a low tolerance to ethanol and ethanol production is product inhibitive, the ethanol concentration in the fermenter is normally below 15 wt% [Hashi *et al.*, 2010]. Therefore, as ethanol is produced and removed, ethanol inhibition is reduced and a greater bioconversion is expected. When the overhead gas is released from the fermenter, the off gas is saturated with water and ethanol vapors. To test the applicability of using PVAm-PVA/TETA membranes for $CO_2$ separation by separating water and ethanol from the gas streams, a $CO_2$-$H_2O$-EtOH ternary mixture was produced by bubbling $CO_2$ through a liquid mixture of ethanol and water, and then the membrane performance for

dehydration and dealcoholization was investigated. Seven ethanol and water liquid mixtures with a broad composition range were used to generate the ternary mixtures, and the experimental results for separating the $CO_2$-$H_2O$-EtOH mixtures are shown in Table 8-1.

Table 8-1 Feed and permeate concentration of $CO_2$, water and ethanol in $CO_2$-$H_2O$-EtOH ternary system

| No. | EtOH wt% in bubbling mixture | Feed gas composition | | | Permeate composition | | | Liquid composition after condensation of permeate vapor (EtOH (wt%)) |
|---|---|---|---|---|---|---|---|---|
| | | $X_{CO2}$ | $X_{H2O}$ | $X_{EtOH}$ | $Y_{CO2}$ | $Y_{H2O}$ | $Y_{EtOH}$ | |
| 1 | 3 | 0.96988 | 0.02785 | 0.00227 | 0.2160 | 0.7820 | 0.0020 | 0.645 |
| 2 | 5 | 0.96868 | 0.02754 | 0.00378 | 0.2342 | 0.7621 | 0.0037 | 1.221 |
| 3 | 10 | 0.96619 | 0.02637 | 0.00743 | 0.2600 | 0.7315 | 0.0085 | 2.894 |
| 4 | 15 | 0.96407 | 0.02490 | 0.01103 | 0.2945 | 0.6916 | 0.0139 | 4.889 |
| 5 | 20 | 0.96187 | 0.02333 | 0.01480 | 0.3302 | 0.6469 | 0.0229 | 8.295 |
| 6 | 30 | 0.95678 | 0.02059 | 0.02264 | 0.3807 | 0.5745 | 0.0448 | 16.61 |
| 7 | 40 | 0.95243 | 0.01751 | 0.03005 | 0.4350 | 0.4870 | 0.0780 | 29.54 |

The permeate stream is significantly enriched in water because of the preferential permeation of water vapor over both ethanol vapor and $CO_2$. In the concentration range relevant to industrial applications (i.e., $CO_2$ saturated with vapor from liquid at EtOH wt%<15 %), the mole fraction of water in the permeate stream can reach 80%, indicating that PVAm-PVA/TETA membranes are effective for purification of $CO_2$ from ethanol fermentation off gas.

For lab studies, the permeate is condensed and collected in liquid nitrogen immersed in a cold trap. For practical applications, a permeate condenser may be designed such that the $CO_2$ can be released and recaptured while the water and ethanol vapors are condensed to liquid. The liquid composition was calculated and shown in Table 8-1.

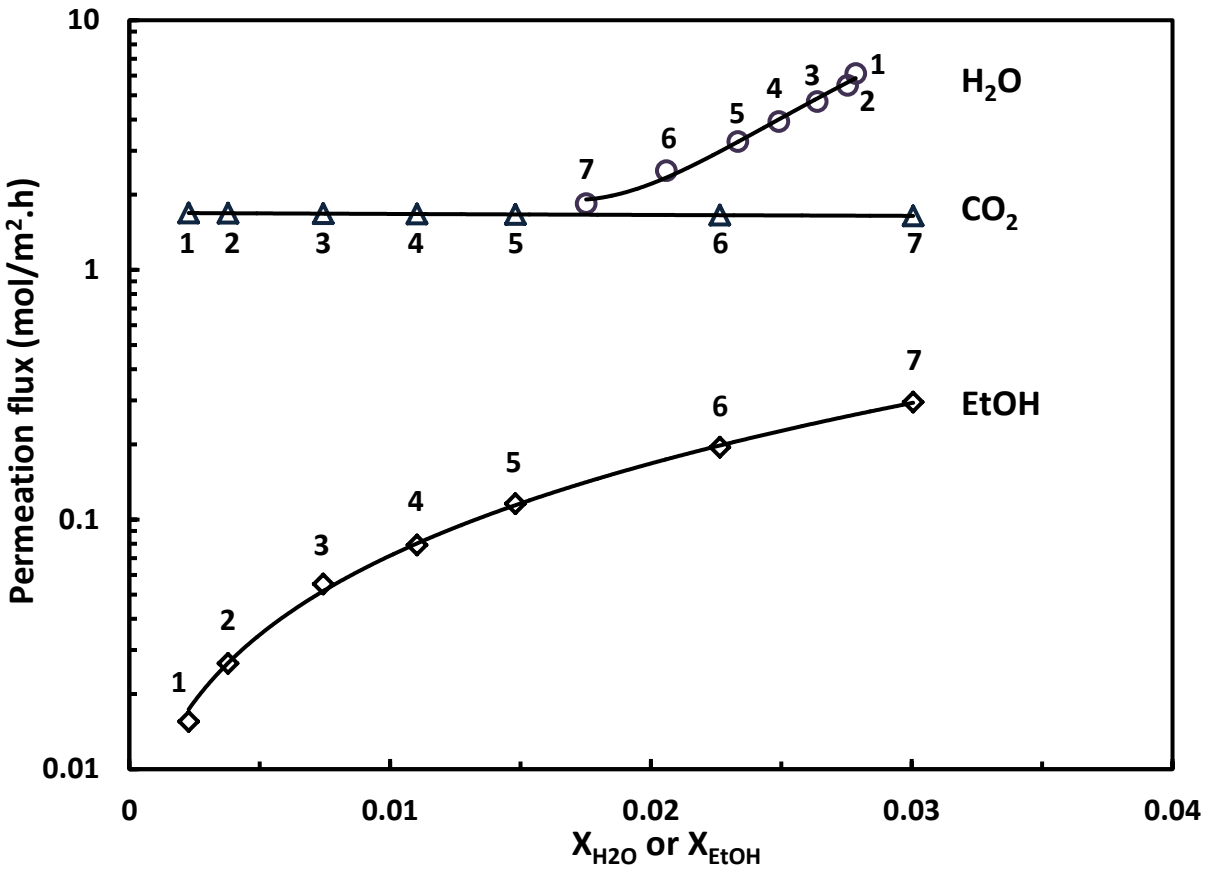


Fig. 8-10 Permeation fluxes of water, ethanol and $CO_2$ for permeation of $CO_2$-$H_2O$-EtOH ternary mixtures. Operating temperature: 25 ℃. Numbers in this figure corresponds to experimental runs listed in Table 8-1.

The permeation flux of water, ethanol and $CO_2$ for $CO_2$-$H_2O$-EtOH ternary mixture permeation is shown in Fig. 8-10. Both permeation fluxes of water and ethanol increase with their concentrations in the feed, and the permeation flux of $CO_2$ basically remains the same, which can be ascribed to the very small changes in partial pressure of $CO_2$ that drives $CO_2$ permeation. The permeance of water and ethanol vapor is displayed in Fig. 8-11. Recalling Figs. 8-5 and 8-6, the increasing trend of water and ethanol permeance with increasing feed water and ethanol concentrations in the ternary system is the same as that for binary $CO_2$-$H_2O$ and $CO_2$-EtOH mixture permeation. For the $CO_2$-$H_2O$-EtOH ternary mixtures, the water vapor permeance was 14600 GPU at a feed water concentration of 2.5 mol%, which was only 12% lower than that for $CO_2$-$H_2O$ binary system (i.e., 16700 GPU) at the same feed water concentration. The water

vapor permeance didn't show a significant difference for $CO_2$-$H_2O$ binary and $CO_2$-$H_2O$-EtOH ternary system. Thus, the $CO_2$ dehydration performance of the PVAm-PVA/TETA membrane is not deteriorated by the presence of ethanol.

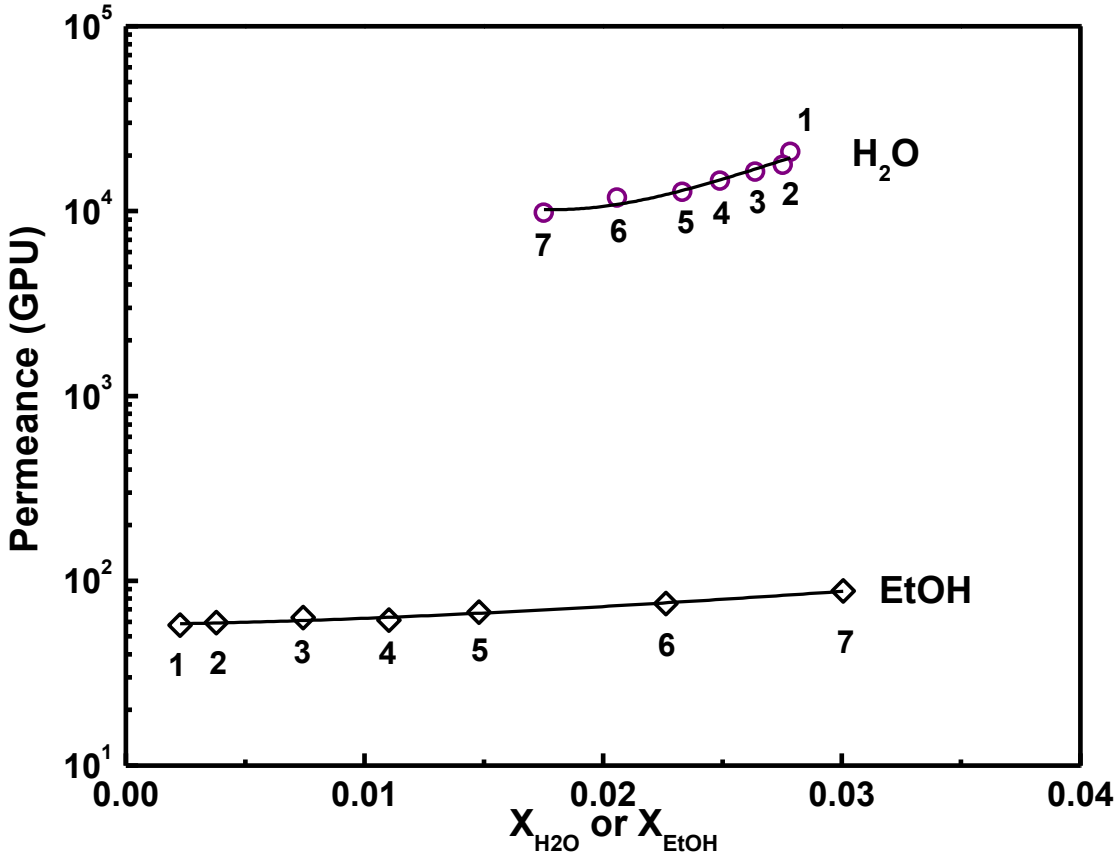


Fig. 8-11 Permeance of water and ethanol vapor for permeation of $CO_2$-$H_2O$-EtOH ternary mixtures. Operating temperature: 25 ℃. Numbers in this figure corresponds to experimental runs listed in Table 8-1.

## 8.4 Conclusions

The use of PVAm-PVA/TETA membranes to purify $CO_2$ emitted from ethanol fermentation was examined, and the performance of the membrane for removal of water and ethanol vapor was evaluated using $CO_2$-$H_2O$ and $CO_2$-EtOH binary mixtures and $CO_2$-$H_2O$-EtOH ternary mixtures. The following conclusions can be drawn:

(1) The permeance of water vapor and ethanol vapor through the membrane was found to increase with an increase in their concentrations in the feed gas stream. A negative temperature dependence of water vapor permeability was observed.

(2) The permeance of water vapor for permeation of $CO_2$-$H_2O$ binary mixtures and $CO_2$-$H_2O$-EtOH ternary mixtures was found to be similar at a given feed water content. The membrane exhibited an outstanding selectivity to permeation of water vapor over $CO_2$, and this membrane can be used for $CO_2$ drying in $CO_2$ capture from fermentation off gas.

# Chapter 9

## General Conclusions, Contributions and Recommendations

---

### 9.1 General Conclusions

PVAm-PVA composite membranes incorporated with CNTs and molecular amines were developed in this work in order to achieve a high permselectivity. The potential applications of these membranes for $CO_2$ separation from flue gas, ethylene glycol dehydration by pervaporation, $H_2$ purification and off gas treatment from ethanol fermentation were explored. The following conclusions can be drawn from this research:

1. The permeability of PVAm/PVA blend polymer membranes to gases followed the order of $N_2 < CH_4 < He \approx O_2 < H_2 < CO_2$, and a higher PVAm/PVA blend ratio was found to correlate to a higher $CO_2/N_2$ permselectivity. The incorporation of acid-treated MWNTs into PVAm/PVA blend polymer was verified by FTIR and Raman spectra, and the membrane crystallinity was shown to decrease with addition of CNTs as characterized by XRD spectra. Adding CNTs in the membrane enhanced $CO_2$ permeability while retaining a similar $CO_2/N_2$ selectivity at a CNT loading up to 2 wt%; a further increase in the CNT loading tended to decrease the gas permeability gradually. Nanocomposite membrane with an increased permeance was obtained by forming a thin film composite membrane where the functional skin layer was supported by a microporous substrate.

2. For pervaporation dehydration of ethylene glycol, the PVAm-PVA/CNT membranes showed good permselectivity as compared with other membranes reported in the literature due to the highly hydrophilic polymer and incorporation of MWNTs into the membrane. At 70℃, a permeation flux of 146 g/($m^2$.h) and a separation factor of 1160 were achieved at 1 wt% water in feed using a PVAm-PVA/CNT composite membrane containing 2 wt% MWNTs. The surface hydrophilicity and bulk liquid sorption uptake tests of the dense membranes showed that a small amount of CNTs in the membrane wouldn't change the permeant solubility in the membrane significantly. The temperature effect on the permeation flux was mainly derived from its effects on the driving force for permeation.
3. The separation of $CO_2$ from $N_2$ by PVAm-PVA composite membranes containing molecular amines (i.e., PZ, and PZ/TEA and PZ/MDEA blend) was investigated using a simulated flue gas containing 15.3 mol% $CO_2$. The $CO_2$ permeance was shown to increase with an increase in the PZ content in the membrane. The effects of various operating conditions (i.e., feed pressure, temperature and composition) on the performance of the membranes were studied. The membrane stability was demonstrated in a continuous permeation process of more than 7 weeks. The facilitation in $CO_2$ transport by the amines was more significant when the mixed amines were used. The mass ratio of PZ to tertiary amine in the range of 67/33 to 80/20 was shown to be appropriate to produce membranes with improved separation performance.
4. PVAm-PVA composite membranes incorporating DETA and TETA were subjected to the removal of $CO_2$ from $N_2$. It was shown that the $CO_2$ permeance increased with an increase in the DETA and TETA content in the membrane initially, and when the amine content is sufficiently high, a further increase in the amine content in the membrane would decrease the membrane permeance. TETA was shown to be more effective in facilitating $CO_2$ transport

than DETA in terms of $CO_2/N_2$ permselectivity. The activation energy for $CO_2$ permeation increased with an increase in DETA and TETA content in the membrane, while the activation energy for $N_2$ permeation didn't change significantly.

5. For the separation of $CO_2$ from syn gas for $H_2$ purification by PVAm-PVA/TETA composite membranes, the effects of TETA content in the membrane and various operating conditions on the performance were investigated. At a given feed pressure, the $CO_2$ permeance didn't change significantly with the feed $CO_2$ concentration, whereas the $H_2$ permeance slightly increased. A $CO_2$ permeance of 23.3 GPU and a $CO_2/H_2$ selectivity of 28.5 were achieved using the composite membrane at a mass ratio of TETA to polymer of 150/100. The membrane was demonstrated to be stable for separating a $CO_2/H_2$ gas mixture.
6. The separation of $CO_2$ from ethanol fermentation off gas by PVAm-PVA/TETA composite membranes was studied using both $CO_2$-$H_2O$ and $CO_2$-EtOH binary mixtures and $CO_2$-$H_2O$-EtOH ternary mixture. The permeance of water vapor was 16700 GPU at 25℃ and 2.5 mol% feed water concentration, and increased with an increase in feed water vapor concentration. The membrane displayed outstanding selectivity to water vapor permeation, making it suitable for separating water vapor and ethanol vapor to purify $CO_2$. A negative temperature dependence of water vapor permeability was observed.

## 9.2 Contributions to Original Research

1. PVAm-PVA nanocomposite membranes incorporated with CNTs were developed in this thesis and employed in $CO_2$ separation and ethylene glycol dehydration by pervaporation. The incorporation of CNTs into the membrane was shown to enhance the permeation (e.g., $CO_2$ permeance or permeation flux) while retaining a similar or improved selectivity (e.g.,

$CO_2/N_2$ selectivity or separation factor). Particularly, the research of membranes embedded with CNTs for pervaporation applications is very lacking, thus, the successful use of PVAm-PVA/CNTs membranes in ethylene glycol dehydration by pervaporation represents an expansion of the scope of applications for CNTs-incorporated membranes.

2. Novel facilitated transport membranes containing both PVAm as fixed carriers and molecular amines as mobile carriers in a crosslinked PVAm-PVA polymer network for $CO_2$ separation were studied in this thesis. All the membranes with molecular amines (including PZ, DETA and TETA) have shown a better separation performance in terms of $CO_2/N_2$ permselectivity as compared to the plain membrane without molecular amines. Among all the molecular amines tested, TETA was shown to be most effective in facilitating $CO_2$ transport due to its multi-amino functionalities. In addition, the use of mixed amines containing PZ and a tertiary amine was also studied. The facilitation in $CO_2$ transport was more significant with membranes containing mixed amines (e.g., PZ/TEA and PZ/MDEA).
3. The PVAm-PVA/TETA thin film composite membranes were employed in $H_2$ purification and $CO_2$ separation from ethanol fermentation off gas in addition to $CO_2$ separation from flue gas. For $CO_2$ separation from $H_2$, this membrane was shown to compare favorably with other membranes reported in the literature in terms of $CO_2/H_2$ permselectivity. For $CO_2$ separation from ethanol fermentation off gas, this membrane exhibited an outstanding selectivity to permeation of water vapor over $CO_2$.

## 9.3 Recommendations for Future Work

1. Although the PVAm-PVA composite membranes incorporating CNTs and molecular amines were developed in this study, the membrane compositions and structures were not optimized.

Reducing the thickness of the skin layer will increase the permeance, but it's more likely to cause pinholes on the membrane surface. Further improvement in the membrane performance can be done by optimizing the membrane structure and the composition of the skin layer.

2. The PVAm-PVA composite membranes incorporated with molecular amines were studied for $CO_2/N_2$, $CO_2/H_2$ separations and $CO_2$ dehydration from ethanol fermentation off gas. Most studies were carried out at low stage cuts in order to keep a relatively constant concentration along the feed side of the membrane. Thus, it is suggested that the separations under various stage cuts are investigated to evaluate the product purity, recovery and productivity of the separation process from an engineering perspective.
3. The flat sheet PVAm-PVA/TETA composite membranes were shown to be promising for permeation of acid gas and water vapor in $CO_2$ separation and gas dehydration. Hollow fibers have a high packing density. Thus, PVAm-PVA/TETA hollow fiber composite membranes comprising a thin skin layer and a microporous substrate are desirable for enhanced productivity. The hollow fiber membranes can be prepared by dip coating the PVAm-PVA/TETA solution onto a microporous hollow fiber substrate (including outside coating and inside coating).
4. Based on the successful construction of PVAm-PVA/TETA flat sheet membrane and hollow fiber membrane, module design is needed to make the membrane commercially viable. For industrial applications, thousands of square meters of membranes need to be packed into modules to perform the separation task on a commercial scale. There are basically three types of module design: plate-and-frame module, spiral wound module and hollow fiber module. For module selection, cost is always important and generally the high-pressure modules are more expensive than low-pressure or vacuum modules. Hollow fiber modules are much

cheaper than spiral wound or plate-and-frame modules for high volume applications, and can withstand high pressures. Hence, it would be of interest to further develop the PVAm-PVA/TETA membranes for hollow fiber modules used for $CO_2$ separation.

# References


Abdalla, M., D. Dean, D. Adibempe, E. Nyairo, P. Robinson, G. Thompson, The effect of interfacial chemistry on molecular mobility and morphology of multiwalled carbon nanotubes epoxy nanocomposite, *Polymer*, 48 (2007) 5662-5670.

Ahn, S.M., J.W. Ha, J.H. Kim, Y.T. Lee, S.B. Lee, Pervaporation of fluoroethanol/water and methacrylic acid/water mixtures through PVA composite membranes, *J. Membr. Sci.*, 247 (2005) 51-57.

Ahn, J., W.J. Chung, I. Pinnau, M.D. Guiver, Polysulfone/silica nanoparticle mixed-matrix membranes for gas separation, *J. Membr. Sci.*, 314 (2008) 123-133.

Akieh, M.N., R.M. Latonen, S. Lindholm, S.F. Ralph, J. Bobacka, A. Ivaska, Electrochemically controlled ion transport across polypyrrole/multi-walled carbon nanotube composite membranes, *Synth. Met.*, 161 (2011) 1906-1914.

Al Marzouqi, M.H., M.A. Abdulkarim, S.A. Marzouk, M.H. El-Naas, H.M. Hasanain, Facilitated transport of $CO_2$ through immobilized liquid membrane, *Ind. Eng. Chem. Res.*, 44 (2005) 9273-9278.

Alper, E., W. Bouhamra, Reaction kinetics of carbonyl sulfide with aqueous ethylenediamine and diethylenetriamine, *Gas Sep. Purif.*, 8 (1994) 237-240.

Amann, J.G., C. Bouallou, A new aqueous solvent based on a blend of N-methyldiethanolamine and triethylene tetramine for $CO_2$ recovery in post-combustion: kinetics study, *Energy Procedia*, 1 (2009) 901-908.

Amnuaypanich, S., J. Patthana, P. Phinyocheep, Mixed matrix membranes prepared from natural rubber/poly(vinyl alcohol) semi-interpenetrating polymer network (NR/PVA semi-IPN) incorporating with zeolite 4A for the pervaporation dehydration of water-ethanol mixtures, *Chem. Eng. Sci.*, 64 (2009) 4908-4918.

Aroon, M.A., A.F. Ismail, M.M. Montazer-Rahmati, T. Matsuura, Effect of chitosan as a functionalization agent on the performance and separation properties of polyimide/multi-walled carbon nanotubes mixed matrix flat sheet membranes, *J. Membr. Sci.*, 364 (2010) 309-317.

Bai, H., W.S.W. Ho, New carbon dioxide-selective membranes based on sulfonated polybenzimidazole (SPBI) copolymer matrix for fuel cell applications, *Ind. Eng. Chem. Res.*, 48 (2009) 2344-2354.

Baker, R.W., *Membrane Technology and Applications, 2nd Edition*, John Wiley & Sons, (2004).

Bao, L., M.C. Trachtenberg, Facilitated transport of $CO_2$ across a liquid membrane: Comparing enzyme, amine, and alkaline, *J. Membr. Sci.*, 280 (2006) 330-334.

Bishnoi, S., G.T. Rochelle, Absorption of carbon dioxide in aqueous piperazine/ methyldiethanolamine, *AIChE J.*, 48 (2002) 2788-2799.

Breck, D.W., Zeolite molecular sieves, Krieger Publishing Company, Malabar, 1974.

Brunetti, A., F. Scura, G. Barbieri, E. Drioli, Membrane technologies for $CO_2$ separation, *J. Membr. Sci.*, 359 (2010) 115-125.

Burshe, M.C., S.B. Sawant, J.B. Joshi, V.G. Pangakar, Dehydration of ethylene glycol by pervaporation using hydrophilic IPNs of PVA, PAA and PAAM membranes, *Sep. Purif. Technol.*, 13 (1998) 47-56.

Cai, Y., Z. Wang, C. Yi, Y. Bai, J. Wang, S. Wang, Gas transport property of polyallylamine-poly(vinyl alcohol)/polysulfone composite membranes, *J. Membr. Sci.*, 310 (2008) 184-196.

Chen, F.R., H.F. Chen, Pervaporation separation of ethylene glycol-water mixtures using crosslinked PVA-PES composite membranes, Part I. Effects of membrane preparation conditions on pervaporation performances, *J. Membr. Sci.*, 109 (1996) 247-256.

Chen, J., M.J. Dyer, M.F. Yu, Cyclodextrin-mediated soft cutting of single-walled carbon nanotubes, *J. Am. Chem. Soc.*, 123 (2001) 6201-6202.

Chen G.Q., C.A. Scholes, G.G. Qiao, S.E. Kentish, Water vapor permeation in polyimide membranes, *J. Membr. Sci.*, 379 (2011) 479-487.

Chen, H.Z., T.S. Chung, $CO_2$-selective membranes for hydrogen purification and the effect of carbon monoxide (CO) on its gas separation performance, *Int. J. Hydrogen Energy*, 37 (2012) 6001-6011.

Choi, J.H., J. Jegal, W.N. Kim, Fabrication and characterization of multi-walled carbon nanotubes/polymer blend membranes, *J. Membr. Sci.*, 284 (2006) 406-415.

Choi, J.H., J. Jegal, W.N. Kim, Modification of performances of various membranes using MWNTs as a modifier, *Macromol. Symp.*, 249-250 (2007) 610-617.

Choi, J.H., J. Jegal, W.N. Kim, H.S. Choi, Incorporation of multiwalled carbon nanotubes into poly(vinyl alcohol) membranes for use in the pervaporation of water/ethanol mixtures, *J. Appl. Polym. Sci.*, 111 (2009) 2186-2193.

Chung, T.S., L. Shao, P.S. Tin, Surface modification of polyimide membranes by diamines for $H_2$ and $CO_2$ separation, *Macromol. Rapid Commun.*, 27 (2006) 998-1003.

Chung, T.S., L.Y. Jiang, Y. Li, S. Kulprathipanja, Mixed matrix membranes (MMMs) comprising organic polymers with dispersed inorganic fillers for gas separation, *Prog. Polym. Sci.*, 32 (2007) 483-507.

Cong, H., M. Radosz, B.F. Towler, Y. Shen, Polymer-inorganic nanocomposite membranes for

gas separation, *Sep. Purif. Technol.*, 55 (2007a) 281-291.

Cong, H., J. Zhang, M. Radosz, Y. Shen, Carbon nanotube composite membranes of brominated poly(2,6-diphenyl-1,4-phenylene oxide) for gas separation, *J. Membr. Sci.*, 294 (2007b) 178-185.

Cong, H., X. Hu, M. Radosz, Y. Shen, Brominated poly(2,6-diphenyl-1,4-phenylene oxide) and its silica nanocomposite membranes for gas separation, *Ind. Eng. Chem. Res.*, 46 (2007c) 2567-2575.

Cussler, E.L., R. Aris, A. Bhown, On the limit of facilitated diffusion, *J. Membr. Sci.*, 43 (1989) 149-164.

Davis, J., G. Rochelle, Amine thermal degradation, Luminant Carbon Management Program Research Review Meeting, Washington DC, 2008.

Deng, L., T.J. Kim, M.B. Hagg, Facilitated transport of $CO_2$ in novel PVAm/PVA blend membrane, *J. Membr. Sci.*, 340 (2009) 154-163.

Deng, L., M.B. Hagg, Swelling behavior and gas permeation performance of PVAm/PVA blend FSC membrane, *J. Membr. Sci.*, 363 (2010) 295-301.

Derks, P.W.J., T. Kleingeld, C. van Aken, J.A. Hogendoorn, G.F. Versteeg, Kinetics of absorption of carbon dioxide in aqueous piperazine solutions, *Chem. Eng. Sci.*, 61 (2006) 6837-6854.

Donaldson, T.L., Y.N. Nguyen, Carbon dioxide kinetics and transport in aqueous amine membranes, *Ind. Eng. Chem. Fundam.*, 19 (1980) 260-266.

Dong, Y., J. Li, Z. Jiang, L. Lu, X. Chen, Chitosan/$TiO_2$ nanocomposite pervaporation membranes for ethanol dehydration, *Chem. Eng. Sci.*, 64 (2009) 3130-3137.

Du, R., X. Feng, A. Chakma, Poly(*N,N*-dimethylaminoethyl methacrylate)/polysulfone composite membranes for gas separations, *J. Membr. Sci.*, 279 (2006) 76-85.

Du, J.R., A. Chakma, X. Feng, Dehydration of ethylene glycol by pervaporation using poly(*N,N*-dimethylaminoethyl methacrylate)/polysulfone composite membranes, *Sep. Purif. Technol.*, 64 (2008) 63-70.

Du, J.R., L. Liu, A. Chakma, X. Feng, Using poly(*N,N*-dimethylaminoethyl methacrylate)/ polyacrylonitrile composite membranes for gas dehydration and humidification, *Chem. Eng. Sci.*, 65 (2010a) 4672-4681.

Du, J.R., L. Liu, A. Chakma, X. Feng, A study of gas transport through interfacially formed poly(*N,N*-dimethylaminoethyl methacrylate) membranes, *Chem. Eng. J.*, 156 (2010b) 33-39.

Duan, S., T. Kouketsu, S. Kazama, K. Yamada, Development of PAMAM dendrimer composite

membranes for $CO_2$ separation, *J. Membr. Sci.*, 283 (2006) 2-6.

Feng, X., R.Y.M. Huang, Pervaporation with chitosan membranes, I. Separation of water from ethylene glycol by a chitosan/polysulfone composite membrane, *J. Membr. Sci.*, 116 (1996) 67-76.

Feng, X., R.Y.M., Huang, Liquid separation by membrane pervaporation: A review, *Ind. Eng. Chem. Res.*, 36 (1997) 1048-1066.

Francisco, G.J., A. Chakma, X. Feng, Membranes comprising of alkanolamines incorporated into poly(vinyl alcohol) matrix for $CO_2/N_2$ separation, *J. Membr. Sci.*, 303 (2007) 54-63.

Francisco, G.J., A. Chakma, X. Feng, Separation of carbon dioxide from nitrogen using diethanolamine-impregnated poly(vinyl alcohol) membranes, *Sep. Purif. Technol.*, 71 (2010) 205-213.

Freeman, B.D., Basis of permeability/selectivity trade-off relations in polymeric gas separation membranes, *Macromolecules*, 32 (1999) 375-380.

Ge, L., Z. Zhu, V. Rudolph, Enhanced gas permeability by fabricating functionalized multi-walled carbon nanotubes and polyethersulfone nanocomposite membrane, *Sep. Purif. Technol.*, 78 (2011) 76-82.

Georgakilas V., K. Kordatos, M. Prato, D.M. Guldi, M. Holzingger, A. Hirsch, Organic functionalization of carbon nanotubes, *J. Am. Chem. Soc.*, 124 (2002) 760-761.

Georgakilas, V., A. Bourlinos, D. Gournis, T. Tsoufis, C. Trapalis, A. Mateo-Alonso, M. Prato, Multipurpose organically modified carbon nanotubes: From functionalization to nanotube composites, *J. Am. Chem. Soc.*, 130 (2008) 8733-8740.

Ghosal, K., B.D. Freeman, Gas separation using polymer membranes: an overview, *Polym. Adv. Technol.*, 5 (1994) 673-697.

Glasscock, D.A., J.E. Critchfield, G.T. Rochelle, $CO_2$ absorption/desorption in mixtures of methyldiethanolamine with monoethanolamine or diethanolamine, *Chem. Eng. Sci.*, 46 (1991) 2829-2845.

Gmehling, J., U. Onken, Vapor-Liquid Equilibrium Data Collection, Chemistry Data Series, Vol. 1, Pt. 1, Aqueous-Organic Systems, DECHEMA, Frankfurt, 1977.

Gomes, D., S.P. Nunes, K.V. Peinemann, Membranes for gas separation based on poly (1-trimetylsilyl-1-propyne)-silica nanocomposites, *J. Membr. Sci.*, 246 (2005) 13-25.

Gorji, A.H., T. Kaghazchi, $CO_2/H_2$ separation by facilitated transport membranes immobilized with aqueous single and mixed amine solutions: experimental and modeling study, *J. Membr. Sci.*, 325 (2008) 40-49.

Guha, A.K., S. Majumdar, K.K. Sirka, Facilitated transport of $CO_2$ through an immobilized

liquid membrane of aqueous diethanolamine, *Ind. Eng. Chem. Res.*, 29 (1990) 2093-2100.

Gunasekaran, S., B. Anita, Spectral investigation and normal coordinate analysis of piperazine, *Indian J. Pure Appl. Phys.*, 46 (2008) 833-838.

Guo, R., C. Hu, F. Pan, H. Wu, Z. Jiang, PVA-GPTMS/TEOS hybrid pervaporation membrane for dehydration of ethylene glycol aqueous solution, *J. Membr. Sci.*, 281 (2006) 454-462.

Guo, R., X. Ma, C. Hu, Z. Jiang, Novel PVA-silica nanocomposite membrane for pervaporative dehydration of ethylene glycol aqueous solution, *Polymer*, 48 (2007) 2939-2945.

Hagewiesche, D.P., S.S. Ashour, H.A. Alghawas, O.C. Sandall, Absorption of carbon dioxide into aqueous blends of monoethanolamine and N-methyldiethanolamine, *Chem. Eng. Sci.*, 50 (1995) 1071-1079.

Hagg, M.B., R. Quinn, Polymeric facilitated transport membranes for hydrogen purification, *MRS Bull.*, 31 (2006) 750-755.

Hartono, A., E.F. da Silva, H. Grasdalen, H.F. Svendsen, Qualitative determination of species in DETA-$H_2O$-$CO_2$ system using 13C NMR spectra, *Ind. Eng. Chem. Res.*, 46 (2007) 249-254.

Hartono, A., H.F. Svendsen, Kinetics reaction of primary and secondary amine group in aqueous solution of diethylenetriamine (DETA) with carbon dioxide, *Energy Procedia*, 1 (2009) 853-859.

Hartono, A., E.F. da Silva, H.F. Svendsen, Kinetics of carbon dioxide absorption in aqueous solution of diethylenetriamine (DETA), *Chem. Eng. Sci.*, 64 (2009) 3205-3213.

Hashi, M., F.H. Tezel, J. Thibault, Ethanol recovery from fermentation broth via carbon dioxide stripping and adsorption, *Energy Fuels*, 24 (2010) 4628-4637.

Hinds, B.J., N. Chopra, T. Rantell, R. Andrews, V. Gavalas, L.G. Bachas, Aligned multiwalled carbon nanotube membranes, *Science*, 303 (2004) 62-65.

Hines, A.L., R.N. Maddox, *Mass Transfer*, Prentice Hall, Upper Saddle River, NJ, (1985), 553.

Holt, J.K., H.G. Park, Y. Wang, M. Stadermann, A.B. Artyukhin, C.P. Grigoropoulos, A. Noy, O. Bakajin, Fast mass transport through sub-2-nanometer carbon nanotubes, *Science*, 312 (2006) 1034-1037.

Horng, S.Y., M.H. Li, Kinetics of absorption of carbon dioxide into aqueous solutions of monoethanolamine + triethanolamine, *Ind. Eng. Chem. Res.*, 41 (2002) 257-266.

Huang, R.Y.M., P. Shao, X. Feng, W.A. Anderson, Separation of ethylene glycol-water mixtures using sulfonated poly(ether ether ketone) pervaporation membranes: membrane relaxation and separation performance analysis, *Ind. Eng. Chem. Res.*, 41 (2002) 2957-

2965.

Huang, J., R.J. Cranford, T. Matsuura, C. Roy, Water vapor permeation properties of aromatic polyimides, *J. Membr. Sci.*, 215 (2003) 129-140.

Huang, Z., Y. Shi, R. Wen, Y. Guo, J. Su, T. Matsuura, Multilayer poly(vinyl alcohol)-zeolite 4A composite membranes for ethanol dehydration by means of pervaporation, *Sep. Purif. Technol.*, 51 (2006) 126-136.

Huang, J., J. Zou, W.S.W. Ho, Carbon dioxide capture using a $CO_2$-selective facilitated transport membrane, *Ind. Eng. Chem. Res.*, 47 (2008) 1261-1267.

Husain, S., W.J. Koros, Mixed matrix hollow fiber membranes made with modified HSSZ-13 zeolite in polyetherimide polymer matrix for gas separation, *J. Membr. Sci.*, 288 (2007) 195-207.

Iijima, S., Helical microtubules of graphitic carbon, *Nature*, 354 (1991) 56.

Inoue, K., Functional dendrimers, hyperbranched and star polymers, *Prog. Polym. Sci.*, 25 (2000) 453-571.

Ismail, A.F., P.S. Goh, J.C. Tee, S.M. Sanip, M. Aziz, A review of purification techniques for carbon nanotubes, *Nano*, 3 (2008) 127-143.

Ismail, A.F., P.S. Goh, S.M. Sanip, M. Aziz, Transport and separation properties of carbon nanotube-mixed matrix membrane, *Sep. Purif. Technol.*, 70 (2009) 12-26.

Karakane, H., M. Tsuyumoto, Y. Maeda, Z. Honda, Separation of water-ethanol by pervaporation through polyion complex composite membrane, *J. Appl. Polym. Sci.*, 42 (1991) 3229-3239.

Khulbe, K.C., T. Matsuura, G. Lamarche, A.M. Lamarche, X-ray diffraction analysis of dense PPO membranes, *J. Membr. Sci.*, 170 (2000) 81-89.

Kim, J.H., Y.M. Lee, Gas permeation properties of poly(amide-6-b-ethylene oxide)-silica hybrid membranes, *J. Membr. Sci.*, 193 (2001) 209-225.

Kim, T.J., B. Li, M.B. Hagg, Novel fixed-site-carrier polyvinylamine membrane for carbon dioxide capture, *J. Polym. Sci., Part B: Polym. Phys.*, 42 (2004) 4326-4336.

Kim, Y.K., H.B. Park, Y.M. Lee, Preparation and characterization of carbon molecular sieve membranes derived from BTDA-ODA polyimide and their gas separation properties, *J. Membr. Sci.*, 255 (2005) 265-273.

Kim, S., T.W. Pechar, E. Marand, Poly(imide siloxane) and carbon nanotube mixed matrix membranes for gas separation, *Desalination*, 192 (2006) 330-339.

Kim, S., J.R. Jinschek, H. Chen, D.S. Sholl, E. Marand, Scalable fabrication of carbon

nanotube/polymer nanocomposite membranes for high flux gas transport, *Nano Lett.*, 7 (2007a) 2806-2811.

Kim, S., L. Chen, J.K. Johnson, E. Marand, Polysulfone and functionalized carbon nanotube mixed matrix membranes for gas separation: theory and experiment, *J. Membr. Sci.*, 294 (2007b) 147-158.

Kim, T.J., H. Vralstad, M. Sandru, M.B. Hagg, Separation performance of PVAm composite membrane for $CO_2$ capture at various pH levels, *J. Membr. Sci.*, 428 (2013) 218-224.

Knudsen, M., *The Kinetic Theory of Gases; Some Modern Aspects;* Methuen's Monographs on Physical Subjects, Methuen, London, (1952).

Koros, W.J., Gas separation membranes: Needs for combined materials science and processing approaches, *Macromol. Symp.*, 188 (2002) 13-22.

Koros, W.J., Evolving beyond the thermal age of separation processes: Membrane can lead the way, *AIChE J.*, 50 (2004) 2326-2334.

Kouketsu, T., S. Duan, T. Kai, S. Kazama, K. Yamada, PAMAM dendrimer composite membrane for $CO_2$ separation: Formation of a chitosan gutter layer, *J. Membr. Sci.*, 287 (2007) 51-59.

Kovvali, A.S., H. Chen, K.K. Sirkar, Dendrimer membranes: A $CO_2$-selective molecular gate, *J. Am. Chem. Soc.*, 122 (2000) 7594-7595.

Kovvali, A.S., K.K. Sirkar, Dendrimer liquid membranes: $CO_2$ separation from gas mixtures, *Ind. Eng. Chem. Res.*, 40 (2001) 2502-2511.

Kruk, M., T. Asefa, M. Jaroniec, G.A. Ozin, Metamorphosis of ordered mesopores to micropores: Periodic silica with unprecedented loading of pendant reactive organic groups transforms to periodic microporous silica with tailorable pore size, *J. Am. Chem. Soc.*, 124 (2002) 6383-6392.

Krull, F.F., C. Fritzmann, T. Melin, Liquid membranes for gas/vapor separations, *J. Membr. Sci.*, 325 (2008) 509-519.

Kumar, S., A. Sharma, B. Tripathi, S. Srivastava, S. Agrawal, M. Singh, K. Awasthi, Y.K. Vijay, Enhancement of hydrogen gas permeability in electrically aligned MWCNT-PMMA composite membranes, *Micron*, 41 (2010) 909-914.

Landro, L.D., M. Pegoraro, L. Bordogna, Interactions of polyether-polyurethanes with water vapour and water-methane separation selectivity, *J. Membr. Sci.*, 64 (1991) 229-236.

Lebrun, L., S. Bruzaud, Y. Grohens, D. Langevin, Elaboration and characterisation of PDMS-$HTiNbO_5$ nanocomposite membranes, *Eur. Polym. J.*, 42 (2006) 1975-1985.

Li, S., Z. Wang, C. Zhang, M. Wang, F. Yuan, J. Wang, S. Wang, Interfacially polymerized thin

film composite membranes containing ethylene oxide groups for $CO_2$ separation, *J. Membr. Sci.*, 436 (2013) 121-131.

Lin, Y., B. Zhou, K.A. Shiral Fernando, P. Liu, L.F. Allard, Y. Sun, Polymeric carbon nanocomposites from carbon nanotubes functionalized with matrix polymer, *Macromolecules*, 36 (2003) 7199-7204.

Lin, H., E. Van Wagner, B.D. Freeman, L.G. Toy, R.P. Gupta, Plasticization-enhanced hydrogen purification using polymeric membranes, *Science*, 311 (2006a) 639-642.

Lin, H., E. Van Wagner, R. Raharjo, B.D. Freeman, I. Roman, High-performance polymer membranes for natural-gas sweetening, *Adv. Mater.*, 18 (2006b) 39-44.

Lin, H., S.M. Thompson, A. Serbanescu-Martin, J.G., Wijmans, K.D. Amo, K.A. Lokhandwala, T.C. Merkel, Dehydration of natural gas using membranes. Part I: Composite membranes, *J. Membr. Sci.*, 413-414 (2012) 70-81.

Littel, R.J., G.F. Versteeg, W.P.M. van Swaaij, Kinetics of $CO_2$ with primary and secondary amines in aqueous solutions, influence of temperature on zwitterion formation and deprotonation rates, *Chem. Eng. Sci.*, 47 (1992) 2037-2045.

Liu, J., A.G. Rinzler, H. Dai, J.H. Hafner, R.K. Bradley, P.J. Boul, A. Lu, T. Iverson, K. Shelimov, C.B. Huffman, F. Rodriguez-Macias, Y.S. Shon, T.R. Lee, D.T. Colbert, R.E. Smalley, Fullerene pipes, *Science*, 280 (1998) 1253-1256.

Liu, L., Chen, Y., Kang, Y., Deng, M., An industrial scale dehydration process for natural gas involving membranes, *Chem. Eng. Technol.*, 24 (2001) 1045-1048.

Liu, Y.L., C.Y. Hsu, Y.H. Su, J.Y. Lai, Chitosan-silica complex membranes from sulfonic acid functionalized silica nanoparticles for pervaporation dehydration of ethanol-water solutions, *Biomacromolecules*, 6 (2005) 368-373.

Liu, Q., T. Wang, J. Qiu, Y. Cao, A novel carbon/ZSM-5 nanocomposite membrane with high performance for oxygen/nitrogen separation, *Chem. Commun.*, 11 (2006) 1230-1232.

Liu, L., A. Chakma, X. Feng, Gas permeation through water-swollen hydrogel membranes, *J. Membr. Sci.*, 310 (2008) 66-75.

Liu, Y.L., W.H. Chen, Y.H. Chang, Preparation and properties of chitosan/carbon nanotube nanocomposites using poly(styrene sulfonic acid)-modified CNTs, *Carbohydr. Polym.*, 76 (2009) 232-238.

Maier, G., Gas separation with polymer membranes, *Angew. Chem. Int. Ed.*, 37 (1998) 2960-2974.

Majeed, S., D. Fierro, K. Buhr, J. Wind, B. Du, A. Boschetti-de-Fierro, V. Abetz, Multi-walled carbon nanotubes (MWCNTs) mixed polyacrylonitrile (PAN) ultrafiltration membranes, *J. Membr. Sci.*, 403-404 (2012) 101-109.

Majumder, M., N. Chopra, R. Andrews, B.J. Hinds, Enhanced flow in carbon nanotubes, *Nature*, 438 (2005) 44.

Makino, H., Y. Kusuki, H. Yoshida, A. Nakamura, Process for preparing aromatic polyimide semipermeable membranes, U.S. Patent 4,378,324, (1983).

Mandal, B.P., M. Guha, A.K. Biswas, S.S. Bandyopadhyay, Removal of carbon dioxide by absorption in mixed amines: modeling of absorption in aqueous MDEA/MEA and AMP/MEA solutions, *Chem. Eng. Sci.*, 56 (2001) 6217-6224.

Matsuyama, H., M. Teramoto, H. Sakakura, K. Iwai, Facilitated transport of $CO_2$ through various ion exchange membranes prepared by plasma graft polymerization, *J. Membr. Sci.*, 117 (1996) 251-260.

Matsuyama, H., K. Matsui, Y. Kitamura, T. Maki, M. Teramoto, Effects of membrane thickness and membrane preparation condition on facilitate transport of $CO_2$ through ionomer membrane, *Sep. Purif. Technol.*, 17 (1999) 235-241.

Matteucci, S., R.D. Raharjo, V.A. Kusuma, S. Swinnea, B.D. Freeman, Gas permeability, solubility and diffusion coefficients in 1,2-Polybutadiene containing magnesium oxide, *Macromolecules*, 41 (2008) 2144-2156.

Maxwell, C., *Treatise on Electricity and Magnetism, vol. 1*, Oxford University Press, London, (1873).

Merkel, T.C., B.D. Freeman, R.J. Spontak, Z. He, I. Pinnau, P. Meakin, A.J. Hill, Ultrapermeable, reverse-selective nanocomposite membranes, *Science*, 296 (2002) 519-522.

Merkel, T.C., B.D. Freeman, R.J. Spontak, Z. He, I. Pinnau, P. Meakin, A.J. Hill, Sorption, transport and structural evidence for enhanced free volume in poly(4-methyl-2-pentyne)/ fumed silica nanocomposite membranes, *Chem. Mater.*, 15 (2003a) 109-123.

Merkel, T.C., Z. He, I. Pinnau, B.D. Freeman, P. Meakin, A.J. Hill, Effect of nanoparticles on gas sorption and transport in poly (1-trimethylsilyl-1-propyne), *Macromolecules*, 36 (2003b) 6844-6855.

Metz, S.J., W.J.C. van de Ven, M.H.V. Mulder, M. Wessling, Mixed gas water vapor/$N_2$ transport in poly(ethylene oxide) poly(butylene terephthalate) block copolymers, *J. Membr. Sci.*, 266 (2005a) 51-61.

Metz, S.J., W.J.C. van de Ven, J. Potreck, M.H.V. Mulder, M. Wessling, Transport of water vapor and inert gas mixtures through highly selective and highly permeable polymer membranes, *J. Membr. Sci.*, 251 (2005b) 29-41.

Modesti, M., C. Dall'Acqua, A. Lorenzetti, E. Florian, Mathematical model and experimental validation of water cluster influence upon vapour permeation through hydrophilic dense membrane, *J. Membr. Sci.*, 229 (2004) 211-223.

Mollersten, K., J. Yan, J.R. Moreira, Potential market niches for biomass energy with $CO_2$ capture and storage – Opportunities for energy supply with negative $CO_2$ emissions, *Biomass Bioenergy*, 25 (2003) 273-285.

Mulder, M., *Basic Principle of Membrane Technology*, Kluwer Academic Publisher, Dordrecht/Boston/London, (1991).

Murali, R.S., S. Sridhar, T. Sankarshana, Y.V.L. Ravikumar, Gas permeation behavior of Pebax-1657 nanocomposite membrane incorporated with multiwalled carbon nanotubes, *Ind. Eng. Chem. Res.*, 49 (2010) 6530-6538.

Nawawi, M., R.Y.M. Huang, Pervaporation dehydration of isopropanol with chitosan membranes, *J. Membr. Sci.*, 124 (1997) 53-62.

Noble, R.D., S.A., Stern, *Membrane Separations Technology-Principles and Applications*, Elsevier: Amsterdam, (1995).

Nureshi, N., H.P. Blaschek, Butanol recovery from model solution/fermentation broth by pervaporation: evaluation of membrane performance, *Biomass Bioenergy*, 17 (1999) 175-184.

Ockwig, N.W., T.M. Nenoff, Membranes for hydrogen separation, *Chem. Rev.*, 107 (2007) 4078-4110.

Ong, Y.T., A.L. Ahmad, S.H.S. Zein, K. Sudesh, S.H. Tan, Poly(3-hydroxybutyrate)-functionalised multi-walled carbon nanotubes/chitosan green nanocomposite membranes and their application in pervaporation, *Sep. Purif. Technol.*, 76 (2011) 419-427.

Pandey, P., R. Chauhan, Membranes for gas separation, *Prog. Polym. Sci.*, 26 (2001) 853-893.

Park, H.B., C.H. Jung, Y.M. Lee, A.J. Hill, S.J. Pas, S.T. Mudie, E. Van Wagner, B.D. Freeman, D.J. Cookson, Polymers with cavities tuned for fast selective transport of small molecules and ions, *Science*, 318 (2007) 254-258.

Patel, N.P., A.C. Miller, R.J. Spontak, Highly $CO_2$-permeable and selective polymer nanocomposite membranes, *Adv. Mater.*, 15 (2003) 729-733.

Patel, N.P., A.C. Miller, R.J. Spontak, Highly $CO_2$-permeable and -selective membranes derived from crosslinked poly(ethylene glycol) and its nanocomposite, *Adv. Funct. Mater.*, 14 (2004) 699-707.

Peng, F., F. Pan, H. Sun, L. Lu, Z. Jiang, Novel nanocomposite pervaporation membranes composed of poly(vinyl alcohol) and chitosan-wrapped carbon nanotube, *J. Membr. Sci.*, 300 (2007a) 13-19.

Peng, F., C. Hu, Z. Jiang, Novel poly(vinyl alcohol)/carbon nanotube hybrid membranes for pervaporation separation of benzene/cyclohexane mixtures, *J. Membr. Sci.*, 297 (2007b) 236-242.

Penkova, A.V., G.A. Polotskaya, V.A. Gavrilova, A.M. Toikka, J.C. Liu, M. Trchova, M. Slouf, Z. Pientka, Polyamide membranes modified by carbon nanotubes: application for pervaporation, *Sep. Sci. Technol.*, 45 (2010) 35-41.

Perry, R.H., D.W. Green (Eds.), Perry's Chemical Engineers' Handbook, McGraw-Hill, (1999).

Pompeo, F., D.E. Resasco, Water solubilization of single-walled carbon nanotubes by functionalization with glucosamine, *Nano Lett.*, 2 (2002) 369-373.

Potreck, J., K. Nijmeijer, T. Kosinski, M. Wessling, Mixed water vapor/gas transport through the rubbery polymer PEBAX 1074, *J. Membr. Sci.*, 338 (2009) 11-16.

Qiao, Z., Z. Wang, C. Zhang, S. Yuan, Y. Zhu, J. Wang, S. Wang, PVAm-PIP/PS composite membrane with high performance for $CO_2/N_2$ separation, *AIChE J.*, 59 (2013) 215-228.

Qin, L., X. Zhao, K. Hirahara, Y. Miyamoto, Y. Ando, S. Iijima, Materials science: The smallest carbon nanotube, *Nature*, 408 (2000) 50.

Qiu, S., L. Wu, G. Shi, L. Zhang, H. Chen, C. Gao, Preparation and pervaporation property of chitosan membrane with functionalized multiwalled carbon nanotubes, *Ind. Eng. Chem. Res.*, 49 (2010) 11667-11675.

Quinn, R., D.V. Laciak, Polyelectrolyte membranes for acid gas separations, *J. Membr. Sci.*, 131 (1997) 49-60.

Rangwala, H.A., B.R. Morrell, A.E. Mather, F.D. Otto, Absorption of $CO_2$ into aqueous tertiary amine/MEA solutions, *Can. J. Chem. Eng.*, 70 (1992) 482-490.

Rao, P.S., S. Sridhar, M.Y. Wey, A. Krishnaiah, Pervaporative separation of ethylene glycol/water mixtures by using cross-linked chitosan membranes, *Ind. Eng. Chem. Res.*, 46 (2007) 2155-2163.

Reid, R.C., J.M. Prausnitz, B.E. Poling, The properties of gases and liquids, McGraw-Hill, New York, 1987.

Reijerkerk, S.R., M.H. Knoef, K. Nijmeijer, M. Wessling, Poly(ethylene glycol) and poly (dimethyl siloxane): combining their advantages into efficient $CO_2$ gas separation membranes, *J. Membr. Sci.*, 352 (2010) 126-135.

Reijerkerk, S.R., R. Jordana, K. Nijmeijer, M. Wessling, Highly hydrophilic, rubbery membranes for $CO_2$ capture and dehydration of flue gas, *Int. J. Greenh. Gas Con.*, 5 (2011a) 26-36.

Reijerkerk, S.R., K. Nijmeijer, C.P. Ribeiro Jr., B.D. Freeman, M. Wessling, On the effects of plasticization of $CO_2$/light gas separation polymeric solubility selective membranes, *J. Membr. Sci.*, 367 (2011b) 33-44.

Robeson, L.M., Correlation of separation factor versus permeability for polymeric membranes, *J. Membr. Sci.*, 62 (1991) 165-185.

Robeson, L.M., The upper bound revisited, *J. Membr. Sci.*, 320 (2008) 390-400.

Rosentrater, K.A., Economics and impacts of ethanol manufacture, *BioCycle*, 47 (2006) 44-52.

Saha, S., A. Chakma, Selective $CO_2$ separation from $CO_2/C_2H_6$ mixtures by immobilized diethanolamine/PEG membranes, *J. Membr. Sci.*, 98 (1995) 157-171.

Sahoo, N.G., S. Rana, J.W. Cho, L. Li, S.H. Chan, Polymer nanocomposites based on functionalized carbon nanotubes, *Prog. Polym. Sci.*, 35 (2010) 837-867.

Sanip, S.M., A.F. Ismail, P.S. Goh, T. Soga, M. Tanemura, H. Yasuhiko, Gas separation properties of functionalized carbon nanotubes mixed matrix membranes, *Sep. Purif. Technol.*, 78 (2011) 208-213.

Schaffer, A., K. Brechtel, G. Scheffknecht, Comparative study on differently concentrated aqueous solutions of MEA and TETA for $CO_2$ capture from flue gas, *Fuel*, 101 (2012) 148-153.

Sears, K., L. Dumee, J. Schutz, M. She, C. Huynh, S. Hawkins, M. Duke, S. Gray, Recent developments in carbon nanotube membranes for water purification and gas separation, *Materials*, 3 (2010) 127-149.

Shao, P., R.Y.M. Huang, Polymeric membrane pervaporation, *J. Membr. Sci.*, 287 (2007) 162-179.

Shao, L., J. Samseth, M.B. Hagg, Crosslinking and stabilization of nanoparticle filled PMP nanocomposite membranes for gas separations, *J. Membr. Sci.*, 326 (2009a) 285-292.

Shao, L., B.T. Low, T.S. Chung, A.R. Greenberg, Polymeric membranes for the hydrogen economy: contemporary approaches and prospects for the future, *J. Membr. Sci.*, 327 (2009b) 18-31.

Sharma, A., S. Kumar, B. Tripathi, M. Singh, Y.K. Vijay, Aligned CNT/polymer nanocomposite membranes for hydrogen separation, *Int. J. Hydrogen Energy*, 34 (2009) 3977-3982.

Sharma, A., B. Tripathi, Y.K. Vijay, Dramatic improvement in properties of magnetically aligned CNT/polymer nanocomposites, *J. Membr. Sci.*, 361 (2010) 89-95.

Shirazi, Y., M.A. Tofighy, T. Mohammadi, Synthesis and characterization of carbon nanotubes/poly vinyl alcohol nanocomposite membranes for dehydration of isopropanol, *J. Membr. Sci.*, 378 (2011) 551-561.

Sieffert, D., C. Staudt, Preparation of hybrid materials containing copolyimides covalently linked with carbon nanotubes, *Sep. Purif. Technol.*, 77 (2011) 99-103.

Sijbesma, H., K. Nymeijer, R. van Marwijk, R. Heijboer, J. Potreck, M. Wessling, Flue gas dehydration using polymer membranes, *J. Membr. Sci.*, 313 (2008) 263-276.

Skoulidas, A.I., D.M. Ackerman, J.K. Johnson, D.S. Sholl, Rapid transport of gases in carbon nanotubes, *Phys. Rev. Lett.*, 89 (2002) 185901.

Smitha, B., D. Suhanya, S. Sridhar, M. Ramakrishna, Separation of organic-organic mixtures by pervaporation: A review, *J. Membr. Sci.*, 241 (2004) 1-21.

Smitha, B., S. Sridhar, A.A. Khan, Synthesis and characterization of poly(vinyl alcohol)-based membranes for direct methanol fuel cell, *J. Appl. Polym. Sci.*, 95 (2005) 1154-1163.

Spitalsky, Z., D. Tasis, K. Papagelis, C. Galiotis, Carbon nanotube-polymer composites: Chemistry, processing, mechanical and electrical properties, *Prog. Polym. Sci.*, 35 (2010) 357-401.

Sridhar, S., G.J. Susheela Reddy, A.A. Khan, Crosslinked chitosan membranes: characterization and study of dimethylhydrazine dehydration by pervaporation, *Polym. Int.*, 50 (2001) 1156-1161.

Surapathi, A., J. Herrera-Alonso, F. Rabie, S. Martin, E. Marand, Fabrication and gas transport properties of SWNT/polyacrylic nanocomposite membranes, *J. Membr. Sci.*, 375 (2011) 150-156.

Tang, C., Q. Zhang, K. Wang, Q. Fu, C. Zhang, Water transport behavior of chitosan porous membranes containing multi-walled carbon nanotubes (MWNTs), *J. Membr. Sci.*, 337 (2009) 240-247.

Tasis, D., N. Tagmatarchis, A. Bianco, M. Prato, Chemistry of carbon nanotubes, *Chem. Rev.*, 106 (2006) 1105-1136.

Tee, Y.H., J. Zou, W.S.W. Ho, $CO_2$-selective membranes containing dimethylglycine mobile carriers and polyethylenimine fixed carrier, *J. Chin. Inst. Chem. Eng.*, 37 (2006) 37-47.

Teramoto, M., K. Nakai, N. Ohnishi, Facilitated transport of carbon dioxide through supported liquid membranes of aqueous amine solutions, *Ind. Eng. Chem. Res.*, 35 (1996) 538-545.

Teramoto, M., Q. Huang, T. Watari, Y. Tokunaga, R. Nakatani, T. Maeda, H. Matsuyama, Facilitated transport of $CO_2$ through supported liquid membranes of various amine solutions - effects of rate and equilibrium of reaction between $CO_2$ and amine, *J. Chem. Eng. Jpn.*, 30 (1997) 328-335.

Vaidya, P.D., E.Y. Kenig, $CO_2$-alkanolamine reaction kinetics: a review of recent studies, *Chem. Eng. Technol.*, 30 (2007) 1467-1474.

Vaidya, P.D., E.Y. Kenig, Termolecular kinetic model for $CO_2$-alkanolamine reactions: an overview, *Chem. Eng. Technol.*, 33 (2010) 1577-1581.

Vijay, Y.K., V. Kulshrestha, K. Awasthi, N.K. Acharya, A. Jain, M. Singh, S.N. Dolia, S.A. Khan, D.K. Avasthi, Characterization of nanocomposite polymeric membrane, *J. Polym. Res.*, 13 (2006) 357-360.

Vu, De Q., W.J. Koros, S.J. Miller, Mixed matrix membranes using carbon molecular sieves: I. Preparation and experimental results, *J. Membr. Sci.*, 211 (2003) 311-334.

Wang, N., Z. Tang, G. Li, J. Chen, Materials science: Single-walled 4A carbon nanotube arrays, *Nature*, 408 (2000) 50-51.

Wang, Z., M. Li, Y. Cai, J. Wang, S. Wang, Novel $CO_2$ selectively permeating membranes containing PETEDA dendrimer, *J. Membr. Sci.*, 290 (2007) 250-258.

Weng, T.H., H.H. Tseng, M.Y. Wey, Preparation and characterization of multi-walled carbon nanotube/PBNPI nanocomposite membrane for $H_2/CH_4$ separation, *Int. J. Hydrogen Energy*, 34 (2009) 8707-8715.

Wijmans, J.G., R.W. Baker, The solution-diffusion model: A review, *J. Membr. Sci.*, 107 (1995) 1-21.

Wu, Y., X. Peng, J. Liu, Q. Kong, B. Shi, M. Tong, Study on the integrated membrane processes of dehumidification of compressed air and vapor permeation processes, *J. Membr. Sci.*, 196 (2002) 179-183.

Wu, H., B. Tang, P. Wu, Novel ultrafiltration membranes prepared from a multi-walled carbon nanotubes/polymer composite, *J. Membr. Sci.*, 362 (2010) 374-383.

Xiao, S., R.Y.M. Huang, X. Feng, Preparation and properties of trimesoyl chloride crosslinked poly(vinyl alcohol) membranes for pervaporation dehydration of isopropanol, *J. Membr. Sci.*, 286 (2006) 245-254.

Xing, R., W.S.W. Ho, Crosslinked polyvinylalcohol-polysiloxane/fumed silica mixed matrix membranes containing amines for $CO_2/H_2$ separation, *J. Membr. Sci.*, 367 (2011) 91-102.

Xu, Z., L. Xiao, J. Wang, J. Springer, Gas separation properties of PMDA/ODA polyimide membranes filling with polymeric nanoparticles, *J. Membr. Sci.*, 202 (2002) 27-34.

Xu, J., C. Gao, X. Feng, Thin-film-composite membranes comprising of self-assembled polyelectrolytes for separation of water from ethylene glycol by pervaporation, *J. Membr. Sci.*, 352 (2010a) 197-204.

Xu, Y., L. Isom, M.A. Hanna, Adding value to carbon dioxide from ethanol fermentations, *Bioresour. Technol.*, 101 (2010b) 3311-3319.

Yaws, C.L., P.K. Narasimhan, C. Gabbula, Yaws' Handbook of Antoine Coefficients for Vapor Pressure, 2nd Electronic ed., Knovel, 2009.

Yi, C., Z. Wang, M. Li, J. Wang, S. Wang, Facilitated transport of $CO_2$ through polyvinylamine/polyethlene glycol blend membranes, *Desalination*, 193 (2006) 90-96.

Yu, X., Z. Wang, Z. Wei, S. Yuan, J. Zhao, J. Wang, S. Wang, Novel tertiary amino containing thin film composite membranes prepared by interfacial polymerization for $CO_2$ capture,

*J. Membr. Sci.*, 362 (2010) 265-278.

Yu, F., Y.H. Lin, Techno-economic evaluation of redox potential-controlled ethanol fermentation processes, *J. Taiwan Inst. Chem. E.*, 43 (2012) 813-819.

Yuan, S., Z. Wang, Z. Qiao, M. Wang, J. Wang, S. Wang, Improvement of $CO_2/N_2$ separation characteristics of polyvinylamine by modifying with ethylenediamine, *J. Membr. Sci.*, 378 (2011) 425-437.

Zhang, X., C. Zhang, S. Qin, Z. Zheng, A kinetics study on the absorption of carbon dioxide into a mixed aqueous solution of methyldiethanolamine and piperazine, *Ind. Eng. Chem. Res.*, 40 (2001) 3785-3791.

Zhang, Y., Z. Wang, S. Wang, Selective permeation of $CO_2$ through new facilitated transport membranes, *Desalination*, 145 (2002a) 385-388.

Zhang, X., C. Zhang, Y. Liu, Kinetics of absorption of $CO_2$ into aqueous solution of MDEA blended with DEA, *Ind. Eng. Chem. Res.*, 41 (2002b) 1135-1141.

Zhang, X., J. Wang, C. Zhang, Y. Yang, J. Xu, Absorption rate into a MDEA aqueous solution blended with piperazine under a high $CO_2$ partial pressure, *Ind. Eng. Chem. Res.*, 42 (2003) 118-122.

Zhang, Q., Q. Liu, Y. Chen, J. Chen, Dehydration of isopropanol by novel poly(vinyl alcohol)-silicone hybrid membranes, *Ind. Eng. Chem. Res.*, 46 (2007) 913-920.

Zhao, X., R.Y.M. Huang, Pervaporation separation of ethanol-water mixtures using crosslinked blended poly(acrylic acid)-nylon 66 membranes, *J. Appl. Polym. Sci.*, 41 (1990) 2133-2145.

Zhao, J., Z. Wang, J. Wang, S. Wang, Influence of heat-treatment on $CO_2$ separation performance of novel fixed carrier composite membranes prepared by interfacial polymerization, *J. Membr. Sci.*, 283 (2006) 346-356.

Zhao, L., E. Riensche, R. Menzer, L. Blum, D. Stolten, A parametric study of $CO_2/N_2$ gas separation membrane processes for post-combustion capture, *J. Membr. Sci.*, 325 (2008a) 284-294.

Zhao, H., Y. Cao, X. Ding, M. Zhou, Q. Yuan, Poly(*N*,*N*-dimethylaminoethyl methacrylate)-poly(ethylene oxide) copolymer membranes for selective separation of $CO_2$, *J. Membr. Sci.*, 310 (2008b) 365-373.

Zhao, Q., J. Qian, C. Zhu, Q. An, T. Xu, Q. Zheng, Y. Song, A novel method for fabricating polyelectrolyte complex/inorganic nanohybrid membranes with high isopropanol dehydration performance, *J. Membr. Sci.*, 345 (2009) 233-241.

Zou, J., W.S.W. Ho, $CO_2$-selective polymeric membranes containing amines in crosslinked poly(vinyl alcohol), *J. Membr. Sci.*, 286 (2006) 310-321.

Zou, H., S. Wu, J. Shen, Polymer/silica nanocomposites: preparation, characterization, properties, and applications, *Chem. Rev.*, 108 (2008) 3893-3957.

# Appendix A - Sample Calculations

## A.1 Sample calculations for pure gas permeation

**Calculation of gas permeance**

The permeance of pure gas was calculated from the following data:

Membrane: PVAm-PVA/PZ membrane at a PZ/polymer mass ratio of 100/100;

Gas: $CO_2$;

Operating temperature: 297 K;

Membrane area: 22.90 $cm^2$;

Feed pressure: 0.6013 MPa;

Downstream pressure: 0.1013 MPa (76 cmHg);

Permeate flow rate: 0.155602 ml/s;

The permeance ($J$) of $CO_2$ can be calculated as follows:

$$J = \frac{V}{At\Delta p}\frac{273.15}{T_0}\frac{p_0}{76} = \frac{0.155602}{22.9 \times (0.6013 - 0.1013) \times 750.063}\frac{273.15}{297.15}\frac{76}{76}$$

$$= 16.731 \times 10^{-6}\ cm^3(STP)/(cm^2.s.cmHg) = 16.731\ GPU$$

For $N_2$, the calculated permeance at the same conditions is $0.198\ GPU$.

**Calculation of ideal selectivity**

The ideal selectivity for $CO_2$ over $N_2$ can be calculated as the ratio of $CO_2$ permeance to $N_2$ permeance.

$$\alpha_{CO_2/N_2} = \frac{J_{CO_2}}{J_{N_2}} = \frac{16.731}{0.198} = 84.5$$

## A.2 Sample calculations for gas mixture permeation

**Calculation of gas permeance**

The permeances of gas mixtures can be obtained from the calculation detailed below:

Membrane: PVAm-PVA/TETA membrane at a TETA/polymer mass ratio of 150/100;

Gas mixture: $CO_2/N_2$;

Operating temperature: 298 K;

Membrane area: 22.90 $cm^2$;

Total feed pressure: 0.6013 MPa;

Feed concentration of $CO_2$: 15.3 mol%;

Permeate concentration of $CO_2$: 74.6 mol%;

Permeate pressure: 0.1013 MPa;

Permeate flow rate: $9.337 \times 10^{-3}\ cm^3/s$;

The permeance of $CO_2$ ($J_{CO_2}$) in the mixture can be calculated as follows:

$$J_{CO_2} = \frac{Vy_{CO_2}}{At(p_f x_{CO_2} - p_p y_{CO_2})}\frac{273.15}{T_0}$$

$$= \frac{9.337 \times 10^{-3} \times 0.746}{22.9 \times (0.6013 \times 0.153 - 0.1013 \times 0.746) \times 750.063}\frac{273.15}{298.15}$$

$$= 22.632 \times 10^{-6}\ cm^3(STP)/(cm^2.s.cmHg) = 22.632\ GPU$$

The permeance of $N_2$ ($J_{N_2}$) in the mixture is:

$$J_{N_2} = \frac{Vy_{N_2}}{At(p_f x_{N_2} - p_p y_{N_2})}\frac{273.15}{T_0}$$

$$= \frac{9.337 \times 10^{-3} \times (1 - 0.746)}{22.9 \times [0.6013 \times (1 - 0.153) - 0.1013 \times (1 - 0.746)] \times 750.063}\frac{273.15}{298.15}$$

$$= 0.262 \times 10^{-6}\ cm^3(STP)/(cm^2.s.cmHg) = 0.262\ GPU$$

**Calculation of selectivity**

The selectivity for $CO_2$ over $N_2$ in the mixture can be calculated as the ratio of $CO_2$ permeance to $N_2$ permeance.

$$\alpha_{CO_2/N_2} = \frac{J_{CO_2}}{J_{N_2}} = \frac{22.632}{0.262} = 86.5$$

## A.3 Temperature dependence on permeance

The temperature dependence of permeance can be expressed by Arrhenius equation and the apparent activation energy can be obtained from $\ln J$ vs. $(1/T)$ plot based on the following form of the equation:

$$\ln J = \ln J_0 + \frac{-E_a}{R}\frac{1}{T} \qquad \text{(A3.1)}$$

$slope\ k = -E_a/R$ (A3.2)

Using the permeation of $CO_2$ through PVAm-PVA/DETA membrane at a DETA/polymer mass ratio of 150/100 at a feed pressure of 0.6013 MPa:

| Temperature (℃) | 1000/T (1/K) | Permeance (GPU) |
|---|---|---|
| 15 | 3.47041 | 17.19429 |
| 25 | 3.35402 | 20.36324 |
| 30 | 3.29870 | 23.66708 |
| 40 | 3.19336 | 29.90967 |
| 50 | 3.09454 | 36.93948 |
| 60 | 3.00165 | 43.77632 |
| 70 | 2.91418 | 50.79966 |

The exponential regression of the plot of $\ln J$ against $(1000/T)$ results to:

$E_a/R = 2.024 \times 10^3$

$E_a = 2.024 \times 10^3 \times 8.3145\ J/mol = 16.83\ kJ/mol$

## A.4 Sample calculations for pervaporation dehydration

The permeation flux and separation factor were calculated from the following data:

Membrane: PVAm-PVA/CNT (0.5 wt% CNTs) membrane;

Liquid mixture: Ethylene glycol/water;

Operating temperature: 311 K;

Membrane area: 16.60 $cm^2$;

Feed concentration of water: 1 wt%;

Permeate concentration of water: 92.22 wt%;

Collected 0.174g of permeate over 5 hrs;

**Calculation of total permeation flux**

$$J = \frac{Q}{At} = \frac{0.174}{16.6 \times 10^{-4} \times 5.0114} = 20.9162\ \ g/(m^2.h)$$

**Calculation of partial permeation flux**

$J_{water} = J \times Y = 20.9162 \times 0.9222 = 19.2889\ \ g/(m^2.h)$

$J_{EG} = J \times (1 - Y) = 20.9162 \times (1 - 0.9222) = 1.6273\ \ g/(m^2.h)$

**Calculation of separation factor**

$$\alpha = \frac{Y/(1-Y)}{X/(1-X)} = \frac{92.22/(100-92.22)}{1/(100-1)} = 1173.5$$

## A.5 Sample calculations for $CO_2$ separation from ethanol fermentation off gas

As mentioned in chapter 8, for $CO_2$-$H_2O$ binary system, the permeance of water vapor can be calculated based on the following equations:

$$Q_{H_2O} = AJ_{H_2O}\left(p_f X - p_p Y\right) \quad \text{(A5.1)}$$

$$Q_{CO_2} = AJ_{CO_2}\left[p_f(1-X) - p_p(1-Y)\right] \quad \text{(A5.2)}$$

$$Y = \frac{Q_{H_2O}}{Q_{H_2O}+Q_{CO_2}} \quad \text{(A5.3)}$$

The water vapor permeance can be calculated from the following data:

Membrane: PVAm-PVA/TETA membrane at a TETA/polymer mass ratio of 150/100;

Feed mixture: $CO_2$/water vapor;

Operating temperature: 298 K;

Membrane area: 22.90 $cm^2$;

Feed concentration of water vapor: 2.52 mol%;

Feed pressure: 101.3 kPa (76 cmHg);

Permeate pressure: 3.3 kPa (2.49 cmHg);

Permeation rate of water: 0.06226 $cm^3$(STP)/s;

Based on the data given above, the water vapor permeance $J_{H_2O}$ and permeate concentration of water vapor $Y$ can be calculated from MATLAB:

$J_{H_2O} = 0.0167\ cm^3(STP)/(cm^2.s.cmHg) = 16700\ GPU$

$Y = 0.7208$